

**Glial contribution to synapse ingestion in Alzheimer's
disease and schizophrenia**

Makis Tzioras



**Doctor of Philosophy (PhD)
The University of Edinburgh
2021**

Abstract

The adaptive and plastic nature of synapses allows the brain to perform complex cognitive tasks, like memory formation and retention. A multitude of disorders affecting the central nervous system are associated with the dysfunction and loss of synapses. These include dementia disorders, schizophrenia, multiple sclerosis, and motor neuron disease. Alzheimer's disease (AD) is the most common form of dementia and is a progressive neurodegenerative disease that affects the elderly population. An estimated 46.8 million people had AD in 2015, with these numbers expected to reach 75 million people by 2030 due to the increasing life-expectancy of people, and growing population. Neurodegeneration in the AD brain can occur as loss of neurons and synapses, with the latter being the strongest pathological correlate to cognitive decline in AD. There are currently no effective treatments to halt disease progression nor provide curative effects. Therapeutic interventions in mice, although promising, have failed to translate to humans, leading to a reproducibility crisis in the field of AD research. Adding to this low success rate is the fact that the majority of clinical interventions have focused on reducing the levels of one of the hallmark protein aggregates found in the AD brain, amyloid- β ($A\beta$). It is now becoming apparent that reducing $A\beta$ levels late in disease is not a successful strategy in halting neurodegeneration and the field has opened its windows to new avenues. Research into non-neuronal cells and their response to AD has emerged as a promising target to resolve AD-related pathologies. For instance, microglia are immune cells in the brain, resembling in morphology and function peripheral macrophages, that have emerged as central players in AD pathogenesis. Specifically, some of the ways that microglia contribute to homeostasis are by regulating neuroinflammation, clearing debris by phagocytosis, and aiding the formation of myelin sheaths. Synapse numbers during development are also adjusted when microglia phagocytose less active ones, in a controlled manner. However, recent evidence from animal models of AD has demonstrated that there is excessive

phagocytosis of synapses in the AD brains, and points to microglia as a contributor to synapse loss, leading to the progressive cognitive decline. Currently, there is little evidence to support these findings in human brains, and given the problem of reproducibility in the AD field, it is crucial to investigate whether this applies to humans prior to any therapeutic targets going to clinical trials. This doctoral thesis has shown that microglia in the human brain ingest more synapses in AD compared to aged controls and that this process is exacerbated near A β plaques. Moreover, isolated pHrodo-tagged synaptoneurosomes from AD and control brains were given to human and mouse microglia and astrocytes *in-vitro*, and were live imaged in a phagocytosis assay. AD-synaptoneurosomes were ingested both more and faster than control synaptoneurosomes, suggesting disease-related alterations to the synaptic preparations makes them more prone to elimination. From a previous proteomic analysis in the lab, it is known that such signals include complement proteins that are upregulated in AD synapses. Mechanistic studies are now ongoing to determine whether the increased phagocytosis of synapses can be modulated by targeting these synaptic changes. Of note, schizophrenia is a psychiatric disorder affecting the mood and personality, where reduced synaptic levels have also been reported. Schizophrenia brains were examined similarly to AD brains, but in this case no significant differences were found between schizophrenia and control brains, suggesting different disease processes affect synapses. Therefore, is it likely that the progressive synapse loss in AD reflects the increased synaptic ingestion, unlike schizophrenia.

Hypothesis: The hypothesis of this thesis is that glial cells contribute to exacerbated synapse loss in the AD and schizophrenia brains by actively removing synapses from brain, and it is predicted that they use opsonin tags on the synapses to induce this change in synaptic ingestion.

Lay abstract

Dementia is commonly thought of as a single disease where a person's memory fades away. In fact, dementia encompasses many distinct disorders affecting the elderly population and one of their common features is progressive cognitive decline, including memory deficits and behavioural changes. Alzheimer's disease (AD) is the most common form of dementia and like in all other dementias, individuals with AD display significant memory problems which worsen over time. An estimated 46.8 million people had AD in 2015, with these numbers expected to reach 75 million people by 2030 due to the increasing life-expectancy of people and growing population. By examining a brain from someone with AD, one can notice remarkable shrinkage in the brain, which is referred to as atrophy. This atrophy is mainly seen because of the loss of nerve cells (neurons) in the brain and the vast network of connections (synapses) between these cells. Neurons and synapses allow the brain to perform complex tasks, like forming new memories and remembering them, learning a new language, or coordinating motor tasks. The loss of these neurons and synapses is known as neurodegeneration, and consequently it results in a failure of the brain to efficiently carry out these tasks. In the AD brain, two proteins known as amyloid- β and tau begin to behave differently and become toxic to synapses and neurons, which in turn kills them and contributes to neurodegeneration. However, treatments focusing on removing amyloid- β plaques have failed to provide any beneficial outcomes for these patients. Sadly, AD is a lethal disease and there are currently no treatments to slow down the disease progression or cure the disease. Currently, an emerging field in neuroscience is the study of glial cells, which are non-neuronal cells in the brain that can aid the function of neurons and support brain health. Microglia and astrocytes are examples of glial cells that help the formation of new synapses but also remove weaker synapses during brain development by eating them. In mice that express AD-like pathology, their microglia eliminate more synapses leading to cognitive impairments.

Interestingly, when this process is stopped, cognition improves and synapses are healthier. This is a potential new avenue for the treatment of AD, but whether microglia contribute to synapse loss by eating them is unknown in humans. This thesis examined human post-mortem brains with and without AD, and found that microglia in AD brains contained more synapses than brains without AD. Interestingly, near these pathological amyloid- β plaques, microglia ate even more synapses. Moreover, synapses from human brains were isolated from control and AD individuals, and they were fed to microglia and astrocytes from mouse and human brains in culture. The synapses from these AD brains were eaten both more and faster than control brains. These data suggest that something about AD synapses makes them more vulnerable for microglia to eat them, and future experiments will address what these signals are and how to limit them. Of note, schizophrenia is a psychiatric disorder affecting the mood and personality, where reduced synaptic levels have been reported. Schizophrenia brains were examined similar to AD brains, but in this case no significant differences were found these cases and controls, suggesting different disease processes affect synapses. It is possible that synapses in schizophrenia are more resilient to degeneration as the age groups are younger in the schizophrenia cohort than the AD group, and that distinct molecular pathways are involved in the disease. Also, it is not clear whether in schizophrenia synapses are lost, like they are in AD, or whether they have never formed properly, suggesting a developmental phenotype, which is different to AD.

Declarations

I declare that this thesis is composed by myself and, except where otherwise stated, is entirely my own work. The presented work has not been submitted for any other degree or professional qualification. The thesis includes work from two published articles and one BioRxiv submission:

Chapter 1 and Appendix: **Tzioras, M.**, Davies, C., Newman, A., Jackson, R. and Spires-Jones, T., 2018. Invited Review: APOE at the interface of inflammation, neurodegeneration and pathological protein spread in Alzheimer's disease. *Neuropathology and Applied Neurobiology*, 45(4), pp.327-346. 10.1111/nan.12529

Chapters 3 and 4: **Tzioras, M.**, Daniels, M., King, D., Popovic, K., Holloway, R., Stevenson, A., Tulloch, J., Kandasamy, J., Sokol, D., Latta, C., Rose, J., Smith, C., Miron, V., Henstridge, C., McColl, B. and Spires-Jones, T., 2019. Altered synaptic ingestion by human microglia in Alzheimer's disease. <https://doi.org/10.1101/795930>

Chapter 5: **Tzioras, M.**, Stevenson, A., Boche, D. and Spires-Jones, T., 2020. Microglial contribution to synaptic uptake in the prefrontal cortex in schizophrenia. *Neuropathology and Applied Neurobiology*, 47(2), pp.346-351. 10.1111/nan.12660

.....
April, 2021

Acknowledgments

It only makes sense to start this section with the person that gave me this opportunity in the first place, and who I am immensely grateful for; Tara. Your generosity has no bounds. I don't think I would be half the person or scientist I am today if it weren't for you. I admire you so much, and I have had the time of my life, whether that is through scientific success, lip syncs, partying it up at conferences, and karaoke extravaganzas. You allowed and encouraged me to live authentically and I grew so much because of you.

Thank you Barry for the support you have given me throughout this PhD, and for providing me with so many valuable teaching opportunities.

Ευχαριστώ την οικογένεια μου που με δεν σταμάτησαν να πιστεύουν σε εμένα. Με έχετε στηρίξει όσο κανείς άλλος και νιώθω πάντα ευπρόσδεκτος (χαχα). Μαμά, θέλω να ξέρεις ότι θαυμάζω τη δύναμη σου. Έμαθα να αγαπώ, να εξερευνώ, να μαθαίνω, να εκτιμώ, να φροντίζω, και να διασκεδάζω χάρεις το παράδειγμα σου. Μπαμπά, σ' ευχαριστώ για όλες σου τις προσπάθειες να μας κάνεις καλύτερους ανθρώπους και να εκτιμάμε τον εαυτό μας, τα κατάφερες. Λάζαρε, ευχαριστώ που είσαι στο πλάι μου και που με στηρίζεις σε όλα τα βήματα μου. Γιαγιά Ματούλα και παππού Λάζαρε, είστε υπέροχοι άνθρωποι και σας αγαπώ πολύ. Γιαγιά Βέτα και παππού Μάκη, σας ευχαριστώ που δώσατε αυτό που μπορούσατε. Μακάρι να μπορούσε η Υβόννη να δει αυτή την εργασία, πιστεύω θα της έδινε μεγάλη χαρά, αλλά ίσως και να τη βλέπει.

My “Mick Michael” Mike Daniels, I want you to know I'm a *mirrorball* and I reflected best because of your *incandescent glow*. Through all the mistakes, the trials and tribulations, I can safely say that *I had a marvellous time ruining everything*. You were *the 1* that made me feel like a brand new *cardigan* when

my tears ricochet, so I can't help but wonder, was there *an invisible string tying you to me*? You helped me *hit my peak* and *live for the hope of it all*. You were there for me during those *clandestine meetings* when I wanted to cry "*this is me trying*". For a while I lost myself and I was in *exile*, *my kingdom come undone*, thinking it was *a shame I went mad*, but you helped me have an *epiphany*, and then *suddenly everything was clear*. So you can bet, I will always *show up at your party* so that we can be FW.

My amazing Jane, did you ever know that you're my hero and everything I would like to be? I can fly higher than an eagle, for you are the wind beneath my wings.

Chris Henstridge, you were a friend and a teacher from day one. I don't think I could admire so much any other person wearing a Wookiee onesie at laser-tag.

Caitlin, you and I defy gravity, and I can safely say that because I knew you, I have been changed for good. We are islands in the stream, how can we be wrong? I loved sharing this experience with you, I cherish all the fun we had together and I know that you made this whole roller coaster ride that much funnier.

Clare Latta, I can't tell you how much I have enjoyed our long walks together. Even the times we walked side by side quietly together, there a mutual connection and understanding that doesn't feel awkward, it just feels like friendship.

Thank you to the lovely people at the Spires-Jones and McColl labs who were a joy to be around. Dec you've been an awesome bro, Hati you've been such a kind-spirit, Carmen it was pure joy being around you, Clare you're such a wonderful person and I love vibing to Taylor Swift with you, Laura you are a

ray of sunshine, Marti you are such a lovely and kind-hearted person, Anna you're such a brilliant person and I had a wonderful time in and outwith the lab, James I have loved our laughs and jokes, Stef you've been a sweet hoooneeyyyy-pot. And thank you to the not-so-lovely people who only magnified the value of a kind heart.

Miruna, I keep looking back at us in high school and how we dreamed of becoming scientists and look at us now! We really have made, and past us would be so proud. You've been such a warm light in my life, much like a cup of coffee at Gilmore Girls. Now that we're doctors maybe they'll hire us at Grey's Anatomy?

Thank you to Virginia Georgiou for being so supportive, I am very grateful.

Laura Kaminioti-Dumont, one of the best things to happen over the last few years was reconnecting and taking our friendship to whole new levels that were so unexpected. I've had so many beautiful memories from our explorations with Ferg and I hope you know how much all this has meant to me.

Laura Barry, I always feel your presence next me and we Ride together. You have been my biggest fan, even when I was so hard on myself. I love you so much and I am so proud of how much you've accomplished. You mean the world to me.

Giulia amorelino, sei stata una amica meravigliosa. Mi sei sempre stata così di supporto e sono così grato di averti avuto nella mia vita. Abbiamo vissuto insieme momenti magici e abbiamo riso con il cuore. Grazie per essere stata un'amica incredibile in tutti questi anni.

A big thank you to Dr. Veronica Miron and her lab for being awesome scientists and people, I had a wonderful time exploring the magic of science with you.

A large part of who I am as a scientist is thanks to Dr. Villy Panoutsakopoulou and her amazing lab. This is in honour of her memory. You showed me the beauty of science and trusted me from day one. Thank you to her and her incredible team, I am so grateful for all you did for me.

Thank you to all the educators in my life who have shared their craft with me.

Thank you to our funders for supporting this work: UK Dementia Research Institute, Alzheimer's Research UK, Alzheimer's Society and the MRC.

And lastly, thank you to myself. I am so proud of how far I have come along.

Table of Contents

Chapter 1: Introduction - 1 -

1. Alzheimer's disease - 1 -

1.1 History of Alzheimer's disease - 1 -

1.2 Clinical progression of AD - 1 -

1.3 Prevalence and cost of AD - 4 -

1.4 Neuropathology of Alzheimer's disease - 4 -

1.5 Synapses: the brains' great communicators - 7 -

1.6 Risk factors for developing Alzheimer's disease - 9 -

1.7 Genetic risk factors and their association to pathologies of Alzheimer's disease - 10 -

1.8 Lack of treatments for AD: paving new ways forward - 11 -

2. Microglia: the brain's Swiss army knife - 12 -

2.1 Introduction into microglia - 12 -

2.2 The role of microglia in synaptic refinement - 14 -

2.3 Flattery will get you everywhere: the complement system and synapse pruning - 17 -

2.4 Intrinsic and extrinsic properties of synapse pruning by microglia - 19 -

2.5 The purinergic system in microglial-mediated synapse pruning - 20 -

2.6 Epigenetic regulation of microglial-mediated synaptic pruning - 20 -

2.7 Astrocytic contribution to synaptic pruning - 21 -

3. Microglia in AD pathogenesis - 24 -

3.1 Genetics implicate microglia in AD - 24 -

4. Microglial contribution to synapse loss - 27 -

4.1 Microglia eliminate synapses in animal models of amyloidopathy - 27 -

4.2 Microglial contribution to synapse loss in mouse models of tauopathy - 32 -

4.3 Non-contact dependent synapse loss by microglia in AD - 34 -

4.4 Microglial contribution to synapse loss in humans - 37 -

5. Schizophrenia - 38 -

5.1 Synaptic changes in schizophrenia brains - 39 -

5.2 Microglial alterations in schizophrenia - 39 -

6. Knowledge gaps - 41 -

7. Hypothesis and aims - 42 -

8. List of publications - 43 -

Chapter 2: Methods - 48 -

1. Overview - 48 -

2. Animals - 49 -

3. Human tissue (Alzheimer's disease study) - 49 -

4. Human tissue (Schizophrenia study) - 51 -

5. Immunohistochemistry for paraffin embedded human tissue - 52 -

6. Confocal microscopy and Image analysis - 55 -

7. Synapse-enriched fraction preparation - 57 -

8. Protein Extraction - 57 -

9. Micro BCA - 58 -

10. Western Blot - 58 -

11. Synaptoneurosome labelling with pHrodo Red-SE - 59 -

12. BV2 microglia phagocytosis assay - 60 -

13. Primary mouse microglia - 61 -

14. Primary human microglia isolation - 62 -

15. Primary mouse astrocyte isolation - 63 -

16. Immunofluorescence of cultured cells - 64 -

17. Statistics - 64 -

18. Software and Data Availability - 65 -

Chapter 3: Human post-mortem analysis of synaptic ingestion by microglia - 66 -

1. Introduction - 66 -

2. Results - 67 -

2.1 Optimization of staining - 67 -

2.2 Increased synaptic ingestion by microglia in human post-mortem tissue - 72 -

2.3 Increased synaptic ingestion by microglia near A β plaques - 82 -

2.4 Astrocytic contribution to synaptic ingestion in AD - 85 -

3. Discussion - 86 -

Chapter 4: *In-vitro* ingestion of human synaptoneuroosomes by glial cells - 91 -

1. Introduction - 91 -

2. Results - 94 -

2.1 Synaptoneuroosomes validation - 94 -

2.2 Loss of synaptophysin but not PSD-95 protein in AD - 96 -

2.3 Phagocytosis validation by BV2 microglia - 97 -

2.4 Phagocytosis assay using primary mouse microglia - 99 -

2.5 Phagocytosis assay using primary human microglia - 104 -

2.6 Phagocytosis assay using primary mouse astrocytes - 113 -

3. Discussion - 117 -

Chapter 5: Microglial contribution to synaptic uptake in the prefrontal cortex in schizophrenia - 121 -

1. Introduction - 121 -

2. Microglial contribution to synaptic uptake in the prefrontal cortex in schizophrenia (attached manuscript) - 123 -

3. Re-analysis of data with 3D segmentation - 137 -

4. Conclusion - 140 -

Chapter 6: Discussion - 142 -

1. Overview - 142 -

2. Synapses: Shantay you stay or sashay away? - 143 -

2.1 Synaptic decorations: “eat-me” and “don’t eat me” signals - 143 -

2.2 APOE, A β , and tau interactions in microglial ingestion of synapses - 144 -

2.3 In-vitro to in-vivo: lost in translation - 146 -

3. Synaptic ingestion by microglia in AD and schizophrenia - 146 -

4. Metabolic disease in AD and synaptic engulfment - 147 -

5. Future experiments - 148 -

6. Conclusion - 149 -

References - 151 -

Appendix - 176 -

Appendix Figure 1. Complete list of Western blot gels and corresponding Ponceau S pages for Chapter 4, Figure 2. - 176 -

Appendix R Script 1. R Studio Script used for the analysis in Chapter 3 (Modified version used for Re-analysis in Chapter 5). - 177 -

Appendix Manuscript 1: Invited Review: APOE at the interface of inflammation, neurodegeneration and pathological protein spread in Alzheimer's disease - 204 -

Epilogue - 262 -

“Here’s to the ones who dream,

foolish as they may seem”

Chapter 1: Introduction

1. Alzheimer's disease

1.1 History of Alzheimer's disease

In 1901, German neuropsychiatrist Alois Alzheimer examined Auguste Dieter, a 51-year old woman who displayed rapid cognitive decline, and psychiatric symptoms like apathy and depression (Hippius and Neundörfer, 2003; Goedert and Spillantini, 2006). She passed away 5 years later in 1906, when Alois Alzheimer examined her brain and presented the pathological findings in 1906. Upon post-mortem examination, Alzheimer found neuropathological lesions that he named neurofibrillary tangles and plaques, as well an accumulation of cells with elongated projections near these pathologies (glial cells). Despite senile dementia being described prior to that study, the disease eventually took its name after him and is now known as Alzheimer's disease (AD). Looking at the hand-drawings Alzheimer made, it can be appreciated that he accurately depicted the landscape of an AD brain as we know it today, and much of what he described more than 100 years ago still holds true. Indeed, diagnosis of Alzheimer's disease still relies on post-mortem identification of plaques and tangles.

1.2 Clinical progression of AD

AD belongs in the family of dementia disorders, which encompasses a number of neurodegenerative diseases primarily affecting the elderly population (Keller, 2006; Prince et al., 2013). Age is the biggest risk factor for developing AD, and with a growing population that also lives longer, there is an increasing

number of people who develop AD (Prince et al., 2015). Disease-associated pathologies, like plaques, tangles and gliosis, precede the onset of clinical symptoms (Ingelsson et al., 2004), which often include memory loss, spatial navigation, mood imbalances, and irritability and confusion (Robinson, Tang and Taylor, 2015). Also, ageing individuals can display mild cognitive impairment (MCI), which can either impair cognitive functions or progress into full-blown dementia (Figure 1) (Petersen, 2004). This is also associated with an increase in neurodegeneration and gliosis. Specifically, individuals with MCI display issues in at least one of the five neurocognitive domains: learning and memory, executive function, complex attention, language, social cognition, and perceptual motor function (Verghese et al., 2007; Hugo and Ganguli, 2014), but their daily life is not significantly impaired by these changes (Knopman and Petersen, 2014). On the other hand, individuals with dementia display problems in more than one cognitive domain, and their daily life is significantly affected by this change in cognition. Once MCI has progressed into dementia, it is not possible to turn back, as dementia disorders are progressive in nature (Petersen et al., 1999; Petersen, 2004). This means that cognitive impairments worsen over time, and new symptoms, like depression or the inability to execute motor function, appear as the disease spreads throughout the brain, making it debilitating to the individual. The average life-span from dementia diagnosis can vary significantly depending on the age of onset with an average of 6.7 years (Wolters et al., 2019), while insufficient pharmacological interventions are currently available to prevent or slow down the disease.

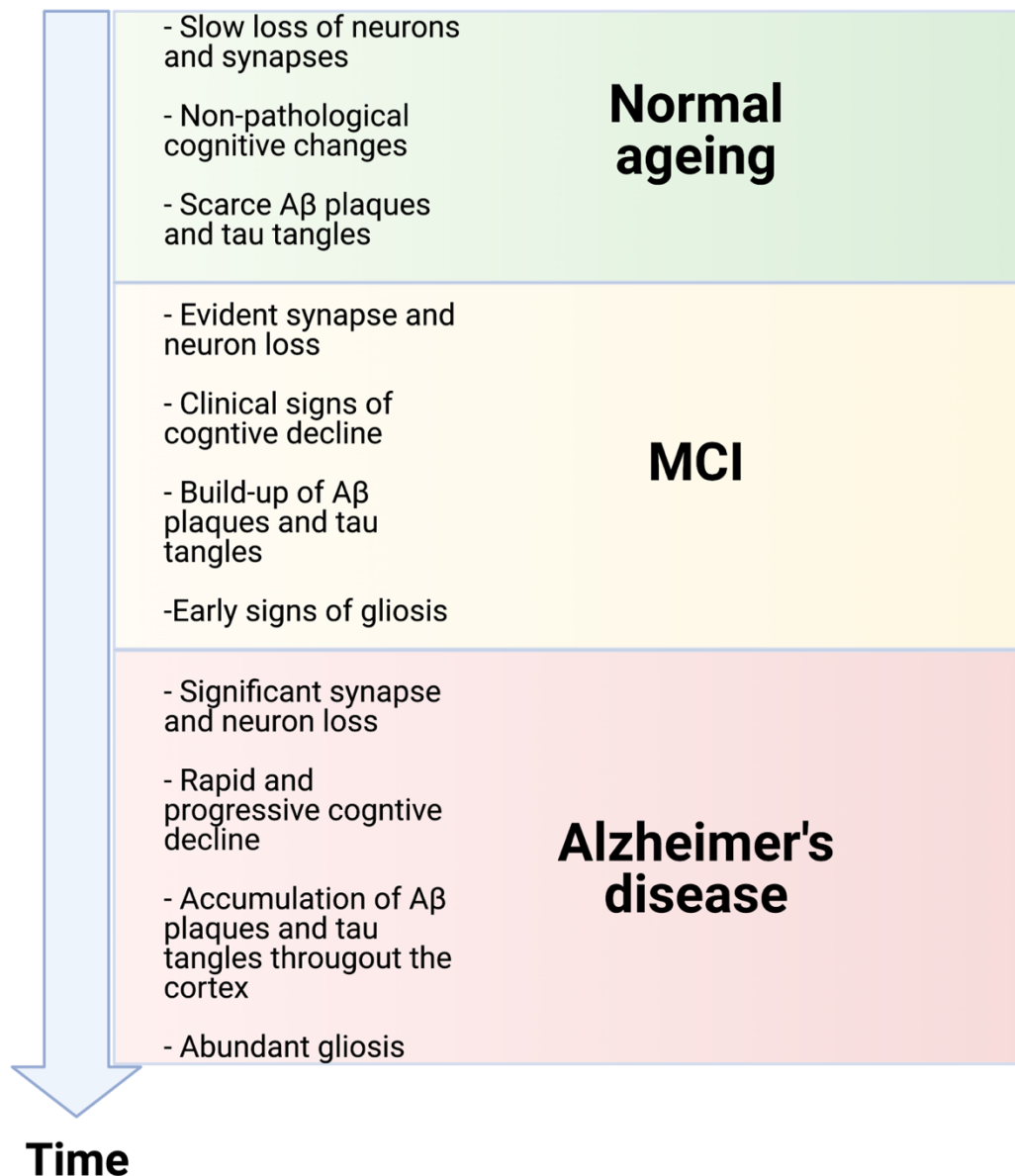


Figure 1. Clinical progression from normal cognitive ageing, to mild cognitive impairment (MCI) and Alzheimer's disease (AD). Hallmark features of AD like synapse loss and pathological protein aggregate accumulations are also seen during normal ageing but in lower levels. As these pathologies increase over time, individuals experience MCI which is considered an intermediate stage between ageing and AD. Not all individuals who develop MCI go on to develop AD, but once they do it is not possible to revert to healthy ageing. It is currently unknown why some people develop AD while others show resilience to cognitive ageing and pathology build-up.

1.3 Prevalence and cost of AD

Currently, AD and dementia are one of the biggest medical challenges worldwide for a multitude of reasons. Dementia currently affects 50 million people worldwide, and at the current rate these numbers are expected to project to a staggering 152 million people by 2050. The most common type of dementia is AD, accounting for approximately 65% of all dementia cases, meaning an estimated 32.5 million people worldwide are affected by AD alone (Prince et al., 2016). The personal cost of people living with dementia and their families is immeasurable; however, the financial cost of dementia is considerably large, costing £26 billion in the United Kingdom (UK) (Lewis et al., 2014), a sum that is projected to increase to £55 billion by 2040 (Prince et al., 2014). To put this in perspective, in the UK the healthcare and social care cost of dementia is greater than cancer and chronic heart disease combined (Luengo-Fernandez, Leal and Gray, 2015).

1.4 Neuropathology of Alzheimer's disease

The underlying causes and symptoms between different forms of dementia can vary but some common features include progressive cognitive decline (memory in particular) and accumulation of pathological protein aggregates (Kent, Spires-Jones and Durrant, 2020; Henstridge, Pickett and Spires-Jones, 2016; Braak and Braak, 1991; Thal, Rüb, Orantes and Braak, 2002). Specifically in AD, the three cardinal neuropathological features of the disease are cortical atrophy, and the presence of two pathological protein aggregates; amyloid- β ($A\beta$) plaques and phosphorylated tau tangles (Figure 2) (Spires-Jones and Hyman, 2014; Ingelsson et al., 2004). The silver-positive stains Alois Alzheimer reported down the microscope are in fact these two pathologies, which can interact to induce neuron and synapse loss in the brain, thus contributing to the cortical atrophy seen in the disease (Koffie et al., 2009; Gomes et al., 2019; Tai et al., 2014; Pickett et al., 2019). To this day, AD

staging relies on the neuropathological spread of these aggregates. Specifically, tau staging is referred to as Braak staging (Braak and Braak, 1991) and A β spread is referred to as Thal staging (Thal et al., 2002). Early stages of these categories represent few and localised incidents of protein aggregates, whereas late stages suggest the majority of grey matter is affected with pathology, indicating the presence of Alzheimer's disease. Brain atrophy is represented by the loss of neurons and synapses, which initially occurs in brain areas important for memory processes, like the hippocampus and temporal lobe (Sheng, Sabatini and Südhof, 2012; Koffie, Hyman and Spires-Jones, 2011). It has been known for almost 30 years that out of all pathological features described above, synapse loss correlates most strongly with cognitive decline in AD. Specifically, in the early 90's two groups showed that poor performance at the Mini Mental Score Exam (MMSE) strongly correlated to lower synaptic counts, counted both by EM and optical density of DAB staining (DeKosky and Scheff, 1990; Terry et al., 1991). Since then, numerous other studies have consistently reported synapse loss in AD, as reported in a recent meta-analysis (de Wilde, Overk, Sijben and Masliah, 2016). That, as well as the highly plastic nature of synapses, has put synaptic biology at the centre of AD research.

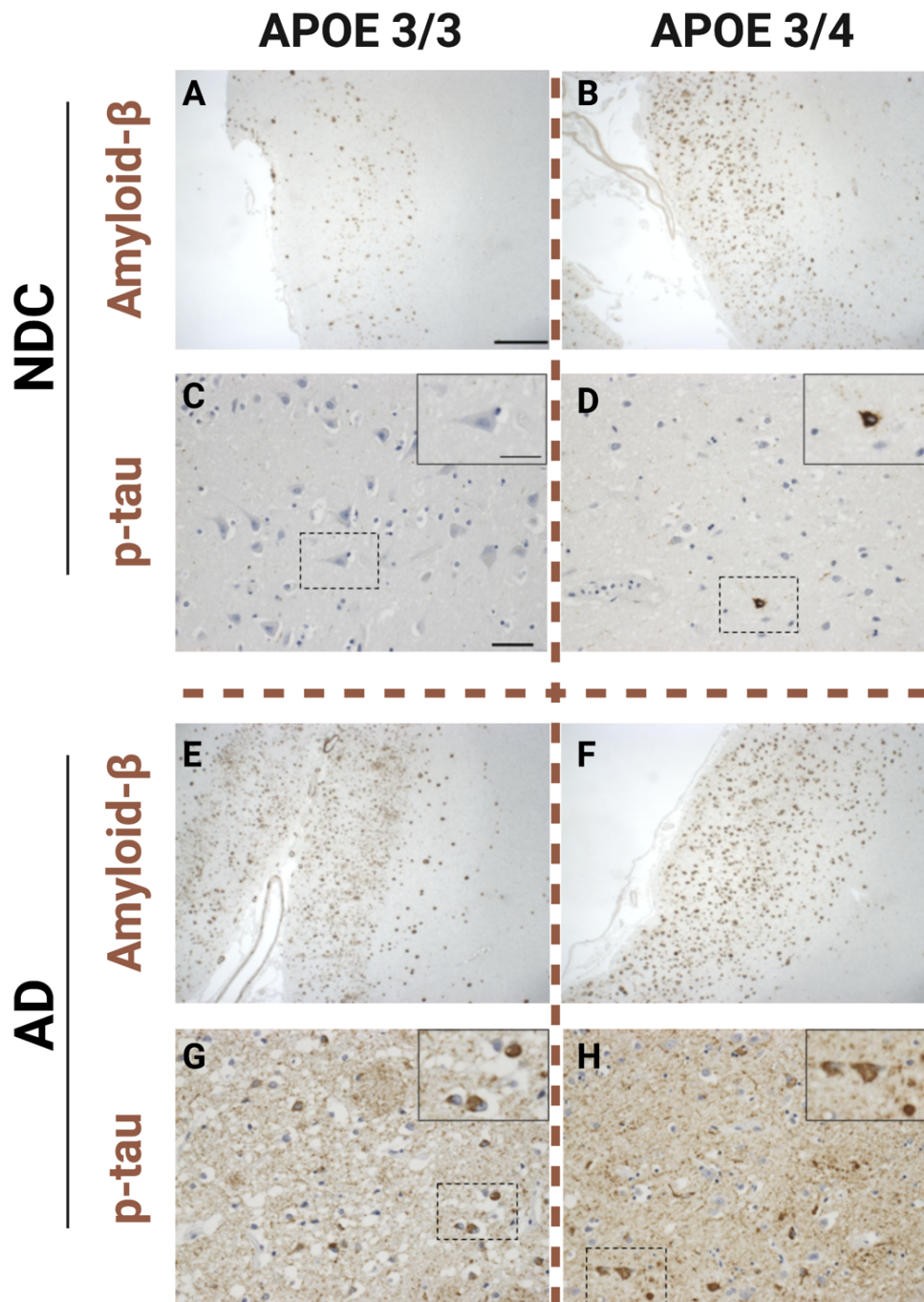


Figure 2. Amyloid- β and phosphorylated tau in ageing and Alzheimer's disease. The figure displays representative images of human post-mortem tissue showing amyloid- β (labelled with BA4) and phosphorylated-tau (labelled with AT8). Tissue was stained with 3,3'-Diaminobenzidine (DAB) and counterstained with haematoxylin to label nuclei. Amyloid- β ($A\beta$) plaques are found both in non-demented control (NDC) brains (A-B), as well as brains with Alzheimer's disease (E-F). More $A\beta$ plaques are found in the AD brain, and the APOE4 genotype is associated to a greater density of these plaques both in NDC and in AD brains. Meanwhile, virtually no phosphorylated tau (p-tau)

tangles are found in NDC brains (C-D), whereas AD brains are packed with misfolded tau tangles (G-H). Scale bar in A, 1mm; scale bar in C 50µm; scale bar in C insert, 25µm. Figure adapted from “Tzioras, M. et al., 2019. Invited Review: APOE at the interface of inflammation, neurodegeneration and pathological protein spread in Alzheimer’s disease. *Neuropathology and Applied Neurobiology*, 45(4), pp.327–346.”

1.5 Synapses: the brains’ great communicators

Synapses are the sub-cellular structures that form a bridge of communication between neurons, and are present both in the central nervous system (CNS) as well as the peripheral nervous system (PNS) (Harris and Weinberg, 2012). They are highly dynamic structures that can be formed and eliminated rapidly to provide quick neuronal responses, which forms the basis of synaptic plasticity (Matsuzaki et al., 2001; Engert and Bonhoeffer, 1999). In turn, synaptic plasticity is critical for learning and retaining information, ranging from motor skills to memory, and beyond (Morris, Anderson, Lynch and Baudry, 1986; Morris, 1989; Dayan and Cohen, 2011). Changes in the voltage properties of a synapse constitute electrical signalling, and specifically, strengthening of a synaptic response after a stimulus constitutes long-term potentiation (LTP), whereas a diminished synaptic response is known as long-term depression (LTD) (Matsuzaki, Honkura, Ellis-Davies and Kasai, 2004). The electrical signals in the synapse are often coupled to a chemical exchange of neurotransmitters, or chemical messengers, from the pre-synapse to the post-synapse. Depending on location and morphology of the synapse, as well as the neurotransmitters exchanged, synapses can be distinguished into two broad categories: excitatory and inhibitory synapses (Penzes et al., 2011; Hensch and Fagiolini, 2005). Live imaging of synapses has elucidated the dynamic nature of these sub-structures, where newly formed dendritic spines can extend or retract when stimulated via learning or sensory experience (Fu, Yu, Lu and Zuo, 2012; Toni et al., 1999; Mostany et al., 2013). Competition between weaker and stronger synapses results in the maintenance of the stronger ones and the removal/elimination of weaker ones, a process known

of as synaptic refinement (Wiesel and Hubel, 1963; Mikuni et al., 2013; Torborg and Feller, 2005; Holtmaat and Svoboda, 2009). Synaptic refinement is a crucial process in development which ensures correct network formation and an appropriate balance of excitation and inhibition in the brain (Turrigiano and Nelson, 2004; Harauzov et al., 2010). Interestingly, such process are not only found in cortical neural networks, but are conserved across other systems, like the retino-thalamic tract (Hong and Chen, 2011) and PNS structures like the neuromuscular junction (Wang et al., 2014). In the case of the retino-thalamic tract, mono-ocular deprivation experiments in mice (known to reduce sensory information) result in greater spine elimination, while binocular deprivation also increases the size of existing spines, with neither forms of deprivation affecting synapse numbers (Zhou, Lai and Gan, 2017). This indicates that synaptic refinement and remodelling is a sensitive and dynamic process in the brain and is crucial to brain function.

Importantly, synaptic refinement and plasticity is also maintained after development, too (Peretti et al., 2015). In the adult mouse cortex, motor-skill learning results in enhanced experienced-dependent plasticity, as shown by live imaging, and changes in LTP facilitate modifications of dendritic spines (Xu et al., 2009). Furthermore, synaptic refinement also persists in the adult hippocampus, an area that is necessary for forming, consolidating, and retrieving memories (Pilz et al., 2016; Morris and Frey, 1997; Takeuchi, Duzskiewicz and Morris, 2014). Due to its high-demand performance, it is not surprising that, through recent advances in hippocampal imaging, spines in the CA1 region display a remarkably high turnover rate of 40% change in 4 days (Pfeiffer et al., 2018). Whether synapse refinement is a cell-autonomous process, non-cell-autonomous process, or a combination of the two is important in understanding synaptic connectivity and its effects in cognitive processes. Over the past 20 years there have been great scientific advances that spotlighted glial cells, in particular microglia and astrocytes, as primary

non-neuronal contributors to synaptic health and function, and have emerged as central players in many forms of neurodegeneration, like AD.

1.6 Risk factors for developing Alzheimer's disease

The classification of AD falls under two main categories: early-onset AD (EOAD) and late-onset AD (LOAD). EOAD is a rare, hereditary form of AD, where mutations can occur in the genes encoding for the amyloid precursor protein (APP) or the proteins involved in cleaving APP to form different forms of A β , known as presenilin proteins (Goate et al., 1991; Hardy and Allsop, 1991; Chartier-Harlin et al., 1991; Tanzi and Hyman, 1991; Wright, Goedert and Hastie, 1991). These mutations are autosomal dominant, and they were discovered in the late 80's and early 90's, revolutionising our understanding of AD aetiology. As the name suggests, individuals with EOAD have an early dementia onset, typically between 50-60 years old (Wragg, Hutton and Talbot, 1996). People with EOAD are afflicted with rapid cognitive decline, and they develop high levels of AD-related pathology, e.g. A β plaques, and tau tangles (Goate et al., 1991; Hardy and Selkoe, 2002). Nevertheless, EOAD accounts for only 1% of total AD cases, and the other 99% develop LOAD (Karch and Goate, 2015). Naturally, the age of onset in LOAD is later than EOAD, often from 65 onwards. Unlike EOAD, the causes for developing LOAD are less understood and at the moment, a mix of environmental, lifestyle, and genetic factors are all linked to developing LOAD (Goate et al., 1991; Silva et al., 2019; Roses, 1996; Karch and Goate, 2015). Having more years in education appears to be protective against cognitive decline late in life, whereas obesity and impairments in vascular health, including traumatic brain injury, contribute negatively to cognition (Profenno, Porsteinsson and Faraone, 2010; Kivipelto et al., 2005). In fact, cognitive reserve is a prominent hypothesis suggesting that more years in education enriches the brain with more synapses, and therefore provides resilience to cognitive decline when synapses are lost

during ageing (Scarmeas and Stern, 2003). Genome-wide association studies (GWAS) in the past decade have revealed a number of variants that predispose individuals to develop LOAD, with the apolipoprotein E (APOE) variant APOE4 being the greatest genetic risk factor. Many of these variants are highly expressed by glial cells in the brain, which has put them on the spotlight of current research (this will be discussed in detail later on).

1.7 Genetic risk factors and their association to pathologies of Alzheimer's disease

In both EOAD and LOAD, various conformations of A β and tau species, like fibrillar and oligomers, accumulate in the brain. A β deposits are primarily extracellular and although the study of plaques had dominated the AD field, it is now understood that oligomeric forms of A β are more harmful to neurons and synapses (Koffie, Hyman and Spires-Jones, 2011; Garcia-Marin et al., 2009; Baglietto-Vargas et al., 2010). A β oligomers induce LTP deficits in hippocampal neurons and increase LTD by interfering with glutamate uptake at the synapse (Li et al., 2009). In culture, neuronal dendritic spines are susceptible to degeneration in response to addition of human A β (Wu et al., 2010), suggesting that spine loss can occur cell-autonomously. In human post-mortem tissue, high-resolution array tomography has revealed that individuals with AD have reduced synapse densities compared to age-matched controls, and that more synapses are lost in the vicinity of A β plaques (Koffie et al., 2012). A β oligomers can be found bound to synapses, but it is unclear what the synaptic ligand for A β is, and how that induces synapse degeneration. Moreover, AD patients with an APOE4 genotype have greater synapse loss compared to ones with APOE3 (Koffie et al., 2012), which partially accounts for the E4 allele being a risk factor for AD. On the other hand, the tau protein (encoded by the *MAPT* gene) is a microtubule-stabilising protein normally found in neuronal axons, and it facilitates transport between the cell body and

the synapse (Kosik, Joachim and Selkoe, 1986). Array tomography images have shown tau localised on human synapses (Largo-Barrientos et al., 2021), which in the context of AD is regarded as exerting synaptotoxic effects. Mice with tau mutations can form toxic aggregates which result in synaptotoxicity (Kopeikina et al., 2013b; a; Tai et al., 2014) and indeed, tau and A β can work in tandem to induce synapse loss and cognitive impairments (Pickett et al., 2019). The APOE4 genotype is also associated to more tangles in the brain (Farfel et al., 2016) (Figure 2) and greater loss of interneurons in mice, as well as deficits in learning and memory (Andrews-Zwilling et al., 2010). The role of APOE and its association to neurodegeneration and neuroinflammation has been extensively reviewed during my PhD has the full manuscript can be found in the Appendix: “Invited Review: APOE at the interface of neurodegeneration, neuroinflammation, and pathological protein spread in Alzheimer’s disease”.

1.8 Lack of treatments for AD: paving new ways forward

Unfortunately, there are no effective treatments in slowing down AD progression, treating symptoms, reducing the mortality rate, or curing any aspects of the disease. Amongst other reasons, this is due to a lack of understanding the underlying causes of the disease, as well the a lack of tools to accurately study the CNS in the past. Importantly, the genetic variants in APP synthesis and its processing in EOAD has pushed clinical trials to focus on reducing the levels of A β in the brains of AD patients. Although these interventions have been promising in mice, none of the clinical trials have provided positive outcomes in humans, and in some cases have even increased mortality and cognitive decline (LaClair et al., 2013; Long and Holtzman, 2019; Gilman et al., 2005). In combination, the increasing prevalence of AD and the lack of therapeutic targets highlight the urgency for effective treatments. The recent GWAS evidence has prompted the field to focus more on non-neuronal cells in the brain, for example the microglia.

Microglia are highly complex and dynamic cells in the brain, and their strong association to AD pathology has made them an excellent candidate for further investigation, and a potential new therapeutic target.

2. Microglia: the brain's Swiss army knife

2.1 Introduction into microglia

Microglia are non-neuronal cells in the brain whose primary functions include immune responses and supporting CNS homeostasis (Prinz and Priller, 2014; Tay et al., 2017; Sierra et al., 2016). These functions are widely varied and include, but are not limited to: phagocytosis (Sierra, Abiega, Shahrzad and Neumann, 2013; Kim et al., 2017; Liu et al., 2013), immune surveillance (like pathogen recognition) (Laudisi et al., 2013; Husemann et al., 2002; Kigerl et al., 2014), detecting and producing cytokines (Zhao et al., 2019; Azevedo et al., 2013; Liddel et al., 2017), myelin sheath formation (Miron et al., 2013), and neural circuit formation (Figure 3) (Vainchtein et al., 2018; Schafer et al., 2012; Oosterhof et al., 2019). In many ways, microglia resemble peripheral macrophages (Ginhoux et al., 2013), which form part of the innate immune response in the body. It is characteristic for macrophages to differ morphologically and transcriptomically depending on their niche environment (Hume, 2015; Schultze, Freeman, Hume and Latz, 2015; Bennett et al., 2016), but also microglia differ in their origin compared to macrophages. While the majority of macrophage populations arise from the bone marrow and foetal liver, yolk sac progenitor cells enter the bloodstream and subsequently populate the brain parenchyma during early stages of embryogenesis (Alliot, Lecain, Grima and Pessac, 1991; Alliot, Godin and Pessac, 1999; Ginhoux et al., 2010). The blood-brain-barrier forms after yolk sac-derived macrophages populate the brain (Ginhoux et al., 2010), thus trapping these cells in the brain where they specialise into microglial cells. In contrast, circulating monocytes

cannot freely enter the brain under homeostasis, although this changes in diseases that involve BBB breakdown, like multiple sclerosis (Correale and Villa, 2007), stroke (McColl, Rothwell and Allan, 2008; Moss and Williams, 2020) or even AD (Montagne et al., 2015). A major challenge in the field has been distinguishing microglia from infiltrating macrophages that are morphologically indistinct but have different functions in the brain (Greenhalgh et al., 2018; Chiot et al., 2020). Even though there are still hurdles to overcome, RNA-sequencing approaches have uncovered a set of microglia-specific markers, like Tmem119, P2Y12, and Sall1 (Bennett et al., 2016; Li et al., 2019; Buttgerit et al., 2016).

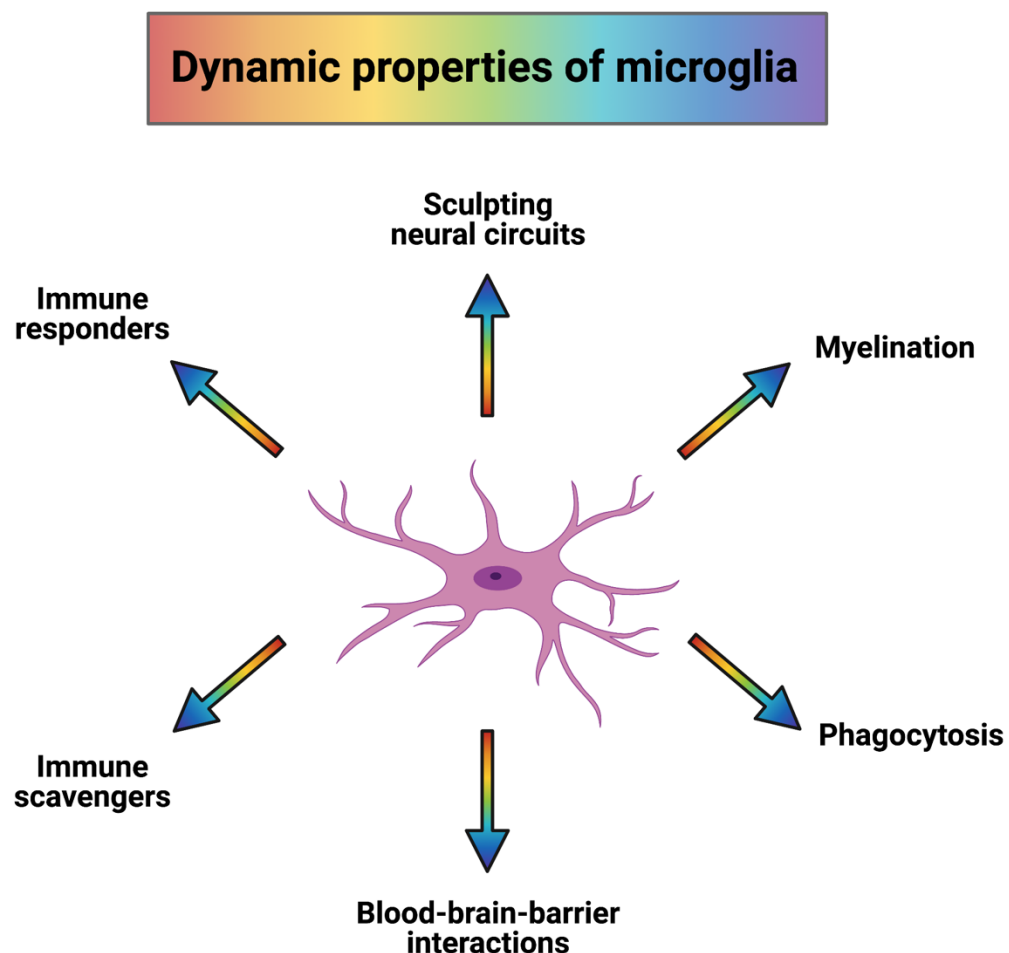


Figure 3. Microglial properties. Microglia have a wide range of functions in the brain and actively participate in achieving brain homeostasis. Microglia are the primary phagocytes of the brain and clear debris via phagocytosis, which

they also employ for sculpting neural circuits by removing weaker synapses. They detect changes in the brain and can regulate immune responses accordingly. They are involved in forming myelin sheaths to protect neuronal axons, and are involved in the remyelination process following myelin damage. They can even co-operate with astrocytes to ensure a tight blood-brain-barrier is achieved.

Microglia are not only dynamic in development, but throughout life. To do this, they are equipped with a plethora of receptors located on their branching protrusions and cell soma in order to sense their environment. These receptors range from scavenger receptors, like MSRA (El Khoury et al., 1998; Husemann et al., 2002), to phagocytosis-associated receptors, like CD11b (or CR3) (Hong et al., 2016), to innate immunity receptors, like toll-like receptor 4 (TLR4) (Kielian, 2006). This extensive assortment of receptors allows microglia to actively alter their morphology to adapt to their surroundings, by extending or retracting their processes, as well as becoming hypertrophic and "amoeboid-like" (Davalos et al., 2005; Nimmerjahn, Kirchhoff and Helmchen, 2005). Indeed, morphologic, functional, and transcriptomic changes are also seen in ageing, as well between different brain areas (Galatro et al., 2017; Tay et al., 2017; Grabert et al., 2016). The powerful phagocytic response by microglia has been studied in the context of clearing debris, but they are far more dynamic than that. One of the main microglial responses is their role in the formation of neural circuits by aiding synaptogenesis as well synapse removal.

2.2 The role of microglia in synaptic refinement

The incredible complexity of the brain requires synaptic connections to be dynamic in nature, and as such both cell autonomous and non-cell autonomous mechanisms have evolved to modify synaptic structures. Neurons possess intrinsic properties to undergo synaptic and spine elimination via apoptotic and necrotic signals localised at the synapse, both in response to refinement (Ertürk, Wang and Sheng, 2014) and degeneration (Wishart,

Parson and Gillingwater, 2006). However, the role of glial cells in the removal of weaker and aberrant synapses in health and disease has expanded our understanding of synaptic remodelling and its complexities (Eroglu and Barres, 2010; Chung et al., 2013; Schafer et al., 2012). In particular, microglia and astrocytes, another abundant glial cell, have been the main non-neuronal contributors to synaptic refinement, as well as aiding the formation of new synapses (Henstridge, Tzioras and Paolicelli, 2019). Growing evidence has implicated microglia as central players in neural circuit formation and learning by contact mediated removal of synapses (Parkhurst et al., 2013), known as synaptic pruning (Figure 4).

The loss of microglia in the human brain has conclusively shown their importance in normal brain function. Mutations in the *colony-stimulating factor 1 receptor (CSF1R)* gene are the cause of a rare type of early-onset dementia; adult-onset leukoencephalopathy with axonal spheroid and pigmented glia, in short ALSA (Konno et al., 2017). Perhaps the most striking example of the importance of microglia in the brain was shown by a recent case study, where congenital absence of microglia in an infant with a homozygous *CSF1R* mutation led to improper grey matter connectivity, seizures, and complete absence of a corpus callosum and cerebellum (Oosterhof et al., 2019). However, microgliopathies do not depend on a reduction of cell numbers, as mutations on microglial *NRROS* (negative regulator of reactive oxygen species) gene can also result in similar radiological findings and death (Smith et al., 2020).

At the start of the decade, the Gross lab visualised microglia engulfing synapses using two super-resolution techniques, electron microscopy (EM) and stimulated emission depletion (STED) microscopy, providing some of the first evidence that microglia are capable of taking up synapses during development (Paolicelli et al., 2011). Reducing microglia via lack of fractalkine signalling in CX3CR1 knock-out (KO) mice resulted in higher dendritic spine

numbers in the CA1 region of the hippocampus at postnatal days 13-16, which are crucial in development. Moreover, greater PSD-95 levels were found inside microglia in the CX3CR1 KO mice, suggesting that microglia phagocytose the excess synapses. Additionally, the KO mice displayed increased LTD and miniature excitatory post-synaptic potentials (mEPSPs), both being signs of poor connectivity and immature synapses (Hsia, Malenka and Nicoll, 1998). More recently, the same group refined the hypothesis that microglia phagocytose entire synapses. Using correlative light-electron microscopy (CLEM), they showed that although sometimes entire synapses are phagocytosed, often only smaller parts of the synapse are engulfed by microglia in a process known as trogocytosis, while other times microglia only contact synapses without undergoing phagocytosis (Weinhard et al., 2018). Indeed, appropriate elimination of synapses in development is crucial, as developmental disorders like autism have been linked to impaired synaptic refinement by microglia (Filipello et al., 2018).

Microglia prune synapses in development

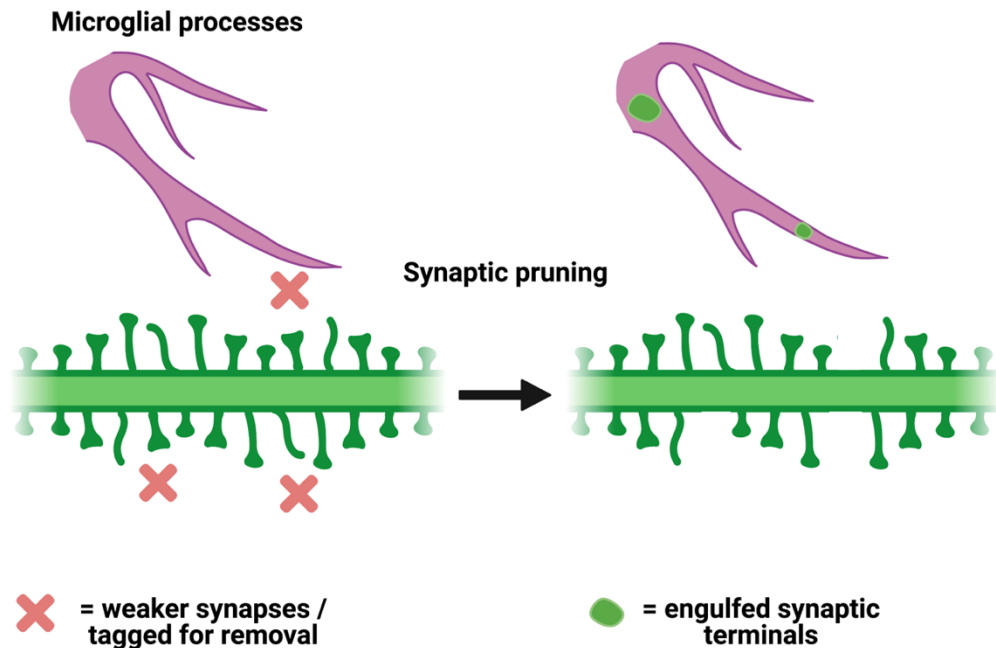


Figure 4. Microglial pruning of synapses. During development, synaptogenesis is a particularly dynamic process leading to an excess number of synapses. The less electrically active, or weaker, synapses are tagged with opsonin proteins, like complement proteins, which facilitate microglia to interact with them and remove them. These weaker synaptic puncta are engulfed by microglia, and later degraded, ensuring an appropriate number of synapses is maintained to allow efficient neural network communication.

2.3 Flattery will get you everywhere: the complement system and synapse pruning

Another widely-accepted theory for synaptic removal in the CNS is the use of the classical complement cascade (CCC). The CCC is a highly complex immunological system whose function is to tag cells and cellular sub-structures for removal by opsonising and attacking them (Michailidou et al., 2018;

Carpanini, Torvell and Morgan, 2019). The tagged substrate can vary from infectious pathogens, like bacteria, to cellular debris. To date, the retinothalamic system has been best studied in its relation to synaptic pruning via the CCC. Specifically, C1q is a molecule of the CCC that appears early in the cascade (Stephan et al., 2013) and is co-localised with the pre-synaptic marker SV2A in a multitude of CNS structures like the cortex, and parts of the retinothalamic system like the dorsal lateral geniculate nucleus (dLGN) and retinal ganglion cells (RGCs), early in development (P5-P8) (Stevens et al., 2007). Moreover, using array tomography, C1q was shown to co-localise less often with paired synaptic puncta (opposing SV2A and PSD-95) and more with individual synaptic puncta, suggesting C1q is present on the more immature synapses tagged for removal. In a separate study, microglia phagocytosed RGCs at the dLGN during this early postnatal stage of development (Schafer et al., 2012). Specifically, when the activity in the ipsilateral eye was blocked with tetrodotoxin, a Na⁺ channel blocker, microglia phagocytosed more RGCs in response to the greater number of weaker inputs. Contrarily, injection of forskolin, a K⁺ channel blocker, increased RGC activity creating stronger synaptic inputs and resulted in fewer RGCs being engulfed by microglia. In a different paradigm, using EM, microglia at the dLGN were shown to engulf synapses and that mice once deprived from light, when re-exposed experience a different microglial phenotype (Tremblay, Lowery and Majewska, 2010). Specifically, under live imaging, microglia contact synapses but upon light re-exposure they contact more synapses, form phagocytic pouches and phagocytose more synapses, demonstrating synaptic pruning is modulated in an experience-dependent manner.

2.4 Intrinsic and extrinsic properties of synapse pruning by microglia

Interestingly, both neurons and microglia have intrinsic signals that can regulate synaptic pruning. For instance, mice lacking progranulin (a protein implicated pathologically in frontotemporal dementia, or FTD) display disturbed homeostasis in microglia, upregulation of C1q synthesis and increased internalisation of synapses by microglia in the ventral thalamus (Lui et al., 2016), leading to OCD-like behaviours. Likewise, conditional knock-out of TDP-43 in microglia results in exacerbated levels of PSD-95 inside microglial lysosomal compartments and greater synapse loss, although microglia also became better at clearing A β (Paolicelli et al., 2017). This shows that phagocytosis is not unilaterally beneficial or detrimental, but rather, it is a nuanced process that can result in both positive and negative outcomes. On the other hand, neurons express the endogenous complement inhibitor SRPX2 which is secreted and binds C1q to prevent complement activation (Sia, Clem and Huganir, 2013). During development, mice lacking SRPX2 show increased microglial and complement activation, combined with enhanced synapse loss in the dLGN and upregulated engulfment of synapses (Cong et al., 2020). Similarly, most mammalian cells express the cell surface marker CD47, which acts as a “don’t eat me signal” against the immune system (Elward and Gasque, 2003). Microglia recognise CD47 through the SIRP1 α receptor, and subsequently, loss of either CD47 or SIRP1 α in mice during postnatal development leads to enhanced phagocytosis of dLGN synapse by microglia (Lehrman et al., 2018). Another signal localised at the cell membrane of the synapse is phosphatidylserine, which was believed to indicate apoptotic cells once flipped and exposed extracellularly (Segawa and Nagata, 2015), in order to recruit phagocytes for removal (Park et al., 2007). Now, it is becoming evident that non-apoptotic cells can also expose phosphatidylserine (Segawa, Suzuki and Nagata, 2011; Brelstaff et al., 2018; Smrz, Dráberová and Dráber, 2007), and that C1q can bind to the extracellular component of phosphatidylserine (Païdassi et al., 2008). In the context of synaptic pruning,

it was recently shown that synapses of viable hippocampal neurons flip phosphatidylserine in a tightly-regulated window of development, and that microglia phagocytose these flipped phosphatidylserine-decorated synapses in a C1q-dependent manner (Scott-Hewitt et al., 2020).

2.5 The purinergic system in microglial-mediated synapse pruning

The purinergic system is also involved in microglia and synaptic refinement. Firstly, microglia use the P2 purinergic receptors to quickly respond to extracellular adenosine tri-phosphate (ATP) as a result of focal injury (Davalos et al., 2005), which would signal cell death and require microglia to clear the debris. Similarly, microglia are also capable of synthesizing and releasing purines, like ATP (George et al., 2015). In hippocampal slice cultures containing mossy fibre neurons of the dentate gyrus, activation of microglia with lipopolysaccharide (LPS) reduced synaptic plasticity via the release of ATP, whereby either blocking microglial release of ATP or the neuronal purinergic receptor P2X4 prevented impairments in synaptic transmission (George, Cunha, Mülle and Amédée, 2016). This is another example of how microglia can modulate synaptic transmission and plasticity without contacting neurons. On the other hand, mono-ocular deprivation in mice increases the number of microglial processes contacting synapses, as well as, synaptic inclusions in microglia shown by EM (Sipe et al., 2016). This process depends on P2Y12 signalling, a crucial purinergic receptor of homeostatic microglia (Krasemann et al., 2017).

2.6 Epigenetic regulation of microglial-mediated synaptic pruning

Synaptic engulfment by microglia under homeostatic conditions varies between brain areas, and can be epigenetically regulated under the polycomb repressive complex 2 (PRC2) (Ayata et al., 2018). Cerebellar microglia express higher levels of the phagocytosis marker CD68 and engage in greater

phagocytosis of apoptotic neurons than striatal microglia. RNA-sequencing and Western blot validation of cerebellar microglia also revealed enhanced expression of phagocytosis and clearance markers, like AXL, APOE, and MHCII. Epigenetic modification of histone H3 lysine 27 trimethylation (H3K27me3) under PRC2 was suggested to account for the differences in synaptic clearance by microglia between brain areas, whereby PRC2 was predicted to silence clearance associated genes. Knocking-out the *Eed* gene, a key component of PRC2, led to loss of H3K27me3 and upregulation of clearance-associated genes in striatal microglia. In turn, this resulted in exacerbated spine loss, enlarged CD68 pouches in microglia, and poorer performance in cognitive tasks, like the open-arm maze. Taken together, these data suggest that the enhanced clearance phenotype in microglia in response to epigenetic cues contributes to synaptic refinement during development and tightly regulate this process depending on the brain area.

2.7 Astrocytic contribution to synaptic pruning

Overall, synaptic pruning during development is currently hypothesised to occur when glial cells detect electrically weaker, or less active, synapses that have become redundant. However, it is worth noting that microglia are not the sole contributors to glial mediated synapse elimination. Astrocytes are glial cells which arise from neural precursors stem cells (radial glial cells) and become one of the most populous cell types of the CNS (Qian et al., 2000). They extend a complex network of long processes, and a single astrocyte in the human brain can in fact contact up to 2 million synapses at once (Oberheim, Wang, Goldman and Nedergaard, 2006). Astrocytes are heterogeneous cells in the human brain, varying in morphology, such as bushy or fibrous (mostly in white matter), and expression of various markers, such as GFAP (Allen and Eroglu, 2017). Although there is some overlap in terms of function between microglia and astrocytes, they are not the same cell types and have distinct roles in the brain. For example, astrocytes are far better

equipped as coupling with the vasculature of the brain and forming the blood-brain-barrier using their astrocytic end-feet, and express proteins like aquaporin 4 to facilitate this (Hubbard, Hsu, Seldin and Binder, 2015).

It is now appreciated that astrocytes are important in secreting neurotrophic factors to stimulate synaptogenesis (Eroglu and Barres, 2010), and they play a very important role in synapse health (Chung et al., 2016; Zhang et al., 2003). Relevant to synapse formation and elimination, astrocytes are capable of engulfment and phagocytosis but at much slower rates than microglia (Byun and Chung, 2018). This means that astrocytes may be involved in facilitating synaptic ingestion at different developmental time points to microglia, in separate brain areas or responding to distinct pathways in recognising synapses for elimination. However, these questions are still being answered and there no definitive answers at the moment.

Interestingly, astrocytes can modulate microglial-mediated synapse phagocytosis by releasing soluble factors like IL-33, C1q, TNF- α , and IL-1 α (Figure 5) (Vainchtein et al., 2018; Liddelow et al., 2017). Furthermore, active phagocytosis of synapses in the mouse hippocampus has been recently shown to be critical for homeostatic control of these circuits (Lee et al., 2021). Therefore, even though microglia are the primary phagocytes of the brain, astrocytes too play an important role in maintaining synapse health.

Glial cells prune synapses in development

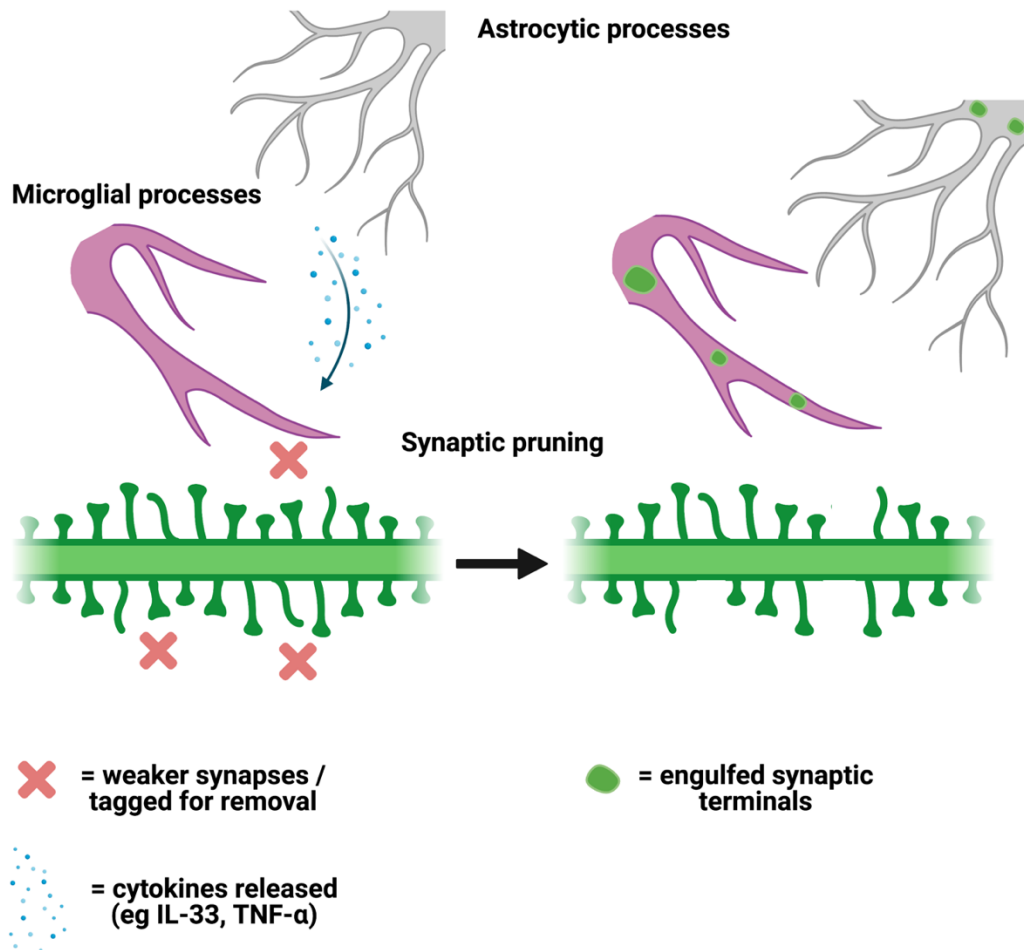


Figure 5. Astrocytes contribute to synaptic pruning directly and indirectly. Astrocytes can prune synapses in the developing mouse brain for appropriate neural network function by actively engulfing synapses. They are also powerful immune responders, and can secrete cytokines, like IL-33 and TNF- α , which modulate microglial pruning of synapses, therefore indirectly influencing synaptic pruning.

3. Microglia in AD pathogenesis

The hypothesis that microglia are involved as mediators in Alzheimer's disease is not a new concept. Over 30 years ago, Paul and Edith McGeer had already started investigating the presence of these macrophage-like cells in diseased brains and linking them to AD pathogenesis due to their close proximity and reactive appearance near A β plaques (Figure 6) (McGeer and McGeer, 1998; Itagaki et al., 1989). Morphologic changes like reduced arborisation of microglia and hypertrophy (Davies, Ma, Jegathees and Goldsbury, 2017) have primed researchers to think that functional changes occur in these cells too. The extent to which these changes are driving AD pathology or are merely a response to it, has been a great debate in the field, and is still actively researched. At the time, the tools to study these cells were scarce and the field lacked basic understanding of glial biology, so research into their roles in neurodegeneration became more prominent over 20 years later.

3.1 Genetics implicate microglia in AD

Many AD risk genes identified by GWAS are expressed by microglia. Accumulating evidence from RNA sequencing studies show that microglia form different expression clusters in AD brains compared to controls, which are associated with pathology. For instance, GWAS revealed mutations on triggering receptor expressed on myeloid cells 2, or TREM2, which is primarily expressed by macrophages and microglia, as a risk-factor for developing AD (Guerreiro et al., 2013; Jonsson et al., 2013). Since then, TREM2 has been strongly implicated in neurodegeneration, showing it is an important receptor for interacting with apoptotic cells, A β species, and regulation the transcription of *APOE* in microglia, as well as microglial pruning of synapses (Krasemann et al., 2017; Kim et al., 2017; McQuade et al., 2020; Filipello et al., 2018). RNA sequencing studies have deduced that microglia change their transcriptome in response to A β pathology and are referred to as "disease-associated

microglia” (Keren-Shaul et al., 2017), complementing the known morphologic changes that happen near these plaques. These changes involve multiple pathways, including upregulation of phagocytosis, something that is reflected in more recent single-cell RNA sequencing of human AD samples (Mathys et al., 2019; Olah et al., 2020; Kunkle et al., 2019). On one hand, upregulation of phagocytosis pathways is beneficial for clearing toxic A β species from the brain, however it can be detrimental to healthy tissue if this process is not tightly regulated. It is likely that this balance is tipped during Alzheimer’s disease, favouring excessive synapse loss.

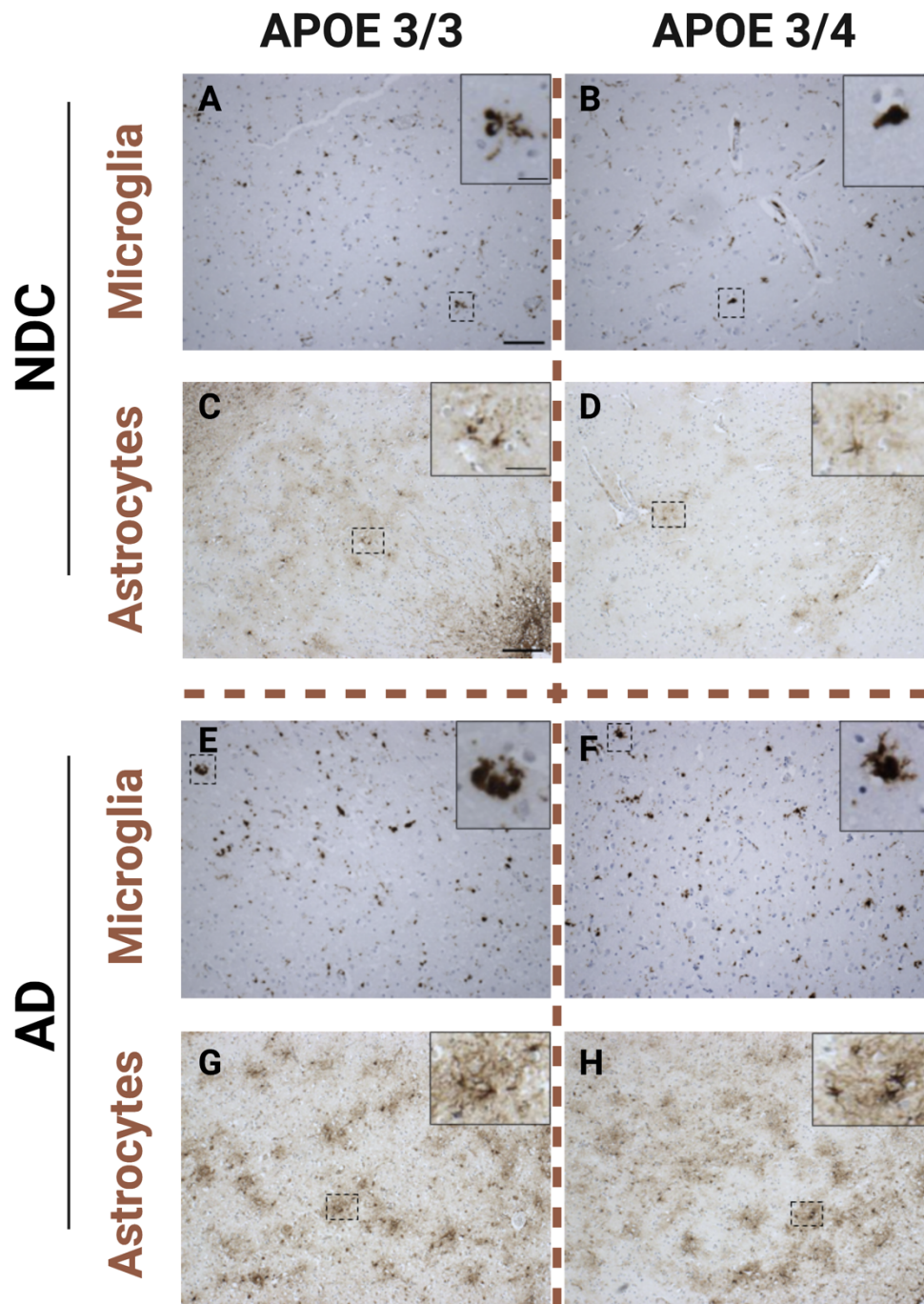


Figure 6. Microglia and astrocytes in ageing and Alzheimer’s disease.

The figure displays representative images of human post-mortem tissue showing microglia (labelled with CD68) and astrocytes (labelled with GFAP). Tissue was stained with 3,3'-Diaminobenzidine (DAB) and counterstained with haematoxylin to label nuclei. The microglial lysosomal marker CD68 is expressed in both non-demented control (NDC) brains (A-B), as well as brains with Alzheimer’s disease (E-F). There is a greater coverage of CD68 in AD brains, indicating an upregulation of lysosomal and phagocytosis pathways. Similarly, GFAP-positive astrocytes are also more prevalent in AD brains (G-

H), compared to NDC brains (C-D). Also, AD astrocytes are more pigmented, suggesting an upregulation of GFAP within cells. The APOE4 genotype is also associated with exacerbated gliosis in AD, compared to APOE3 carrying individuals. Scale bar in A, 100µm; scale bar in A insert, 25µm; scale bar in C 200µm; scale bar in C insert, 100µm. Figure adapted from “Tzioras, M. et al., 2019. Invited Review: APOE at the interface of inflammation, neurodegeneration and pathological protein spread in Alzheimer’s disease. *Neuropathology and Applied Neurobiology*, 45(4), pp.327–346.”

4. Microglial contribution to synapse loss

The role of microglia in synaptic pruning during development has been extensively studied, highlighting systems like the classical complement cascade, purinergic signalling, and fractalkine signalling which are selected to remove weaker synapses and shape neural circuits. Microglial activation (measured by TSPO ligand binding) occurs prior to disease onset in AD (Long and Holtzman, 2019; Boche, Gerhard, Rodriguez-Vieitez and MINC Faculty, 2019; Parhizkar et al., 2019), and concomitantly with synapse loss, which suggests that microglia may interact with synapses in a pathological manner in asymptomatic individuals. Indeed, there is accumulating evidence from mouse models of AD to suggest microglia aberrantly engage in phagocytosis of both healthy and dysfunctional synapses. At the moment, mice expressing different forms of the AD-associated pathological proteins Aβ and tau (either genetically or injected) have constituted the basis of this hypothesis, supplemented by, so far, indirect human evidence (Figure 7).

4.1 Microglia eliminate synapses in animal models of amyloidopathy

Similar to development, the CCC has been strongly implicated in microglial-driven synaptic loss and dysfunction during ageing and AD. Primarily, the levels of C1q drastically increase in the ageing mouse and human brain (Stephan et al., 2013). Regardless of disease, ageing mice display neuron and synapse loss in the hippocampus, and cognitive impairments such as memory

deficits in the Morris water maze (Shi et al., 2015). Interestingly, though, C3 knock-out mice do not display such synapse and neuron loss, they perform better at the aforementioned cognitive task, and they display enhanced LTP. Furthermore, in two amyloidopathy mouse models (Tg2576 and APP/PS1) lacking C1q, there was decreased microgliosis surrounding A β plaques and a rescue of synaptophysin loss in the hippocampus, even though the levels of A β were unchanged in C1q deficient mice (Fonseca, Zhou, Botto and Tenner, 2004). This suggests that complement can act as a synaptic tag and can operate in combination to microglia to induce synapse loss. So far, the evidence that microglia phagocytose synapses via the CCC is indirect.

The first evidence that microglia eliminate synapses in AD came from the Stevens lab in 2016 using the J20 and APP/PS1 amyloidosis models, and injection of oligomeric A β in WT mice (Hong et al., 2016). The J20 mouse model develops early synapse loss, cognitive impairments, and LTP deficits (3-4 months) prior to plaque deposition at 5-7 months. Using structural illumination microscopy (SIM), C1q depositions were found at the synapse during this early period of synapse loss, independent to plaques, and they were upregulated in multiple brain areas of the J20 mice, with the hippocampus and frontal cortex showing marked increase. Similarly, oligomeric A β in tail-vein injections to WT mice also upregulated C1q at the synapse, induced synapse loss, and increased the expression of CD68 in microglia, indicating a more phagocytic phenotype. Co-administration of a C1q blocking antibody partially protected against synaptic loss and rescued LTP deficits caused by oligomeric A β . In a separate AD model, the APP/PS1, C3 colocalised more with PSD-95, and APP/PS1 mice lacking C3 did not show marked synapse loss in the dentate gyrus and CA1 of the hippocampus, unlike their APP/PS1 counterparts. Importantly, mice injected with oligomeric A β showed high levels of synapse (post-synaptic Homer 3) engulfment by microglia and increased synapse loss, although both of these deficits were ameliorated in mice lacking the receptor for C3 (CR3). Altogether, these data

suggest that the complement system plays an important role in synaptic loss during neurodegeneration, and that microglia can recognise complement tags on synapses to remove them. It is worth noting that although blockade of C1q improves LTP and prevents synapse loss, the levels do not reach that of the WT mouse, suggesting that microglia are not solely responsible for synapse elimination and plasticity, and other mechanisms are involved in these processes.

In addition to Hong et al (2016), the Lemere group also explored the interference of complement C3 in microglial-mediated synapse loss in the APP/PS1 mice (Shi et al., 2017a). Sixteen-month old mice with the APP/PS1 transgenes had impaired cognitive performance, shown by a poorer outcomes at the water T-maze while the APP/PS1 mice crossed with C3 knock-out mice performed at the level of the control group. Although the APP/PS1;C3-KO mice developed a greater plaque burden, they had fewer microglia and astrocytes associated with plaques than the APP/PS1 mice, and had more neurons present in the hippocampus. Interestingly, in a separate amyloidopathy model, the PS2APP, there was reduced synapse loss near A β plaques when crossed to the C3-KO mice, suggesting that although C3 may act upstream of plaque formation, it is also important in synapse signalling. Furthermore, ELISAs of brain homogenates showed that compared to APP/PS1 mice, the APP/PS1;C3-KO mice had lower levels of pro-inflammatory cytokines like TNF- α and INF- γ , and higher levels of anti-inflammatory cytokines, like IL-10 (Shi et al., 2017a). Apart from the expected reduction of synapses in the APP/PS1 brains, mice lacking C3 (without the APP/PS1 transgenes) had a greater number of synaptic pairs (GluR1 + VGlut2) and Western blot analysis showed there was an increase in plasticity-related proteins, like TrkB, mBDNF, CREB, and pCREB. These results are complementary to the hypothesis that microglia induce synapse elimination in AD via the CCC by showing how C3 affects synaptic plasticity, glial kinetics near plaques, and how these together are involved in cognitive function.

The APP/PS1 and oligomeric A β paradigms have been used again in the context of microglial engulfment of excitatory synapses by Bie et al. (2019). Firstly, oligomeric A β induces cognitive impairments in mice, indicated by mice spending more time in each quadrant during the Morris water maze, and additionally, CD68 expression per Iba1 cell was also increased (Bie, Wu, Foss and Naguib, 2019). Furthermore, they have shown that there were higher levels of PSD-95 and synaptophysin inside the CD68 lysosomal compartment in Iba1+ cells in these two models of amyloidopathy. Short inhibitory RNA against C1q (siC1q) normalises cognitive performance in the A β injected mice, and reduces synaptic engulfment by microglia, similar to what has been previously shown. Interestingly, blocking excitatory activity at the synapse via the mGluR1 inhibitor JNJ16259685, also improved the cognitive performance of oligomeric A β injected mice and markedly reduced synaptic puncta inside microglia. The same was validated in APP/PS1 mice crossed with mGluR1 knock-out mice (Grm1 $^{-/-}$), suggesting that excitatory activity at the synapse may work in tandem with complement components, like C1q, for tagging synapses for degradation. Although in development it appears that weaker synapses are specifically eliminated by microglia, it is possible that during neurodegeneration a different electrophysiological signature at the synapse induces this altered form of synaptic pruning.

The use of non-human primates has offered a translation leap into the research of microglial-mediated synapse loss. Oligomeric A β injections into the dorsolateral prefrontal cortex of rhesus monkeys have successfully recapitulated previous findings in rodent animal models of AD (Beckman et al., 2019). Indeed, there was a significant reduction in spine density, although the spine head diameter was increased, potentially as a compensatory mechanism. Microglia in the rhesus monkey engulfed more PSD-95 puncta in response to oligomeric A β injections, but not scrambled A β injections. Interestingly, oligomeric A β also induced a spike in TNF- α in the CSF 30 days

after injection, suggesting neuroinflammation is a result of the accumulation of A β species in the brain.

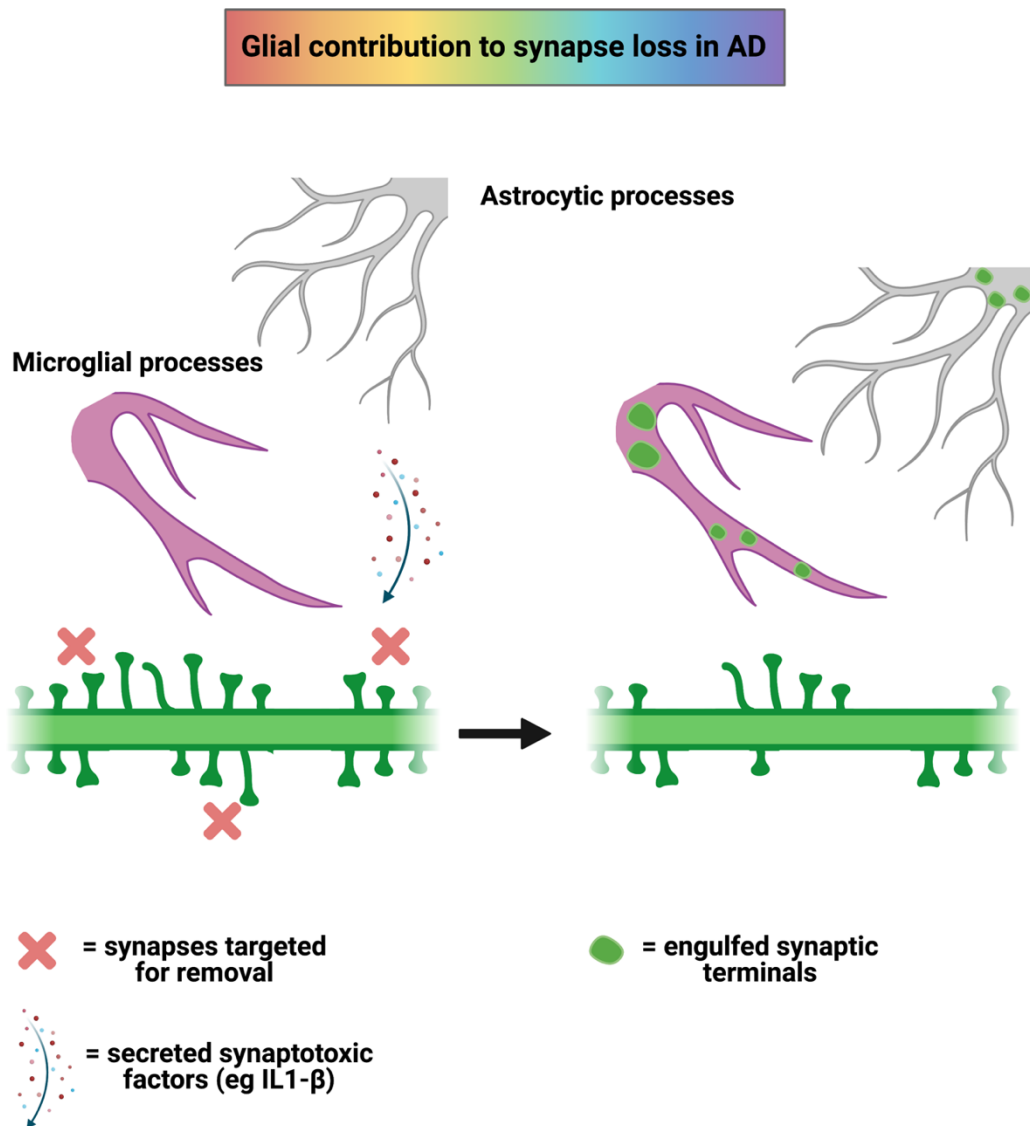


Figure 7. Glial contribution to synapse loss in AD. During development, synaptogenesis is a particularly dynamic process leading to an excess number of synapses. The less electrically active, or weaker, synapses are tagged with opsonin proteins, like the complement cascade proteins and MFG-E8, which facilitate microglia to recognise them as signals for removal.

4.2 Microglial contribution to synapse loss in mouse models of tauopathy

Nevertheless, amyloid is not the only pathological protein aggregate in the AD pathogenesis, with phosphorylated tau being a known glial activator inducing synaptotoxicity (Shi et al., 2017b; Streit, Braak, Xue and Bechmann, 2009). A widely used mouse model of tauopathy is the P301S line, expressing a MAPT transgene associated with FTD, and these mice develop synapse loss and glial activation prior to phosphorylated tau tangles at 6 months old (Yoshiyama et al., 2007). Dorsal root ganglion (DRG) neurons isolated in culture from P301S 5mo mice were phagocytosed by microglia in a non-complement mediated way (Brelstaff et al., 2018). Non-apoptotic neurons (shown by expressing calcineurin but not expressing caspase-3 and propidium iodide) can contain phosphorylated clumps of tau, which induces aberrant exposure of phosphatidylserine outside the cell membrane. In turn, microglia release factors like nitric oxide and milk-fat globule 8 EGF-factor-8 (MFG-E8) which bind extracellular phosphatidylserine on neurons and mediate phagocytosis of whole, living, neurons by microglia. However, the data presented here pertain to exposed phosphatidylserine in the neuronal cell body, and not specifically at the synapse, as well as to DRG neurons which are not primarily affected in AD.

More recently, P301S mice have been used as a tauopathy model to demonstrate specific synaptic alterations, as well as implicating microglia in eliminating synapses via the CCC (Dejanovic et al., 2018). Specifically, magnetic resonance imaging (MRI) of whole mouse brains showed no changes in brain volume until 12 months, but tau aggregation at the synapse and gliosis were observed at 9 months. Mass spectrometry and immunoblotting revealed multiple GTPases being downregulated in hippocampal synaptic fractions of P301S mice, which is likely contributing to synaptic dysfunction and PSD collapse. Synapses in the transgenic mice were

also richer in C1q, validated by STED, immunoblots and EM. Immunoblots of the superior temporal gyrus in humans with AD also confirmed increased levels of C1q, both in total lysates and specifically in isolated PSD fractions. Moreover, C3 was also increased in the human AD brains compared to age-matched controls, and both C1q and C3 significantly correlate to phosphorylated-tau. Similar to the amyloidopathy models of AD, microglia contained more synaptic proteins inside them in the P301S mice, shown by high-resolution confocal images of synapsin and PSD-95 inside CD68 positive cells. Blockade of C1q with an anti-C1q antibody reduced the levels of C1q in the mouse brain, partially rescued the synaptic loss observed in the P301S mice, and decreased the levels of synaptic proteins inside microglia. Furthermore, P301S mice crossed to C3-knockout mice displayed reduced levels of synapsin inside CD68-positive microglia (Wu et al., 2019), similar to C1q blockade, and resembling the results by Hong et al (2016) and Shi et al (2017) in the amyloidopathy mouse models.

The rTg4510, containing the P301L mutation on the MAPT gene, is another model of tauopathy widely used in neurodegeneration, with the difference that tau expression is inducible. At 6 months, rTg4510 mice display a thinner CA1 cell layers of the hippocampus than same-age WT mice, as well as increased caspase-3 expression and phosphatidylserine exposure, indicating apoptosis (Benetatos et al., 2020). Like the P301S mice, rTg4510 mice show age-dependent C1q increase, concomitantly with a reduction in PSD-95 puncta and increased C1q+PSD-95 colocalisation. This is accompanied by higher levels of Iba1 and CD68 in the transgenic mice, and increased engulfment of PSD-95 by CD68-positive microglia. In this study, unlike the previous work on tauopathy, microglia are suggested to engulf synapses by PTEN activation rather than complement activation and deposition at the synapse. PTEN is an important protein for synaptic plasticity during brain development (Kwon et al., 2006), but its relevance to synapse loss and degeneration in AD is less understood. In this study, they found higher levels of the catalytically active

(dephosphorylated) form of PTEN in hippocampal synaptosomes of 4 and 6 month-old rTg4510 mice compared to control ones, which precedes the spike in caspase-3 activation. In subsequent experiments, inhibition of PTEN dephosphorylation with bisperoxovanadium (bpV), and therefore decreasing the levels of active PTEN, rescues synaptic and neuronal loss in the transgenic mice and also reduces the engulfment of synaptic proteins by microglia in the CA1 of the hippocampus. However, in human AD and FTD brains, the levels of activated PTEN negatively correlates with age, while there is a positive correlation in the control group. This is somewhat contradictory to the findings in the transgenic line, and highlights the importance of understanding the translational barriers between mouse and human research.

4.3 Non-contact dependent synapse loss by microglia in AD

Increased levels of complement proteins can act as an opsonin on synapses for elimination, and although this appears to be precisely tuned during development, it is possible that neuroinflammation during AD can amplify the number of synapses tagged for elimination in an aberrant way. The release of inflammatory cytokines by microglia in relation to synapse loss is a less explored, but an equally interesting, field of research.

Firstly, administration of A β species in mice is linked to microgliosis, and release of pro-inflammatory cytokines and enhanced complement production by microglia. For instance, addition of A β to isolated complement C3 fractions led to activation of the CCC, yielding higher levels of the membrane attack complex C5a-9, which is toxic to neural precursor cells (Bradt, Kolb and Cooper, 1998). In culture, A β stimulated microglia to produce high levels of pro-inflammatory cytokines, including TNF- α , and nitric oxide synthase (NOS) which were neurotoxic (Combs, Karlo, Kao and Landreth, 2001). Furthermore, peripherally injected fibrillar A β (A25T) induced microgliosis and

neuroinflammation *in-vivo*, by boosting the production of TNF- α and interleukin 6 (IL6) (Azevedo et al., 2013). This boost in pro-inflammatory markers was also accompanied by synapse loss, measured by immunostaining of synaptophysin and PSD-95, and cognitive decline, shown by short-term memory impairment in the novel object recognition task. Interestingly, treatment with minocycline, an antibiotic which kills microglia, rescued mice from this cognitive deficit, indicating that microglial-mediated neuroinflammation is synaptotoxic, and consequently detrimental to cognition.

Moreover, transgenic mice containing 3 familial AD mutations on A β production and processing (3xTg-AD), were afflicted with increased TNF- α expression both in neurons, leading to increased cell death in a cell-autonomous manner (Janelsins et al., 2008), and increased TNF- α release by microglia, leading to non-cell autonomous neurotoxicity in the entorhinal cortex (Janelsins et al., 2005). Other inflammatory markers are also key players in neuroinflammation and neurotoxicity. For example, murine interferon-gamma (mIFN- γ) was transgenically expressed in mouse brains of the amyloidosis model of AD, the TgCRND8 mice (Chakrabarty et al., 2010). This increase in mIFN- γ was associated to increased microgliosis, TNF- α secretion by microglia, and complement C1q and C3 deposition in the brain, while surprisingly, reduced A β pathology was also observed. This highlights the importance of a balance between pro- and anti-inflammatory cytokines in the brain in order to control toxicity and also prevent plaque formation.

Injection of LPS in mouse brains has also provided indirect evidence of microglial-mediated synapse loss in response to neuroinflammation. LPS-injected mice displayed considerable microgliosis and astrogliosis, as well as marked increase in neuroinflammatory markers like TNF- α , IL-6 and IL-1 β (Zhu et al., 2012). Apart from neuroinflammation, these mice also had reduced levels of pre- and post-synaptic proteins levels, including synaptophysin, drebrin and PSD-95. Of note, neuroinflammation, microgliosis, and synapse

loss were all higher in mice expressing human APOE4, compared to mice expressing APOE2 and APOE3. This is in agreement with data from individuals with APOE4 genotypes who have more severe AD-associated pathology (Tzioras et al., 2019). On the other hand, peripheral injection of LPS in mice decreased brain and serum levels of the anti-inflammatory cytokines IL-4 and IL-10, and similar to brain injections of LPS, also induced higher levels of TNF- α , IL-1 β , nitric oxide, and prostaglandin E2 (PGE2) (Zhao et al., 2019). In relation to microglial involvement in neuroinflammation-induced synapse loss, it was shown that LPS injected mice had impaired performance in the Morris water maze and displayed problems in learning and memory retention, all of which are associated with synapse loss.

It is not clear which type of synapses are more vulnerable during neuroinflammation. In organotypic hippocampal slice cultures, pre-synaptic terminals are more vulnerable to degeneration in response to LPS than post-synapses, in a microglial-driven IL-1 β pathway (Sheppard, Coleman and Durrant, 2019; Tai et al., 2014; Di Filippo et al., 2013). Lastly, vascular breakdown and BBB leakage is a common feature in AD, allowing blood factors like fibrinogen to enter the brain. Indeed, fibrinogen levels are negligible in the brain of a WT mouse, but are increased in the APP/PS1 mice (Merlini et al., 2019). Live-imaging of dendritic spines showed synaptic vulnerability and degeneration near fibrinogen deposits, similar to A β plaques. Although it is not clear if this spine loss is cell-autonomous, fibrinogen can induce spine loss in a non-cell autonomous way via microglia. Fibrinogen binds to the CD11b receptor on microglia, which induces the production of nitric oxide species in the vicinity of these fibrinogen deposits near the dendrites, therefore killing spines in a non-contact mediated pathway.

4.4 Microglial contribution to synapse loss in humans

Although there is accumulating evidence showing microglia are key players in synapse elimination in various AD mouse models via multiple pathways, there is very little direct evidence to support that this is relevant in human brains. In the context of human AD, there are no quantitative studies that have assessed microglial engulfment of synapses, but there is some evidence to suggest that data from mouse models are physiologically relevant to humans as well. Super-resolution EM images from AD human post-mortem tissue have revealed synaptic vesicles inside microglial cells, indicating that microglia are likely engulfing or phagocytosing synapses in the human brain (El Hajj et al., 2019). Likewise, there is some limited evidence to suggest astrocytes are phagocytosing pre-synaptic terminals in AD, possibly clearing dystrophic neurites (Gomez-Arboledas et al., 2018). Multiple studies have shown complement protein levels increase in human AD brains compared to age-matched non-neurological controls (Wu et al., 2019; Dejanovic et al., 2018; McGeer, Akiyama, Itagaki and McGeer, 1989), which is a promising pathway by which microglia can recognise and uptake synapses, similar to mice. We have recently shown with unbiased proteomics and mass spectrometry that isolated synaptoneurosomes from AD patient brains are enriched for complement proteins, like C1q and C4 subunits (Hesse et al., 2019). It should be noted that IPA analysis of the phagocytosis pathway in our samples has revealed other interesting proteins involved in microglial-mediated neuron and synapse elimination, like MFG-E8 and CD33. These results are promising because they suggest that such proteins opsonise synapses for phagocytosis, with microglia being a prominent candidate to phagocytose the opsonised structures.

Overall, it is clear that a balance is needed between “eat-me” and “don’t eat-me” for the healthy elimination of synapses, which is tipped in disease. For example, complement tags or MFG-E8 opsonisation of the synapse in a

disease setting is vital for flagging degenerating synapses that need to be cleared away, but if healthy synapses are wrongly tagged in the vicinity (for example, near A β plaques) then a cascade of aberrant synapse loss would ensue.

5. Schizophrenia

Schizophrenia is a neuropsychiatric disorder where just like in AD, reduced synapse burdens are also present. However, schizophrenia has an average age of onset in the mid to late 20's, unlike AD which affects the elderly (Kahn et al., 2015; Gogtay et al., 2011). In addition, AD is progressive in terms of cognitive decline and pathology, whereas schizophrenia is not considered a progressive disorder. Individuals with schizophrenia experience affective symptoms, including hallucinations, delusions, severe mood imbalances, and other comorbid symptoms like psychosis and depression (Kahn et al., 2015). Both genetic mutations and environmental triggers can act as risk factors for developing schizophrenia; for example, less than 1% of the population develops schizophrenia, while monozygotic twins have a 40% chance of both developing the disease (Cardno et al., 1999), suggesting strong genetic links. Neuroimaging studies have shown reduced frontal lobe volume in individuals with schizophrenia (Kikinis et al., 2010; Wible et al., 2001) and poorer white matter connectivity associated with the frontal lobe (Klauser et al., 2017). The frontal lobe is associated to personality and behaviour, explaining the affective and psychiatric symptoms of the disease. Importantly, synapse loss and microglial activation are also present in the frontal lobe of patients with schizophrenia, but the aetiology and underlying pathologies are distinct to AD. Therefore, schizophrenia provides a good foil to AD for comparing the microglial involvement to synaptic ingestion (Figure 8).

5.1 Synaptic changes in schizophrenia brains

Firstly, it is still unclear whether schizophrenia brains with reduced synaptic levels have suffered synapse loss, or if synapses never formed properly. Whilst synapse loss in AD is consistently reported and is a widely accepted feature of the disease, there is mixed evidence regarding reduced synaptic levels in schizophrenia (Osimo, Beck, Reis Marques and Howes, 2019). At the moment, the two main discrepancies regarding this depend on the synaptic marker used and the brain area examined. For instance, the levels of the presynaptic marker SV2A, measured by positron emission tomography (PET), were shown to be reduced in the frontal lobe and anterior cingulate cortex of individuals with schizophrenia compared to healthy controls, but not in the hippocampus (Onwordi et al., 2020). Others have shown reduction in the pre-synaptic marker synapsin I, but not synaptophysin, in schizophrenia brains (Browning et al., 1993), while the post-synaptic marker PSD-95 is also decreased in the frontal lobe of patients with schizophrenia (Funk et al., 2017). These examples demonstrate the variability that exists in terms of reporting synaptic changes in the schizophrenia literature, but also beg the question on what mechanisms are involved in this synaptic reduction. Unlike AD, schizophrenia is not characterised by the accumulation of toxic protein aggregates that are synaptotoxic, so the mechanisms of altered synaptic connections are likely different. Given that microglia are actively pruning synapses in the developing brain, it is possible that they are also contributing to some synapse loss in brains with schizophrenia.

5.2 Microglial alterations in schizophrenia

Recent GWAS have revealed several loci on the MHC gene (major histocompatibility complex) as risk factors for developing schizophrenia (Schizophrenia Psychiatric Genome-Wide Association Study (GWAS)

Consortium, 2011; Schizophrenia Working Group of the Psychiatric Genomics Consortium, 2014). In the brain, MHC is expressed by microglial cells, and is an important component of immune signalling, suggesting a link between immunity and schizophrenia. Furthermore, PET scans using TSPO to track microglia and inflammation in the brain have suggested microglial activation following the onset of schizophrenia. Firstly, although gliosis is a common feature in neurodegeneration and injury, human post-mortem brains with and without schizophrenia do not differ in glial burdens, measured by CD68 for microglia and GFAP for astrocytes (Arnold et al., 1998). This suggests an increase in inflammatory signals is not due an increased number of glial cells. The current evidence that TSPO signals are upregulated in schizophrenia has been recently reviewed in a meta-analysis (De Picker, Morrens, Chance and Boche, 2017). In the grey matter of the frontal lobe, TSPO signals were increased in schizophrenia patients for up to 5 years from the age of disease onset (van Berckel et al., 2008), as well during psychosis phases (Doorduyn et al., 2009). However, these findings have not been replicated in more recent studies (Kenk et al., 2015; Coughlin et al., 2016), further emphasising the variability seen between different schizophrenia cohorts. Of interest, two studies have reported that administration of minocycline orally, an antibiotic drug that can cross the blood-brain-barrier to diminish microglial numbers, reduced negative symptoms of schizophrenia, and that these effects lasted a month after treatment (Miyaoaka et al., 2008; Levkovitz et al., 2010). This suggests that dampening inflammation is beneficial for individuals with schizophrenia, although it's unclear whether these mechanisms act on the peripheral or CNS immune systems. Lastly, a recent report has provided evidence of microglia being involved in excessive synaptic pruning in schizophrenia (Sellgren et al., 2019). Co-cultures of human induced pluripotent stem cells from control and schizophrenia lines were differentiated into neurons and microglia-like cells. Interestingly, the microglia from the schizophrenia lines were more phagocytic than the control ones, and showed increased synaptic phagocytosis *in-vitro*. Whether similar mechanisms to AD

apply in schizophrenia too are unclear, but the complement system has been implicated to schizophrenia through mutations in C4 being risk factors for the disease (Sekar et al., 2016). Like in AD, there is lack of any human evidence to support the hypothesis that microglia undergo excessive phagocytosis of synapses in schizophrenia brains.

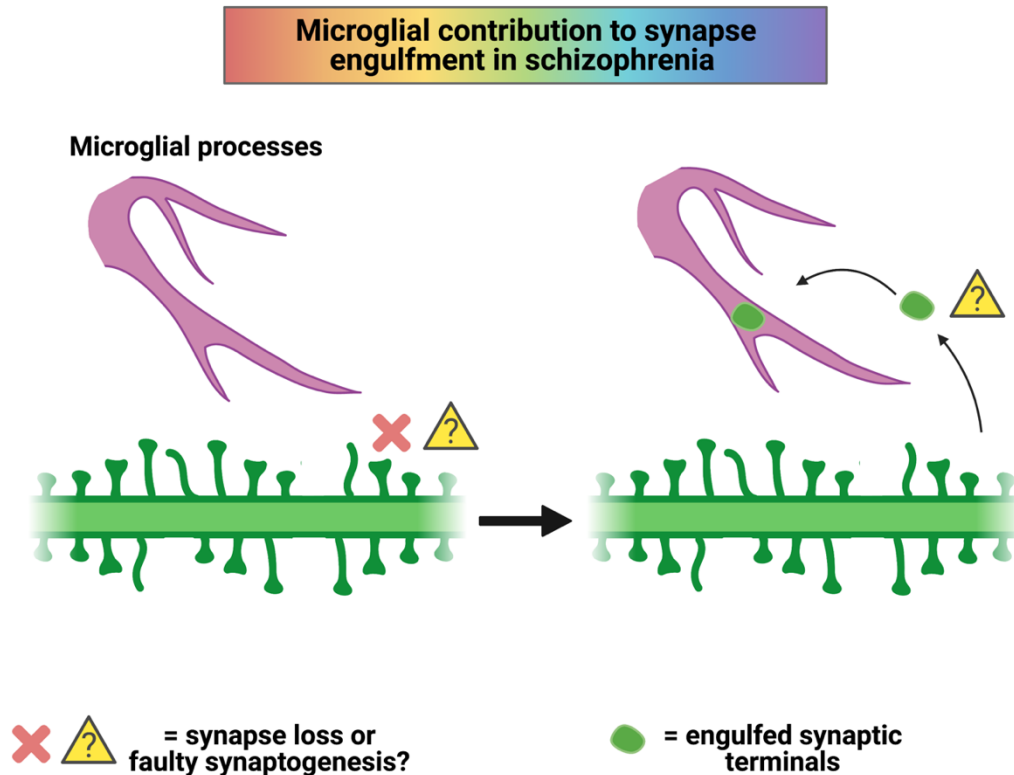


Figure 8. Synaptic uptake by microglia in schizophrenia. Unlike AD, it is not clear whether the reduced synaptic puncta in brains with schizophrenia are due to synapse loss or synaptic failure to properly form. There is limited evidence to suggest microglia in schizophrenia are more prone to exacerbated synaptic pruning, leaving important questions unanswered, like if this occurs only during development or throughout the lifespan, and what the mechanisms for synaptic uptake are.

6. Knowledge gaps

There is substantial lack of evidence in humans to suggest that the pruning hypothesis holds, and despite the compelling arguments made by a mouse-

dominated field, all the evidence surrounding human research is circumstantial and indirect. It is therefore essential to investigate whether human glial cells ingest more synapses in AD brains, like in the mouse models of AD. Similarly, the schizophrenia field is even further behind in understanding how microglia are involved in the disease (if at all), and the field can greatly benefit from more studies of the human post-mortem.

7. Hypothesis and aims

Hypothesis: Microglia and astrocytes in the human brain participate in exacerbated synaptic ingestion in individuals with AD compared to age-matched, healthy controls. This difference in synaptic uptake by glial cells is likely the outcome of both intrinsic changes in glial properties, as well as opsonisation of AD synapses, possibly as a response to increased neuropathology in the AD brains. Furthermore, it is hypothesised that microglia also contribute to synaptic ingestion in schizophrenia brains, and it is predicted that more ingestion occurs in schizophrenia brains compared to control brains.

Aims:

- 1) Quantify the presence of synaptic markers inside microglial lysosomes in AD and age-matched control brains, near and far from plaques.
- 2) Incubate human synaptoneurosomes from control and AD brains with microglia and astrocytes, in-vitro, and quantify synaptic ingestion.
- 3) Quantify the presence of synaptic markers inside microglial lysosomes in schizophrenia and age-matched control brains.

8. List of publications

Published work

- 1) **Tzioras, M.**, Easter, J., Harris, S., McKenzie, C., Smith, C., Deary, I., Henstridge, C. and Spires-Jones, T., 2017. Assessing amyloid- β , tau, and glial features in Lothian Birth Cohort 1936 participants post-mortem. *Matters*, 10.19185/matters.201708000003

Contribution: Microscopy, statistical analysis, manuscript writing and editing, figure design

Chapter discussed in: Not discussed

- 2) Henstridge, C., Sideris, D., Carroll, E., Rotariu, S., Salomonsson, S., **Tzioras, M.**, McKenzie, C., Smith, C., von Arnim, C., Ludolph, A., Lulé, D., Leighton, D., Warner, J., Cleary, E., Newton, J., Swinger, R., Chandran, S., Gillingwater, T., Abrahams, S. and Spires-Jones, T., 2017. Synapse loss in the prefrontal cortex is associated with cognitive decline in amyotrophic lateral sclerosis. *Acta Neuropathologica*, 135(2), pp.213-226. 10.1007/s00401-017-1797-4

Contribution: immunohistochemistry, microscopy, manuscript editing

Chapter discussed in: Not discussed

- 3) Brown, R., Lam, A., Gonzalez-Sulser, A., Ying, A., Jones, M., Chou, R., **Tzioras, M.**, Jordan, C., Jedrasiak-Cape, I., Hemonnot, A., Abou Jaoude, M., Cole, A., Cash, S., Saito, T., Saido, T., Ribchester, R., Hashemi, K. and Oren, I., 2018. Circadian and Brain State Modulation of Network Hyperexcitability in Alzheimer's Disease. *eneuro*, 5(2), pp.ENEURO.0426-17.2018. 10.1523/ENEURO.0426-17.2018

Contribution: immunohistochemistry, microscopy, manuscript editing

Chapter discussed in: Not discussed

- 4) **Tzioras, M.**, Davies, C., Newman, A., Jackson, R. and Spires-Jones, T., 2018. Invited Review: APOE at the interface of inflammation, neurodegeneration and pathological protein spread in Alzheimer's disease. *Neuropathology and Applied Neurobiology*, 45(4), pp.327-346. 10.1111/nan.12529

Contribution: Study design, systematic literature review, manuscript writing and editing, microscopy, figure design

Chapter discussed in: Figures adapted for Chapter 1

- 5) Henstridge, C., **Tzioras, M.** and Paolicelli, R., 2019. Glial Contribution to Excitatory and Inhibitory Synapse Loss in Neurodegeneration. *Frontiers in Cellular Neuroscience*, 13. 10.3389/fncel.2019.00063

Contribution: design, literature review, manuscript writing and editing, figure design

Chapter discussed in: Mentioned in Chapter 1

- 6) Pickett, E., Herrmann, A., McQueen, J., Abt, K., Dando, O., Tulloch, J., Jain, P., Dunnett, S., Sohrabi, S., Fjeldstad, M., Calkin, W., Murison, L., Jackson, R., **Tzioras, M.**, Stevenson, A., d'Orange, M., Hooley, M., Davies, C., Colom-Cadena, M., Anton-Fernandez, A., King, D., Oren, I., Rose, J., McKenzie, C., Allison, E., Smith, C., Hardt, O., Henstridge, C., Hardingham, G. and Spires-Jones, T., 2019. Amyloid Beta and Tau Cooperate to Cause Reversible Behavioral and Transcriptional Deficits in a Model of Alzheimer's Disease. *Cell Reports*, 29(11), pp.3592-3604.e5. 10.1016/j.celrep.2019.11.044

Contribution: immunohistochemistry of microglia and astrocytes, statistical analysis, microscopy, figure design

Chapter discussed in: Mentioned in Chapter 1

- 7) Hesse, R., Hurtado, M., Jackson, R., Eaton, S., Herrmann, A., Colom-Cadena, M., **Tzioras, M.**, King, D., Rose, J., Tulloch, J., McKenzie, C., Smith, C., Henstridge, C., Lamont, D., Wishart, T. and Spires-Jones, T., 2019. Comparative profiling of the synaptic proteome from Alzheimer's disease patients with focus on the APOE genotype. *Acta Neuropathologica Communications*, 7(1). 10.1186/s40478-019-0847-7

Contribution: Western blot of GFAP, data and statistical analysis

Chapter discussed in: Mentioned in Chapters 1-3

- 8) **Tzioras, M.**, Stevenson, A., Boche, D. and Spires-Jones, T., 2020. Microglial contribution to synaptic uptake in the prefrontal cortex in schizophrenia. *Neuropathology and Applied Neurobiology*, 47(2), pp.346-351. 10.1111/nan.12660

Contribution: Study design, staining tissue, confocal microscopy, statistical analysis, manuscript writing and editing, figure design

Chapter discussed in: Chapter 4

- 9) Kurucu, H., Colom-Cadena, M., Davies, C., Wilkins, L., King, D., Rose, J., **Tzioras, M.**, Tulloch, J., Smith, C. and Spires-Jones, T., 2021. Inhibitory synapse loss and accumulation of amyloid beta in inhibitory presynaptic terminals in Alzheimer's disease. *European Journal of Neurology*.

Contribution: Technical assistance and editing

Chapter discussed in: Not mentioned

- 1) **Tzioras, M.**, Daniels, M., King, D., Popovic, K., Holloway, R., Stevenson, A., Tulloch, J., Kandasamy, J., Sokol, D., Latta, C., Rose, J., Smith, C., Miron, V., Henstridge, C., McColl, B. and Spires-Jones, T., 2019. Altered synaptic ingestion by human microglia in Alzheimer's disease. <https://doi.org/10.1101/795930>

Contribution: Study design, performed all experiments (in collaboration to M Daniels), data and statistical analysis, manuscript writing and editing, figure design

Chapter discussed in: Chapters 3 and 4

- 2) Lorenzini, I., Alsop, E., Levy, J., Gittings, L., Rabichow, B., Lall, D., Moore, S., Bustos, L., Pevey, R., Burciu, C., Saul, J., McQuade, A., **Tzioras, M.**, Mota, T., Logemann, A., Rose, J., Almeida, S., Gao, F., Bowser, R., Spires-Jones, T., Blurton-Jones, M., Gendron, T., Baloh, R., Van Keuren-Jensen, K. and Sattler, R., 2020. Activated iPSC-microglia from C9orf72 ALS/FTD patients exhibit endosomal-lysosomal dysfunction. <https://doi.org/10.1101/2020.09.03.277459>

Contribution: preparation of human synaptoneurosomes, Western blots, statistical analysis, manuscript editing

Chapter discussed in: Not discussed

- 3) Mondal, M., Bali, J., **Tzioras, M.**, Paolicelli, R., Jawaid, A., Malnar, M., Dominko, K., Udayar, V., Halima, S., Vadodaria, K., Manesso, E., Thakur, G., Decressac, M., Petit, C., Sudharshan, R., Hecimovic, S., Simons, M., Klumperman, J., Brüstle, O., Ferguson, S., Nitsch, R., Schulz, P., Spires-Jones, T., Koch, P., Gunawan, R. and Rajendran, L., 2020. Nutrient signaling pathways regulate amyloid clearance and synaptic loss in Alzheimer's disease. <https://doi.org/10.1101/2020.11.13.381186>

Contribution: design of experiments involving human tissue, human tissue staining, data and statistical analysis, manuscript writing and editing, figure design

Chapter discussed in: Mentioned in Chapter 6

- 4) Stevenson, A., McCartney, D., Shireby, G., Hillary, R., King, D., **Tzioras, M.**, Wrobel, N., McCafferty, S., Murphy, L., McColl, B., Redmond, P., Taylor, A., Harris, S., Russ, T., Hannon, E., McIntosh, A., Mill, J., Smith, C., Deary, I., Cox, S., Marioni, R. and Spires-Jones, T., 2020. A comparison of blood and brain-derived ageing and inflammation-related DNA methylation signatures and their association with microglial burdens. <https://doi.org/10.1101/2020.11.30.404228>

Contribution: human tissue staining, data and statistical analysis, manuscript editing

Chapter discussed in: Not discussed

- 5) Colom-Cadena, M., Tulloch, J., Jackson, R., Catterson, J., Rose, J., Davies, C., Hooley, M., Anton-Fernandez, A., Dunnett, S., Tempelaar, R., **Tzioras, M.**, Izzo, N., Catalano, S., Smith, C. and Spires-Jones, T., 2021. TMEM97 increases in synapses and is a potential synaptic A β binding partner in human Alzheimer's disease. <https://doi.org/10.1101/2021.02.01.428238>

Contribution: mouse culling and brain processing

Chapter discussed in: Not discussed

Chapter 2: Methods

1. Overview

The overall aims of the thesis are to investigate synaptic ingestion by microglia and astrocytes in diseases like Alzheimer's disease and schizophrenia. Human post-mortem tissue was chosen to address some of these aims. This tissue was from non-demented and non-neurological control cases, Alzheimer's disease cases and schizophrenia cases. Tissue was cut from paraffin blocks and it was stained by immunofluorescence for glial markers, synaptic markers, and amyloid β plaques. The aim was to assess synaptic internalisation by microglia in disease situations. Human tissue was chosen here because, so far, there is evidence of synaptic internalisation by microglia only in mouse models of disease and there is a translational gap from basic research to humans. It is therefore important to investigate whether these mechanisms are relevant to humans. However, human tissue is limited studying a snap-shot at the end-stage of disease and lacks mechanistic insight. For this reason, cultured glial cells from mice and humans were challenged with synaptoneurosomes from human post-mortem brains, from control and Alzheimer's disease brains. The aim of this part of the study is to investigate whether there are synaptic changes associated with disease that make them more prone for glial cells to ingest them. Where possible, the conditions and the experimenter were blinded to disease status, and mice were randomised (more details on this to follow).

2. Animals

Experiments were performed using male C57Bl/6J mice (Charles River Laboratories). Mice were maintained under a standard 12 h light/ dark cycle and provided with *ad libitum* access to food and water. Mice were housed in groups of up to five mice and were acclimatized for a minimum of 1 week prior to procedures. All experiments were conducted under the UK Home Office Animals (Scientific Procedures) Act 1986, in agreement with local ethical and veterinary approval (Biomedical Research Resources, University of Edinburgh).

3. Human tissue (Alzheimer's disease study)

All tissue was provided by the MRC Edinburgh Brain Bank, following all appropriate ethical approval. For paraffin embedding, tissue was dehydrated via increasing ethanol solutions, fixed in formalin, and baked in paraffin-embedded blocks. Tissue from the inferior temporal lobe (Brodmann area 20/21) and primary visual cortex (Brodmann area 17) was cut using a microtome at 4µm thickness and mounted on glass slides for use in immunohistochemistry. The locations of these areas in the brain are visualised in Figure 1. AD cases were cross-checked neuropathologically and were confirmed to be Braak Stages V-VI. In one case (BBN: 24527) no plaques were measured in BA17 and was excluded as a whole from the near plaque analysis. Case BBN31495 has a Braak Stage of VI but has been cognitively tested upon 3 waves and was cognitively unimpaired. Data about subjects included in the study are found in Table 1.

Use of human tissue for post-mortem studies has been reviewed and approved by the Edinburgh Brain Bank ethics committee and the ACCORD medical research ethics committee, AMREC (approval number 15-HV-016; ACCORD is the Academic and Clinical Central Office for Research and Development, a

joint office of the University of Edinburgh and NHS Lothian). The Edinburgh Brain Bank is a Medical Research Council funded facility with research ethics committee (REC) approval (11/ES/0022).

Table 1. Participant information used for post mortem AD experiments described in Chapters 3 and 4. For the study, we included in total 17 non-demented control cases (NDC) and 23 Alzheimer’s disease (AD) cases, that are age-matched and of mixed APOE genotypes. Age-matching was based on Student’s t-test, where $p=0.1064$. All AD cases are end-stage of disease. Some cases were only used for the staining study (no asterisk), and some for both the staining and making synaptoneurosomes (*) [synaptoneurosomes preparations seen in the next chapter]. NA denotes information is not available.

MRC BBN	APOE status (3vs4)	Condition	Age	Gender (F/M)	PMI (hours)	Brain weight (g)	Brain pH	Braak stage
19686*	3/3	NDC	76	F	75	1320	6.5	I
28797*	3/3	NDC	79	M	57	1301	6.11	NA
28406*	3/3	NDC	79	M	72	1437	6.13	II
28402*	3/3	NDC	78	M	49	1503	6.33	I
26495*	3/3	NDC	78	M	39	1290	6.17	I
14395*	3/3	NDC	74	F	41	1520	6.3	NA
20122*	3/3	NDC	59	M	74	1500	6.1	NA
22612*	3/3	NDC	61	M	70	1300	6.1	NA
001.32577	3/3	NDC	81	M	74	1313	6.07	NA
29086*	3/3	NDC	79	F	68	1468	6.2	NA
29082*	3/4	NDC	79	F	80	1339	5.96	III
31495*	3/4	NDC	81	M	38	1318	5.79	VI
20593*	3/4	NDC	60	M	52	1460	6	NA
22629*	3/4	NDC	59	F	53	1280	6.3	NA
15809*	3/4	NDC	58	M	90	1470	5.9	NA
16425*	3/4	NDC	61	M	99	1270	6.2	NA
001.34131	3/4	NDC	82	M	95	1472	5.97	IV
Group mean	10/7		72.00	5/12	66.24	1385.94	6.13	
24527	3/3	AD	81	M	74	1160	6.1	V
28410	3/3	AD	62	F	109	1029	6.04	VI
28771	3/3	AD	85	M	91	1183	5.95	VI
15258	3/3	AD	65	M	80	1335	6.1	VI
19595	3/3	AD	87	M	58	1420	6.5	VI
19994	3/3	AD	87	F	89	1270	5.9	VI
22223	3/3	AD	87	F	83	1200	6.7	IV
001.32929	3/3	AD	85	F	80	1354	6.08	VI
19690*	3/4	AD	57	M	58	1200	5.9	VI
24322*	3/4	AD	80	M	101	1410	6	VI
25739*	3/4	AD	85	F	45	1375	5.77	VI
26718*	3/4	AD	78	M	74	1367	6.13	VI
29521*	3/4	AD	95	M	96	1221	6.08	VI
29695*	3/4	AD	86	M	72	1200	6.1	VI
10591*	3/4	AD	86	M	76	1470	NA	VI
15810	4/4	AD	73	F	96	1090	6.2	VI
15811	3/4	AD	81	F	41	1457	6.3	VI
23394*	3/4	AD	88	F	59	1165	6.3	V
001.26732*	3/4	AD	76	M	66	1467	6.48	VI
20995*	4/4	AD	60	M	86	1244	5.9	VI
001.26500	4/4	AD	81	M	83	1315	6.25	VI
15256	4/4	AD	60	M	28	1389	NA	V-VI
001.28796	4/4	AD	60	F	54	1150	5.95	VI
Group mean	8/15		77.6086957	9/14	73.86956522	1281.347826	6.13	

4. Human tissue (Schizophrenia study)

Ethical approval was provided by BRAIN UK, a virtual brain bank which encompasses the archives of neuropathology departments in the UK and the Corsellis Collection, ethics reference 14/SC/0098. The study was registered under the Ethics and Research Governance (ERGO) of the Southampton University (Reference 19791). Ten cases with a confirmed diagnosis of schizophrenia (mean age 64.80 ± 20.37) and 10 non- neurological and non-neuropathological controls (mean age 64.40 ± 19.78) were obtained from the Corsellis Collection (Table 1). Dorsal prefrontal cortex (DPFC, or Brodmann area 46) (Figure 1), an area showing neuroimaging abnormalities with reduction of the grey matter volume in chronic schizophrenia, was investigated for all cases. Cases with any other significant brain pathologies such as infarct, tumour, or traumatic brain injury were excluded from the study. Controls with no history of neurological or psychiatric disease or symptoms of cognitive impairment were matched to cases as possible. No difference in age at death and in post- mortem delay was detected between the 2 groups. To minimize the time in formalin, which has an effect on the quality of the immunostaining, the selection was performed on the availability of formalin-fixed paraffin embedded tissue, and thus on blocks processed at the time of the original post-mortem examination. Characteristics of the cohorts are provided in Table 2.

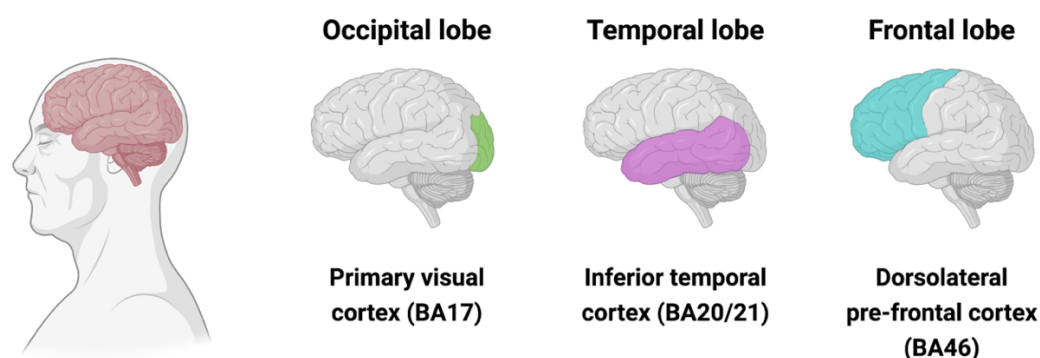


Figure 1. Location of the different brain areas used in the AD and schizophrenia study.

Table 2: Demographic, clinical and *post-mortem* characteristics of control and schizophrenia cases

Cases	Ctrl (n=10)	Sz (n=10)	P value
Sex	4F:6M	2F:8M	
Age at death (years, mean \pm SD)	64.40 \pm 19.78	64.80 \pm 20.37	P = 0.94
Post-mortem delay (hours, mean \pm SD)	61.90 \pm 51.23	50.60 \pm 24.52	P = 0.61
Age of onset (years, mean \pm SD)	NA	36.50 \pm 13.81	
Duration of illness (years, mean \pm SD)	NA	35.13 \pm 21.85	
Cause of death			
<i>Cardiovascular disease</i>	8	5	
<i>infection/inflammation</i>	1	3	
<i>Trauma</i>	1	1	
<i>Others*</i>	0	1	

Ctrl, neurologically/cognitively normal controls; *Sz*, Schizophrenia cases; *F*, female, *M*, male; *SD*, standard deviation; *NA*, Not Applicable; *foreign body in respiratory tract

5. Immunohistochemistry for paraffin embedded human tissue

Paraffin-embedded sections were provided by the Sudden Death MRC Edinburgh Brain Bank and the Corsellis collection (schizophrenia study). Tissue was resected from post-mortem brains and dehydrated with ethanol, prior to paraffin-embedding. Sections were cut using a microtome at 4 μ m thickness (7 μ m thickness for the schizophrenia study) and provided upon a justified tissue request. Slides with embedded tissue were dewaxed in xylene for 6 minutes, followed by rehydration using descending ethanol-to-water solutions: 100% EtOH, 90% EtOH, 70% EtOH, 50% EtOH, 100% water, of 3 minutes each. For antigen retrieval, samples were pressure cooked for 3 minutes at the steam setting in citrate buffer, pH 6 (Vector labs, H3300).

Specifically, citric acid concentrate was diluted from 100x stock in de-ionised water for use, and made fresh each time. Slides were allowed to cool down under running water, and then immersed in 70% ethanol for 5 minutes. Slides were incubated with an autofluorescence eliminator reagent (Merck, 2160) for 5 minutes and washed with 70% ethanol, followed by two 5-minute washes using PBS-0.3% Triton X-100 (Sigma-Aldrich, T8787-100ML), and one wash with 1x PBS (Thermo Fisher, 70011036). Using a wax pen (Vector labs, H4000), the tissue was outlined and incubated with blocking solution for 1 hour. Blocking solutions consisted of 10% normal donkey serum (Sigma-Aldrich, D96663) and 0.3% Triton X-100. Primary antibodies were diluted appropriately (Table 3) at a final volume of 500 μ l per slide, and were allowed to incubate overnight (14-16 hours) in the cold room, at 4-6°C, in a humid chamber using wet paper towel in the staining box. On the second day of staining, slides were washed once in PBS-0.3% Triton X-100, followed by two 5 minute washes in PBS. Secondary antibodies were then applied at a volume of 500 μ l per slide (Table 4). All cross-adsorbed secondary antibodies were made-up to a final concentration of 1:500 (4 μ g/ml) in PBS, and applied for 1 hour at room temperature. Nuclei were counterstained with DAPI (1 μ g/ml) (D9542-10MG, Sigma-Aldrich). For Thioflavin S (Sigma-Aldrich, T1892), slides were dipped in 0.001% Thioflavin S, made in 50% ethanol, for 8 minutes and differentiated in 80% ethanol for 1 minute. In the end, one drop of Immumount (Thermo Fisher, 9990402) was added per slide to allow for coverslip adherence. Coverslips size was No 1.5, corresponding to 22x40mm (VWR, 631-0136). Coverslips were pressed gently to remove excess mounting media and remove bubbles, and were allowed to dry at room temperature for at least 1 hour. Slides were kept in the fridge for long term storage and were allowed to reach room temperature prior to imaging.

Table 3. Primary antibody information.

Antibody	Company and catalogue number	Species (isotype)	Dilution
CD68	DAKO M0876	Mouse polyclonal (IgG3)	1:100
Synapsin I	Merck Millipore AB1543P	Rabbit (IgG)	1:750
Synaptophysin (Sy38)	Abcam ab8049	Mouse monoclonal (IgG1)	1:500
Synaptophysin (Sy38)	R&D Systems AF5555	Goat polyclonal IgG	1:500
PSD-95 (PDZ domain)	Synaptic systems 124 014	Guinea pig polyclonal (IgG)	1:500
Iba1	Abcam ab5076	Goat polyclonal (IgG)	1:500
TMEM119	Abcam ab185333	Rabbit polyclonal (IgG)	1:500
AW7	Provided by Dominic Walsh	Rabbit (IgG)	1:5,000
GFAP	Abcam ab53554	Goat (IgY)	1:3,000
GAD65/67	Abcam ab183999	Rabbit polyclonal (IgG)	1:500

Table 4. Secondary antibody information.

Antibody	Company and catalogue number	Dilution
Donkey anti-rabbit A647 (highly cross-adsorbed, IgG)	Thermo Fisher (Invitrogen), A-31573	1:500
Donkey anti-mouse A594 (highly cross-adsorbed, IgG)	Thermo Fisher (Invitrogen), A-21203	1:500
Donkey anti-rabbit A488 (highly cross-adsorbed, IgG)	Thermo Fisher (Invitrogen), A-21206	1:500
Donkey anti-goat A647 (highly cross-adsorbed, IgG)	Thermo Fisher (Invitrogen), A32849	1:500
Donkey anti-rabbit A594 (highly cross-adsorbed, IgG)	Thermo Fisher (Invitrogen), A-21207	1:500
Goat anti-chicken A647 (highly cross-adsorbed, IgY)	Thermo Fisher (Invitrogen), A32933	1:500

6. Confocal microscopy and Image analysis

Slides were imaged on a confocal microscope (Leica TCS8) with a 63x oil immersion objective. Laser and detector settings were kept constant between samples. During imaging and analysis, the experimenter was blinded to brain area and disease status. Twenty images from the grey matter were taken per case, sampling randomly through all six cortical layers. The synaptic stain was used to confidently separate grey matter versus white matter. The resolution of the confocal microscopy was $0.18\mu\text{m} \times 0.18\mu\text{m} \times 0.3\mu\text{m}$ (xyz).

For the schizophrenia study, analysis was performed by using a custom written macro on FIJI where images were automatically thresholded to perform a mask of the microglial and synaptic stains, which were multiplied to show the percent area of colocalisation. Analysis was done of max-projected images

and a 2D colocalization mask was used to calculate burdens (followed by re-analysis with 3D). 3D reconstruction images were generated in Imaris (Alzheimer's disease study) and ParaView 5.8.0 (Schizophrenia study). All experiments and analyses were blinded to the experimenter.

For the AD and SZ analysis an improved analysis flowthrough was generated in order to analyse data in 3D images rather than 2D. Image stacks were segmented in 3D in Matlab under the auto-local threshold function with custom made scripts. For the CD68 stain, the Matlab segmentation settings were: window size=70, Factor C=0.2, method=mean, no minimum size selected. For the synapsin I stain the settings were: window size=10, Factor C=10, method=mean, no minimum size selected. This analysis removes noise and non-specific staining by removing objects that are not found in the same location in sequential slices. The same segmentation parameters were used for all images to keep the final outputs similar and not influence the final burdens between cases. Once the segmentation was completed, the images were processed with a custom Python script in order to obtain their volumetric measurements (i.e. density of objects/mm³ of tissue). This provided density measurements for stained markers, like the total objects of CD68-positive staining per image slice in a Z-stack. This allowed further analysis on Python for calculating the area of colocalisation between CD68 and SynI objects in 3D. To allow colocalization, two objects need to overlap at least 25% of their whole structure. Images were processed again with FIJI in order to add all segmented slices in their respective stacks in order to calculate the volume occupied by all of the staining in the stack. Each stack was normalised to the volume of the entire stack (different stacks have different amounts of slices, so the final volume differs). All scripts can be found in the following link: <https://github.com/lewiswilkins/Array-Tomography-Tool>.

7. Synapse-enriched fraction preparation

Preparation of synaptoneurosomes was performed as described previously (Tai et al., 2014). Snap-frozen human tissue of 300-500mg from BA38 (temporal cortex) was homogenised using a Dounce homogeniser with 1ml of a protease inhibitor buffer, termed here Buffer A. Buffer A consists of 25mM HEPES, 120mM NaCl, 5mM KCl, 1mM MgCl₂, 2mM CaCl₂, protease inhibitors (Merck, 11836170001) and phosphatase inhibitors (Merck, 524629-1SET) made up in sterile water, and was prepared fresh each day. The Dounce homogeniser and Buffer A were kept ice-cold throughout the procedure to avoid further degradation. We allowed 10 passes for full homogenisation but minimise cellular disruption that would lead to an impure final fraction. Once homogenised, the homogenate was aspirated in a 1ml syringe and passed through an 80-micron filter (Merck, NY8002500) to remove debris and yielded the total homogenate (TH). The filter was pre-washed with 1ml of Buffer A to maximise yield. A sample of the TH was snap-frozen on dry ice for Western blot analysis, and the rest was split in half for Western blot analysis and the phagocytosis assays. A subsequent filtration took place using a 5-micron filter (Merck, SLSV025LS) followed by centrifugation at 1000xg for 7 minutes to yield the synaptoneurosome (SN) pellet. In this step, extra care was taken to slowly pass the homogenate through the filter in order to prevent the filter breaking. The filter was pre-washed with 1ml of Buffer A to maximise yield. The pellet was washed with Buffer A and pelleted down again to ensure purity. Pellets were snap frozen on dry ice and stored at -80°C for long-term storage.

8. Protein Extraction

For protein extraction, samples were diluted five-fold with Tris-HCl buffer pH 7.6 (100mM Tris-HCl, 4% SDS, and Protease inhibitor cocktail EDTA-free [ThermoFisher Scientific, 78447]), followed by centrifuging for 25 minutes at 13,300 RPM at 4°C. Then, the supernatant was collected in fresh tubes and

heated at 70°C for 10 minutes. Samples were kept at -80°C for long-term storage.

9. Micro BCA

Micro BCA kit (ThermoFisher Scientific, 23235) was used to quantify protein levels, following manufacturer's instructions. Briefly, 1 µl of sample was added in 1 ml of working solution and heated at 60°C for 1 hour. Working solution was made fresh right before required, consisting of 50% Buffer A, 48% Buffer B and 2% Buffer C, all provided in kit. Albumin was provided in the kit for determining a standard curve of the following concentration: 2 µg/ml, 4 µg/ml, 6 µg/ml, 8 µg/ml, 10 µg/ml, and 20 µg/ml. Absorbance values were obtained using spectrophotometry at 562nm with working solution used as the blank value to calibrate the machine.

10. Western Blot

After protein extraction, each sample was made-up to 20µg of protein as calculated by the micro BCA (protein extract diluted in de-ionised water) and diluted in half with Laemmli buffer (2x stock) (S3401-10VL). In each well, 15µl of sample were loaded in 4-12% Bis-Tris gels (ThermoFisher Scientific, NP0323BOX). Each gel was run with 5µl of molecular weight marker (Licor, 928-40000) in the first well. Gels were washed with de-ionised water and diluted NuPAGE buffer (ThermoFisher Scientific, NP0002) (20x stock) to remove bits of broken gel and residual acrylamide. Western blot chambers were filled with diluted NuPAGE buffer (600ml per chamber), making sure each chamber compartment was locked securely and there was no leaking. Gels were run at 80V for 5 minutes, 100V for 1.5 hours and 120V for 30 minutes. Then, using a scraper tool, gels were cracked open from their plastic casing and soaked in 20% ethanol for 10 minutes prior to transferring using the iBlot

2 Dry Blotting System (IB21001). Pre-packed transfer stacks containing a PVDF membrane (ThermoFisher Scientific, IB24002) were assembled as per manufacturers recommendations, and samples were transferred for 8.5 minutes at 25V. After transferring, the PVDF membranes were stained for 5 minutes with Ponceau S in 5% acetic acid (P7170-1L), and washed 3 times with 5% acetic acid to stain for total protein. Ponceau S stained membranes were scanned and analysed on FIJI to obtain a measurement of total protein per sample. Ponceau S was washed out with PBS and the PVDF membranes were blocked using Odyssey blocking buffer (Licor, 927-40000) for 30 minutes, following overnight incubation with primary antibodies made up in Odyssey block with 0.1% Tween-20, at 4°C with gentle shaking. The following primary antibodies were used: Synaptophysin (mouse, Abcam ab8049, 1:1000), PSD-95 (rabbit, Cell signalling D27E11, 1:1000), and Histone (rabbit, Abcam ab1791, 1:1000). The next day, membranes were washed 6 times with PBS-0.1% Tween-20, and incubated with the following Licor secondary antibodies for 30 minutes: IRDye 680RD Donkey anti-Mouse IgG, highly cross-adsorbed (Licor, 925-68072, 1:5000) and IRDye 800CW Donkey anti-Rabbit IgG, highly cross-adsorbed (Licor, 925-32213, 1:5000). All gels were imaged using the same exposure times and intensities using a Licor Scanner. The images were then uploaded on ImageStudio for analysis. For each band, the same size box was used to ensure all samples are measured equally. Each sample was normalised to its corresponding value of total protein.

11. Synaptoneurosome labelling with pHrodo Red-SE

First, pHrodo Red-SE (ThermoFisher Scientific, P36600) was diluted with DMSO according to manufacturers instructions to reach a concentration of 10mM. Synaptoneurosome (SNS) pellets were resuspended in 100mM sodium carbonate buffer pH 9, adapted from a previously described protocol (Byun and Chung, 2018). SNSs were tagged with pHrodo Red-SE based on protein concentration, roughly at 4mg/ml, as calculated by the micro BCA, and

incubated at room-temperature under gentle shaking for 1 hour, covered in foil. Samples were centrifuged at 13,000 RPM for 10 minutes to obtain the labelled SNS pellet, followed by 3 rounds of washing with PBS and centrifugation to wash out any unbound dye. The pHrodo-labelled SNS pellets were then resuspended in 5% DMSO-PBS and aliquoted for storage at -80°C. Aliquots of pooled AD and NDC samples were prepared fresh.

12. BV2 microglia phagocytosis assay

Phagocytosis assays were optimised using the BV2 immortalised murine microglia cell line. BV2 microglia were cultured in DMEM + GlutaMAX (ThermoFisher Scientific, 31966-021) and were supplemented with 10% fetal bovine serum (FBS, ThermoFisher Scientific) and 1% penicillin/streptomycin (PenStrep, ThermoFisher Scientific). Cells were grown in a humidity-controlled incubator at 37°C with 5% CO₂. One day prior to the phagocytosis assay, BV2 microglia were seeded in a 96-well flat bottom plate (ThermoFisher Scientific, 165305) at a density of 12,500 cells/well. Cells were stained with Hoechst (2µg/ml, ThermoFisher, H3570) to visualise nuclei and cytochalasin D treated cells (10µM, Sigma-Aldrich, C8273) were used as negative controls. BV2 cells were challenged with pHrodo-tagged synaptoneuroosomes, and immediately taken to an ImageExpress high-throughput microscope (Molecular Devices) for live-imaging using a 20x air objective (37°C, 5% CO₂). Images were taken every 5-10 minutes for 3 hours, using the same settings for all imaging sessions. All conditions were repeated in triplicate with 4 fields of view per well. For analysis, MetaXpress 6 (Molecular Devices) software was used to automatically calculate the number of cells per field of view and detect fluorescence around cells by thresholding. A phagocytosis index was calculated by normalising the number of cells phagocytosing to total number of cells in an automated and unbiased way. The same exposure settings were used for each set of experiments. Videos taken with phase contrast and were

recorded on a Zeiss Observer Z1 microscope using 20x air objective (37°C, 5% CO₂), with images taken every 5 minutes.

13. Primary mouse microglia

Primary adult mouse microglia were isolated and cultured as described previously (Grabert and McColl, 2018). Brains from 12-week-old male C57/Bl6 (Charles-River) mice were isolated by terminally anaesthetizing with 3% isoflurane (33.3% O₂ and 66.6% N₂O) and transcardial perfusion with ice-cold 0.9% NaCl. Brains were immediately placed into ice-cold HBSS (ThermoFisher Scientific) and minced using a 22A scalpel before centrifugation (300 x g, 2 min) and digestion using the MACS Neural Dissociation Kit (Miltenyi) according to manufacturer's instructions. Briefly, brain tissue was incubated in enzyme P (50 µL/brain) diluted in buffer X (1900 µL/brain) for 15 min at 37°C under gentle rotation before addition of enzyme A (10 µL/brain) in buffer Y (20 µL/brain) and further incubation for 20 min at 37°C under gentle rotation. Following digest tissue was dissociated mechanically using a Dounce homogenizer (loose Pestle, 20 passes) on ice and centrifuged (400 x g, 5 min at 4°C). To remove myelin, tissue was resuspended in 35% isotonic Percoll (GE Healthcare) overlaid with HBSS and centrifuged (800 x g, 40 min, 4°C). Following centrifugation, the supernatant and myelin layers were discarded and the pellet resuspended in MACS buffer (PBS, 0.5% low endotoxin BSA (Sigma-Aldrich), 2 mM EDTA, 90 µL/brain). Anti-CD11b microbeads (Miltneyi) were added (10 µL/brain) and the suspension incubated for 15 min at 4°C. before running through pre-rinsed (MACS buffer) LS columns attached to a magnet (Miltenyi). After washing with 12 mL MACS buffer columns were removed from the magnet and cells retained (microglia) were flushed in 5 mL MACS buffer. Microglia were resuspended in DMEM/F-12 (ThermoFisher Scientific) supplemented with 1% PenStrep, 10% FBS, 500 pg/mL rhTGFβ-1 (Miltenyi), 10 pg/µL mCSF1 (R&D Systems). Microglia were

counted using a haemocytometer and plated out at 40,000 cells/well onto a black-walled, optical bottom 96-well plate (ThermoFisher Scientific) coated with poly-L-lysine. Cells were cultured for 7 days with a half media change on day 3. Phagocytosis assay was performed and analysed as described above with 9 fields of view per well.

14. Primary human microglia isolation

Use of human temporal lobe resections for research was approved by National Health Service Lothian under protocol number 2017/0125/SR/720 issued to V.E.M. The protocol for isolating primary human microglia was adapted from a previously established one (Blain et al., 2010). Fresh brain tissue was donated from a 23-year-old male undergoing epilepsy surgery. Resected brain specimen came from healthy tissue of the temporal lobe. Briefly, blood was removed by multiple washes of PBS followed by treatment with 0.25% trypsin and 100ug/ml DNase in PBS for 30 minutes at 37°C, with gentle rotation. Trypsin was then deactivated with 10% FCS. Samples were centrifuged at 1,200 RPM for 10 minutes (high brakes) at 4°C and the supernatant was discarded followed by addition of PBS and Percoll (GE Healthcare) with further ultra-centrifugation at 15,000 RPM for 30 minutes at 4°C (no brakes). The myelin layer was aspirated off and cell layer was transferred in a clean tube, leaving behind a layer of red blood cells. The transferred cells were topped-up with PBS and centrifuged again at 1,200 RPM for 10 minutes (high brakes) at 4°C and resuspended in warm media containing 5% FCS and 0.1% glucose. Subsequently, isolated mixed cells were cultured in T12.5 flasks for 3 days. Three days later, microglia were trypsinised and collected from the flasks, following centrifugation to yield the microglia cell pellet. After the isolation, microglia were counted using a haemocytometer and plated out at 40,000 cells/well onto a black-walled, optical bottom 96-well plate (ThermoFisher

Scientific) coated with poly-L-lysine, and were allowed to rest for 5 days prior to phagocytosis assays. Phagocytosis assay was performed and analysed as described above with 9 fields of view per well. For the glioblastoma cases, a modified protocol of CD11b immunomagnetic bead isolation was used, as described above.

15. Primary mouse astrocyte isolation

Astrocyte isolation and culturing has been previously described by (Hasel et al., 2017). Glia cultures were achieved by passaging a mixed neuron/glia culture with trypsin consequently removing neurons. All reagents were purchased from Merck unless otherwise stated. Briefly, E17.5 mouse CD1 embryos were decapitated in accordance with schedule 1 of UK home office guidelines for humane killing of animals. The cortices were removed in a dissociation medium (81.8mM Na₂SO₄, 30 mM K₂SO₄, 5.84 mM MgCl₂, 0.252 mM CaCl₂, 1 mM HEPES, 20 mM D-glucose, 1 mM kynurenic acid, 0.001% Phenol Red) and then enzymatically digested with papain at 36,000 USP units/ml for 40 minutes. The cortices were then washed twice with dissociation medium followed by twice with plating media (DMEM+10% FBS+1X antibiotic-antimycotic agent (all Thermofisher)). Cortices were homogenized using a 5ml pipette by sequential suction/expulsion and plated a density of 2 cortices/T75 flask in plating medium. After 6-7 days in vitro, the mixed neuron/glia culture was trypsinized, centrifuged at 800 RPM for 5 minutes and the pellet re-suspended in plating medium. 1/3 of the total cell suspension was plated into a new T75 which reached maximum confluency 4-5 days later. This cell population now predominately contains astrocytes with a smaller proportion of microglia which can be detached by shaking. Plating of astrocytes was done similar to microglia, as described above. Human astrocytes were purchased by Caltag Medsystems (SC-1800) and cultured under the same conditions as the mouse ones.

16. Immunofluorescence of cultured cells

Plated cells were fixed for 10 minutes with 4% PFA. Subsequently cells were washed with PBS (pH 7.4) and incubated with 0.1% TritonX-100 for 30 minutes. After washing, blocking solution was applied for 1 hour (10% NDS, 3% Bovine serum albumin [A8806-5G], 0.1% TritonX-100, 0.1% Tween-20 in PBS). Primary antibodies were diluted in blocking solution and used in the same concentrations as in the human paraffin tissue, and left overnight at 4°C. Cells were washed 3 times with PBS and secondary antibodies were applied for 30 minutes with DAPI (1 µg/ml). Secondaries and DAPI were washed, and cells were topped with PBS and kept in the fridge. Images were taken with 10x and 20x objectives using a Zeiss Axio Observer Z1 microscope.

17. Statistics

Statistical analyses were performed in Graphpad Prism and R Studio (Team, 2020). No a priori calculations were conducted for determining sample sizes because of tissue availability constraints. The experiments in Chapter 4 involving mouse tissue are ongoing, and power calculations will be made for the continuation of this study. For human post-mortem tissue imaging, data were not normally distributed according to residual plots. In order to use a linear regression model the data must meet the assumption of normal distribution. For this reason, the data presented in Chapters 3 and 5 (human post-mortem) were transformed with a Tukey transformation after adding 1 to all datapoints (lambda value -1082) for normalisation. We used a linear mixed-effects model with disease, APOE genotype, brain region, plaques, and sex as fixed effects and case as a random effect to account for multiple measurements per case (Full code found in the Appendix R Script 1, modified for Chapter 5). This allows for a more powerful analysis which considers more data points per case, rather a single mean from the 20 images. Post-hoc comparisons of groups were done using pairwise comparisons in the

emmeans function of R. Data is presented in the figures in its untransformed format to allow for scientific interpretation. For all other comparisons, analysis was conducted in GraphPad Prism 8 and appropriate statistical tests were chosen on the basis of normality (residual plots). In all experiments, for significance we considered $p < 0.05$.

18. Software and Data Availability

Figures were made using BioRender, GraphPad Prism, and R Studio.

The code generated for statistical analysis with R Studio is found in the Appendix R Script 1.

Chapter 3: Human post-mortem analysis of synaptic ingestion by microglia

1. Introduction

In the past, microglia have been suggested to become activated by A β or tau pathologies in the brain, but that they remain by-standers without playing any active roles in driving disease progression . Now, a plethora of genetic, pharmacological, and mechanistic studies implicate microglia as key players in disease driving pathologies, including aberrant phagocytosis (Sierra et al., 2013; Podleśny-Drabiniok, Marcora and Goate, 2020; Kim et al., 2017) and contributing to synapse degeneration and elimination (Hong et al., 2016; Paolicelli et al., 2017; Bie et al., 2019). Mouse-models of AD have shown that microglia internalise more synaptic proteins than control mice, and have suggested that microglia actively phagocytose synapses, rather than just clearing debris of degenerated ones. Importantly, preventing microglia from eliminating synapses results in improved cognition and synapse health suggesting that they remove active synapses, as well as degenerating ones (Hong et al., 2016; Shi et al., 2017a, 2015). EM images have shown synaptic terminals inside microglial processes in human AD brains (El Hajj et al., 2019) but to date there has never been a quantitative analysis of synaptic ingestion by microglia in human brains. Therefore, a key knowledge gap is whether in human brains, microglia also contribute to synapse loss in AD by ingesting healthy synapses.

In this chapter, human brain sections were examined, provided by the Edinburgh Brain Bank. Two brain areas were assessed in this study: the inferior temporal lobe (BA20/21) and primary visual cortex (BA17). The temporal lobe was chosen because it is affected early during AD and has high

levels of pathology, including significant synapse loss (Ingelsson et al., 2004; Braak and Braak, 1991; Keller, 2006). On the other hand, BA17 is affected during late stage AD, and so this area has been affected for less time, and to a lesser extent (Keller, 2006), providing an internal control. Non-demented control (NDC) brains are compared to confirmed late-stage AD cases (Braak stages V and VI), of mixed sex and APOE genotypes. It is hypothesised that given the pathological landscape of the AD brain and APOE4's role in neurodegeneration, that both these factors are associated to exacerbated synapse engulfment by microglia (Tzioras and Spires-Jones, 2018). The tissue was stained for glial, synaptic, and A β markers.

This chapter will examine quantitatively the evidence for synaptic ingestion by microglia and astrocytes in human post-mortem brain tissue.

2. Results

2.1 Optimization of staining

Iba1 (ionised calcium binding adaptor protein 1) has been commonly used to label microglial cells in the brain in immunohistochemistry studies, as it is expressed in the cell cytoplasm and is a good indicator of microglial morphology (Minett et al., 2016; Davies et al., 2017). Moreover, it is typical to observe increased numbers of Iba1-positive microglial cells in mouse brains with AD-associated pathology (Krasemann et al., 2017; Parhizkar et al., 2019; Pickett et al., 2019; Hong et al., 2016; Shi et al., 2017b). Iba1 can also label microglia in human brains (Davies et al., 2017; Oosterhof et al., 2019; Olmos-Alonso et al., 2016), and this staining has been previously optimised in the lab for both immunofluorescence (Paolicelli et al., 2017) and DAB staining (Henstridge et al., 2018); therefore, it was chosen as a preferred microglial marker at the outset of this project for staining human tissue. Example images

are shown in Figure 1 (B-D), showing Iba1-positive microglia clustering near A β plaques (stained with AW7). In Figure 1E-F, microglia have ingested pre-synaptic terminals, labelled with synaptophysin (white arrows). However, there were significant inconsistencies with the Iba1 staining quality between cases, and sometimes within single sections from the same brain. Specifically, in some cases the antibody labelled microglia successfully (Figure 2A-D), while in others labelling was patchy and the staining was faint (Figures 2E-F, Figure 3B). Both outcomes were observed in the same batch of staining, suggesting it's not a methodological issue (for example staining problems or antibody issues). To this extent, Iba1 inconsistencies were seen in both brain areas of one case (BA17 and BA20/21), which suggests issues with post-mortem interval, tissue processing, or protein expression, rather than staining problems (Figure 2). Importantly, it was recently shown that the expression of Iba1 in AD human tissue does not follow the same trajectory as in mouse tissue, and its expression in the grey matter of AD cases has been reported to be unchanged or even decreased (Olmos-Alonso et al., 2016; Tischer et al., 2016; Minett et al., 2016; Waller et al., 2019). Altogether, these factors made Iba1 not suitable for staining human post-mortem AD tissue. Alternatively, Tmem119 is a microglia-specific marker which is a good candidate for staining human microglia (Bennett et al., 2016; Satoh et al., 2016). Staining human post-mortem tissue with Tmem119 was successful (Figure 3), however, it has been previously confirmed that the marker is sensitive to changes in homeostasis (Zrzavy et al., 2017) and its expression is downregulated in the context of AD and injury, making it also unsuitable for consistently labelling microglia between NDC and AD (Bennett et al., 2016; Krasemann et al., 2017; Kenkhuis et al., 2021). Similarly, other microglial-specific markers like P2Y12 are also sensitive to loss of homeostasis and would not be suitable for consistently labelling microglia in the AD brain (Mildner et al., 2017). A microglial marker whose expression increases in disease and is associated with phagocytosis is CD68 (Minett et al., 2016; Parhizkar et al., 2019), which is found in the lysosome of microglia and macrophages. CD68 labelled

microglia consistently in control and AD tissue (Figure 4), and so it was chosen as the preferred microglial marker. However, CD68 comes with its own set of limitations, including not being microglial specific as it also labels macrophages too, and it does not stain the cell cytoplasm. In mice, microglia phagocytosing synapses have usually reported synaptic markers inside CD68 lysosomes, and those inside Iba1-positive cells (Schafer et al., 2012; Paolicelli et al., 2017). However, for the aforementioned reasons, this was not possible with the human tissue. Nevertheless, an example image is shown demonstrating CD68 is found within Iba1/Tmem119-positive microglia, and that CD68 expression is increased near an A β plaque (Figure 3). On the other hand, Iba1 staining is poor near the plaque. Due to antibody incompatibilities between CD68 and synaptophysin, the synaptophysin antibody was also replaced for synapsin I, which is also a pre-synaptic marker.

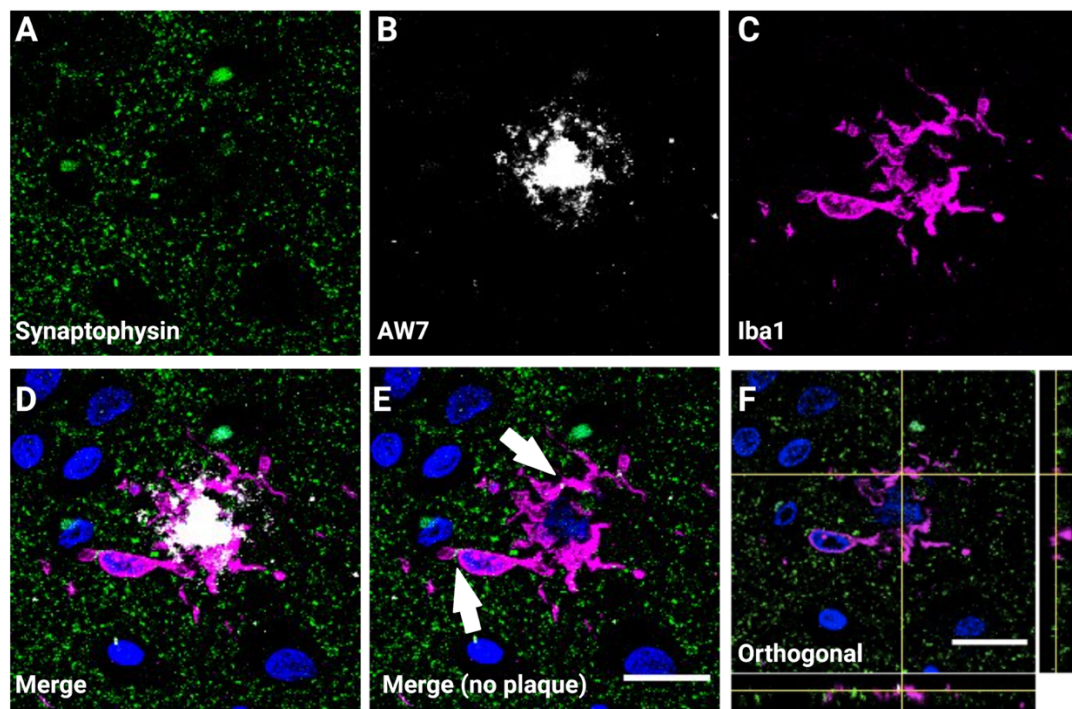


Figure 1. Microglia cluster around A β plaques and ingest synapses. Example confocal images acquired using a 63x oil-immersion lens demonstrating the staining quality of: (A) Synaptophysin (green), (B) AW7 labelling A β plaques (grey), (C) Iba1 labelling microglia (magenta) and counterstained nuclei with DAPI (blue) in non-demented Alzheimer's disease (AD) tissue. (D) Merged channels showing microglia clustering near the A β

plaque. (E) Merged channels showing ingested synaptophysin puncta inside Iba1-positive microglia (white arrows). (F) Orthogonal view of ingested synaptic material by microglia. Scale bars represent 20µm.

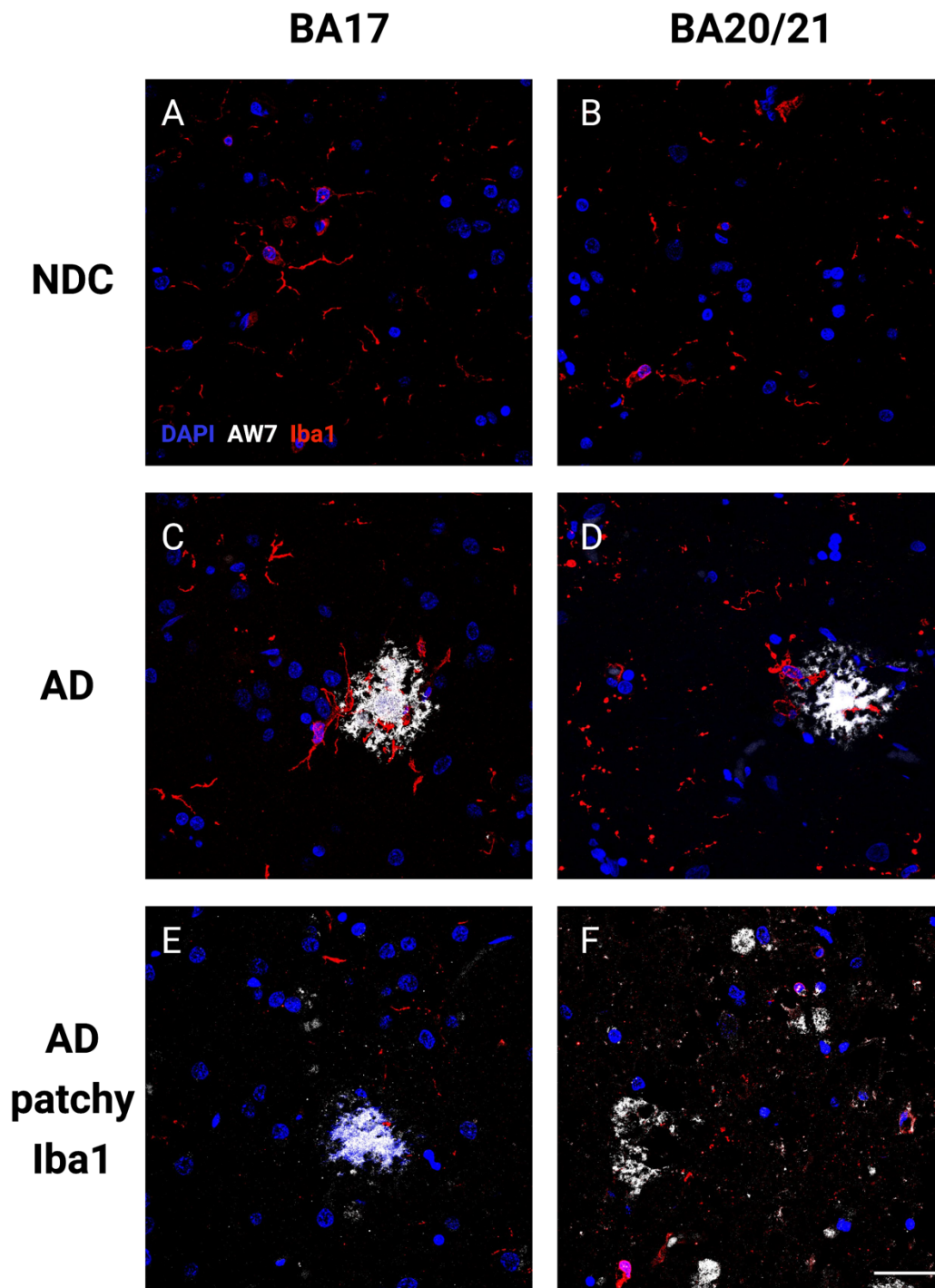
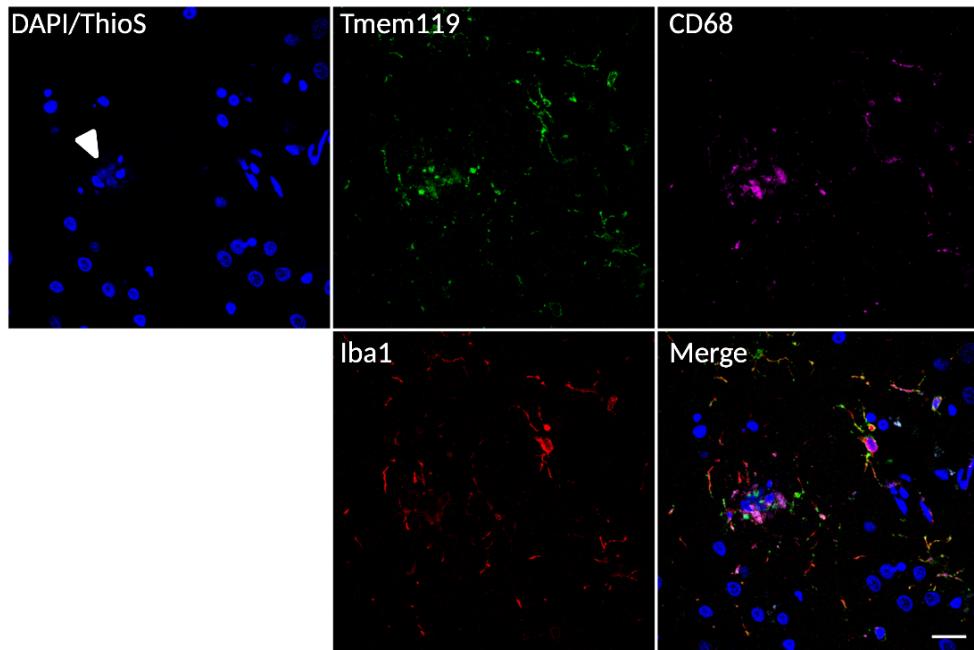


Figure 2. Iba1 staining of human post-mortem tissue. Example confocal images acquired using a 63x oil-immersion lens demonstrating the staining quality of Iba1 (red), AW7 labelling A β plaques (grey), and counterstained

nuclei with DAPI (blue) in non-demented control (NDC) and Alzheimer's disease (AD) tissue. Two brain areas were assessed, Brodmann area 17 (BA17) representing the primary visual cortex and Brodmann area 20/21 (BA20/21) representing the inferior temporal lobe. For each condition, the two brain areas come from the same case (i.e A and B come from the brain, and the same for C and D, and E and F). Images are max intensity projections of 4 μ m thick sections (step size 0.3 μ m). Scale bar 30 μ m.

A



B

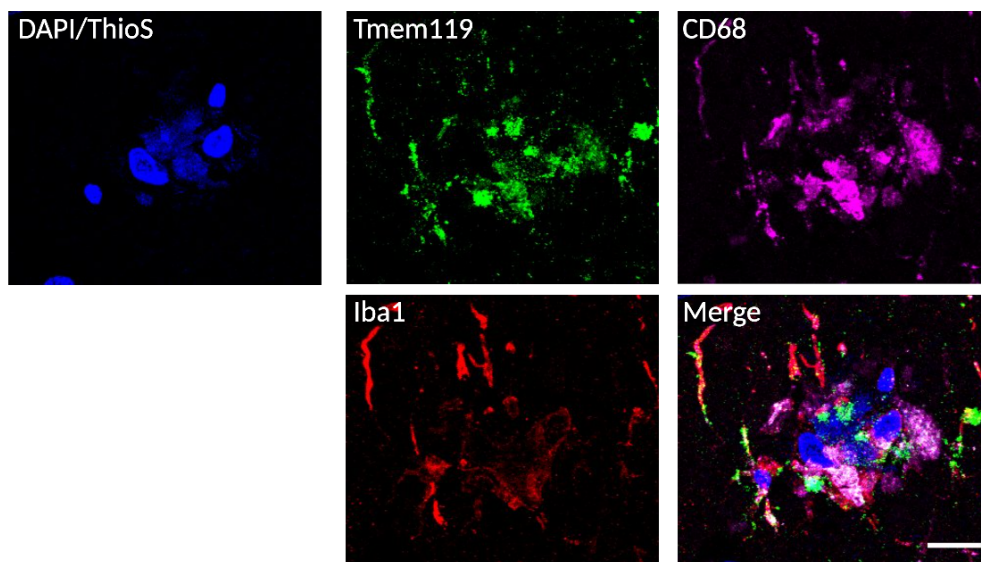
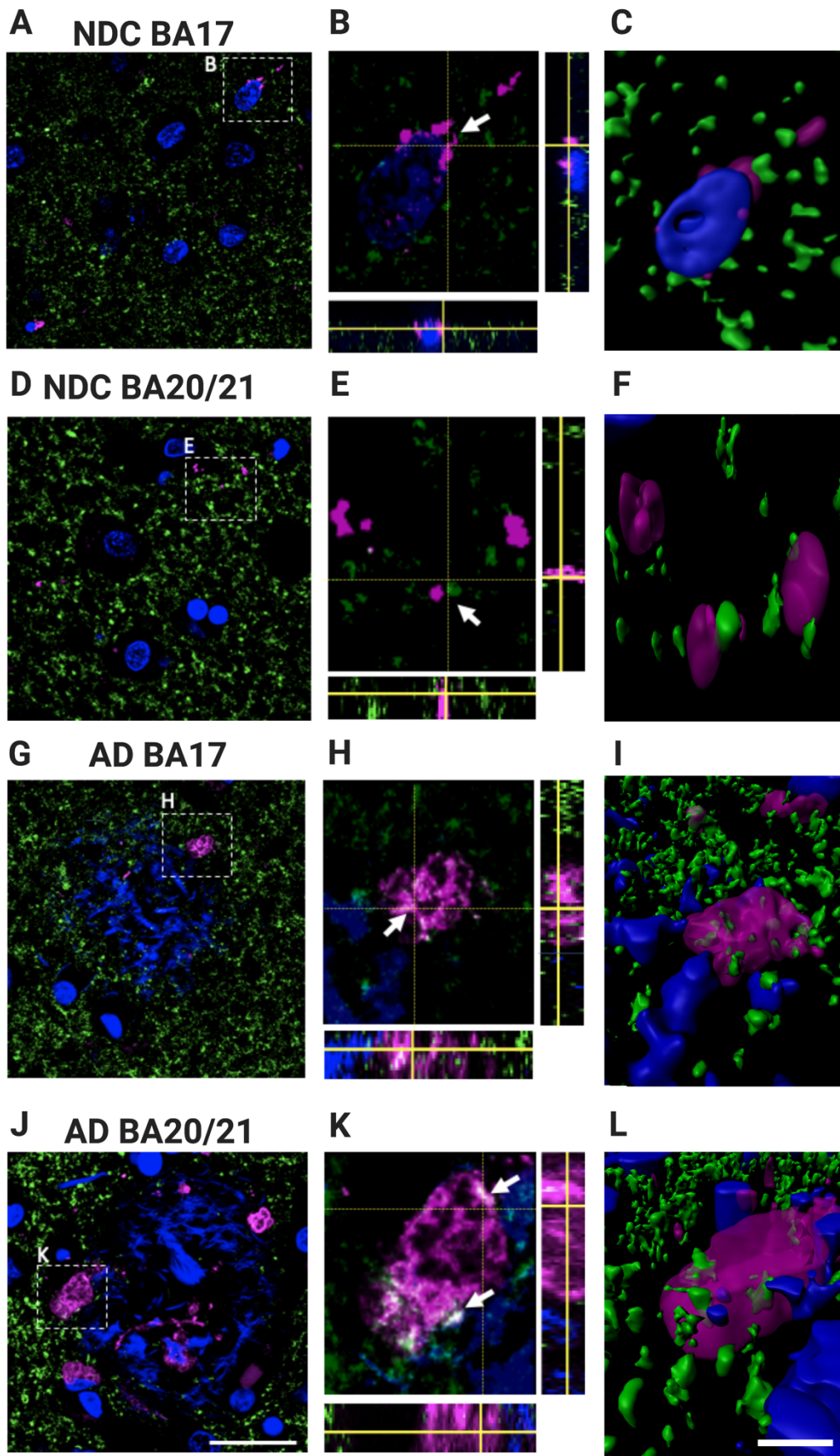


Figure 3. Validation of microglial markers in human post-mortem tissue. (A) Representative confocal images acquired using a 63x oil-immersion lens, showing DAPI-positive cells expressing the microglial specific marker Tmem119, which colocalises extensively with Iba1 (red) the lysosomal marker CD68 (magenta). A very low concentration of Thioflavin S was used to show Abeta plaques in blue (arrowhead), demonstrating an evident upregulation of CD68. Scale bar represents 20µm. (B) Insert from plaque-region shown in panel A. Scale bar represents 10µm.

2.2 Increased synaptic ingestion by microglia in human post-mortem tissue

Based on the staining optimization described above, we used CD68 to label microglial lysosomes alongside synapsin I (SynI) staining to label presynaptic proteins and thioflavin S to label plaques, in order to examine synaptic protein ingestion by microglia in AD. To assess synaptic internalisation, image stacks were 3D rendered and segmented on Matlab, followed by colocalisation thresholding of the images on FIJI. This provided a volumetric analysis of burdens and colocalisation. SynI signal localised within CD68+ microglia was observed in both control and AD brains, suggesting synaptic internalisation occurs in the ageing brain independently of disease (Fig. 4A-C, D-F, G-I, J-L). There was significantly increased colocalisation of CD68 and SynI in AD compared to control brains in both brain regions examined (Fig. 5A, linear mixed-effects model on Tukey transformed data: $F [1,73.8]=15.1$, $p=0.0002181$). Interestingly, there was also a significant effect of brain area with BA17 showing an increased CD68+SynI burden compared to BA20/21 ($F [1,73.9]=11.8$, $p=0.0009558$). Since microgliosis is a prominent feature of the AD brain (Itagaki et al., 1989; McGeer et al., 1993), CD68 burdens (% volume) were quantified. A significantly higher burden of CD68 was found in AD patients' brains compared to controls (Fig. 5B, $F [1,73.95]=34.5$, $p=1.12 \times 10^{-7}$), in line with previous literature (Minett et al., 2016). No significant brain area effects were established in CD68 burdens ($F [1,73.97]=0.5704$, $p=0.4525$). It is unclear whether individual microglia internalise synapses during AD more readily, or whether the increased microglial burden results in greater overall synapse ingestion. To examine this, the area of colocalisation between CD68

and Syn1 was normalised by the area occupied by CD68. When normalised, no significant difference between AD and controls were found (Fig. 5C, F [1,85.9]=0.663, p=0.418). Similar to the unnormalised data, there was a significant effect of brain area favouring increased CD68+Syn1 normalised to CD68 in BA17 compared to BA20/21 (F [1,74.15]=24.05, p=5.37x10⁻⁶). This could suggest more ingestion occurs in the AD brain because more microglia are present, although a caveat to this is that microglia numbers have not been measured (microglia burden as % volume covered by CD68 measured instead).



CD68 **SynI** **ThioS/DAPI**

Figure 4. Increased presence of synapsin 1 in CD68-positive microglial cells in Alzheimer's disease. (A, D, G, J) Confocal images reveal Syn1 staining (green) localised within or contacting CD68-positive microglial lysosomes (magenta) in both Alzheimer's disease (AD, n=23) and non-demented control (NDC, n=17) brain (arrows). Nuclei are labelled with DAPI and plaque fibrils with thioflavin S (blue). Large images in A, D, G, J (75x75 μm) show average projections of a stack of 10 optical sections. Scale bar represents 20 μm . (b, e, h, k) Insets (15x15 μm) show zoomed-in and orthogonal views of the stacks. Scale bar represents 5 μm . (C, F, I, L) 3-D reconstructions using Imaris. Scale bar represents 5 μm .

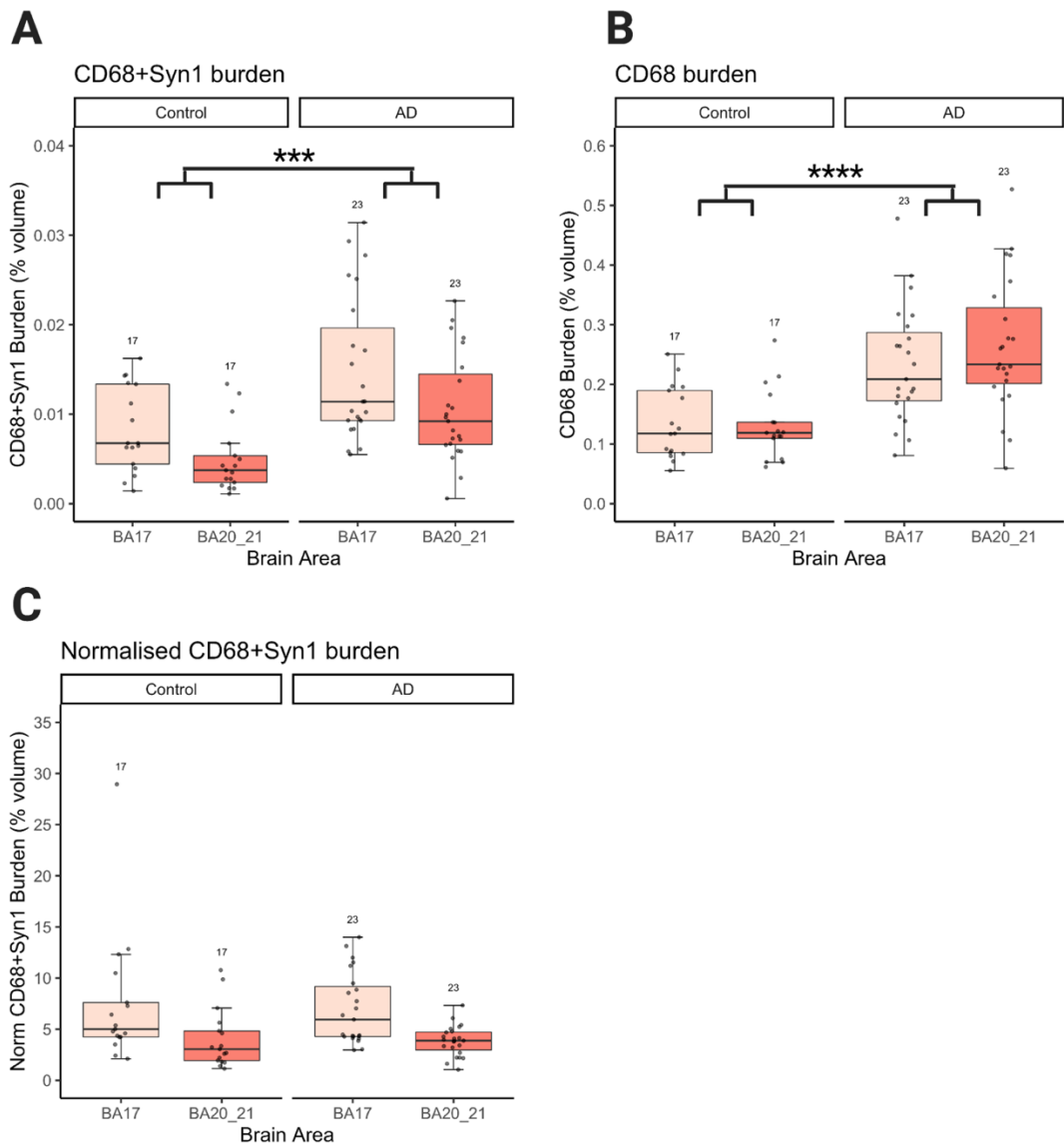


Figure 5. Increased presence of synapsin 1 in CD68-positive microglial cells in Alzheimer's disease. (A) Percent volume of colocalising CD68 and SynI staining in image stacks from BA17 (occipital lobe) and BA20/21 (inferior temporal lobe). Increased CD68+SynI burdens found in AD patients (n=23) compared to controls (n=17), $F [1,73.8]=15.1$, $p=0.0002181$. (B) Percent volume covered by CD68 staining (burden) in control and AD cases. Increased CD68 burdens found in AD patients compared to controls, $F [1,73.95]=34.5$, $p=1.12 \times 10^{-7}$. (C) CD68+SynI colocalisation volume normalised to the CD68 burden of corresponding case. Data were analysed with a linear mixed effects model on Tukey transformed data to fit the assumptions of the model (untransformed shown here). No differences were found in CD68+SynI burdens between AD and control cases in normalised data, $F [1,85.9]=0.663$, $p=0.418$. Each dot in bar graphs represents the mean of 20 values for a single case. The tops and bottoms of the bar graph represent the interquartile range, the line in the bar represents the median, and the error bars represent 1.5x interquartile range. For statistics, significance is considered for $p < 0.05$, and $***=p < 0.001$, $****p < 0.0001$.

In this cohort, three APOE genotypes were assessed, namely APOE3/3, APOE3/4, and APOE4/4. As discussed in the introduction, the presence of an APOE4 allele is a risk-factor for developing LOAD in a dose-dependent manner, and is associated with greater burdens of AD-related pathologies. The first set of analysis was based only if an APOE4 allele was present instead of taking into account all three different genotypes. The mixed-effect model showed that, overall, having an APOE4 allele was significantly associated to increased CD68+SynI colocalisation in AD cases (Fig. 6A, $F [1,73.9]=5.83$, $p=0.0182$). When the data are stratified based on the APOE4 allele, it can be seen that the E4 allele doesn't affect all groups the same, meaning that disease and brain area are likely influencing the outcome of the test. Indeed, when the APOE4 allele was set as the main variable and disease and brain area were set as the co-variables, both disease and brain area were found to significantly influence CD68+SynI colocalisation in an increasing manner ($F [1,73.89]=15.01$, $p=0.0002288$, and $F [1,73.94]=11.27$, $p=0.0012477$, respectively). However, the interaction between the APOE4 allele was not significant for neither disease nor brain area, which means it is statistically unwise to pursue with a posthoc test to find where these differences lie (F

[1,73.87]=0.0095, $p=0.922$, and $F [1,73.93]=0.0155$, $p=0.901$, respectively). In addition, the E4 allele was not associated to any changes in the CD68 burdens between AD and control cases (Fig 6B, $F [1,73.96]=0.0144$, $p=0.905$). Surprisingly, although when previously the data were normalised to the CD68 burden no differences were found between AD and control, when stratified based on the APOE4 allele the differences between AD and control from the unnormalised data are maintained (Fig 6C, $F [1,74.1]=8.395$, $p=0.004944$).

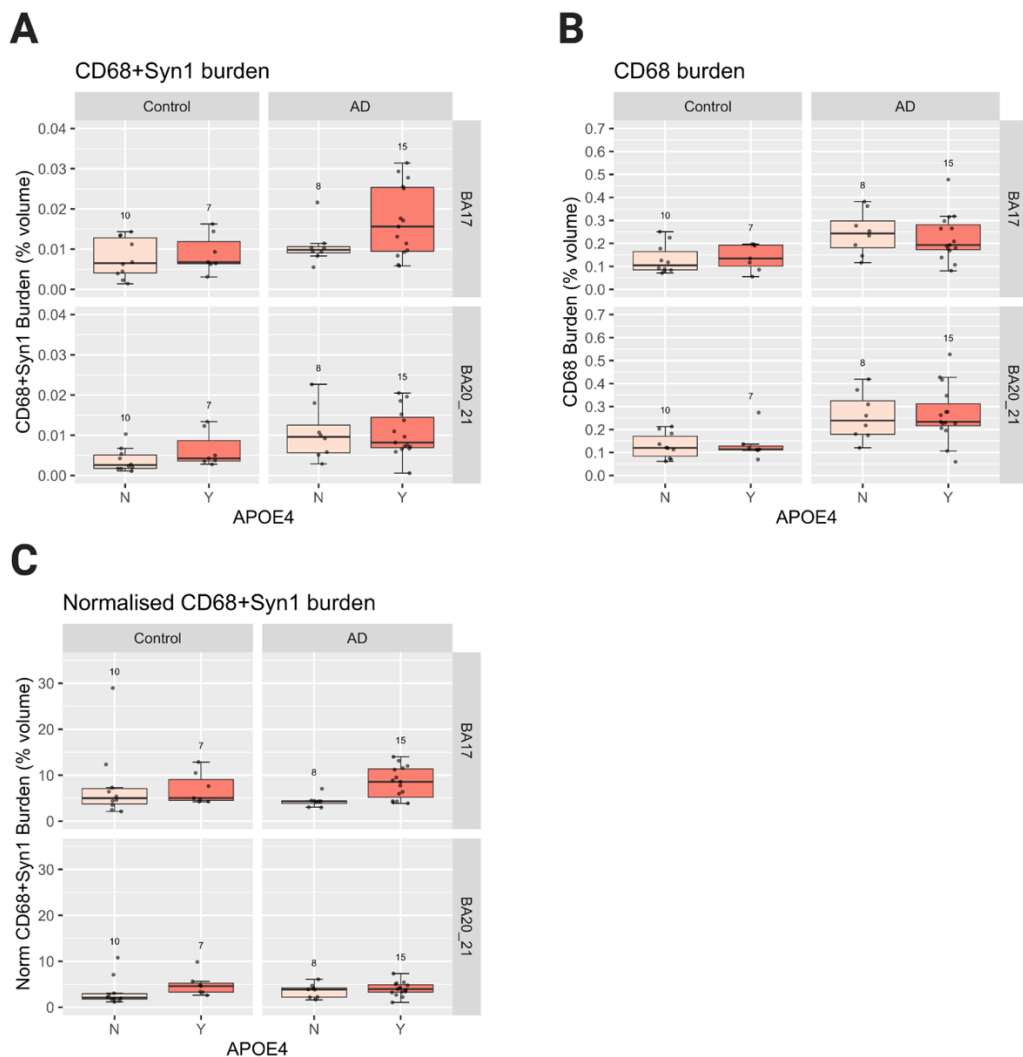


Figure 6. Data stratified by the presence of an APOE4 allele. Cases were assigned a no (N) or yes (Y) based on whether they had at least one APOE4 allele in their genotype. (A) Percent volume of colocalising CD68 and Syn1 staining in image stacks from BA17 (occipital lobe) and BA20/21 (inferior temporal lobe). Overall, the presence of an APOE4 allele was associated with

increased CD68+SynI burdens found in AD patients (n=23, APOE3 n=8, APOE4 n=15) compared to controls (n=17, APOE3 n=10, APOE4 n=7), $F [1,73.9]=5.83$, $p=0.0182$. (B) Percent volume covered by CD68 staining (burden) in control and AD cases. No changes in CD68 burdens found in AD patients compared to controls based on the APOE4 allele, $F [1,73.97]=0.0144$, $p=0.905$. (C) CD68+SynI colocalisation volume normalised to the CD68 burden of corresponding case. Data were analysed with a linear mixed effects model on Tukey transformed data to fit the assumptions of the model (untransformed shown here). When stratified by the APOE4 allele, the differences found in unnormalized data still stand when CD68+SynI burdens are normalised to CD68 between AD and control cases, $F [1,74.1]=8.395$, $p=0.004944$. Each dot in bar graphs represents the mean of 20 values for a single case. The tops and bottoms of the bar graph represent the interquartile range, the line in the bar represents the median, and the error bars represent 1.5x interquartile range. For statistics, significance is considered for $p<0.05$.

Next, the data was re-analysed using all APOE genotypes present in the cohort (3/3, 3/4, and 4/4). However, a limitation to this analysis is that no APOE4/4 control cases were used as the Brain Bank did have any cases with these criteria. Similarly to the APOE4 data, when all genotypes were considered, there was a significant increase of CD68+SynI colocalisation in AD cases compared to controls (Fig. 7A, $F [1,72.86]=14.80$, $p=0.0002534$). However, unlike the APOE4 only analysis, when considering all APOE genotypes the mixed-effects model deduced a significant effect of APOE to CD68 burdens (Fig. 7B, $F [1,72.94]=32.05$, $p=2.78 \times 10^{-7}$). Lastly, in agreement with the APOE4 analysis, when normalising the CD68+SynI burdens to CD68 and stratifying based on APOE there was a significant difference between AD and control cases (Fig. 7C, $F [1,73]=0.146$, $p=6.35 \times 10^{-6}$). Again, none of these variables showed a significant interaction in the test, so it is unclear whether how the other co-factors like brain area are affecting the data.

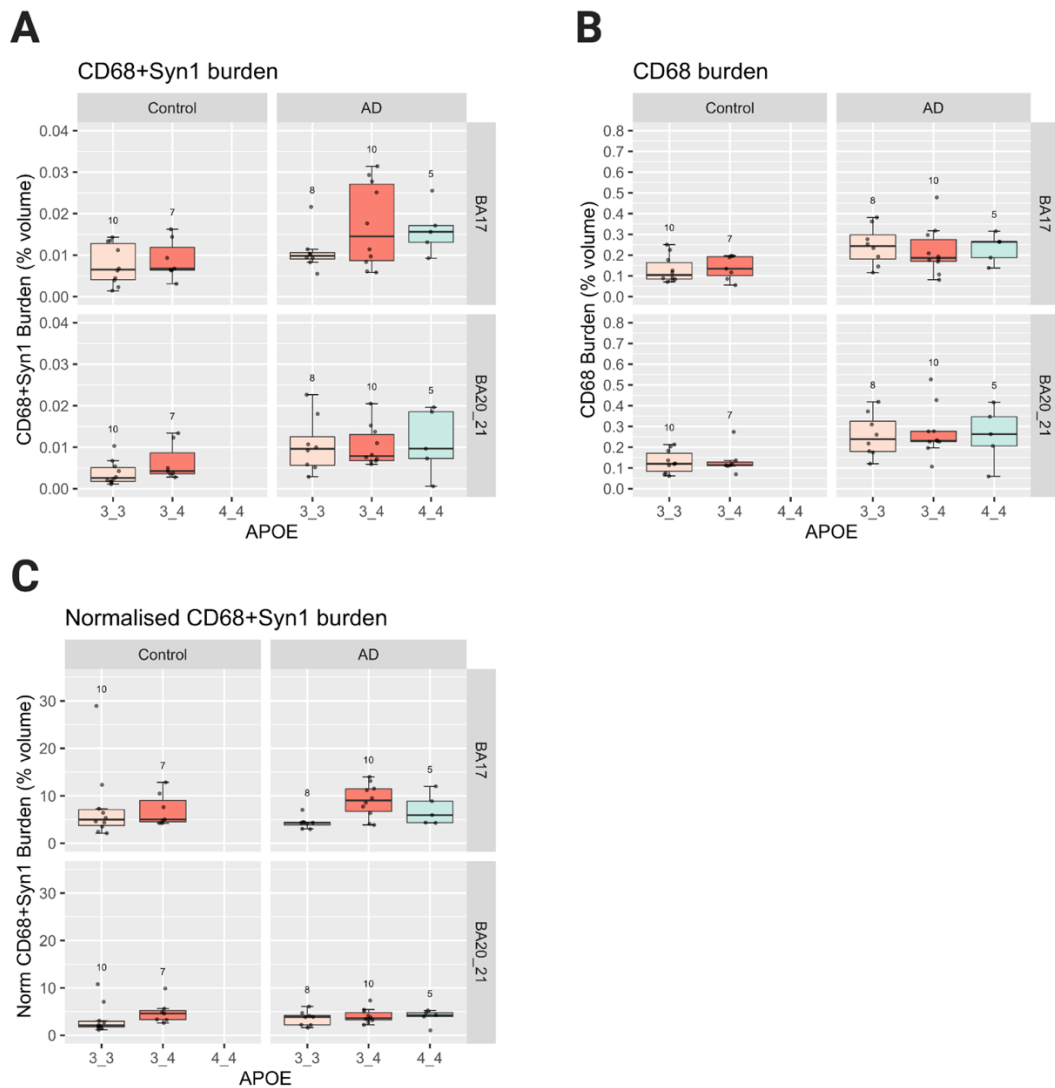


Figure 7. Data stratified by the presence of all APOE genotypes found in the cohort. (A) Percent volume of colocalising CD68 and Syn1 staining in image stacks from BA17 (occipital lobe) and BA20/21 (inferior temporal lobe). Overall, the APOE genotype significantly influenced CD68+Syn1 burdens found in AD patients by increasing the burdens (n=23, APOE3/3 n=8, APOE3/4 n=10, APOE4/4 n=5) compared to controls (n=17, APOE3/3 n=10, APOE3/4 n=7), $F [1,72.86]=14.80$, $p=0.0002534$. (B) Percent volume covered by CD68 staining (burden) in control and AD cases. The APOE genotypes account to variability in CD68 burdens found in AD patients compared to controls, $F [1,72.94]=32.05$, $p=2.78 \times 10^{-7}$. (C) CD68+Syn1 colocalisation volume normalised to the CD68 burden of corresponding case. Data were analysed with a linear mixed effects model on Tukey transformed data to fit the assumptions of the model (untransformed shown here). When stratified by the APOE genotypes, the differences found in unnormalized data still stand when CD68+Syn1 burdens are normalised to CD68 between AD and control cases, $F [1,73]=0.146$, $p=6.35 \times 10^{-6}$. Each dot in bar graphs represents the mean of 20 values for a single case. The tops and bottoms of the bar graph

represent the interquartile range, the line in the bar represents the median, and the error bars represent 1.5x interquartile range. For statistics, significance is considered for $p < 0.05$.

Sex is also a risk factor, with women having an increased prevalence of developing AD than men (Podcasy and Epperson, 2016; Viña and Lloret, 2010). Whether or not sex affects the process of synaptic ingestion by microglia and synapse loss overall is unknown. Here, the mixed-effects analysis showed a trend towards significance in CD68+SynI burdens in women compared to men (Fig. 8A, $F [1,73.98]=3.80$, $p=0.0549$). On the other hand, no sex effects were found to influence the CD68 burdens (Fig. 8B, $F [1,74.01]=0.3844$, $p=0.5372$). Lastly, a non-significant trend towards increased the normalized CD68+SynI burden was also in women (Fig. 8C, $F [1,74.09]=3.75$, $p=0.0565$).

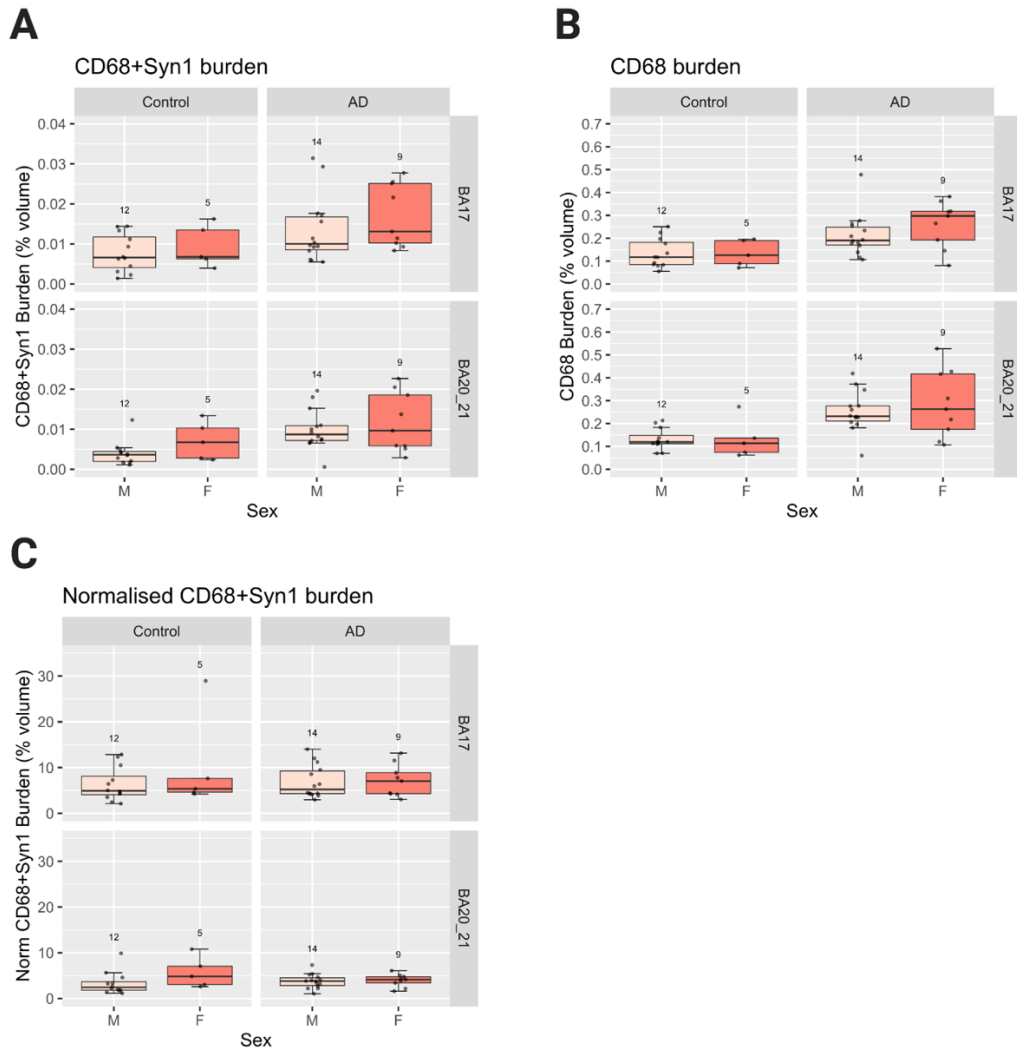


Figure 8. Data stratified by sex. (A) Percent volume of colocalising CD68 and Syn1 staining in image stacks from BA17 (occipital lobe) and BA20/21 (inferior temporal lobe) in male (M) and female (F) patients. Overall, stratifying by sex resulted in a trend towards increasing CD68+Syn1 burdens (F [1,73.98]=3.80, $p=0.0549$). (B) Percent volume covered by CD68 staining (burden) in control and AD cases. The APOE genotypes account to variability in CD68 burdens found in AD patients compared to controls, F [1,72.94]=32.05, $p=2.78 \times 10^{-7}$. (C) CD68+Syn1 colocalisation volume normalised to the CD68 burden of corresponding case. Data were analysed with a linear mixed effects model on Tukey transformed data to fit the assumptions of the model (untransformed shown here). When stratified by the APOE genotypes, the differences found in unnormalized data still stand when CD68+Syn1 burdens are normalised to CD68 between AD and control cases, F [1,73]=0.146, $p=6.35 \times 10^{-6}$. Each dot in bar graphs represents the mean of 20 values for a single case. The tops and bottoms of the bar graph represent the interquartile range, the line in the bar represents the median, and the error bars represent 1.5x interquartile range. For statistics, significance is considered for $p < 0.05$.

2.3 Increased synaptic ingestion by microglia near A β plaques

To date, one of the most well established mechanisms for synapse loss in AD is the synaptic accumulation of toxic oligomeric A β , which surround senile plaques (Koffie et al., 2012; Jackson et al., 2019). Furthermore, microglia aggregate near A β plaques and upregulate inflammatory and phagocytic markers (Keren-Shaul et al., 2017; Rodriguez, Tai, LaDu and Rebeck, 2014; Itagaki et al., 1989; Krasemann et al., 2017; Reed-Geaghan, Croxford, Becher and Landreth, 2020). Hence, it was hypothesised that microglia phagocytose more synapses close to A β plaques in AD cases, contributing to the exacerbated synapse loss near plaques. Each confocal stack was marked on whether it contained a plaque, and a plaque analysis on all AD cases based on this parameter. Indeed, images with A β plaques showed a marked increase in CD68 and SynI colocalisation (Fig. 9) (Fig. 10A, F [1,877.14]=24.78, $p=7.73 \times 10^{-7}$). Moreover, there was a significant interaction between the presence of a plaque and brain area (F [1,877.38]=13.99, $p=0.0001955$). Post-hoc analysis (estimated marginal means) showed that the main significant effect is an increase in CD68+SynI burden only in BA17 and not BA20/21 ($p<0.0001$). Similarly, there was an increased CD68 burden when plaques were present in the confocal stacks (Fig. 10B, F [1,869.74]=48.35, $p=6.99 \times 10^{-6}$) and a significant interaction between plaques and brain area (F [1,869.93]=11.20, $p=0.0008535$). Specifically, the CD68 burden is increased in plaque-containing images in BA17, but not BA/2021 ($p<0.0001$). Of note, synaptic internalisation was also evident in regions distant from plaques, suggesting it is not an entirely plaque-dependent phenomenon (Figs. 10B and D). When normalised to CD68 burden, the synaptic colocalisation in microglia in plaque-containing images was not found to be increased (Fig. 10C, F [1,882.30]=0.7264, $p=0.394$).

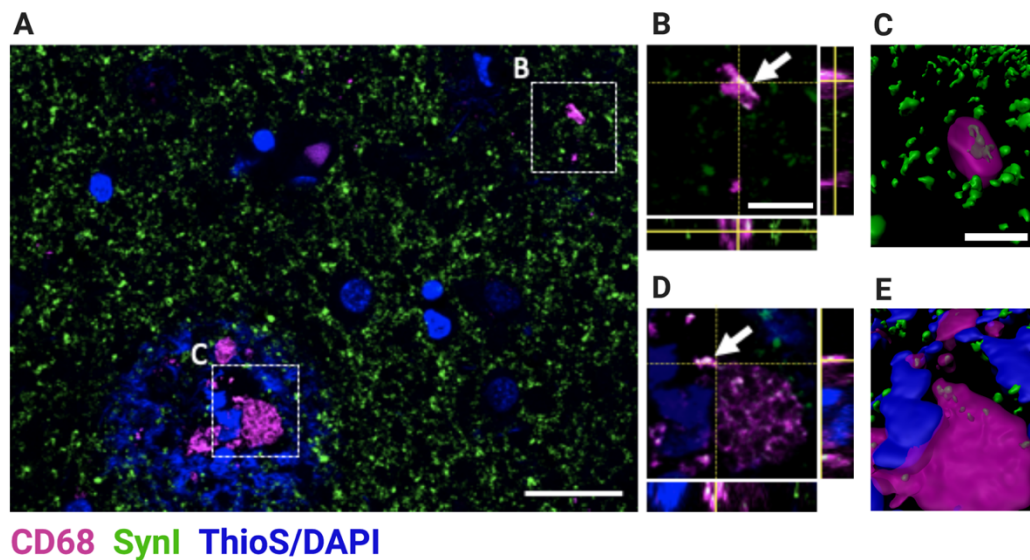


Figure 9. Plaque-associated CD68-positive microglial cells internalise synapsin I in Alzheimer's disease. (A) Confocal image (average projections of a stack of 10 optical sections) reveals Syn1 staining (green) localised within or contacting CD68-positive microglial lysosomes (magenta) in Alzheimer's disease (AD, n=22-23). Nuclei are labelled with DAPI and plaque fibrils with thioflavin S (blue). (B and C) Insets (15x15 μm) show zoomed-in and orthogonal views of the stacks, respectively. (D and E) 3-D reconstructions using Imaris. Scale bar: A, 20 μm ; B, 5 μm , D, 5 μm .

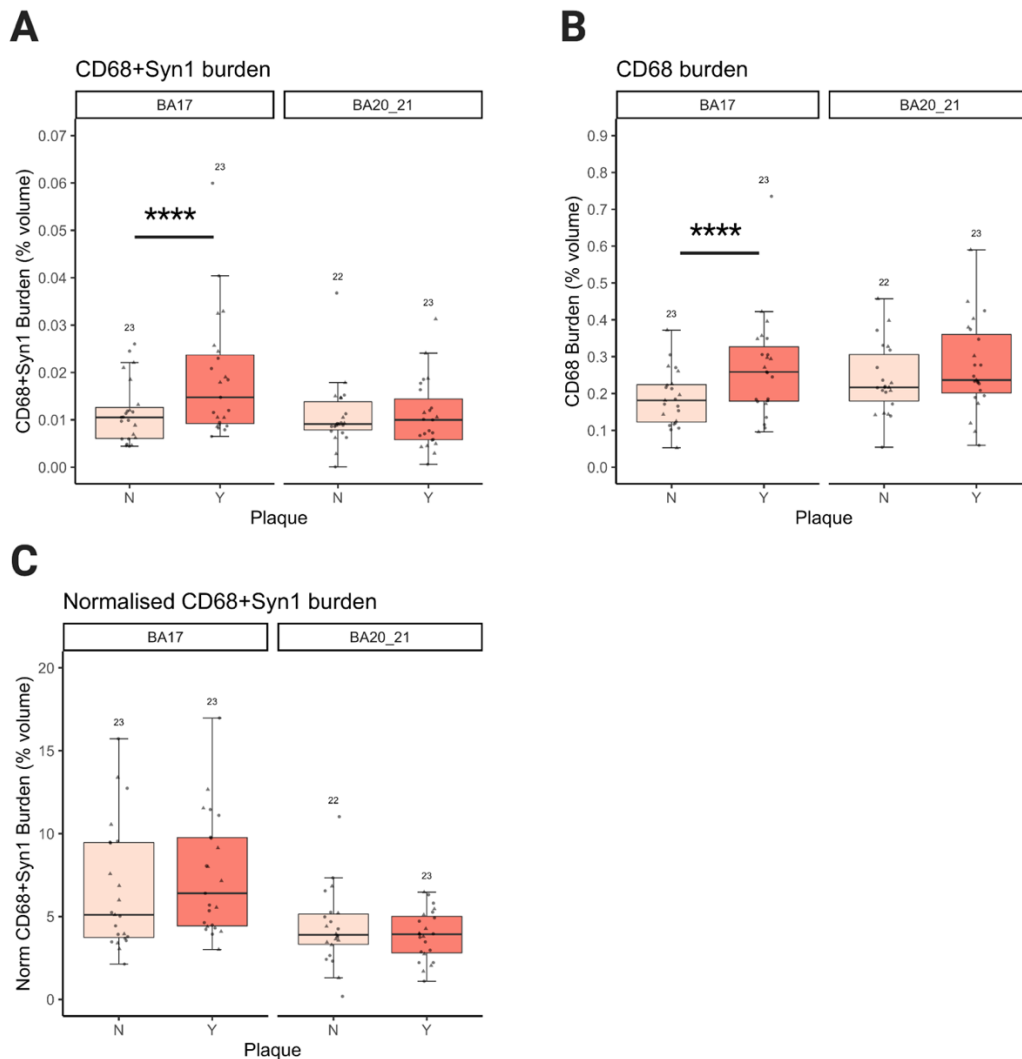
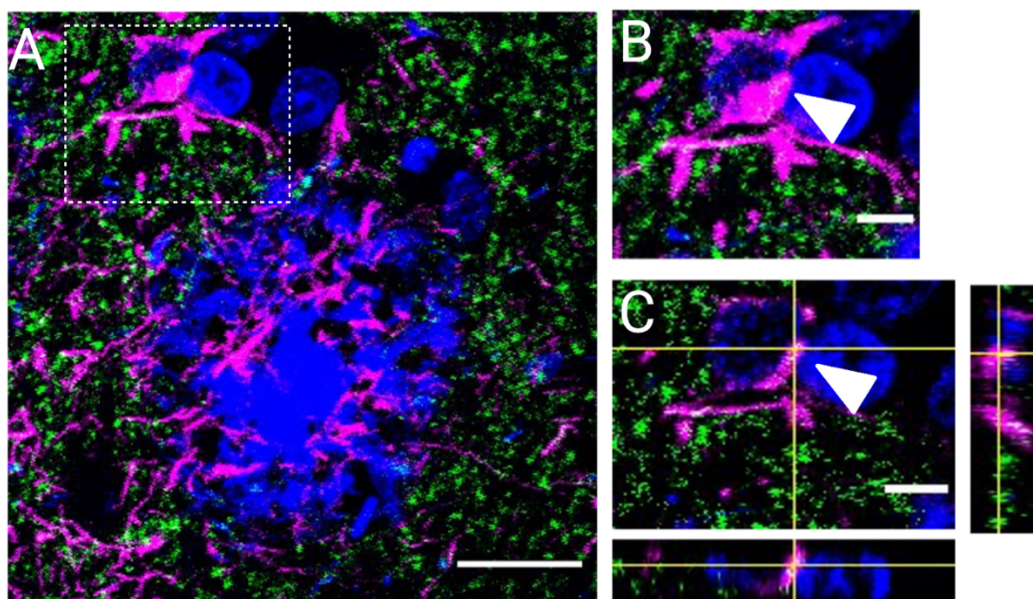


Figure 10. Plaque-associated increased synapsin I in CD68-positive microglial cells in Alzheimer’s disease. Images were stratified based on whether they had a plaques (Y) or not (N). (A) Percent volume of colocalising CD68 and Syn1 staining in image stacks from BA17 (occipital lobe) and BA20/21 (inferior temporal lobe). Increased CD68+Syn1 burdens found in AD patients in images containing A β plaques, $F [1,877.14]=24.78$, $p=7.73 \times 10^{-7}$. (B) Percent volume covered by CD68 staining (burden) in AD cases with and without plaques. Increased CD68 burdens found in images containing A β plaques, $F [1,869.74]=48.35$, $p=6.99 \times 10^{-6}$. (C) CD68+Syn1 colocalisation volume normalised to the CD68 burden of corresponding case. No differences were found in CD68+Syn1 burdens between images with and without plaques in normalised data, $F [1,882.30]=0.7264$, $p=0.394$. Each dot in bar graphs represents the mean of 20 values for a single case. Data were analysed with a linear mixed effects model on Tukey transformed data to fit the assumptions of the model (untransformed shown here). The tops and bottoms of the bar graph represent the interquartile range, the line in the bar represents the median, and the error bars represent 1.5x interquartile range. For statistics, significance is considered for $p < 0.05$, and **** $p < 0.0001$.

2.4 Astrocytic contribution to synaptic ingestion in AD

So far, microglia have been shown to ingest more synapses in AD brains compared to NDC brains, particularly near A β plaques. Astrocytes are also capable of phagocytosis, and have been shown to engulf synapses in the developing mouse brain. In human AD brains, astrocytes contain dystrophic pre-synaptic terminals, suggesting they contribute to debris clearance, but whether they contribute to healthy synapse elimination is unknown. By applying the same approaches, human tissue has been stained for the cytoskeletal astrocytic marker GFAP (glial fibrillary acidic protein) along with synapsin I and ThioS for plaques (Figure 11A-B). Preliminary images show SynI inside GFAP-positive cells too in orthogonal sections (Figure 11C), suggesting astrocytes can also ingest synapses in the human brain.



GFAP **SynI** **ThioS/DAPI**

Figure 11. Pre-synaptic ingestion by astrocytes. Example confocal image acquired using a 63x oil-immersion lens from human post-mortem tissue from an AD brain was stained with the cytoskeletal marker of astrocytes GFAP (magenta), and pre-synaptic terminals were stained with synapsin I (SynI, green). Nuclei are labelled with DAPI and plaque fibrils with thioflavin S (both blue). (A) Max-intensity projection of 4 μ m thick stack (step size 0.3 μ m) showing astrocytes near the plaque, as well as astrocytic projections surrounding the plaque core. Scale bar 15 μ m. (B) Insert from A (size) showing

colocalisation between GFAP and SynI (white). White arrows point towards these sites of co-localisation. Scale bar 5 μ m. (C) Orthogonal section of B indicating SynI puncta inside GFAP-positive cells. Scale bar 5 μ m.

3. Discussion

In recent years, microglial interactions with synapses have been shown to be an important part of healthy brain development in mice. Synaptic internalisation by microglia is a vital process during development in order to ensure correct synaptic densities and network connectivity (Filipello et al., 2018; Paolicelli et al., 2011; Schafer et al., 2012; Oosterhof et al., 2019). Microglia can also directly contact neuronal cell bodies using purinergic signalling as a protective phenotype (Cserép et al., 2020) and can also help the formation of synapses via their secretome (Lim et al., 2013; Parkhurst et al., 2013). However physiological functions of microglia may be compromised in diseases associated with changes in gene expression, morphology and neurodegeneration (Keren-Shaul et al., 2017). For instance, in animal models of AD microglia are aberrantly involved in synaptic elimination. Mice and non-human primates challenged with oligomeric A β display reduced synaptic densities and increased levels of synaptic proteins inside microglial CD68-positive compartments (Hong et al., 2016; Beckman et al., 2019). Similarly, in tauopathy mouse models, microglia also contain more synaptic proteins (Dejanovic et al., 2018; Benetatos et al., 2020), and the classical complement cascade has been suggested as a possible mechanism for this synaptic elimination. In individuals with AD, C3 protein levels have been shown to increase comparably to non-neurological controls, suggesting microglia in AD may recognise synapses via the complement system similar to mice (Wu et al., 2019). Nevertheless, evidence for this process in human AD is negligible and suggested only from morphological analysis by electron microscopy on two cases showing synaptic vesicles inside microglia (El Hajj et al., 2019).

Currently, there are no studies that have quantitatively addressed the presence of synaptic proteins inside microglia in human brains. This work on human post-mortem tissue comparing 23 confirmed AD cases to 17 age-matched controls provides evidence that microglia in human AD indeed contain more synapses, shown by greater levels of synapsin I present in CD68-positive microglial lysosomes. Furthermore, this effect is magnified near A β plaques which are known to alter microglial phenotypes (Itagaki et al., 1989; Rodriguez et al., 2014; Keren-Shaul et al., 2017), but only in the occipital cortex (BA17). Interestingly, when the synaptic ingestion by microglia is normalised to the microglial burdens, there is no longer a statistical difference between control and AD cases. These data imply that the increased ingestion of synaptic protein by microglia in AD is either due to increased numbers of microglia or that hypertrophy of microglia accounts for the greater CD68 burden and thus reflects more synaptic protein per microglial cell (due to tissue thickness reliable cell counts for normalisation could not be generated). It is still possible, however, that increased synaptic ingestion and higher CD68 burdens are unrelated. Furthermore, astrocytes have been shown to clear dystrophic pre-synaptic terminals in human AD brains, suggesting a role in removing degenerating synapses. To this extent, immunohistochemistry parameters have been optimised to replicate this study with the astrocytic marker GFAP. Pre-synaptic inclusions have been found inside GFAP-positive cells in AD tissue, and whether more synapses are ingested by astrocytes in AD will be determined in future experiments. A limitation to this is the use of only one synaptic marker, and that it is a pre-synaptic that is non-specific to excitatory and inhibitory synapses. Staining with PSD-95 for excitatory post-synapses was not ideal because of non-specific staining of nuclei and high background levels, which becomes problematic when assessing phagocytosis. Pilot stains have been optimised to look into whether inhibitory synapses are also ingested more by microglia in human AD brains. To this extent, the inhibitory neuronal marker GAD65/67 was used in combination to

CD68 and Iba1, where it is evident that inhibitory neuronal markers are also ingested by microglia in AD brains (Figure 12).

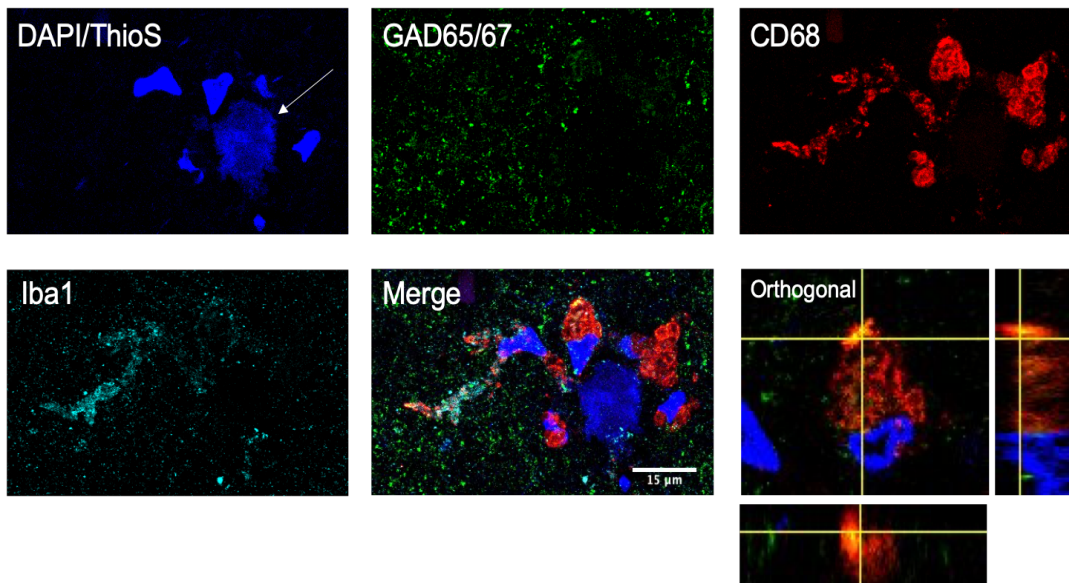


Figure 12. Inhibitory cells are ingested by human microglia. Example confocal image acquired using a 63x oil-immersion lens from human post-mortem tissue from an AD brain was stained with the inhibitory neuronal marker GAD65/67 (green), lysosomal microglia/macrophage marker CD68 (red) and cytoplasmic microglia/macrophage marker Iba1 (cyan). Nuclei are labelled with DAPI and plaque fibrils with thioflavin S (both blue).

An interesting finding was that although BA17 is a brain area that displays more protection from AD pathologies until later stages, it was also associated with a greater amount of synaptic ingestion by microglia than BA20/21 which is affected earlier on. Also, plaque-associated enhanced synaptic ingestion was only present in BA17. Although this appears counter-intuitive, it is possible that most damage to synapses has already occurred by the time the tissue is donated and microglia have cleared most synapses already. On the other hand, this process is occurring at an earlier stage in BA17 where the pathology is more recent, and it is possible modelling an earlier stage of AD. Of note, by comparing example images of microglia ingesting synapses in mouse brains with AD-like pathology, it can be appreciated that more synapses are internalised by mouse microglia compared to human microglia, and that often

these inclusions are larger. It is possible this happens because mouse models catch this process during disease peak, whereas the human brains come from late-stage AD. Also, mouse models of AD tend to overexpress pathological proteins and are considered aggressive due to the accelerated pathology. It would be interesting, therefore, to not only investigate synaptic ingestion by microglia in earlier stages of AD, but also in younger controls to determine whether this process is influenced by age. One key downside to this idea is that Braak stage V and VI are definitive of AD (in combination with plaque pathology and cognitive decline pre-mortem), but early Braak stages could signify MCI (therefore absence of dementia) or other forms of dementia, like FTD and vascular dementia.

An exciting outcome from the analysis of human post-mortem tissue is that a significant association between the APOE4 allele and increased synaptic ingestion by microglia was found. To briefly summarise the points discussed in the introduction, APOE4 is associated to greater synapse loss, more A β and tau pathology, and a more reactive microglial phenotype. It is likely that all these factors come together to induce more synaptic ingestion by human microglia in AD brains. These are observational data however, and the question remains: does APOE4 make microglia more phagocytic or are more synapses degenerating and thus need to be cleared away? Both are plausible explanations, and in tandem are potential contributors to synapse loss and cognitive decline.

The data from this analysis could be improved by complementing them with super resolution imaging. In collaboration with the Horrocks lab that specialises in super-resolution imaging, many attempts were made at staining tissue to allow for super-resolution with photo-activated fluorophores and photoactivated localisation microscopy (PALM). The idea behind this is that primary antibodies are conjugated with secondary antibodies that become photoactivated, or “blink”, when they are in close proximity. Unfortunately, this

was unsuccessful because there was a lot of background “blinking” due to the human tissue which masks any real signal.

Although it is important to address synaptic ingestion in human AD brains, post-mortem human tissue is limited in that it only provides a snapshot of the disease and does not allow for studies of the kinetics of synaptic phagocytosis. Importantly, a considerable limitation of observational data such as these is that they do not address whether the synapses ingested were active and healthy, which would mean aberrant phagocytosis is taking place, or that neurons and synapses which are degenerating are being cleared by microglia, which would be physiological. While this question has not been answered by the data here, mouse models of AD where the complement proteins are reduced genetically or pharmacologically, have shown a rescue of synaptic LTP and a reduction of microglial elimination of synapses (Bie et al., 2019; Hong et al., 2016; Shi et al., 2017a; Dejanovic et al., 2018). Taking this into consideration, it is likely that components of the complement cascade, like C3 and C1q, are upregulated in response to the neurodegeneration and pathology found in the AD brain, but instead of the finely tuned tagging of synapses seen in development, in disease this process is uncontrolled and healthy synapses are aberrantly ingested too. The increased levels of complement proteins found in the AD and diseased brains (Wu et al., 2019; Michailidou et al., 2015; Stephan et al., 2013), and particularly the synapses (Hesse et al., 2019), support this hypothesis and warrant further investigation into the mechanisms by which more synapses are ingested in the AD.

Chapter 4: *In-vitro* ingestion of human synaptoneuroosomes by glial cells

1. Introduction

In the previous chapter, it was observed that microglia contain greater levels of the pre-synaptic marker synapsin I inside the CD68 lysosomal compartment in AD brains compared to NDC brains. The use of human post-mortem tissue is, however, limited by a single snap-shot at the end of disease. It is therefore difficult to establish a molecular or cellular mechanism for this observation. Moreover, it is unknown whether the transcriptome changes that occur in microglia in AD (Srinivasan et al., 2020; Mathys et al., 2019; Keren-Shaul et al., 2017) induce an enhanced phagocytosis profile leading to greater synaptic uptake, or if synapses themselves are becoming more prone to elimination. For example, synapses can be tagged with complement proteins, like C1q or C3, inviting microglia to eliminate them in both health and disease (Michailidou et al., 2015; Stevens et al., 2007; Hong et al., 2016; Shi et al., 2017a). Alternatively, proteins like MFG-E8 can bind on the exposed phosphatidylserine of neurons which in turns signals microglia to undergo phagocytosis of those neurons (Brelstaff et al., 2018). On the other hand, it is possible that “don’t eat me” signals at the synapse, like CD47, are downregulated in AD leading to enhanced phagocytosis of synapses (Lehrman et al., 2018). Indeed, the lab has previously shown that complement proteins and MFG-E8 protein levels go up in AD synapses, while CD47 goes down (Hesse et al., 2019). This chapter aims to test the hypothesis that such synaptic changes contribute to the enhanced synaptic ingestion seen in AD microglia of the human post-mortem. To do this, snap-frozen tissue from the temporal tip (Brodmann area 38) of NDC and AD brains were processed to yield synaptoneurosome preparations, or synapse-enriched fractions. These

fractions were tagged with pHrodo-RED, a pH indicator that fluoresces red in acidic conditions, like those found in the lysosomes of cells (Byun and Chung, 2018; Lehrman et al., 2018; Liddel et al., 2017). Then, these pHrodo-tagged synaptoneurosomes were incubated with primary microglia isolated from surgically resected human tissue, as well as primary microglia from adult mice. Using live imaging, the phagocytosis of human synaptoneurosomes was tracked using the pHrodo indicator over time in order to determine whether the amount and rate of phagocytosis of microglia differs between AD and NDC brains. Lastly, having shown in the previous chapter that astrocytes are also capable of ingesting synapses in human brains, a similar approach was used to assess phagocytosis of pHrodo-tagged synaptoneurosomes by primary mouse astrocytes.

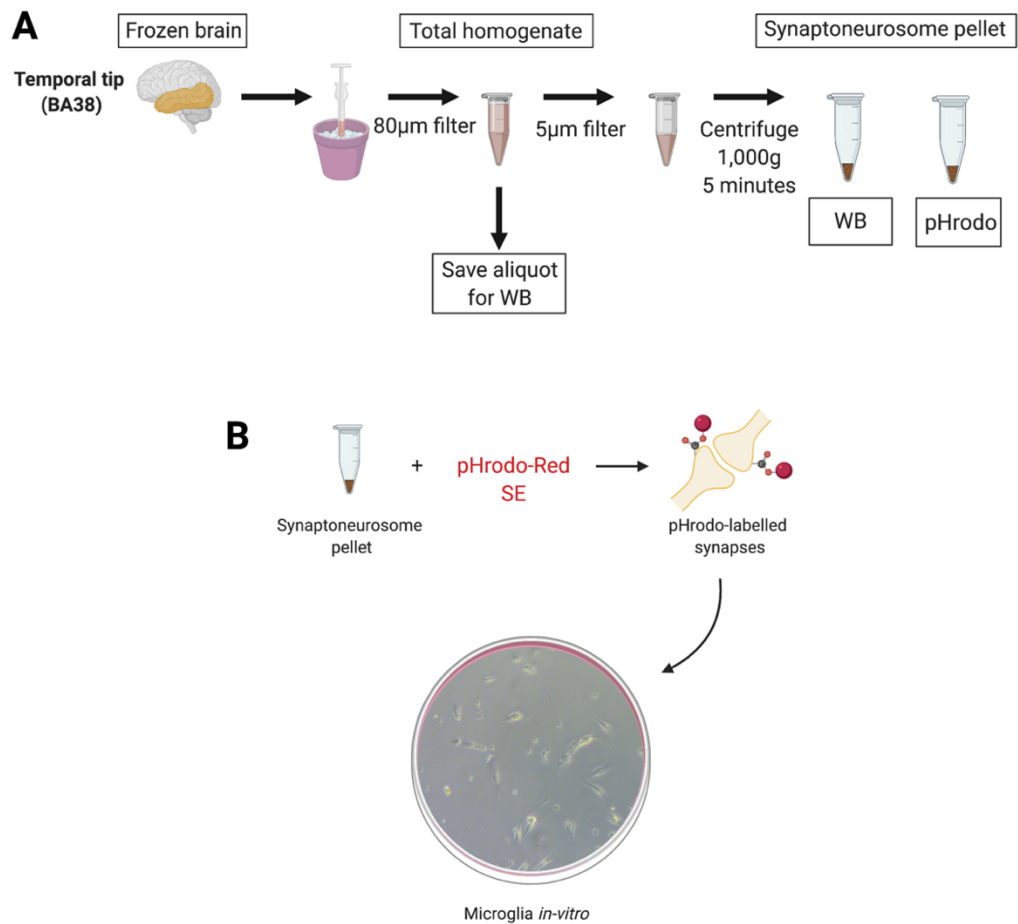


Figure 1. Schematic diagram of synaptoneurosomes preparation and pHrodo-conjugation for phagocytosis assays. (A) The temporal tip, or BA38, from non-demented control and Alzheimer's disease brains was Dounce homogenised and filtered to yield the total homogenate, a part of which was collected for Western blot (WB) validation. Through another round of filtering and centrifugation a synaptoneurosomes pellet was achieved, which was split into two equal parts, one of WB validation and the other for the phagocytosis assays in B. (B) The isolated synaptoneurosomes pellets were tagged with pHrodo-Red Succinimidyl Ester (SE). These preparations were then given to primary microglia *in-vitro*.

2. Results

2.1 Synaptoneurosomes validation

The preparation of human synaptoneurosomes was performed following a previously validated protocol, showing in EM detail re-annealed pre- and post-synaptic puncta tethered together (Tai et al., 2014). Synaptoneurosomes from 16 NDC cases and 15 AD cases were pooled separately for challenging glial cells in culture. Prior to any assays, these synaptoneurosomes were quality checked to test for synaptic enrichment. Aliquots from the total homogenate and the synaptoneurosome fractions for each brain were protein extracted and prepared for Western blotting (see Methods chapter). The pre-synaptic marker synaptophysin and excitatory post-synaptic marker PSD-95 were chosen to assess synaptic enrichment, while histone (H3) was chosen as a nuclear marker that should not be found in abundant levels at the synapse. The full-length Western blot is shown in Figure 2A, and total protein levels were measured with Ponceau S stain (Figure 2B) to normalise protein levels. Comparing the total homogenate to the synaptoneurosomes preparations showed that both synaptophysin and PSD-95 were enriched in the synaptic fractions, while histone levels were de-enriched (Figure 2C). Cases in which histone H3 levels were not de-enriched were either made from scratch or excluded, depending on tissue availability. Therefore, the synaptoneurosome preparations were successfully enriched in synapses from human brains. A full list of all gels generated for these experiments can be found in Appendix Figure 1.

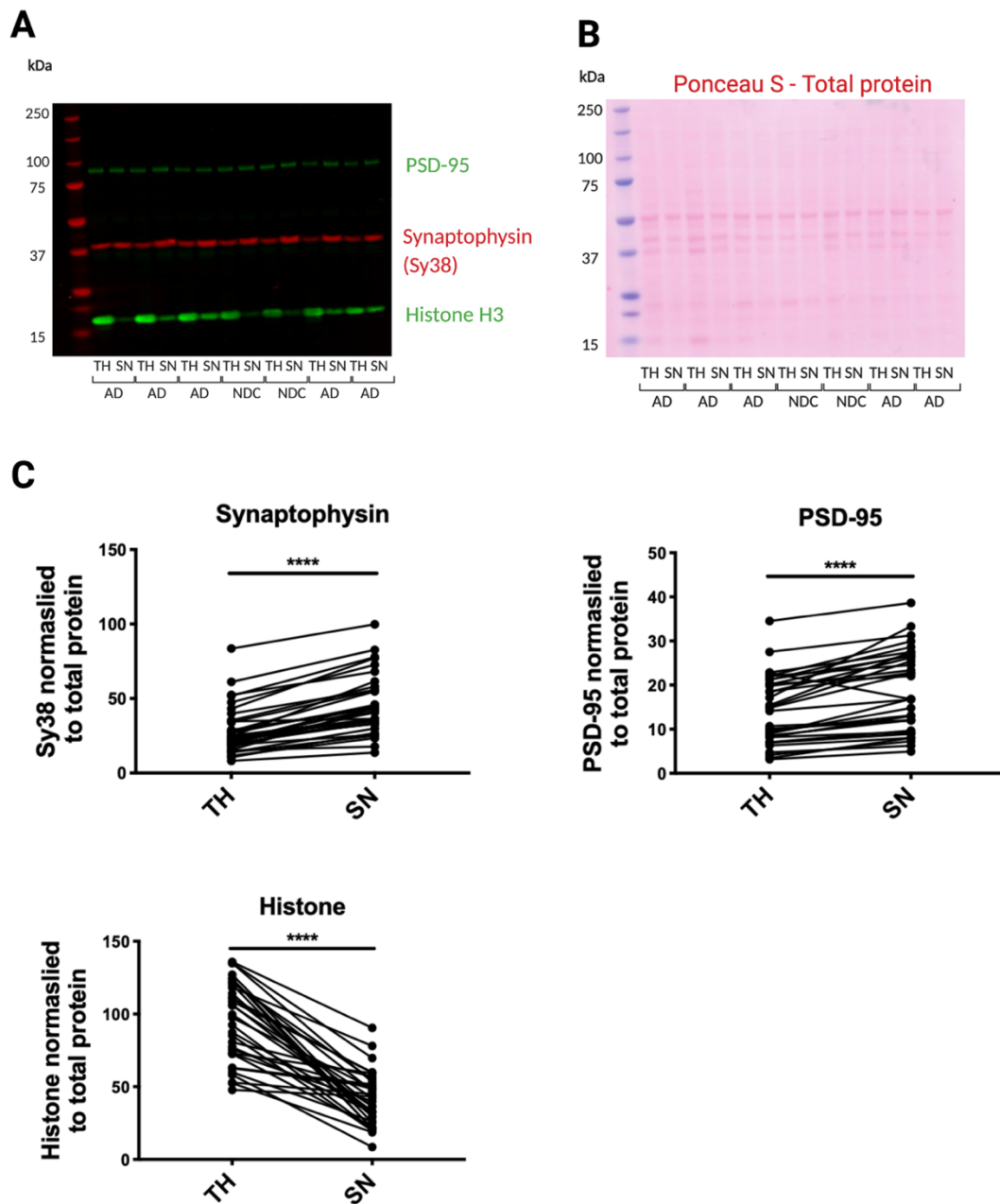


Figure 2. Validation of synaptoneurosome preparations. (A) Representative image of full-length Western blot, indicating whether a sample is from total homogenate (TH) or synaptoneurosome (SN), and their corresponding disease status. Bands were quantified on Image Studio, and normalised to total protein, quantified by Ponceau S. (B) Ponceau S staining for total protein from gel shown in A. (C) Significantly increased protein levels of the pre- and post-synaptic markers synaptophysin (Sy38) and PSD-95, respectively, as well as decreased protein levels of histone (H3), indicating exclusion of non-synaptic material (Wilcoxon matched-pairs signed rank test, **** $p < 0.0001$, $n = 31$). Lines link the two different preparations from the same case.

2.2 Loss of synaptophysin but not PSD-95 protein in AD

As discussed in the Introduction Chapter, synapse loss is a key feature of AD and it is consistently reported both in human brains and in mouse models of AD. The Western blots from the synaptoneurosome validation not only validated synaptic enrichment, but also provided the opportunity to measure the levels of synaptic proteins and compare them between AD and NDC brains. A significant reduction in the levels of synaptophysin protein was found in both the total homogenate and synaptoneurosome fractions of AD brains compared to NDC ones (Figure 3A-B). However, no change was found in the levels of PSD-95 (Figure 3C-D).

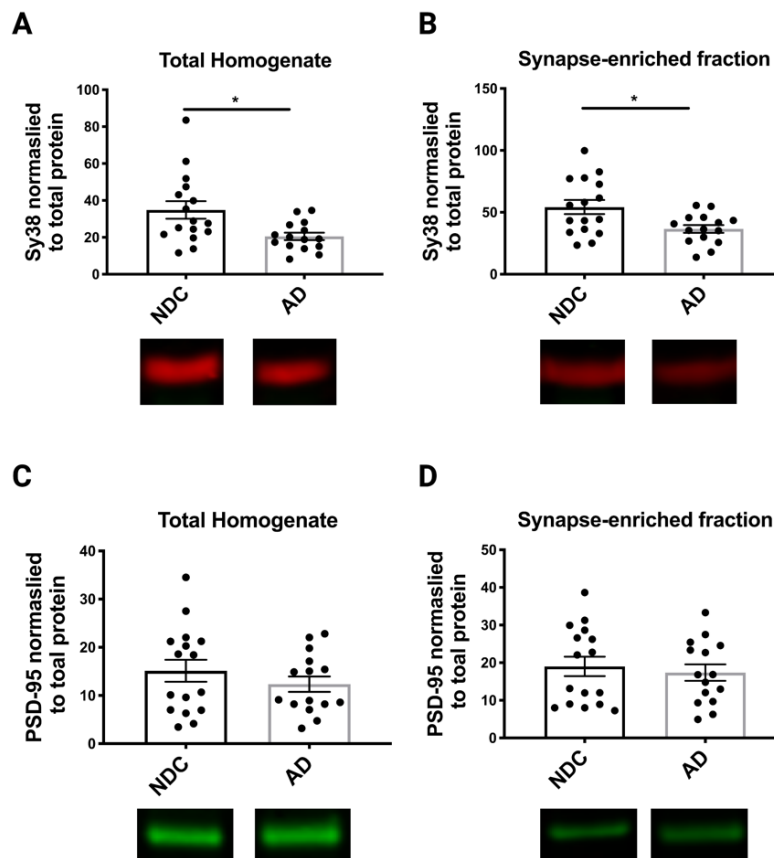


Figure 3. Pre-synaptic, but not post-synaptic, protein loss in AD. (A) Decreased levels of synaptophysin (Sy38) in the total homogenate of AD cases (n=15), compared to age-matched non-demented control (NDC) cases

(n=16), as detected by Western blot (Mann-Whitney test, $p=0.0106$). (B) Same as (A) for synapse-enriched fraction (unpaired Student's t-test, $p=0.0121$). (C) Unchanged PSD-95 protein levels in total homogenate between AD and NDC groups (unpaired Student's t-test, $p=0.332$). (D) Same as in (C) but in synapse-enriched fraction ($p=0.627$). For statistics, $*p<0.05$.

2.3 Phagocytosis validation by BV2 microglia

Although mouse synaptosomes have been previously pHrodo-tagged for phagocytosis assays by others, there is negligible information on using human synaptoneuroosomes for such assays. It was therefore imperative to test how the human synaptoneuroosomes behaved in a phagocytosis assay. BV2 cells were chosen to optimise this assay because they are an immortalised line of murine microglia, meaning they multiply fast and can be frozen-down and thawed to generate new ones rapidly. Like primary microglia, BV2 cells are seen to have ramified extensions under phase contrast microscopy (Figure 4) before the synaptoneuroosomes are added. By 50 minutes, BV2 cells have a red signal building up in the cell cytoplasm around the nuclei (cyan), indicating phagocytosis of synaptoneuroosomes is taking place. At 100 minutes, the red signal is stronger and more abundant.

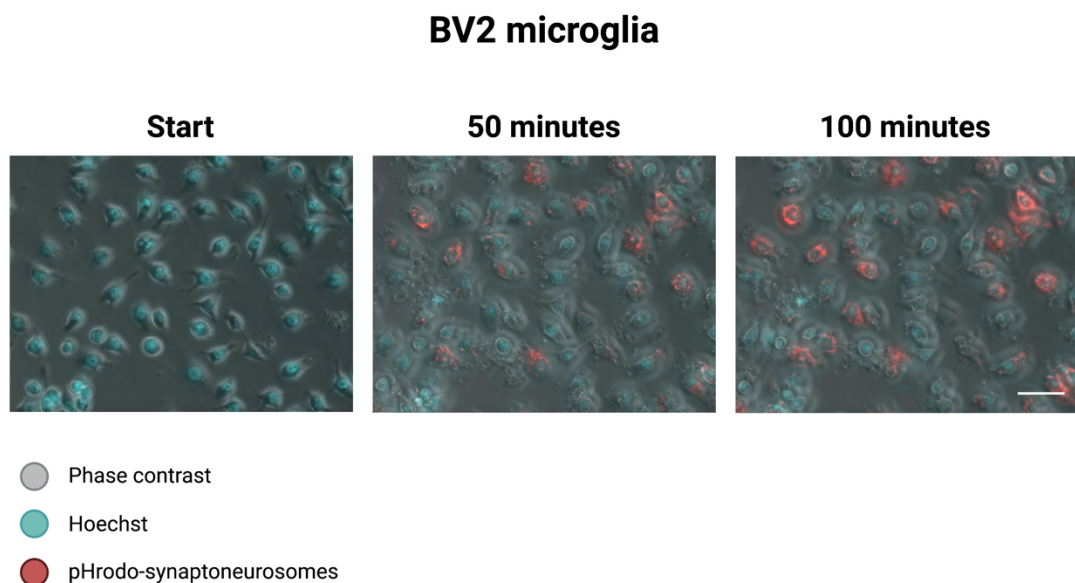


Figure 4. Pilot phagocytosis assay of human synaptoneurosomes using BV2 microglia. Live imaging of BV2 microglia (phase with Hoechst-positive nuclei in cyan) undergoing phagocytosis of human synaptoneurosomes tagged with pHrodo (can be seen as small spheroids on phase contrast). Synaptoneurosomes become red once they enter the acidic phago-lysosomal compartment of the cell. Each panel represents an image 50 minutes apart. Scale bar represents 50 μ m.

Knowing that BV2 cells are capable of undergoing phagocytosis of these human synaptoneurosomes was key in extending this study to test NDC vs AD effects. To do this, the high throughput ImageExpress microscope was chosen, as it can take multiple images per well from multiple wells, in an automated way. Another advantage of this microscope is that it allows for analysis of phagocytosis by providing a phagocytosis index. This index is measured by normalising the pHrodo-signal around Hoechst-positive nuclei to the respective total number of Hoechst-positive nuclei in an image. However, a disadvantage is that that microscope was not equipped with phase contrast, so the microglial morphology was not available.

BV2 cells were plated in a 96-well plate and labelled with Hoechst prior to the assay, labelling the nuclei (pseudocoloured grey) (Figure 5). By 2 hours phagocytosis had peaked and the ingested synaptoneurosomes became red, similar to the previous validation experiment (Figure 5A). In non-acidic conditions, pHrodo-Red can auto-fluoresce because of its strong signal. To control for this, BV2 cells were treated with the actin polymerisation inhibitor cytochalasin D (10 μ M) which subsequently inhibits phagocytosis. At the start of the assay a very faint red signal can be seen (suggesting background noise) which quickly subsides and by 2 hours no phagocytosis is observed in the cultures (Figure 5B). This validates that the synaptoneurosomes do not acidify over time and express a red signal, but become red only when ingested. These experiments provided the necessary foundation for developing a high-throughput assay for testing phagocytosis of synaptoneurosomes from AD and NDC brains by primary microglia in an efficient way.

BV2 microglia

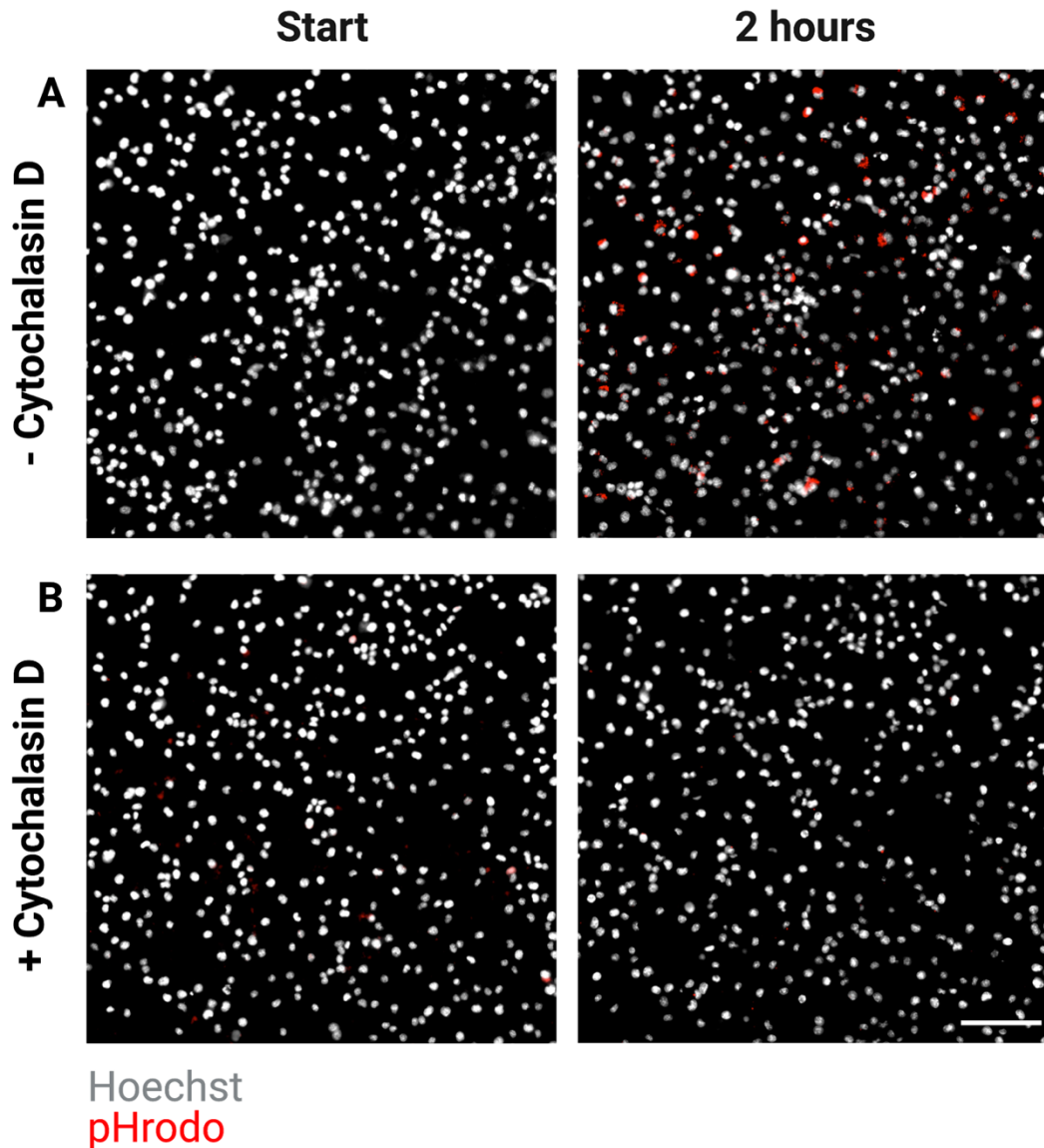


Figure 5. BV2 microglia challenged with pHrodo-tagged synaptoneurosomes in ImageExpress. (A) Still images from live imaging of BV2 microglia (Hoechst-positive nuclei in grey) undergoing phagocytosis of human synaptoneurosomes tagged with pHrodo. Synaptoneurosomes can be seen in red as they enter the acidic phago-lysosomal compartment of the cell. (B) Cells treated with 10 μ M of Cytochalasin D 30 minutes prior to the experiment showed no phagocytosis. Scale bar represents 30 μ m.

2.4 Phagocytosis assay using primary mouse microglia

Firstly, microglia from 2 month-old male mice were isolated using CD11b immunomagnetic beads, a previously established technique in the lab (Grabert and McColl, 2018). To validate that murine microglia are also capable of phagocytosis they were incubated with the pHrodo-tagged synaptoneurosomes and were live-imaged with phase contrast (Figure 6A). Primary microglia had their characteristic elongated shape at the start of the assay and by 1 hour they had started ingesting the synaptoneurosomes, by which point most process had retracted. By 2 hours, a clear pHrodo signal had developed around Hoechst-positive nuclei, suggesting successful ingestion of the synaptoneurosomes. ImageExpress could successfully capture the primary mouse microglia ingesting the pHrodo-synaptoneurosomes, making it possible to compare NDC and AD effects next (Figure 6B).

Synaptoneurosomes from both AD and NDC brains were rapidly taken up with a peak of 60% of cells actively phagocytosing by 60 mins (Figure 7A). When synaptoneurosomes from AD brains were incubated with primary mouse microglia (n=8 mice), a significantly greater proportion of microglial cells phagocytosed synaptoneurosomes compared to controls, as shown by the increased area under the curve (Figure 7B). Specifically, the area under the curve for NDC brains was 5068 ± 111.7 (error represented as standard error of mean) and for AD brains 5766 ± 90.8 (unpaired Student's t-test, $p=0.0097$). Moreover, AD-derived synaptoneurosomes were phagocytosed more rapidly by microglia compared to NDC-derived synaptoneurosomes, indicated by the reduced time to reach a half maximum value on the phagocytotic index (Figure 7C). The time to reach half-max decreased from 35.2 ± 0.53 minutes in NDC-synaptoneurosomes to 29.12 ± 0.45 minutes for AD preparations (unpaired Student's t-test, $p < 0.0001$). It is important to note that microglia from the same mice were plated in two wells in order for NDC-synaptoneurosomes and AD-synaptoneurosomes to be comparable. By doing so, the data from AD-synaptoneurosomes can be normalised to their NDC counterparts and transformed into a percentage for comparison. A non-significant trend towards

increased ingestion of AD-synaptoneuroosomes was observed once the data were normalised (one sample t-test, hypothetical value=100, $p=0.0522$), but a significant reduction in time to half-maximum was still observed (one sample t-test, hypothetical value=100, $p<0.0001$). Phagocytosis was also stratified based on the APOE genotype of the synaptoneuroosomes (APOE3/3 and APOE3/4). No significant differences in synaptic ingestion were found based on APOE genotype in the NDC group (one-way ANOVA with Tukey's multiple corrections, $p=0.904$) nor in the AD group (one-way ANOVA with Tukey's multiple corrections, $p>0.999$).

Primary mouse microglia

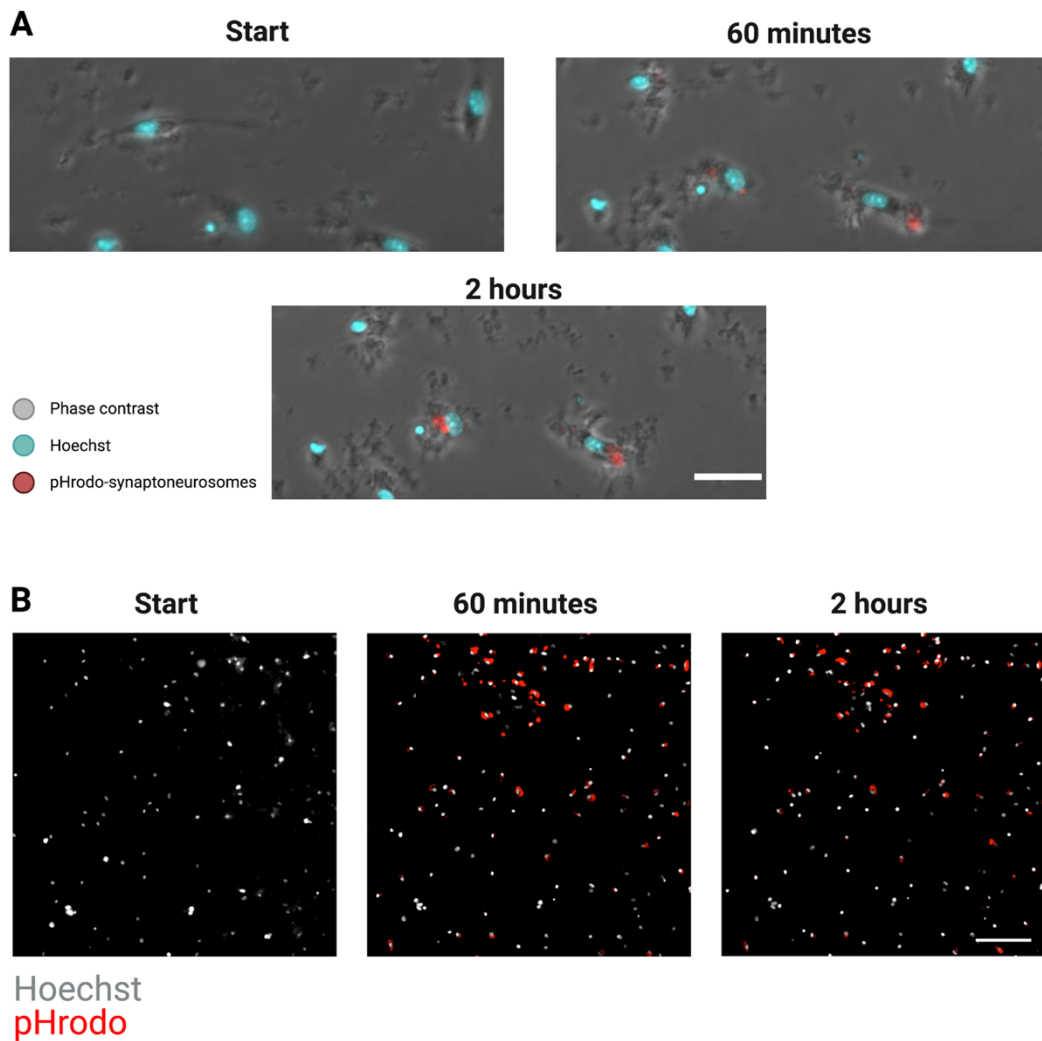


Figure 6. Phagocytosis assay of human synaptoneuroosomes using primary mouse microglia. (A) Live imaging of primary mouse microglia (phase with Hoechst-positive nuclei in cyan) undergoing phagocytosis of human synaptoneuroosomes tagged with pHrodo-RED (can be seen as small spheroids on phase contrast). Synaptoneuroosomes become red once they enter the acidic phago-lysosomal compartment of the cell. Each panel represents an image 60 minutes apart. Scale bar represents 50 μ m. (B) Stills from ImageExpress over 2 hours. Primary microglia (Hoechst-positive nuclei in grey) undergoing phagocytosis of human synaptoneuroosomes tagged with pHrodo. Synaptoneuroosomes can be seen in red as they enter the acidic phago-lysosomal compartment of the cell. Scale bar represents 30 μ m.

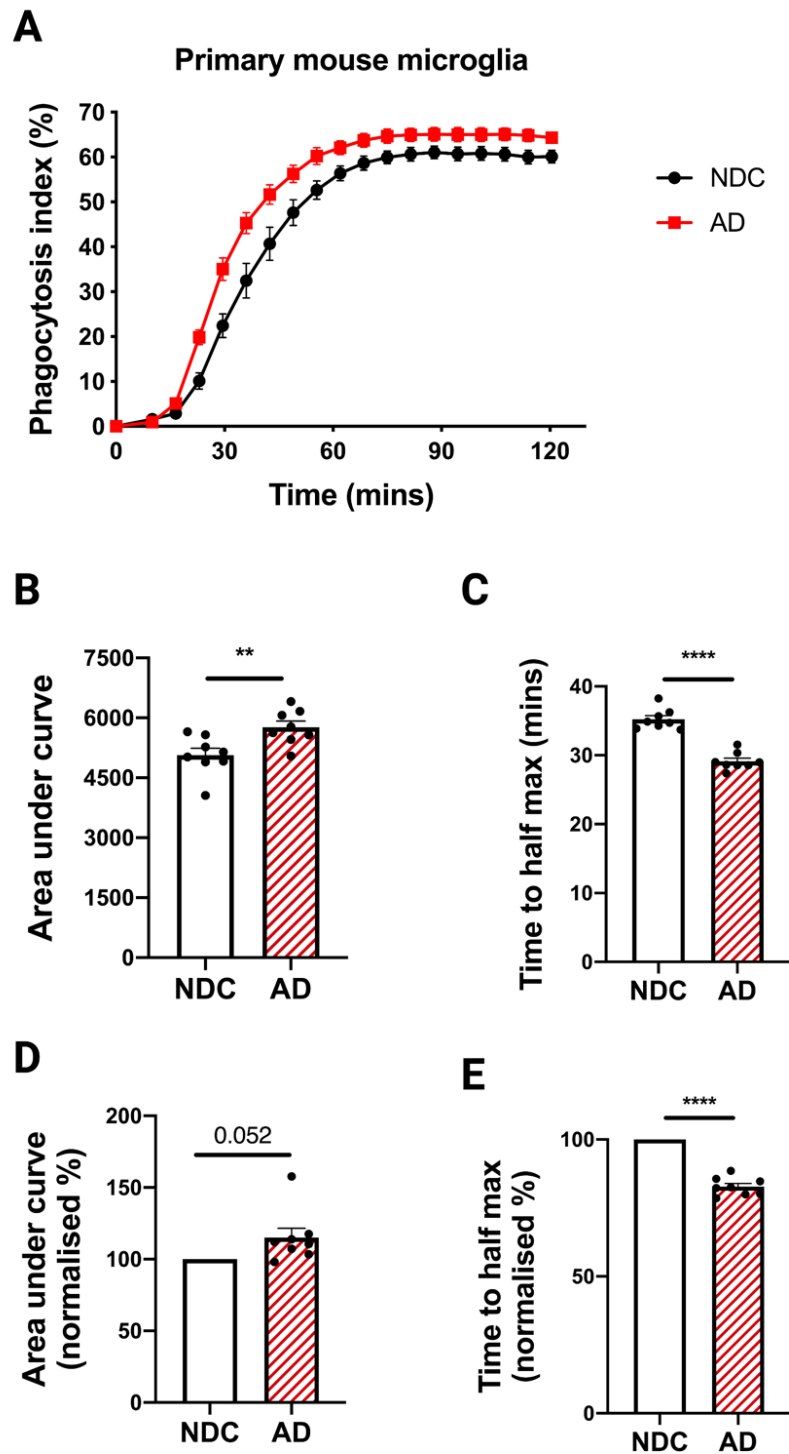


Figure 7. Increased phagocytosis of AD-derived synaptoneurosomes by primary mouse microglia. (A) Phagocytosis index of primary mouse microglia engulfing human synaptoneurosomes (n=8 mice, average of 9 images per well). (B) Area under curve from A (unpaired Student's t-test, p=0.003). (C) Time to half-maximum phagocytosis was calculated from the curve shown in A (unpaired Student's t-test, p<0.0001). (D) Area under curve

from AD-treated wells normalised to their respective NDC well and transformed into a percentage (one sample t-test, hypothetical value=100, $p=0.0522$). (E) Time to half maximum from AD-treated wells normalised to their respective NDC well and transformed into a percentage (one sample t-test, hypothetical value=100, $p<0.0001$). For statistics, $**p<0.01$, and $****p<0.0001$. Data shown as mean \pm SEM.

2.5 Phagocytosis assay using primary human microglia

By using mouse microglia, it was previously shown that AD-synaptoneuroosomes are more prone to be ingested than NDC ones. The next step was to replicate this assay using primary human microglia. However, the ability to generate primary human microglia from living tissue is limited to preparation from surgically resected samples. The microglial yield is typically smaller because of constraints on tissue size, and the survival of human microglia varies between cases. Also, the tissue donated comes from surgically resected brain and the underlying causes that require the surgery differ. A total of nine different sources of human microglia have been successfully cultured and incubated with the pHrodo-synaptoneuroosomes, one from a patient with epilepsy and eight with glioblastoma, a type of brain tumour. The tissue provided comes from outwith the pathologic foci. Of note, microglia isolated from surgical resection have been shown to have comparable transcriptomic signatures between non-affected cortex and ex-vivo isolated microglia (Galatro et al., 2017). The microglia from the epilepsy biopsy were isolated with a lift-off method, as described previously (Blain et al., 2010), and provided by the Miron lab (courtesy of Rebecca Holloway, tissue provided Dr. Jothy Kandasamy and Dr. Drahus Sokolov). The remaining eight glioblastoma cases were isolated using the CD11b immunomagnetic beads similar to the mouse microglia.

Firstly, microglia from the epilepsy case were in sufficient numbers to do three replicates and also treat with cytochalasin D. Tissue from the temporal lobe was donated by a 20-year old male. Still images from live imaging with and

without phase (Figure 8A-B) show pHrodo-positive inclusions in plated microglial cells over time, similar to the mouse and BV2 microglia. Synaptoneurosomes from both AD and control brains were rapidly taken up with a peak of 45% of cells actively phagocytosing by 60 mins (Figure 9A). When synaptoneurosomes from AD brains were incubated with microglia, a significantly greater proportion of cells phagocytosed synaptoneurosomes compared to controls, as shown by the increased area under the curve (Figure 9B). Specifically, the area under curve in AD-synaptoneurosome ingestion was 4482.33 ± 46 while for NDC-synaptoneurosomes it dropped to 4125 ± 23.96 (ordinary one-way ANOVA with Tukey's multiple comparisons test, $p=0.0004$, $n=1$ from 3 replicates). Moreover, AD-derived synaptoneurosomes were phagocytosed more rapidly by human microglia cells compared to controls, indicated by the reduced time to half maximum value for the phagocytotic index (Figure 9C). The time to reach half max decreased from 23.67 ± 0.71 minutes in NDC to 19.46 ± 0.57 in AD (unpaired Student's t-test, $p < 0.0001$, $n=1$ from 3 replicates). Importantly, phagocytosis of synaptoneurosomes was significantly suppressed in CytD treated cells (ordinary one-way ANOVA with Tukey's multiple comparisons test, $p < 0.0001$, $n=1$ from 3 replicates) (Figure 9A-B).

Primary human microglia (epilepsy case)

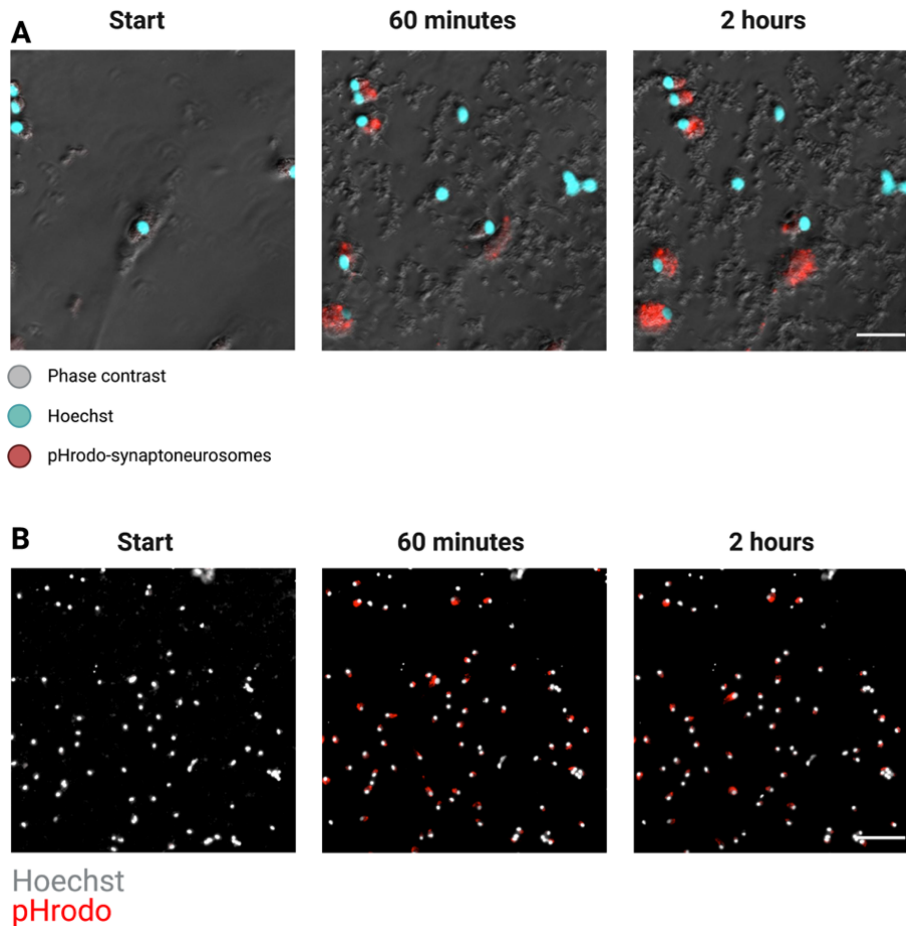


Figure 8. Phagocytosis assay of human synaptoneuroosomes using primary human microglia from an epilepsy case. (A) Live imaging of primary human microglia (phase with Hoechst-positive nuclei in cyan) undergoing phagocytosis of human synaptoneuroosomes tagged with pHrodo (can be seen as small spheroids on phase contrast). Synaptoneuroosomes become red once they enter the acidic phago-lysosomal compartment of the cell. Each panel represents an image 60 minutes apart. Scale bar represents 50 μ m. (B) Stills from ImageExpress over 2 hours. Primary microglia (Hoechst-positive nuclei in grey) undergoing phagocytosis of human synaptoneuroosomes tagged with pHrodo. Scale bar represents 30 μ m.

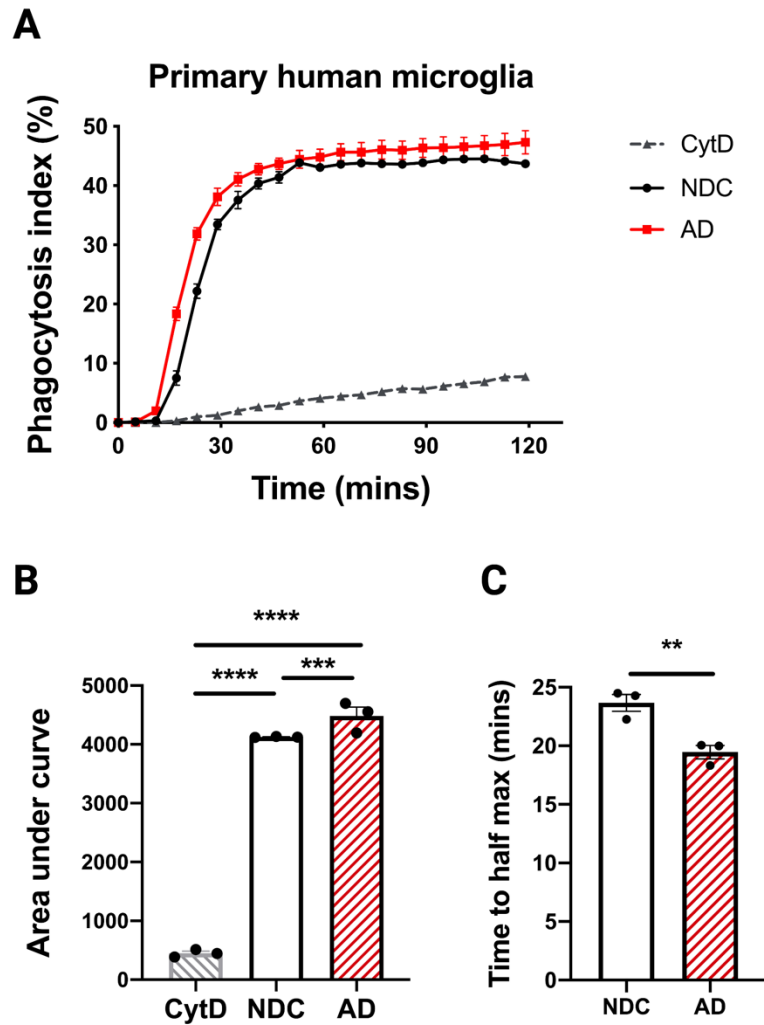


Figure 9. Increased phagocytosis of AD-derived synaptoneuroosomes by primary human microglia (epilepsy). (A) Phagocytosis index of primary human microglia engulfing human synaptoneuroosomes (n=1 human sample, replicated in 3 wells from an average of 9 images per well). (B) Area under curve from A (ordinary one-way ANOVA with Tukey's multiple comparisons test, $p=0.0004$). (C) Time to half-maximum phagocytosis was calculated from the curve shown in A (unpaired Student's t-test, $p=0.0098$). For statistics, $**p<0.01$, $***p<0.001$, $****p<0.0001$. Data shown as mean \pm SEM.

Human microglia were also provided from peri-tumoral tissue from eight different patients by Dr. Paul Brennan. At the moment, information on sex, age, and brain area are not available for all cases and have not been included in this thesis. Microglia from these cases were isolated using CD11b immunomagnetic beads, like the murine microglia. Both the CD11b+ and CD11b- cells were cultured. The CD11b+ cells resembled microglial cells and by 6 days *in-vitro* showed typical branching processes, whereas the CD11b- cells do not appear morphologically microglial (Figure 10A). Immunostaining of these cells showed that Cd11b+ cells were positive for the microglial specific marker Tmem119, while CD11b- cells contained GFAP-positive cells, which are most likely astrocytic (Figure 10C&D). Tmem119 cells were not found in the Cd11b- population, and GFAP positive cells were not found in the Cd11b+ population (data not shown). The resected tissue provided from these cases was limited and allowed for only one replicate of NDC and AD-synaptoneurosome treated wells per case.

Primary human microglia (glioblastoma)

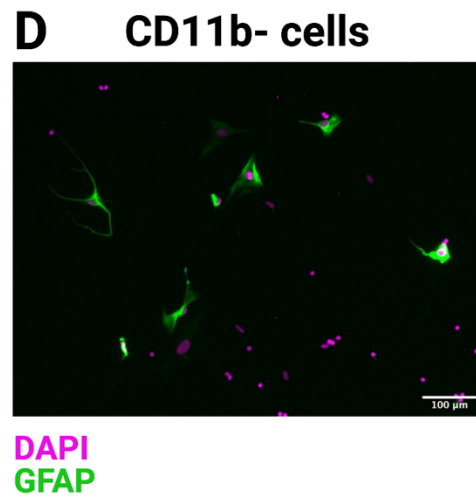
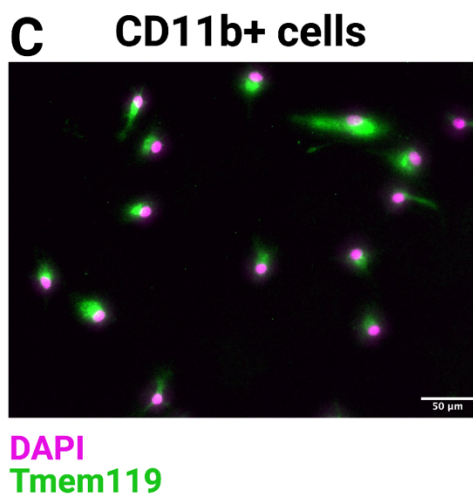
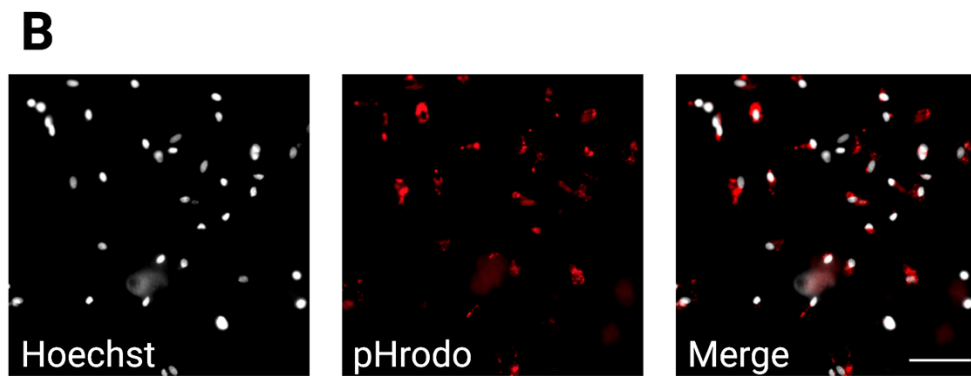
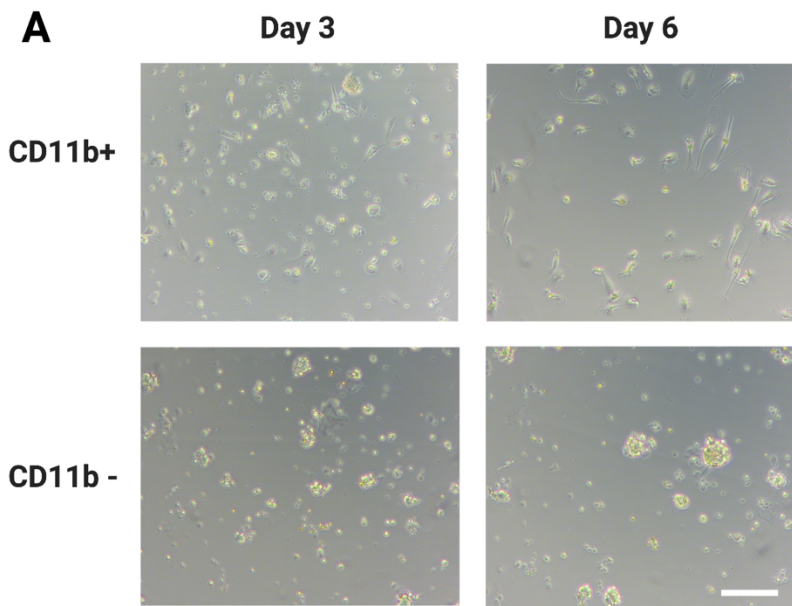


Figure 10. Human microglia from peri-tumoral tissue from glioblastoma surgery. (A) CD11b+ microglia were selected from surgery resected tissue from the peri-tumoral region. Scale bar represents 20 μ m. (B) Stills from ImageExpress showing CD11b+ primary microglia (Hoechst-positive nuclei in grey) undergoing phagocytosis of human synaptoneurosomes tagged with pHrodo. Scale bar represents 30 μ m. (C) CD11b+ cells fixed and stained for the microglial specific marker Tmem119 (green) and DAPI for nuclei (magenta). Scale bar 100 μ m. (D) CD11b- cells fixed and stained for the astrocytic marker GFAP (green) and DAPI for nuclei (magenta). Scale bar 100 μ m.

Microglia isolated from the glioblastoma cases were also capable of synaptoneurosome phagocytosis, as indicated by the pHrodo-positive signal captured in live microscopy (Figure 10B). Figure 11 shows the phagocytosis profiles of all eight glioblastoma cases individually, with control synaptoneurosomes seen in black and AD synaptoneurosomes in red. The cases have been plotted individually to demonstrate the large amount of variability seen from individual to individual, both in terms of NDC to AD phagocytosis response but also for peak phagocytosis, ranging from 35% to 85%. In some cases, there is no difference between NDC and AD synaptoneurosomes (Figure 11D and G), in some cases there is a small increase in AD compared to NDC (Figure 11B, E, and F), and finally in some cases there is a large increase in phagocytosis of AD compared to NDC (Figure 11A, C, and H). Altogether, these differences could arise from tissue friability due to age, surgery and tumour effects, brain area, and sex. Due to the high variability in the human assays, the AD phagocytosis response (area under the curve and time to half maximum) was normalised to their respective NDC values, and turned into a percentage (similar to Figure 7).

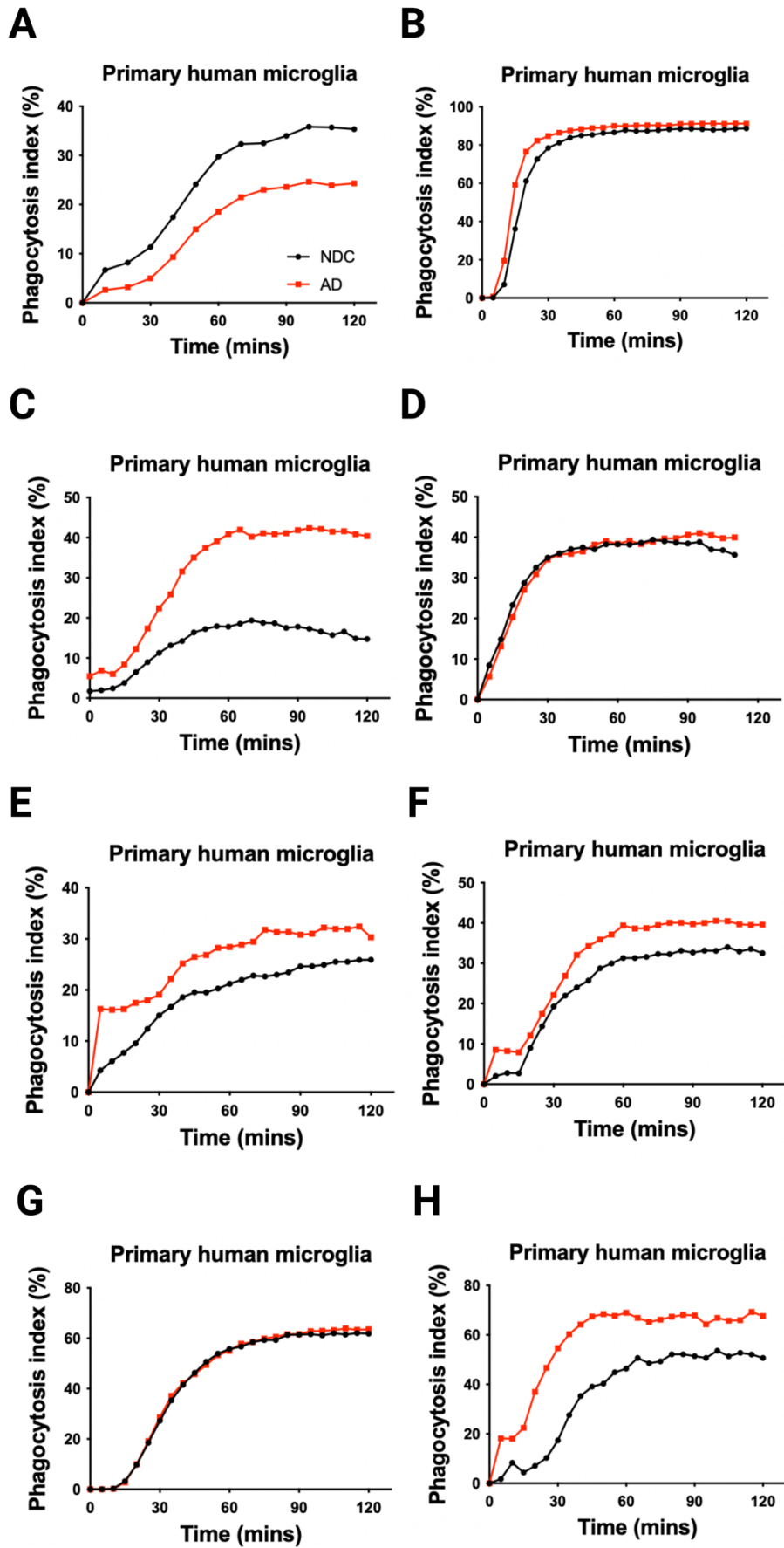


Figure 11. Phagocytosis of human synaptoneurosomes by primary human microglia (glioblastoma). Phagocytosis index of primary human microglia from eight glioblastoma cases engulfing human synaptoneurosomes. NDC synaptoneurosomes shown in black lines with circles and AD synaptoneurosomes in red lines with squares. Each plot represents a single individual.

The data from the eight human cases (glioblastoma only) were then pooled and analysed together, based on the normalised data. A significant increase in ingestion of AD synaptoneurosomes is seen compared to the NDC ones (Figure 12B) (one sample t-test, hypothetical value=100, $p=0.0363$), and a significant decrease in the time to half max is also observed (one sample t-test, hypothetical value=100, $p=0.0123$) (Figure 12B).

Human microglia (GBM) pooled

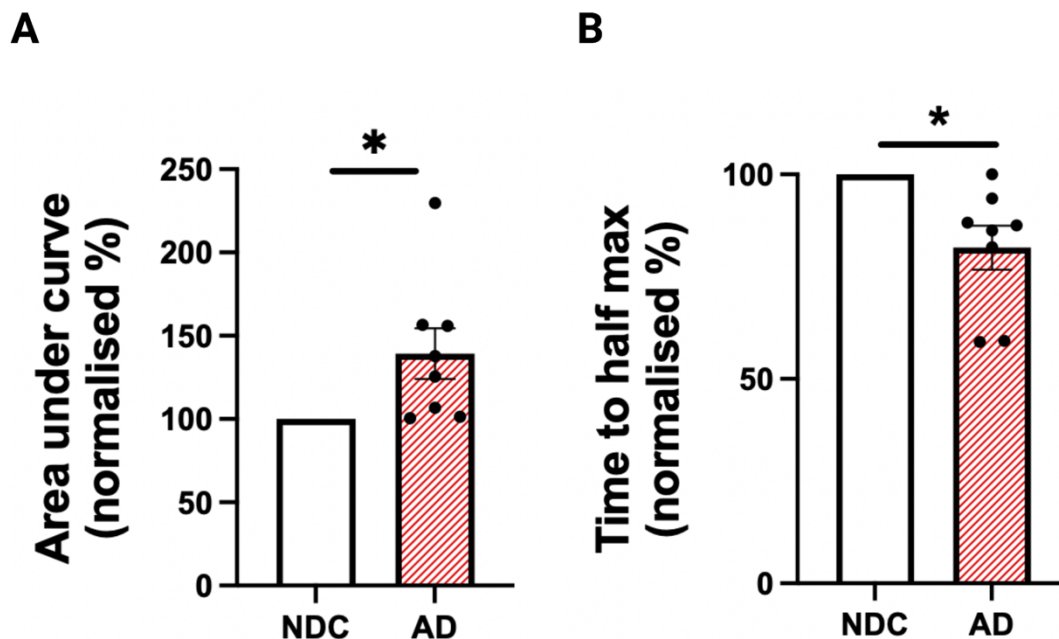


Figure 12. Phagocytosis of human synaptoneurosomes by primary human microglia pooled from all 3 cases. (A) Area under curve from AD-treated wells normalised to their respective NDC well and transformed into a percentage (one sample t-test, hypothetical value=100, $p=0.0363$). (B) Time to half maximum from AD-treated wells normalised to their respective NDC well and transformed into a percentage (one sample t-test, hypothetical value=100, $p=0.0123$). For statistics, $*p < 0.05$. Data shown as mean \pm SEM.

2.6 Phagocytosis assay using primary mouse astrocytes

Although microglia are the primary phagocytes of the brain, astrocytes are also capable of phagocytosis of synapses both in the developing and adult brain. Having established a phagocytosis assay for testing synaptoneurosome ingestion by microglia, it was possible to extend this using primary astrocytes in culture. To do this, cultured primary astrocytes were provided by the Hardingham lab (courtesy of Dr. Sean McKay). Astrocytes were purified from mixed-sex E17.5 mice. Briefly, mouse brains were dissociated into mixed cell suspensions which were cultured for 7 days, followed by trypsin treatment to kill neurons. Seven days later, microglia were lifted-off and discarded to yield a 99% pure astrocyte culture (Hasel et al., 2017). An example of image GFAP-positive mouse astrocytes can be found in Figure 13A. The isolated astrocytes were then plated in 96-well plates and allowed to settle for 3 days, prior to the assay. Additionally, primary human astrocytes have been purchased from Caltag Medsystems and cultured in the lab under the same conditions as the mouse astrocytes. These astrocytes are foetal so are also modelling developmental glia rather than adult ones, like in the primary microglia. Human astrocytes also express GFAP (Figure 13B). Astrocytes have a larger cytoplasmic area than microglia meaning that ingesting synapses can happen far from the nucleus, and so ImageExpress was not deemed suitable for imaging and analysing in the same way as the microglia. Instead, Incucyte was chosen for imaging and analysis because it allows live imaging with phase contrast to detect cells and the red channel for detecting pHrodo. This way, prior to synaptoneurosome addition, an image of the astrocytes was taken and thresholded to create a mask of the astrocytes in each well. Once the synaptoneurosomes were added, the pHrodo signal was tracked over time, and phagocytosis was normalised to the phase mask of each well to account for any differences in cell numbers.

Astrocytes successfully ingested the human synaptoneurosomes as shown by the pHrodo-positive signal that develops over time (Figure 14). Importantly, treatment with cytochalasin D inhibited the development of any pHrodo signal (Figure 14) suggesting a successful prevention of synaptoneurosomes phagocytosis. Unlike microglia, astrocytic ingestion has been reported to be slow (Byun and Chung, 2018) and so imaging lasted longer. For example, more pHrodo signal was observed at 48 hours in culture compared to 24 hours, suggesting phagocytosis happens even after 24 hours in culture (Figure 14).

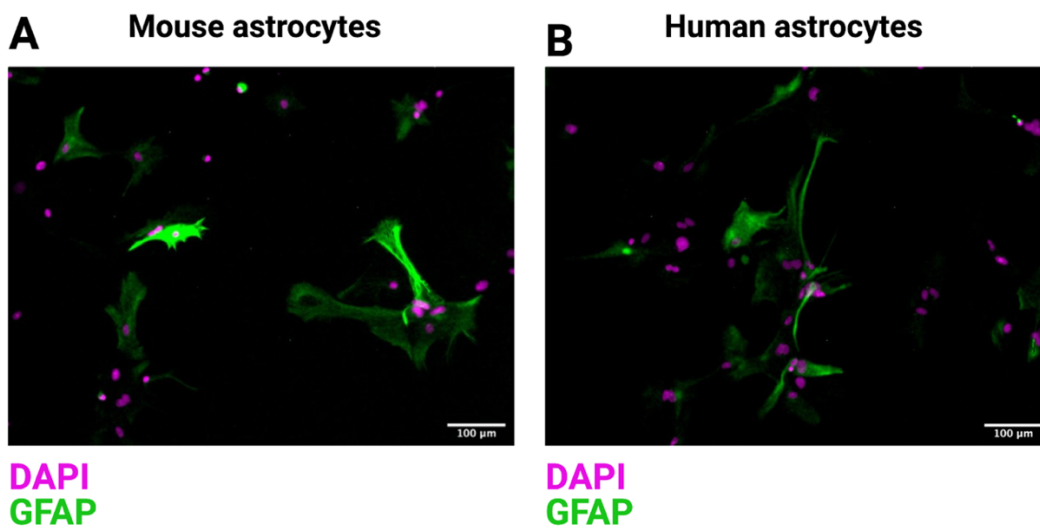


Figure 13. Primary mouse astrocytes ingest human synaptoneurosomes in culture. (A) Primary mouse astrocytes stained for GFAP (green) shows most cells express the marker, indicating a pure astrocytic culture. (B) Primary human astrocytes stained for GFAP (green) shows cells express the marker, although some cells do not. Scale bars represent 100µm.

Primary mouse astrocytes

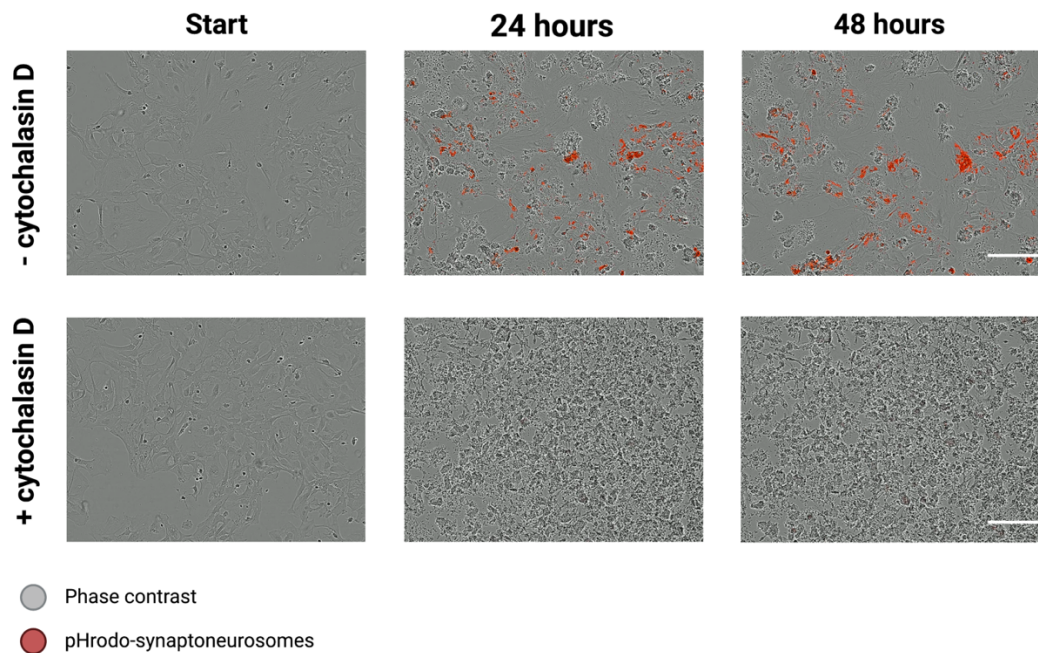
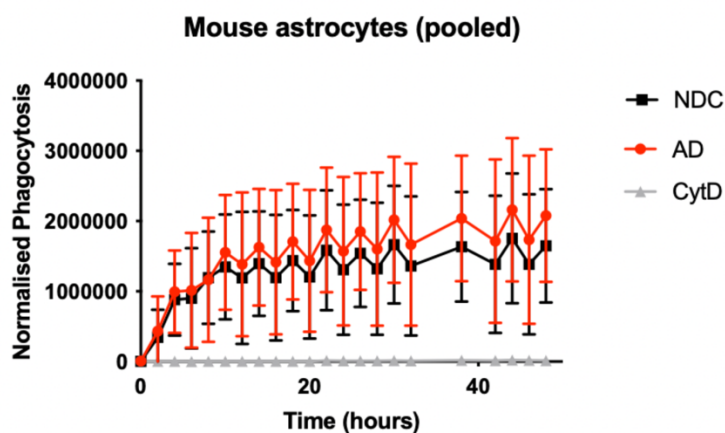


Figure 14. Primary mouse astrocytes ingest human synaptoneurosomes in culture. Live imaging of primary mouse astrocytes (phase in grey) undergoing phagocytosis of human synaptoneurosomes tagged with pHrodo (can be seen as small spheroids on phase contrast). Synaptoneurosomes become red once they enter the acidic phago-lysosomal compartment of the cell. Each panel represents an image 24 hours apart. Cells treated with $10\mu\text{M}$ of Cytochalasin D 30 minutes prior to the experiment showed no phagocytosis. Scale bars represent $200\mu\text{m}$.

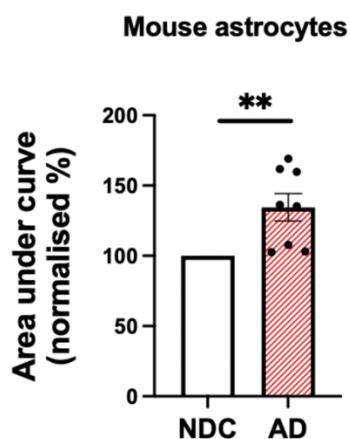
A total of 8 independent runs have been made using primary mouse astrocytes and 7 with the purchased human astrocytes. A phagocytosis assay profile has been plotted in Figure 15A showing that there is great variability between each run, verified by the large error bars. Therefore, all analysis was done by normalising the AD phagocytosis area under the curve to its respective NDC area under the curve as a percentage. Firstly, it was evident that synaptoneurosomes were fluorescing red by means of phagocytosis as there was no phagocytosis occurring in cytochalasin D treated cells (Figure 15A).

When normalised, there was a significant increase in the ingestion of AD-synaptoneurosomes compared to control ones both by mouse astrocytes (Figure 15B, one sample t-test, hypothetical value=100, $p=0.0095$) and by the human astrocytes (Figure 15C, one sample t-test, hypothetical value=100, $p=0.0008$). Specifically, mouse astrocytes achieved a phagocytosis index of 134.4% phagocytosis and the human astrocytes 119.3%, suggesting similar phagocytosis profiles.

A



B



C

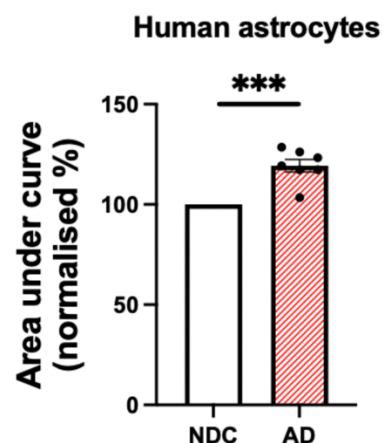


Figure 15. Phagocytosis of human synaptoneurosomes by primary mouse astrocytes. (A) Normalised phagocytosis of primary mouse astrocytes engulfing human synaptoneurosomes over 48 hours (n=8). Cytochalasin D treatment prevented phagocytosis. (B) Area under curve from A (mouse), normalised AD to their respective NDC well and transformed into a percentage (one sample t-test, hypothetical value=100, p=0095) (n=8 preparations from 8 independent mice). (C) Area under curve (human) with normalised AD to their respective NDC well and transformed into a percentage (one sample t-test, hypothetical value=100, p=0095) (n=7 independent preparations). For statistics, **p<0.01, ***p<0.001. Data shown as mean \pm SEM.

3. Discussion

Overall, the data presented in this chapter suggest that synaptic changes in the AD brain makes them more prone to be engulfed by microglia. This is in support of the hypothesis that synapses in AD are tagged for removal by glia, and that microglial changes are not solely responsible for synaptic pruning, as the microglia incubated with NDC or AD synaptoneurosomes come from the same mice. Microglia from both murine and human brains preferably ingested AD-derived synaptoneurosomes compared to ones from control brains. Interestingly, astrocytes too showed a preference for ingesting AD-synaptoneurosomes, further supporting the above hypothesis. Nevertheless, these experiments are accompanied by their own set of limitations that need to be addressed.

First, the biologically relevant details for the human cases are unknown and there could be key differences between them, including age, the underlying disease, and brain area, all of which could influence microglial phenotypes (Grabert et al., 2016; Galatro et al., 2017; Tay et al., 2017; Gibson et al., 2019; Gibson and Monje, 2021). Also, the microglia provided from the epilepsy case were purified in a different way to those from the glioblastoma cases, which could affect microglial phenotypes and alter phagocytosis. Altogether, these differences between samples and the low sample size of the human primary microglia require extra caution when interpreting the results and rely on

validation from mouse microglia. Also, astrocytes were cultured from embryonic brains rather than adult, so it would be more comparable to culture astrocytes from adult mouse brains. This is because younger glial cells are more phagocytic than adult ones (Njie et al., 2012; Ritzel et al., 2015), and so the phenotype observed here may reflect an exaggerated phagocytic response. The human astrocytes are also of embryonic stages and they too model an earlier glial phenotype. Importantly, the data between the mouse and human astrocytes are very similar which validates the two experiments.

The use of serum in cell culture is standard practice as it provides cells with necessary hormones, growth factors, adhesion factors and nutrients. Both human and mouse microglia are supplemented with 10% heat-inactivated serum. Recently, a debate has sparked on whether serum should be given to microglia *in-vitro* as it is associated with microglial activation, and can therefore alter their phenotypes (Bohlen et al., 2017). More relevant to these experiments is that serum may contain opsonin molecules that bind to the synaptoneuroosomes and exacerbate phagocytosis. Even though the serum has been heat-inactivated (denaturing complement proteins that can opsonise synapses), it is not possible to exclude this hypothesis, and it needs to be addressed by culturing microglia in serum and serum-free conditions. This should be done both in short- and long-term experiments; one, changing the media right before the assay to test the presence of opsonin proteins in serum, and two, culturing microglia in serum or serum-free media to test the effects of microglial activation in response to phagocytosis of synaptoneuroosomes.

Another limitation is the use of microglia from only male mice in the *in-vitro* experiments. Microglia exhibit sexual dimorphism both in terms of their density in the brain and morphology (Lenz, Nugent, Haliyur and McCarthy, 2013). More amoeboid microglia are found in the male neonatal mouse preoptic area, a phenotype associated with microglial activation. However, in the hippocampus of female mice there are more microglia undergoing

phagocytosis of neuronal debris (Nelson, Warden and Lenz, 2017). In another study, female mice from the maternal immune activation model (a mouse model for schizophrenia-like behaviour) showed increased levels of Iba1 and CD68 in the dentate gyrus compared to male mice, suggesting reactive gliosis (Hui et al., 2020). Also, quantitative PCR demonstrated higher levels of C1q in female brains. These data highlight sex differences in the phagocytosis profiles of microglia between male and female mice, and it would be important to test whether these differences apply in the synaptoneurosome phagocytosis paradigm.

Furthermore, flow cytometry quantification of synaptic markers and potential opsonin proteins decorating those synapses can elucidate whether there are differences in synaptic composition, as well as any relevant tagged signals pertaining to phagocytosis.

Ultimately, the biggest question that arises from these results is what are the signals on the AD synaptoneurosome that lead to a greater and faster ingestion. In the introduction chapter, the classical complement cascade was shown to bind on synapses and signal to microglia to undergo synaptic elimination, both in the context of brain development and disease. The data presented here are in support of these hypotheses but mechanistic experiments are required to dissect what these signals are. Previously, the lab found higher levels of phagocytosis-associated proteins on AD synaptoneurosome by an unbiased proteomic screen, like C4, C1q, and MFG-E8 (Hesse et al., 2019). Currently, blocking antibodies against MFG-E8 are being tested on synaptoneurosome to determine whether they suppress microglial ingestion of AD-derived synaptoneurosome. Also, mice lacking the complement 3 receptor have been purchased and are being bred in the lab in order to isolate microglia from their brains and challenge them with the synaptoneurosome. The hypothesis is that complement tags on the synaptoneurosome make them more preferable for phagocytosis and lacking

a receptor that is crucial for complement recognition will result in reduced phagocytosis of AD synaptoneuroosomes specifically. Moreover, it is possible that different soluble factors are present between the NDC and AD preparations that stimulate microglia to ingest more synaptoneuroosomes. An experiment to test this would be to incubate the synaptoneuroosomes with GFP-labelled beads and quantify whether the GFP beads are ingested differently between NDC and AD treated wells. Lastly, a caveat to the *in-vitro* data is that it is difficult to extrapolate what the rates of phagocytosis are *in-vivo*, and how the differences shown here translate to a human brain.

The results of this chapter can be strengthened by validating the purity of these cultures by immunohistochemistry (as performed) and by quantification of these samples. For example, microglia can be stained with the microglial specific markers Tmem119 and P2RY12, and compare the percentage of cells (Hoechst/DAPI positive) of microglial-specific cells. Co-labelling with Iba1 will allow to differentiate between microglia and macrophages in these cultures. The same can be applied for the astrocyte cultures, where the astrocyte specific marker Aldh1.1 can be used to stain astrocytes for checking the purity of the culture. Other markers for non-astrocytic cells (like Tmem119 for microglia and Olig2 for oligodendrocytes) can be used for excluding the presence of other cell types. By immune-labelling the glial cells in a low-pH buffer, it is possible to measure pHrodo-positive puncta inside these cells, providing an alternative measurement to the live-imaging assays.

In conclusion, the results of this chapter build-up on those of the previous chapter showing increased synaptic ingestion of microglia in AD human post-mortem brains, but also implicated synapses too as culprits of this enhanced ingestion.

Chapter 5: Microglial contribution to synaptic uptake in the prefrontal cortex in schizophrenia

1. Introduction

So far, synaptic loss by microglia has been addressed in the context of ageing and Alzheimer's disease. This chapter is focused on published data (on Neuropathology and Applied Neurobiology) showing synaptic engulfment by microglia in schizophrenia, a psychiatric disorder affecting 20 million people worldwide. In the introduction, the importance of fine-tuned synaptic pruning during normal brain development was discussed. Interestingly, disproportionate pruning by microglia is linked to developmental CNS disorders, including schizophrenia. Schizophrenia is an affective disorder that primarily affects the frontal lobe of the brain, and its symptoms include hallucinations, delusions, mood imbalances, and personality disturbances (Kahn et al., 2015; Wible et al., 2001). The onset of the disease varies, but it is more prevalent in teenagers/young-adults. The cause of the disease is unknown, although both environmental and genetic factors can contribute to an increased predisposition of developing schizophrenia (Schizophrenia Psychiatric Genome-Wide Association Study (GWAS) Consortium, 2011). Synapse and spine loss in patients' brains with schizophrenia have been reported in some studies, depending on the brain area, synaptic marker, and cohort investigated (Faludi and Mirnics, 2011; Feinberg, 1982; Funk et al., 2017; Osimo et al., 2019). Research into schizophrenia has primarily been neuron-centric, but more recently glial activation and its role in synaptic pruning has been applied to the field of schizophrenia. Co-cultures of human iPSC-derived microglia and neurons from schizophrenia and control sources, have indicated increased synaptic pruning in schizophrenia (Sellgren et al., 2019). Genetic variants on the complement component C4A gene implicate

the immune system as a risk factor for schizophrenia (Sekar et al., 2016; Comer et al., 2020). Moreover, PET scans using TSPO ligand binding as marker of cerebral inflammation show higher levels of brain inflammation in patients with schizophrenia (Doorduyn et al., 2009; van Berckel et al., 2008), although these data have been recently refuted (Coughlin et al., 2016; Kenk et al., 2015; De Picker et al., 2019). Altogether, it is intriguing to ask whether microglia play a part in actively removing synapses in schizophrenia, leading to cognitive and behavioural changes. Similar to previous chapters, this question was addressed using donated human post-mortem tissue.

2. Microglial contribution to synaptic uptake in the prefrontal cortex in schizophrenia (attached manuscript)

Scientific Correspondence

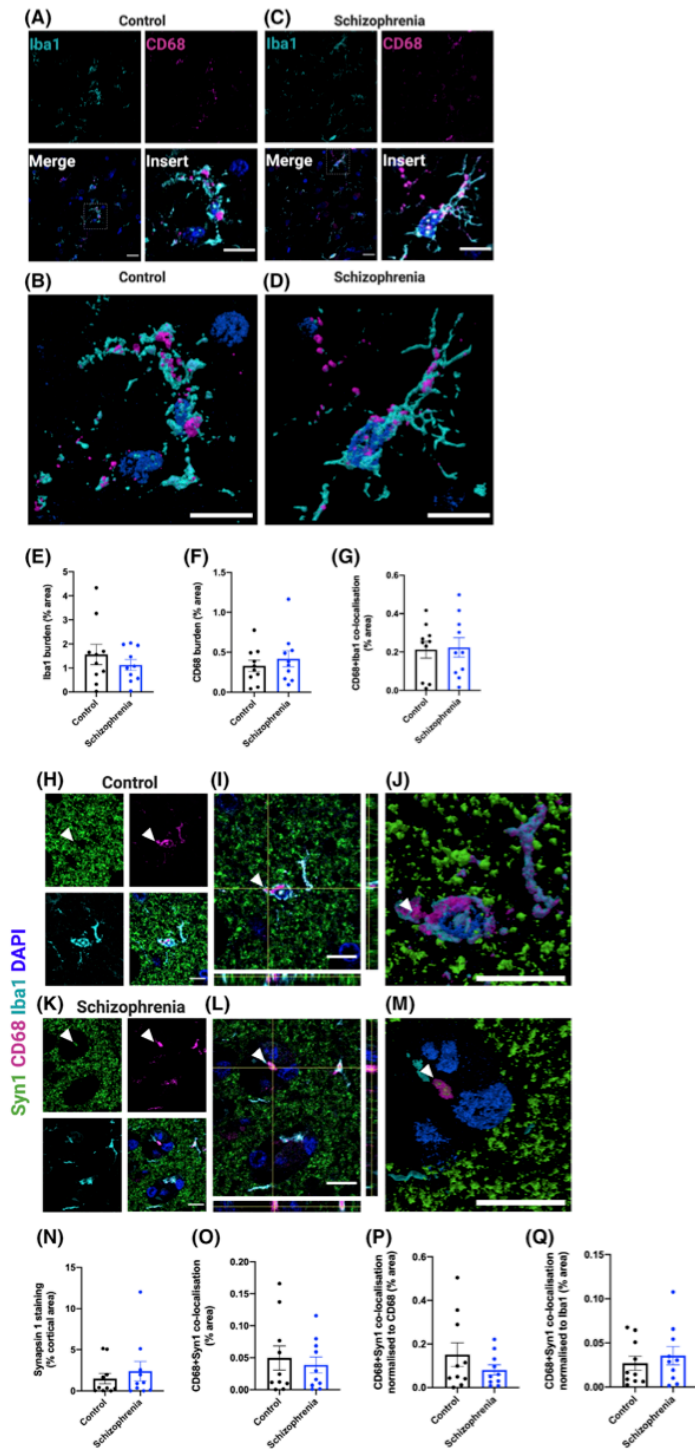
Microglial contribution to synaptic uptake in the prefrontal cortex in schizophrenia

Efficient synaptic communication is crucial to maintain healthy behavioural and cognitive processes. In neurodevelopmental diseases, like schizophrenia, affected individuals can exhibit behavioural symptoms like psychosis, hallucinations and alterations in decision-making. A reduction in cortical grey matter volume and enlarged ventricles in the brains of schizophrenia cases has been consistently reported [1,2]. This reduction in cortical volume is likely to be an outcome of neuronal and synaptic loss, which has also been reported in schizophrenia but the results have varied between brain area and synaptic markers examined [3–7]. A meta-analysis of the expression of synaptic markers in the disease has shown reduced levels of presynaptic markers in the frontal cortex which are heavily implicated in schizophrenia, but not in unaffected areas like the temporal and occipital lobes [8]. Synapses are crucial mediators of brain communication [9], and so, such synaptic alterations can have an impact on brain network connectivity, a process known to be affected in schizophrenia [10]. There are several factors during brain development that influence brain connectivity, with nonneuronal contributors playing an important role in synaptic formation and network maturation [11,12]. One of these nonneuronal contributors are microglia, the resident brain immune cells and primary phagocytes of the brain [12,13]. Gliosis is commonly

observed during loss of brain homeostasis. Microglia have also been shown to facilitate neural network shaping in development by phagocytosing synapses using the complement system [14]. However, microglia can be aberrantly involved in synaptic elimination in nonphysiological contexts, as observed in animal models of Alzheimer's disease [15]. Here, we performed a human post mortem study to investigate the role of microglia in synaptic engulfment in schizophrenia. We examined microglial burden using Iba1 which labels the microglial cytoplasm and reflects microglial motility and homeostasis. Iba1 is considered as a pan-microglial marker and has been observed to be increased in a subset of neurodegenerative diseases [16]. Our other microglial marker, CD68, labels the lysosomal compartment of microglia [17].

We studied post mortem brains from 10 control and 10 schizophrenia cases from the dorsolateral prefrontal cortex which is affected in schizophrenia [1]. Cortical sections were stained with Iba1 and CD68 to label microglia (Figure 1A–D). We observed that there was no difference in either Iba1 ($P = 0.315$) or CD68 ($P = 0.794$) area coverage of the cortex (burden) between the schizophrenia and control cohorts (Figure 1E,F) (full statistical results found in Table S1). Furthermore, there was no difference in the co-localization between CD68 and Iba1 in controls and schizophrenia brains ($P = 0.639$), suggesting the co-expression of the two markers per single cell is unchanged (Figure 1G).

Figure 1. Microgliosis burdens unchanged in control and schizophrenia tissue. Representative confocal images of immunohistochemistry stained sections for the microglial markers Iba1 (cyan) and CD68 (magenta) in control (A,B) and schizophrenia (C,D) tissue. Nuclei are counterstained with 4',6-diamidino-2-phenylindole (DAPI). Scale bars in large images represent 20 and 10 μm in the expanded inserts (denoted by dotted white lines). The insert images of A and B are represented as 3D-reconstruction in B and D, respectively (scale bar, 10 μm). 3-D reconstructions made on ParaView. Quantification of Iba1 burdens (% area), CD68 burdens (% area) and Iba1 + CD68 co-expression (% area) are shown in panels E, F, and G, respectively. Representative confocal images of the pre-synaptic marker synapsin I (green) engulfed by CD68 (magenta) and Iba1 (cyan) in control (H–J) and schizophrenia tissue (K–M). H and K show individual panels of each stain and lastly the merged image, with white arrowheads pointing to sites of co-localisation between CD68 and synapsin I. I and L are expanded images of H and K, with orthogonal views indicating where CD68 and synapsin I co-localise inside Iba1 positive cells. J and M represent 3D reconstructions from H and K, generated on ParaView. Synapsin I burdens are shown in panel N. In O, the co-localisation index of CD68 and synapsin I is quantified for control and schizophrenia cases, where similar levels of synaptic engulfment by microglia are observed. By normalising each image to their respective CD68 burden or Iba1 burden there is still no statistical change in the engulfment of synapsin I by CD68 (P and Q, respectively). Each data point represents a mean average of 20 images taken per case, where $n = 10$ per group. Linear mixed-effects model assessed statistical significance, considering $P \leq 0.05$ for significance. All scale bars in H–M represent 10 μm .



© 2020 The Authors. *Neuropathology and Applied Neurobiology* published by John Wiley & Sons Ltd on behalf of British Neuropathological Society

Figure 1. Microgliosis burdens unchanged in control and schizophrenia tissue. Representative confocal images of immunohistochemistry stained sections for the microglial markers Iba1 (cyan) and CD68 (magenta) in control (A,B) and schizophrenia (C,D) tissue. Nuclei are counterstained with 4',6-diamidino-2-phenylindole (DAPI). Scale bars in large images represent 20 and 10 μm in the expanded inserts (denoted by dotted white lines). The insert images of A and B are represented as 3D-reconstruction in B and D, respectively (scale bar, 10 μm). 3-D reconstructions made on ParaView. Quantification of Iba1 burdens (% area), CD68 burdens (% area) and Iba1 + CD68 co-expression (% area) are shown in panels E, F, and G, respectively. Representative confocal images of the pre-synaptic marker synapsin I (green) engulfed by CD68 (magenta) and Iba1 (cyan) in control (H–J) and schizophrenia tissue (K–M). H and K show individual panels of each stain and lastly the merged image, with white arrowheads pointing to sites of co-localisation between CD68 and synapsin I. I and L are expanded images of H and K, with orthogonal views indicating where CD68 and synapsin I co-localise inside Iba1 positive cells. J and M represent 3D reconstructions from H and K, generated on ParaView. Synapsin I burdens are shown in panel N. In O, the co-localisation index of CD68 and synapsin I is quantified for control and schizophrenia cases, where similar levels of synaptic engulfment by microglia are observed. By normalising each image to their respective CD68 burden or Iba1 burden there is still no statistical change in the engulfment of synapsin I by CD68 (P and Q, respectively). Each data point represents a mean average of 20 images taken per case, where $n = 10$ per group. Linear mixed-effects model assessed statistical significance, considering $P \leq 0.05$ for significance. All scale bars in H–M represent 10 μm

found presynaptic proteins inside microglial cells in the frontal cortex of the brain, but no difference in the levels of synaptic internalization between the two groups. A limitation of our post mortem tissue is that it provides a snapshot of the disease many years after onset, which does not address the mechanism involved in synaptic internalization by microglia. A greater sample size in an independent cohort will be useful to assess the reproducibility of these results and to stratify by confounding variables like sex and age. This would also allow us to assess whether confounding factors like depression, psychosis, systemic inflammation and use of antipsychotic drugs affect these microglial and synaptic interactions. Furthermore, we have looked through all six cortical layers in a nonbiased manner, but we cannot exclude layer specific differences in gliosis, synapse loss or synaptic engulfment by microglia. However, this study is unique by the type of assessment performed on schizophrenia tissue is scarce.

With gliosis being reported in multiple brain disorders, we assessed microgliosis in schizophrenia. As described above, we found no differences in microglial burden between disease and control groups. This suggests that microglial activation is not a sustained event in chronic schizophrenia, and if any changes do occur in these cells it would instead likely involve functional alterations. Previous literature looking at CD68 expression in control and schizophrenia cases has also reported a similar outcome [18]. It is possible that if any changes in glial dynamics were to occur, they may be seen closer to disease onset, and that by the time the brains were donated approximately 35 years later, any changes would have subsided. This would be consistent with the observations published to visualize and quantify microglial activation *in vivo* with positron

emission computed tomography (PET) using specific ligands of the translocator protein TSPO [19]. The PET studies have revealed that activated microglia are present in patients within the first 5 years of disease onset or during a psychotic state, whereas other PET studies in chronic schizophrenia have shown no difference in microglial activation between healthy controls and these patients. Nevertheless, TSPO signals are not a perfect read-out of microglia-mediated inflammation as they are influenced by age and are not microglia-specific [20,21].

Although developmental synaptic alterations, like synapse loss, have been characterized in individuals with schizophrenia [3,8], there are key unanswered questions that remain. For instance, it is not clear how the synapse elimination is mediated, the extent to which it drives behavioural symptoms, or whether it is the outcome of other disease-specific pathologies. Right now, a prominent mechanism for synaptic elimination in development is the use of the classical complement cascade (CCC), where it has been shown to sculpt neural circuits by tagging less electrically active synapses [14]. Recent research has now implicated complement as a signal for aberrant synapse elimination in disease [12,22]. Specifically, variants of C4 of the CCC are associated with a greater risk of developing schizophrenia [23], as well as poorer brain connectivity and schizophrenia-like behavioural deficits in mice [24].

Currently, a suggested mechanism by which complement-tagged synapses are cleared is by microglial recruitment for synaptic removal. In co-cultured neuron and microglia-like cells from human induced pluripotent stem cells from control and schizophrenia lines, increased levels of the excitatory post-synaptic protein PSD-95 was reported phagocytosed in the schizophrenia

co-cultures [25]. Interestingly, this increased phagocytic activity was mainly driven by the presence of schizophrenia-derived microglia. Indeed, when schizophrenia neurons were co-cultured with microglia from control patients, the phagocytic index was reduced, indicating that in schizophrenia microglia have intrinsic differences in their phagocytic response. It is worth noting that induced stem cells are a good model for understanding human disease but represent a developmentally earlier phenotype, and not that of the age of the donor. Therefore, this supports a role for phagocytic microglia in early stages of the illness and may explain why we did not see any changes in phagocytic ability of microglia towards synapses in chronic schizophrenia, as we are not studying the developmental time-frame.

In conclusion, we report that microglia in human post mortem tissue internalize presynaptic proteins physiologically, and that this does not appear to be altered in the chronic form of schizophrenia, in contrast with our observation in AD. Nevertheless, given the typically early onset of schizophrenia and that synapse loss is likely to have occurred years before brain collection, we cannot make assumptions on the role of microglia in synaptic clearance at the start of the disease. Looking forward, it would be interesting to study the difference between young vs. older cases in terms of synaptic uptake by microglia, and phenotype these changes in several brain areas to investigate any region-specific differences. Lastly, longitudinal PET imaging of the presynaptic marker SV2A [26] and TSPO microglial marker would enable exploration of any microglia-synapse association during the course of the illnesses.

Acknowledgements

We would like to thank our funders, specifically the UK Dementia Research Institute which receives funding from Alzheimer's Research UK, the Alzheimer's Society, and the Medical Research Council. We also would like to thank the Wellcome Trust for funding AJS and TLSJ. Tissue samples were obtained from The Corsellis Collection as part of the UK Brain Archive Information Network (BRAIN UK) which is funded by the Medical Research Council and Brain Tumour Research. Ethics approval was provided by BRAIN UK, a virtual brain bank which encompasses the archives of neuropathology departments in the UK and the Corsellis Collection,

© 2020 The Authors. *Neuropathology and Applied Neurobiology* published by John Wiley & Sons Ltd on behalf of British Neuropathological Society


ethics reference 14/SC/0098. The study was registered under the Ethics and Research Governance (ERGO) of the Southampton University (Reference 19791). Authors contributed in the following ways: MT contributed to the study design, performed experiments and imaging, statistical analysis and manuscript preparation; AJS contributed to statistical analysis and manuscript editing; DB contributed by providing cut paraffin-embedded section, study design and manuscript editing; TLSJ contributed the study design, statistical analysis and manuscript editing. TLSJ is on the Scientific Advisory Board of Cognition Therapeutics and receives collaborative grant funding from two industry partners. None of these had any influence over this paper. None of remaining authors declare any conflicts of interest. Figures were created with BioRender.com.

Peer Review


The peer review history for this article is available at <https://publons.com/publon/10.1111/nan.12660>.

Data availability statement

The data that support the findings of this study are available from the corresponding author upon reasonable request.

M. Tzioras*† 

A. J. Stevenson*† 

D. Boche†¹ 

T. L. Spires-Jones*†¹ 

*UK Dementia Research Institute, †Centre for Brain Discovery Sciences, The University of Edinburgh, Edinburgh, and ‡Clinical Neurosciences, Clinical and Experimental Sciences Academic Unit, Faculty of Medicine, University of Southampton, Southampton, UK

¹Equal contribution.

References

- 1 Kikinis Z, Fallon JH, Niznikiewicz M, Nestor P, Davidson C, Bobrow L, et al. Gray matter volume reduction in rostral middle frontal gyrus in patients with chronic schizophrenia. *Schizophr Res* 2010; **123**: 153–9
- 2 Kahn RS, Sommer IE, Murray RM, Meyer-Lindenberg A, Weinberger DR, Cannon TD, et al. Schizophrenia. *Nat Rev Dis Primers* 2015; **1**: 15067

- 3 Feinberg I. Schizophrenia: caused by a fault in programmed synaptic elimination during adolescence? *J Psychiatr Res* 1982; 17: 319–34
- 4 Faludi G, Mirnics K. Synaptic changes in the brain of subjects with schizophrenia. *Int J Dev Neurosci* 2011; 29: 305–9
- 5 Onwordi EC, Half EF, Whitehurst T, Mansur A, Cotel M-C, Wells L, et al. Synaptic density marker SV2A is reduced in schizophrenia patients and unaffected by antipsychotics in rats. *Nat Commun* 2020; 11: 246
- 6 Browning MD, Dudek EM, Rapier JL, Leonard S, Freedman R. Significant reductions in synapsin but not synaptophysin specific activity in the brains of some schizophrenics. *Biol Psychiatry* 1993; 34: 529–35
- 7 Funk AJ, Mielnik CA, Koene R, Newburn E, Ramsey AJ, Lipska BK, et al. Postsynaptic density-95 isoform abnormalities in schizophrenia. *Schizophr Bull* 2017; 43: 891–9
- 8 Osimo EF, Beck K, Reis Marques T, Howes OD. Synaptic loss in schizophrenia: a meta-analysis and systematic review of synaptic protein and mRNA measures. *Mol Psychiatry* 2019; 24: 549–61
- 9 Matsuzaki M, Ellis-Davies GC, Nemoto T, Miyashita Y, Iino M, Kasai H. Dendritic spine geometry is critical for AMPA receptor expression in hippocampal CA1 pyramidal neurons. *Nat Neurosci* 2001; 4: 1086–92
- 10 Klausner P, Baker ST, Cropley VL, Bousman C, Fornito A, Cocchi L, et al. White matter disruptions in schizophrenia are spatially widespread and topologically converge on brain network hubs. *Schizophr Bull* 2017; 43: 425–35
- 11 Eroglu C, Barres BA. Regulation of synaptic connectivity by glia. *Nature* 2010; 468: 223–31
- 12 Henstridge CM, Tzioras M, Paolicelli RC. Glial contribution to excitatory and inhibitory synapse loss in neurodegeneration. *Front Cell Neurosci* 2019; 13: 63
- 13 Sierra A, Abiega O, Shahraz A, Neumann H. Janus-faced microglia: beneficial and detrimental consequences of microglial phagocytosis. *Front Cell Neurosci* 2013; 7: 6
- 14 Schafer DP, Lehrman EK, Kautzman AG, Koyama R, Mardinly AR, Yamasaki R, et al. Microglia sculpt postnatal neural circuits in an activity and complement-dependent manner. *Neuron* 2012; 74: 691–705
- 15 Hong S, Beja-Glasser VF, Nfonoyim BM, Frouin A, Li S, Ramakrishnan S, et al. Complement and microglia mediate early synapse loss in Alzheimer mouse models. *Science* 2016; 352: 712–6
- 16 Boche D, Perry VH, Nicoll JAR. Review: activation patterns of microglia and their identification in the human brain. *Neuropathol Appl Neurobiol* 2013; 39: 3–18
- 17 Franco-Bocanegra DK, McAuley C, Nicoll JAR, Boche D. Molecular mechanisms of microglial motility: changes in ageing and Alzheimer's disease. *Cells* 2019; 8: <https://doi.org/10.3390/cells8060639>
- 18 Arnold SE, Trojanowski JQ, Gur RE, Blackwell P, Han LY, Choi C. Absence of neurodegeneration and neural injury in the cerebral cortex in a sample of elderly patients with schizophrenia. *Arch Gen Psychiatry* 1998; 55: 225–32
- 19 De Picker LJ, Morrens M, Chance SA, Boche D. Microglia and brain plasticity in acute psychosis and schizophrenia illness course: a meta-review. *Front Psychiatry* 2017; 8: 238
- 20 De Picker L, Ottoy J, Verhaeghe J, Deleze S, Wyffels L, Fransen E, et al. State-associated changes in longitudinal [18F]-PBR111 TSPO PET imaging of psychosis patients: Evidence for the accelerated ageing hypothesis? *Brain Behav Immun* 2019; 77: 46–54
- 21 Notter T, Schalbetter SM, Clifton NE, Mattei D, Richetto J, Thomas K, et al. Neuronal activity increases translocator protein (TSPO) levels. *Mol Psychiatry* 2020; 12: <https://doi.org/10.1038/s41380-020-0745-1>
- 22 Carpanini SM, Torvell M, Morgan BP. Therapeutic inhibition of the complement system in diseases of the central nervous system. *Front Immunol* 2019; 10: 362
- 23 Sekar A, Bialas AR, de Rivera H, Davis A, Hammond TR, Kamitaki N, et al. Schizophrenia risk from complex variation of complement component 4. *Nature* 2016; 530: 177–83
- 24 Comer AL, Jinadasa T, Sriram B, Phadke RA, Kretsge LN, Nguyen TPH, et al. Increased expression of schizophrenia-associated gene C4 leads to hypoconnectivity of prefrontal cortex and reduced social interaction. *PLoS Biol* 2020; 18: e3000604
- 25 Sellgren CM, Gracias J, Watmuff B, Biag JD, Thanos JM, Whittredge PB, et al. Increased synapse elimination by microglia in schizophrenia patient-derived models of synaptic pruning. *Nat Neurosci* 2019; 22: 374–85
- 26 Colom-Cadena M, Spires-Jones T, Zetterberg H, Blennow K, Caggiano A, DeKosky ST, et al. The clinical promise of biomarkers of synapse damage or loss in Alzheimer's disease. *Alzheimers Res Ther* 2020; 12: 21

Supporting information

Additional Supporting Information may be found in the online version of this article at the publisher's web-site:

Figure S1. Microglia can engulf synaptophysin in control and schizophrenia human post mortem tissue. Representative confocal images of the presynaptic marker synaptophysin, Sy38, (green), CD68 (magenta) and Iba1 (cyan) in control (A–C) and schizophrenia tissue (D–F). Nuclei are counterstained with DAPI. A and D show individual panels of each stain and lastly the merged image, with white arrowheads pointing to sites

of co-localization between CD68 and synaptophysin. **B** and **E** are expanded images of **A** and **D**, with orthogonal views indicating where CD68 and synaptophysin co-localize. **C** and **F** represent 3D reconstructions from **A** and **D**, generated on ParaView. All scale bars represent 10 μm .

Figure S2. Microglia can engulf PSD-95 in control and schizophrenia human post mortem tissue. Representative confocal images of the presynaptic marker PSD-95 (green), CD68 (magenta) and Iba1 (cyan) in control (**A–C**) and schizophrenia tissue (**D–F**). Nuclei are counterstained with DAPI. **A** and **D** show individual panels of each stain and lastly the merged image, with white

arrowheads pointing to sites of co-localization between CD68 and PSD-95. **B** and **E** are expanded images of **A** and **D**, with orthogonal views indicating where CD68 and PSD-95 co-localize. **C** and **F** represent 3D reconstructions from **A** and **D**, generated on ParaView. All scale bars represent 5 μm .

Table S1. Linear mixed-effects model outcomes from R Studio.

Appendix S1. Methods.

Received 26 May 2020

Accepted after revision 22 August 2020

Published online Article Accepted on 6 September 2020

Methods

Human tissue

Ten cases with a confirmed diagnosis of schizophrenia (mean age 64.80 ± 20.37) and 10 non-neurological and non-neuropathological controls (mean age 64.40 ± 19.78) were obtained from the Corsellis Collection (Table 1). Dorsal prefrontal cortex (DPFC, or Brodmann area 46), an area showing neuroimaging abnormalities with reduction of the grey matter volume in chronic schizophrenia [1], was investigated for all cases. Cases with any other significant brain pathologies such as infarct, tumour, or traumatic brain injury were excluded from the study. Controls with no history of neurological or psychiatric disease or symptoms of cognitive impairment were matched to cases as possible. No difference in age at death and in post-mortem delay was detected between the 2 groups. To minimize the time in formalin, which has an effect on the quality of the immunostaining, the selection was performed on the availability of formalin-fixed paraffin embedded tissue, and thus on blocks processed at the time of the original post-mortem examination. Characteristics of the cohorts are provided in Table 1.

Table 1: Demographic, clinical and *post-mortem* characteristics of control and schizophrenia cases

Cases	Ctrl (n=10)	Sz (n=10)	P value
Sex	4F:6M	2F:8M	
Age at death (years, mean \pm SD)	64.40 ± 19.78	64.80 ± 20.37	P = 0.94
Post-mortem delay (hours, mean \pm SD)	61.90 ± 51.23	50.60 ± 24.52	P = 0.61
Age of onset (years, mean \pm SD)	NA	36.50 ± 13.81	
Duration of illness (years, mean \pm SD)	NA	35.13 ± 21.85	
Cause of death			
<i>Cardiovascular disease</i>	8	5	
<i>infection/inflammation</i>	1	3	
<i>Trauma</i>	1	1	
<i>Others*</i>	0	1	

Ctrl, neurologically/cognitively normal controls; Sz, Schizophrenia cases; F, female, M, male; SD, standard deviation; NA, Not Applicable; *foreign body in respiratory tract

Immunohistochemistry

Paraffin-embedded tissue was cut at 7 μ m thickness on a microtome and mounted on Superfrost glass slides. The tissue was dewaxed in xylene, followed by rehydration in 100% EtOH, 90% EtOH, 70% EtOH, 50% EtOH, and finally water for 3 minutes each. Citric acid pH6 (VectorLabs, H-3300) was used for heat-mediated antigen retrieval by pressure cooking for 3 minutes at the steam setting. The slides were incubated for 5 minutes with autofluorescence eliminator reagent (Merck Millipore, 2160) to reduce background, followed by another 5 minutes incubation with Vector TrueView autofluorescence quenching kit (VectorLabs, SP-8400) to reduce red blood cell autofluorescence. Sections were blocked in 10% normal donkey serum (Sigma Aldrich, D9663-10ML) and 0.3% Triton X-100 (T8787-100ML) for 1 hour at room temperature. Microglia were stained with Iba1 (Abcam, ab5079, goat polyclonal, 1:500), and CD68 (DAKO, M0876, mouse monoclonal, 1:100), and pre-synaptic terminals with synapsin I (Sigma Aldrich, AB1543P, rabbit polyclonal, 1:750) or synaptophysin (R&D Systems, AF5555, goat polyclonal, 1:500) overnight at 4°C in a humid chamber. For post-synaptic staining, PSD-95 was used to label excitatory post-synaptic densities (Synaptic Systems, 124 014, Guinea pig, 1:500), with the addition of salmon sperm DNA (Thermo Fisher Scientific, AM9680, diluted to 200 μ g/ml) in the blocking solution. All primary antibodies were diluted in the blocking solution described above. The following cross-adsorbed secondary antibodies were used: donkey anti-goat A647 (Thermo Fisher Scientific, A32849), donkey anti-mouse A594 (Thermo Fisher Scientific, A32744), and donkey anti-rabbit A488 (Thermo Fisher Scientific, A32790), donkey anti-Guinea pig A488 (Jackson ImmunoResearch, 706-545-148). All secondary antibodies were diluted in phosphate buffer saline (PBS) (Thermo Fisher Scientific, 70011036). For tissue washes, 10X PBS was diluted in water to 1X concentration, with the addition of 0.3% Triton X-100 in washes prior to primary antibody incubation. Nuclei were counterstained with DAPI (1 μ g/ml) (D9542-10MG, Sigma-Aldrich).

Confocal microscopy and image analysis

Twenty images were taken randomly throughout all cortical layers of the grey matter for each case using a Leica TCS8 confocal microscope with a 63x oil immersion objective. Acquisition parameters were kept constant for all images and cases. Lif files were split into tiff files, and batch analysed on ImageJ (version 1.52p, Wayne Rasband, NIH, USA) using a custom co-localisation and thresholding macro. Images from different cases were also manually analysed to ensure the macro was accurately detecting positive signal and excluding background. For

synaptic internalisation by microglia we chose to analyse the colocalization of CD68 with Syn1, and also normalised to either CD68 or Iba1 burden. Data are expressed as protein burden (%) defined as the area fraction of each image labelled by the antibody. 3D reconstruction images were generated in ParaView 5.8.0. All experiments and analyses were blinded to the experimenter.

Ethics

Ethical approval was provided by BRAIN UK, a virtual brain bank which encompasses the archives of neuropathology departments in the UK and the Corsellis Collection, ethics reference 14/SC/0098. The study was registered under the Ethics and Research Governance (ERGO) of the Southampton University (Reference 19791).

Statistics

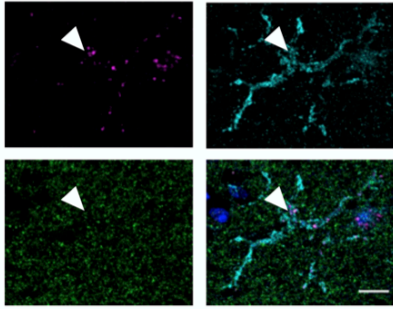
R Studio version 3.6.0 (2019-04-26) was used for statistical analysis [2]. Linear mixed-effects models were used to examine the effect of disease status on microglial burdens and CD68-Synapsin I co-localisation. This test was chosen because it allows all 20 images taken per case to be considered while accounting for non-independence, instead of a single mean value per case, allowing for a more powerful analysis on the results. QQ plots were generated in R Studio to check the residuals were normally distributed, which is an assumption of the mixed-effects model. To meet the assumptions of the test, all datasets were Tukey transformed prior to analysis (untransformed data presented in graphs). GraphPad Prism 8 was used for generating bar graphs with a mean value plotted per case, represented as a dot. We considered $p \leq 0.05$ as significant.

References

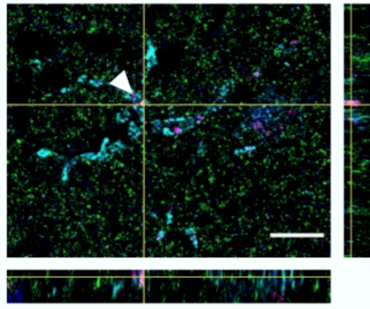
- 1 Kikinis Z, Fallon JH, Niznikiewicz M, Nestor P, Davidson C, Bobrow L, *et al.* Gray matter volume reduction in rostral middle frontal gyrus in patients with chronic schizophrenia. *Schizophr Res* 2010;**123**:153–9.
- 2 Team RC. R: A language and environment for statistical computing. R Foundation for Statistical Computing, Vienna, Austria. 2012. URL [http://www R](http://www.R-project.org/)

Control

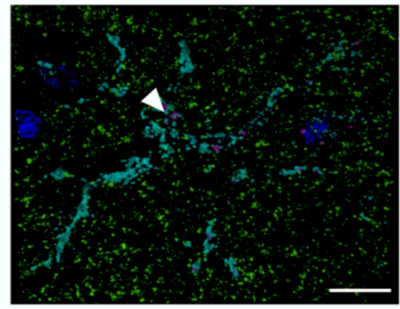
A



B

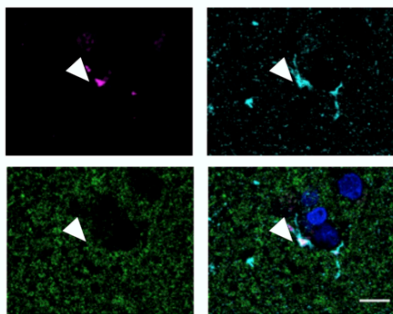


C

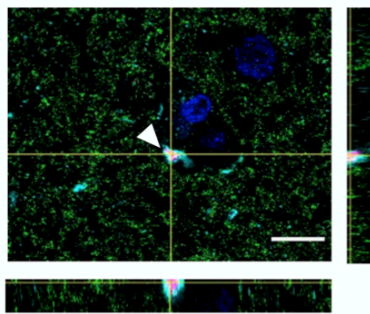


Schizophrenia

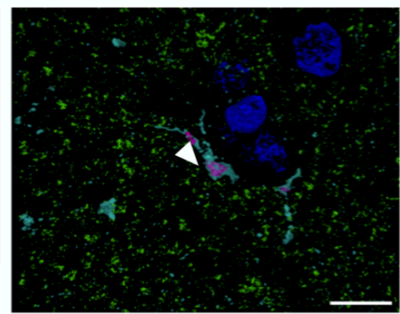
D



E

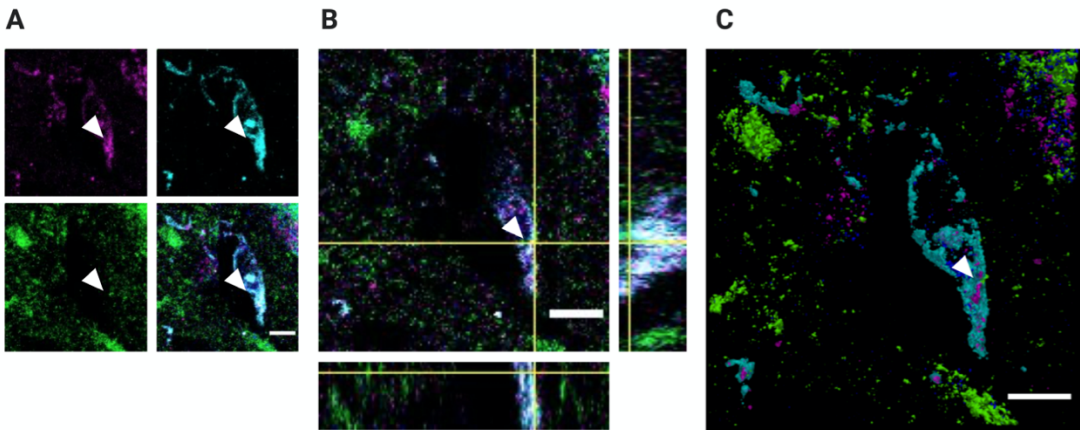


F

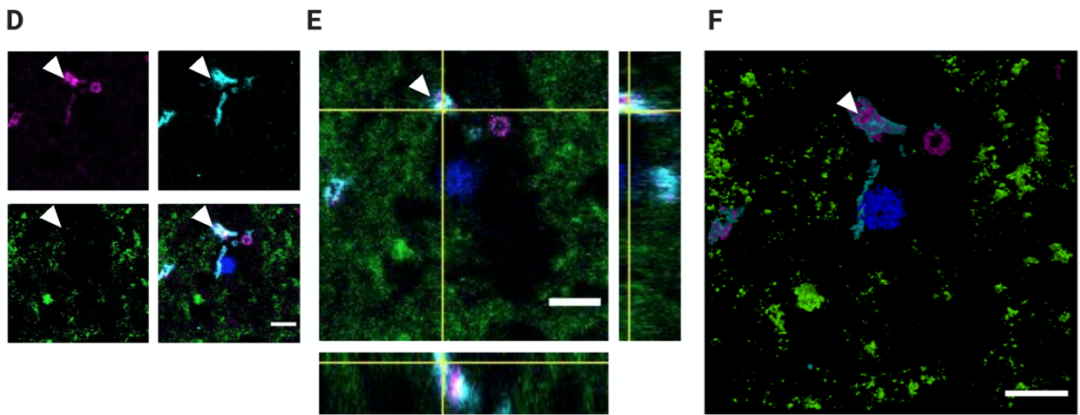


Sy38 CD68 Iba1 DAPI

Control



Schizophrenia



PSD-95 CD68 Iba1 DAPI

Supplementary Table 1: Linear mixed-effects model outcomes from R Studio.

Measurement	Effect size	Standard Error	p-value
Iba1 burden (% area)	-0.1637	0.1580	0.315
CD68 burden (% area)	0.0165	0.06215	0.794
Synapsin 1 burden (% area)	0.01049	0.1862	0.956
CD68+Iba1 colocalisation (% area)	-0.0378	0.0792	0.639
CD68+Syn1 colocalisation (% area)	-0.0772	0.0917	0.413
CD68+Syn1 colocalisation /CD68 (% area)	-0.1414	0.0980	0.167
CD68+Syn1 colocalisation /Iba1 (% area)	-0.0044	0.0958	0.964

3. Re-analysis of data with 3D segmentation

A limitation of the analysis used in the manuscript is that images were max projected in FIJI and colocalisation was based on the projected 2D images. Given that synapses are smaller than the step size used in the confocal imaging (less than $0.3\mu\text{m}$), it is possible this analysis gives false-positives by showing colocalisation of Synapsin I with CD68-positive cells, even if the synapse exists on a different Z plate to the microglia. For this reason, the images acquired for the manuscript were 3D segmented and re-analysed using the same segmentation pipeline described in the Methods and Chapter 3 (Human post-mortem AD chapter). Briefly, 3D segmented images provided a volumetric measurement of burdens and colocalisation between different markers. The data came from 10 neurologically control individuals and 10 individuals with schizophrenia, where 20 images were taken per case from the grey matter. Data were analysed with a mixed effects linear model (R Studio) in order to compare all images taken per case and assess confounding variables like sex. Overall, the new 3D analysis has found no statistically significant differences between the control and schizophrenia groups in any measurements, just like the 2D analysis.

Specifically, no differences were seen between the control and schizophrenia groups in terms of Iba1 burdens (Figure 2A) ($F [1,17]=0.4517$, $p=0.5106$), CD68 burdens (Figure 2B) ($F [1,17]=0.6654$, $p=0.4259$), Iba1+CD68 colocalisation (Figure 2C) ($F [1,17]=0.0013$, $p=0.9719$), and Synapsin I burdens (Figure 2D) ($F [1,17]=0.2764$, $p=0.6058$). Also, no significant differences were found between these measurements regarding sex, specifically in Iba1 burdens $F [1,17]=0.0002$, $p=0.9886$, in CD68 burdens $F [1,17]=1.4117$, $p=0.2511$, in Iba1+CD68 colocalisation $F [1,17]=0.3317$, $p=0.5722$, and in Synapsin I burdens $F [1,17]=0.4030$, $p=0.5340$.

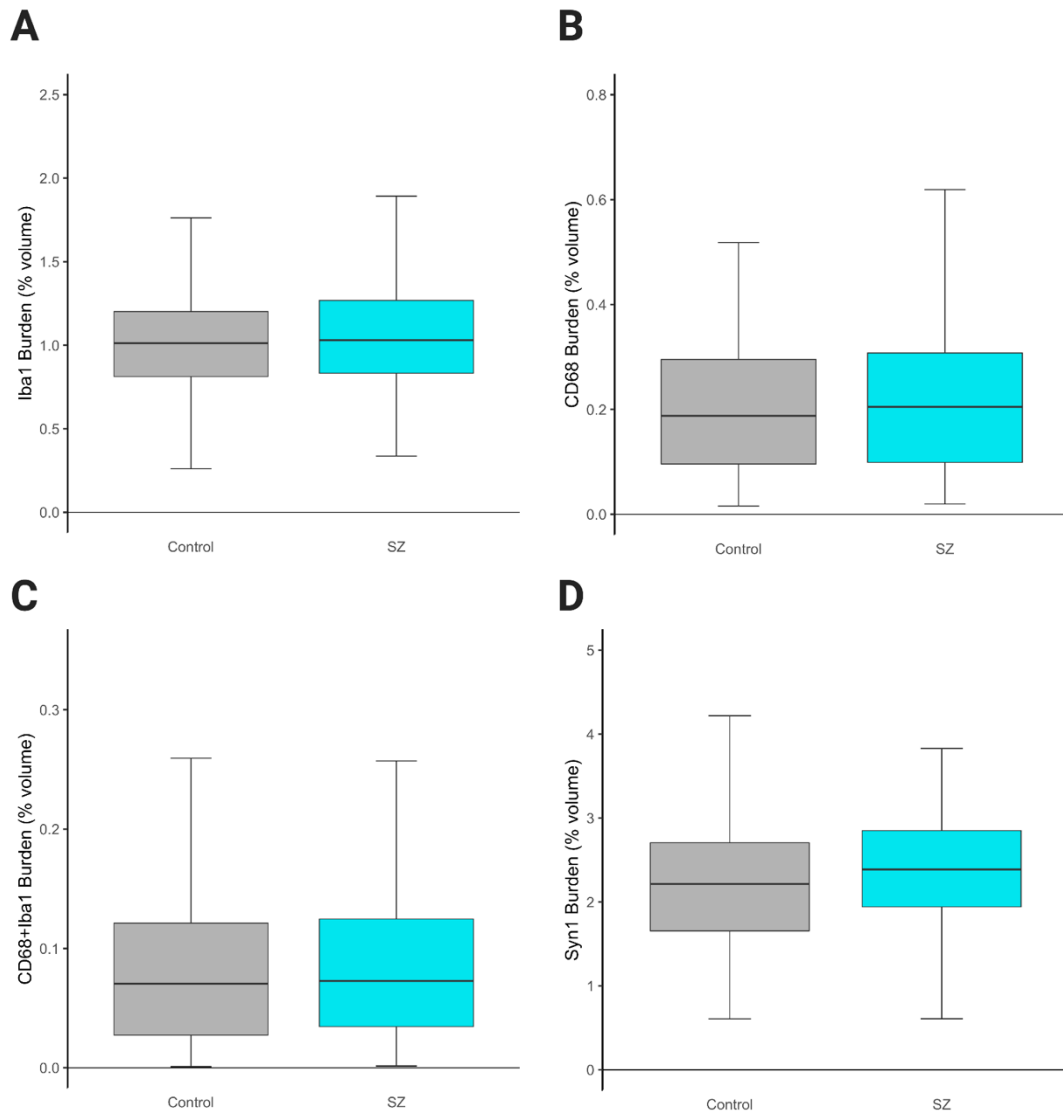


Figure 2. Glial and synaptic burdens in the dorsolateral pre-frontal cortex from control and schizophrenia (SZ) human post-mortem brains. (A) Percent volume covered by Iba1 staining (burden) in control and SZ cases. No significant differences found between the groups. (B) Percent volume covered by CD68 staining (burden) in control and SZ cases. No significant differences found between the groups. (C) Percent volume of colocalising CD68 and Iba1 staining. No significant differences found between the groups. (D) Percent volume covered by Synapsin 1 staining (burden) in control and SZ cases. No significant differences found between the groups. The tops and bottoms of the bar graph represent the interquartile range, the line in the bar represents the median, and the error bars represent 1.5x interquartile range. For statistics, significance is considered for $p < 0.05$.

Moreover, much like the 2D analysis, no statistically significant differences were found between any synaptic ingestion measurements, neither when comparing control and schizophrenia cases nor sexes. Specifically, no significant changes were reported in CD68+Syn1 colocalisation (Figure 3A) (Disease: $F [1,17]=0.2764$, $p=0.6058$, Sex: $F [1,17]=0.4030$, $p=0.5340$), CD68+Syn1 colocalisation normalised to CD68 burdens (Figure 3B) (Disease: $F [1,17]=0.0658$, $p=0.8007$, Sex: $F [1,17]=2.1191$, $p=0.1637$), nor CD68+Syn1 colocalisation normalised to Iba1 burdens (Figure 3C) (Disease: $F [1,17]=0.2523$, $p=0.6219$, Sex: $F [1,17]=0.7805$, $p=0.3893$).

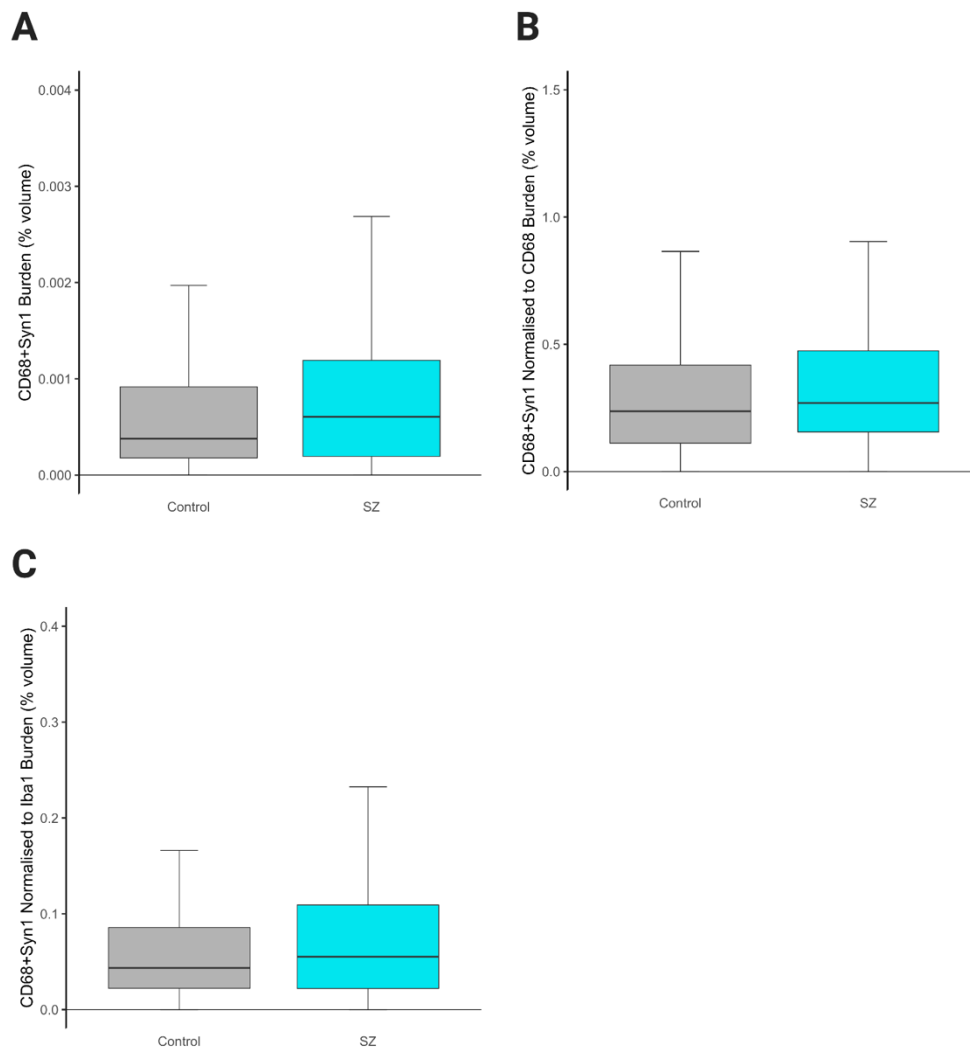


Figure 3. Colocalisation of CD68+Syn1 burdens in the dorsolateral pre-frontal cortex from control and schizophrenia (SZ) human post-mortem brains. (A) Percent volume of colocalising CD68 and Syn1 staining (burden) in control and SZ cases. No significant differences found between the groups. (B) Percent volume of colocalising CD68 and Syn1 staining normalised to CD68 burdens (burden) in control and SZ cases. No significant differences found between the groups. (C) Percent volume of colocalising CD68 and Syn1 staining normalised to Iba1 burdens (burden) in control and SZ cases. No significant differences found between the groups. The tops and bottoms of the bar graph represent the interquartile range, the line in the bar represents the median, and the error bars represent 1.5x interquartile range. For statistics, significance is considered for $p < 0.05$.

4. Conclusion

This study presented evidence of synaptic protein inside microglial lysosomes in the brains of control participants as well as from individuals with schizophrenia. No differences were found between the two groups in terms of glial burdens, nor synaptic engulfment by microglia, whether the images were analysed with 2D or 3D segmentation. The study assessed at 10 control and 10 schizophrenia cases, which did not allow for results to be stratified by factors like sex, age, comorbid symptoms (like psychosis or depression), and drug treatment, although all of these would provide valuable insight (Tzioras, Stevenson, Boche and Spires-Jones, 2021).

The use of human tissue is a precious resource in understanding schizophrenia pathogenesis, especially given the lack of appropriate animal models of the disease. However, the disadvantage is that it only provides a snap-shot of the brain at the time of death, and limits any efforts of exploring mechanistic changes at the cellular or molecular level. It is therefore unclear from this preliminary study whether microglia always prune synapses at similar levels between control and schizophrenia brains, or if there are differences closer to disease onset, where inflammation is at its peak. *In-vitro* work using hiPSCs showed that microglia phagocytose more synapses when

derived from schizophrenia patients than control ones (Sellgren et al., 2019). Stem cells display a more developmental phenotype in cells, which also favours phagocytosis pathways and so may better resemble what happens earlier in the disease. In order to mirror these experiments in human PM tissue, it would require a cohort with brain donation occurring shortly after disease onset.

The complement system pathways have been involved both as risk factors for developing schizophrenia and as a potential culprit in deficient neuronal function. It is also possible that similar to how the complement system tags weaker synapses for pruning in development and pathologically in AD, in schizophrenia too microglia eliminate synapses instructed by complement signalling.

Lastly, neurodegenerative diseases like AD are progressive in nature, where synapse loss is ongoing. Schizophrenia has not been characterised as a progressive disease, but does display synapse loss and glial changes. It can be speculated that not seeing differences in synaptic ingestion by microglia in schizophrenia, but seeing them in AD, is an exciting outcome and acts as an internal control to the AD data in Chapters 3 and 4. Overall, this study was only the beginning in understanding novel mechanisms that drive synapse loss in schizophrenia.

Chapter 6: Discussion

1. Overview

The results of this thesis have demonstrated that microglia and astrocytes exhibit increased synaptic ingestion in Alzheimer's disease, but not in schizophrenia. Specifically, microglia in human post-mortem tissue contained greater amounts of the pre-synaptic marker synapsin I, and interestingly this was heightened near A β plaques. Furthermore, isolated synaptoneurosomes from AD brains were ingested both more and faster by microglia and astrocytes in culture. However, human brains with schizophrenia did not differ in the amounts of synapsin I found inside microglial phago-lysosomes with age-matched neurological controls. It would be interesting to examine whether synaptoneurosomes from brains with schizophrenia are ingested similar to control levels. The data presented here are novel in the field of neuroscience as there has never been a quantification of synaptic ingestion by microglia in the AD human brain published in the literature. These outcomes, in combination with data from mouse models of AD that have shown microglia eliminate synapses in a pathological way, provide an exciting new avenue for targeting synapse loss in AD with the goal of preventing the cognitive decline associated with the disease. The aim of this chapter is to discuss how these data fit in the wider context of AD and schizophrenia, as well as which new questions have emerged and which questions remain.

2. Synapses: Shantay you stay or sashay away?

2.1 Synaptic decorations: “eat-me” and “don’t eat me” signals

As alluded to in Chapter 4, a gain of “eat-me” signals and a loss of “don’t eat-me” signals at the synapse has been seen in AD synaptoneurons by proteomics, and is a possible explanation to the increased synaptic ingestion by microglia in culture (Figure 1). These include increased levels of MFG-E8 bound on exposed phosphatidylserine, C1q, C3, and loss of CD47. However, a question that has been left unanswered in this thesis is whether the synaptic material ingested by microglia in the human brains comes from degenerating synapses that need to be cleared or whether the synapses are active and healthy. The resolution of confocal microscopy is not sufficient to detect structural changes in the synapse in order to determine whether they are degenerating, and there are currently no synaptic markers of degeneration to stain human tissue with. In mice, targeting the complement pathway in amyloidopathy models is beneficial for synaptic function and cognitive performance whilst microglial-mediated synapse elimination is reduced (Hong et al., 2016; Bie et al., 2019; Shi et al., 2017a), suggesting that to a certain extent microglia pathologically engulf synapse. This is not specific to AD however, as in multiple sclerosis, an autoimmune demyelinating disease (Dutta et al., 2011; Aggelakopoulou et al., 2016), the complement system also pathologically tags synapses for removal, both in human tissue and experimental mouse models (Michailidou et al., 2015; Watkins et al., 2016; Michailidou et al., 2017, 2018; Werneburg et al., 2020). As it is difficult to mechanistically explore this using donated human tissue, a future experiment that would shed more light on this would be correlating cognitive function to the amount of synaptic ingestion occurring.

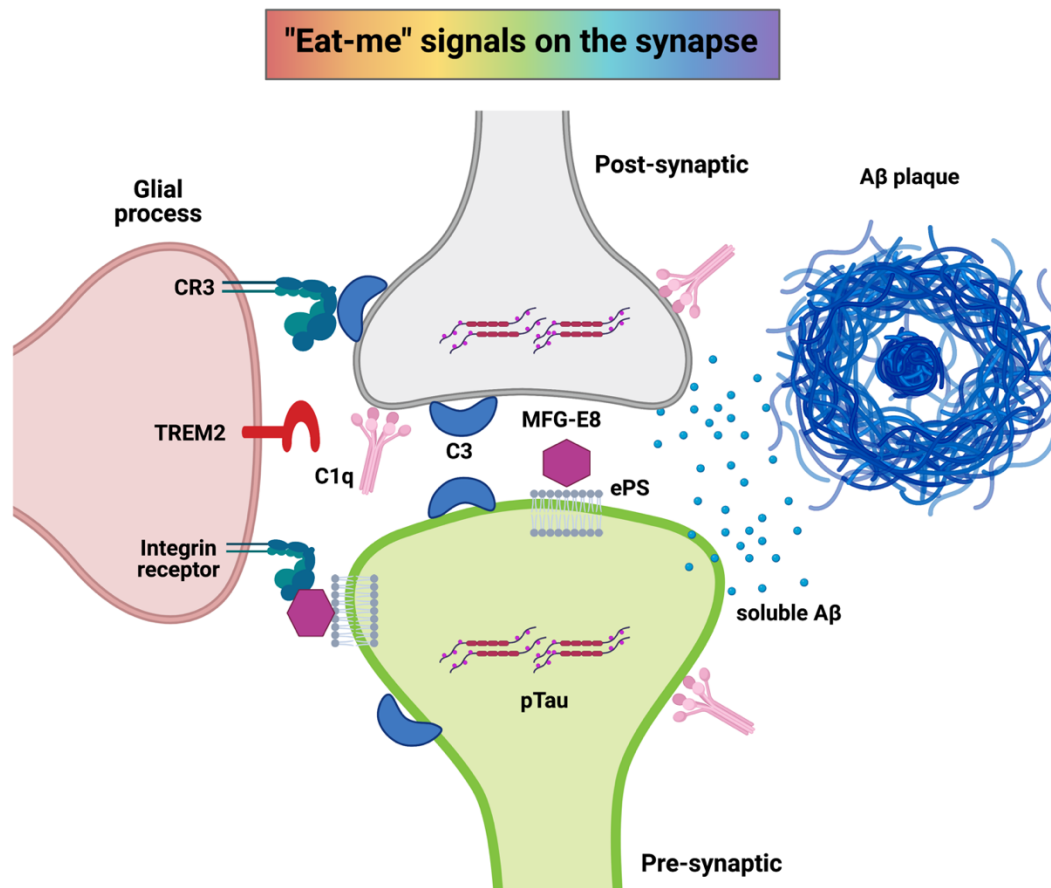


Figure 1. Schematic diagram of the tri-partite synapse and “eat-me” signals in AD. These signals include C1q, C3, MFG-E8 which binds on exposed phosphatidylserine, and soluble Aβ. Microglia use integrins receptors (complement receptor 3, or CR3 being one of them) and TREM2 to sense their environments and bind to these opsonin molecules on the synapses. Phosphorylated tau (pTau) and Aβ plaques are key features of the AD synapse pathology.

2.2 APOE, Aβ, and tau interactions in microglial ingestion of synapses

The greatest genetic risk factor for developing sporadic AD is the possession of an APOE4 allele, which, as discussed in Chapter 1 (Introduction), is also associated to greater synapse loss and reactive gliosis (Zhu et al., 2012; Colton et al., 2002; Caberlotto et al., 2016; Tzioras et al., 2019; Rodriguez et al., 2014). Consequently, it was hypothesised that APOE4 carriers will display greater synaptic ingestion, particularly in the AD group. Microglial ingestion in

human tissue was analysed in 3D segmented images by a mixed-effect linear regression model that allows for stratification based on factors like sex or APOE status. Interestingly, individuals with an E4 allele were inflicted by higher burdens of CD68+SynI, meaning greater synaptic ingestion by microglia. To date, no evidence has been published in neither mice nor humans showing APOE playing a direct role in synaptic engulfment by microglia. It is also possible that microglia mediate increased synapse loss in APOE4 carriers but in non-contact dependent mechanisms, for example by secretion of synaptotoxic inflammatory cytokines like IL1- β and IL-6. No APOE effects were seen in the *in-vitro* study, suggesting that the levels of the signals on the synapse that microglia recognise for phagocytosis are not considerably different. One way to further test this hypothesis is by isolating microglia from the APOE knock-in (human APOE2,3,or4) and knock-out mice that are currently bred in the lab and incubating them with the human synaptoneuroosomes. It is likely that APOE4-expressing microglia are more phagocytic towards the synaptoneuroosomes.

The concept that APOE4 is also associated to greater A β and tau burdens, as well as more neurodegeneration in AD has already been examined in this thesis. It is not clear, however, if there is an interaction between APOE, A β and tau in inducing exacerbated glial-mediated synapse loss in AD, but recent evidence suggests that this is indeed possible. A β can bind on the transmembrane receptor 97 (TMEM97), which in combination to phosphorylated tau is predicted to induce neurodegeneration (Colom-Cadena et al., 2020; Pickett et al., 2019). Knowing that the two pathological proteins are found at higher levels in APOE4 carriers, it would not be surprising if their interaction results in increased synapse loss in AD. Although not shown directly so far, it is possible that stress and danger signals accumulate in such synapses in the form complement tags, in tandem to losing protective signals like CD47.

2.3 *In-vitro* to *in-vivo*: lost in translation

In this thesis, an indirect approach was necessary to study how human synapses (in the form of synaptoneurosomes) were ingested by microglia in culture. Although such experiments can and have been conducted in model organisms *in-vivo*, it is not possible to replicate in humans. Nevertheless, it is important to understand and appreciate the strengths and limitations of using an *in-vitro* system to study human synapses and microglia. The obvious strength of using an *in-vitro* approach is the ability to study how human microglia ingest synapses, which cannot be studied or modulated in a living human brain. One of the limitations of this system is the use of frozen human brains, which disrupts the shape (and likely function) of the synaptic proteins, and the opsonin tags. However, it would be extremely rare to be able to get a donation of live tissue for isolating microglia, alongside a donation of AD brain tissue for making synaptoneurosomes from fresh tissue. Another limitation is that microglia are sensitive to their environments, and monocultures of microglia display significant differences in morphology and function, compared to those *in-vivo*. Ultimately, the rates of phagocytosis in a culture system cannot be extrapolated to represent what would happen to a living human brain, but it does allow to important questions to be answered, as presented in this thesis.

3. Synaptic ingestion by microglia in AD and schizophrenia

A growing amount of literature has implicated microglia as a pathological eliminators of synapses in AD mouse models, so it was not surprising that in human post-mortem tissue microglia were observed ingesting more synapses than in age-matched controls. Very recently, hiPSC co-cultures derived from patients with AD have also shown microglia engulfing PSD-95 puncta (Guttikonda et al., 2021), while human synaptosomes are also phagocytosed

by hiPSC-derived microglia (McQuade et al., 2020). Similarly, as discussed in Chapter 5 (Schizophrenia), hiPSC microglia derived from patients with schizophrenia phagocytose more post-synapses in culture than microglia derived from control lines (Sellgren et al., 2019). However, in this work no differences were observed in pre-synaptic ingestion by microglia in the prefrontal cortex of patients with schizophrenia compared to controls (Tzioras et al., 2021). As explained in Chapter 5, schizophrenia is not considered to be a progressive disease and it is not clear whether the lower synaptic burdens reflect synapse loss or failure to form synapses properly. On the other hand, AD is a progressive disease with ongoing synapse loss. It is therefore interesting that increased synaptic ingestion is detected in AD brains, but not in brains with schizophrenia. In a way, the study looking at schizophrenia has acted as a negative control to the AD study by showing that the presence of neurological disease is not sufficient to induce microglial uptake of synapses and that AD effects are more likely due to the specific disease.

4. Metabolic disease in AD and synaptic engulfment

It is known that sporadic AD is highly influenced by non-genetic factors, like lifestyle. Specifically, metabolic diseases during midlife like obesity, hyperlipidaemia and type 2 diabetes (T2D) all increase the risk of developing AD later in life, and can accelerate the transition from MCI to AD (Kivipelto et al., 2005; Profenno, Porsteinsson and Faraone, 2010; Xu et al., 2010). Moreover, APP/PS1 mice crossed with a diabetic line showed exacerbated cognitive decline, more A β plaques, vascular damage and reduced spine density (Infante-Garcia, Ramos-Rodriguez, Galindo-Gonzalez and Garcia-Alloza, 2016). When these mice were treated with the antidiabetic agent Empagliflozin there was a significant reduction in the aforementioned pathologies, as well as reduced microgliosis (Hierro-Bujalance et al., 2020). To this extent, the Rajedran lab in King's College London have hypothesised that in early stages of AD these metabolic disorders negatively contribute to

AD-pathologies, like impaired amyloid clearance and synapse dysfunction, but in late stages the increased levels of insulin and hyperlipidaemia provide metabolic support to microglia to assuage phagocytosis. Also, they have recently shown that BV2 microglia depleted of nutrients phagocytose more synaptosomes. To assist them with testing this hypothesis, human post-mortem tissue was stained in the lab similarly to Chapters 3 and 5 to label microglia and synapses, which has been published as a BioRxiv pre-print (Mondal et al., 2020). In this case, individuals were stratified based on the presence of hyperlipidaemia and T2D (neither of which were present in the cases of this thesis). Surprisingly, individuals with AD and hyperlipidaemia showed significantly reduced synaptic ingestion by microglia and performed better at the MMSE tests, indicating better cognitive function. Therefore, it is important to be aware of these factors when looking at microglia in human tissue.

5. Future experiments

In the short term, the aim is to increase the sample size of the phagocytosis assays using mouse astrocytes and human microglia, depending on tissue availability. Female mice are also expected to be used for isolating microglia and challenging them with pHrodo-synaptoneuroosomes to test for any sex effects. Next, a flow cytometry panel has been established to detect levels of complement proteins in the human synaptoneuroosomes to validate the changes seen in the proteomic study. The antibodies used for this are C1q, C3d (an activated form of C3), and C4, as well as histone H3 and synaptophysin to cross-validate with the Western blots. To this extent, mice lacking the complement 3 receptor (CR3-knock-out mice) are being bred in the lab and aged to 2 months to isolate microglia from their brains and challenge with the synaptoneuroosomes. CR3 is also known as CD11b which the target of the immunomagnetic beads used to isolate microglia, so immunomagnetic beads against P2RY12 have been purchased for isolating microglia.

Moreover, given MFGE-8's role in tagging neurons for microglial-mediated phagocytosis, an MFGE-8 blocking antibody has been purchased to attempt blocking bound MFGE-8 on the synaptoneuroosomes with the hypothesis that ingestion will be reduced. Furthermore, human post-mortem tissue from the same control and AD cases has been stained with the astrocytic marker GFAP and analysed for the presence of synapsin I inside astrocytes. In order to address the issue of whether living or degenerating synapses are targeted by microglia, an ex-vivo model of organotypic hippocampal slice cultures can be used. These slices provide an intact cytoarchitecture of the mouse hippocampus, and Dr. Claire Durrant who has joined the lab as a Race Against Dementia fellow is an expert in generating these preparations. One way of labelling living neurons and dendrites is by virally expressing GCaMP-GFP constructs and labelling microglia with isolectin-A594. These preps can be challenged with human brain homogenate from AD brains to mimic the AD brain environment and live image the cultures using 2-photon microscopy to detect whether microglia engulf active synapses.

6. Conclusion

To conclude, this thesis has expanded the fields of neuroscience and glial biology by demonstrating that in human AD brains there is greater synaptic ingestion by microglia, but not in schizophrenia. Moreover, A β plaques are associated with greater microgliosis and increased ingestion of synapses by microglia. This was shown to be true in two brain areas, the inferior temporal lobe and the primary visual cortex. Interestingly, mouse microglia and astrocytes, as well as human microglia, preferentially phagocytose AD-derived synaptoneuroosomes from the temporal lobe compared to synaptoneuroosomes from control brains. These data are exciting and promising because they show a potential candidate to be therapeutically targeted for limiting synapse loss and preventing cognitive decline in AD patients.

References

- Aggelakopoulou, M., Kourepini, E., Paschalidis, N., Simoes, D.C.M., Kalavrizioti, D., Dimisianos, N., Papathanasopoulos, P., Mouzaki, A., and Panoutsakopoulou, V., 2016. ER β -Dependent Direct Suppression of Human and Murine Th17 Cells and Treatment of Established Central Nervous System Autoimmunity by a Neurosteroid. *Journal of Immunology*, 197(7), pp.2598–2609.
- Allen, N.J., and Eroglu, C., 2017. Cell Biology of Astrocyte-Synapse Interactions. *Neuron*, 96(3), pp.697–708.
- Alliot, F., Godin, I., and Pessac, B., 1999. Microglia derive from progenitors, originating from the yolk sac, and which proliferate in the brain. *Brain research. Developmental brain research*, 117(2), pp.145–152.
- Alliot, F., Lecain, E., Grima, B., and Pessac, B., 1991. Microglial progenitors with a high proliferative potential in the embryonic and adult mouse brain. *Proceedings of the National Academy of Sciences of the United States of America*, 88(4), pp.1541–1545.
- Andrews-Zwilling, Y., Bien-Ly, N., Xu, Q., Li, G., Bernardo, A., Yoon, S.Y., Zwilling, D., Yan, T.X., Chen, L., and Huang, Y., 2010. Apolipoprotein E4 causes age- and Tau-dependent impairment of GABAergic interneurons, leading to learning and memory deficits in mice. *The Journal of Neuroscience*, 30(41), pp.13707–13717.
- Arnold, S.E., Trojanowski, J.Q., Gur, R.E., Blackwell, P., Han, L.Y., and Choi, C., 1998. Absence of neurodegeneration and neural injury in the cerebral cortex in a sample of elderly patients with schizophrenia. *Archives of General Psychiatry*, 55(3), pp.225–232.
- Ayata, P., Badimon, A., Strasburger, H.J., Duff, M.K., Montgomery, S.E., Loh, Y.-H.E., Ebert, A., Pimenova, A.A., Ramirez, B.R., Chan, A.T., Sullivan, J.M., Purushothaman, I., Scarpa, J.R., Goate, A.M., Busslinger, M., Shen, L., Losic, B., and Schaefer, A., 2018. Epigenetic regulation of brain region-specific microglia clearance activity. *Nature Neuroscience*, 21(8), pp.1049–1060.
- Azevedo, E.P., Ledo, J.H., Barbosa, G., Sobrinho, M., Diniz, L., Fonseca, A.C.C., Gomes, F., Romão, L., Lima, F.R.S., Palhano, F.L., Ferreira, S.T., and Foguel, D., 2013. Activated microglia mediate synapse loss and short-term memory deficits in a mouse model of transthyretin-related oculoleptomeningeal amyloidosis. *Cell death & disease*, 4, p.e789.
- Baglietto-Vargas, D., Moreno-Gonzalez, I., Sanchez-Varo, R., Jimenez, S., Trujillo-Estrada, L., Sanchez-Mejias, E., Torres, M., Romero-Acebal, M., Ruano, D., Vizuete, M., Vitorica, J., and Gutierrez, A., 2010. Calretinin interneurons are early targets of extracellular amyloid-beta pathology in PS1/AbetaPP Alzheimer mice hippocampus. *Journal of Alzheimer's Disease*, 21(1), pp.119–132.
- Beckman, D., Ott, S., Donis-Cox, K., Janssen, W.G., Bliss-Moreau, E., Rudebeck, P.H., Baxter, M.G., and Morrison, J.H., 2019. Oligomeric A β in the monkey brain

impacts synaptic integrity and induces accelerated cortical aging. *Proceedings of the National Academy of Sciences of the United States of America*.

Benetatos, J., Bennett, R.E., Evans, H.T., Ellis, S.A., Hyman, B.T., Bodea, L.-G., and Götz, J., 2020. PTEN activation contributes to neuronal and synaptic engulfment by microglia in tauopathy. *Acta Neuropathologica*.

Bennett, M.L., Bennett, F.C., Liddel, S.A., Ajami, B., Zamanian, J.L., Fernhoff, N.B., Mulinyawe, S.B., Bohlen, C.J., Adil, A., Tucker, A., Weissman, I.L., Chang, E.F., Li, G., Grant, G.A., Hayden Gephart, M.G., and Barres, B.A., 2016. New tools for studying microglia in the mouse and human CNS. *Proceedings of the National Academy of Sciences of the United States of America*, 113(12), pp.E1738-46.

van Berckel, B.N., Bossong, M.G., Boellaard, R., Kloet, R., Schuitmaker, A., Caspers, E., Luurtsema, G., Windhorst, A.D., Cahn, W., Lammertsma, A.A., and Kahn, R.S., 2008. Microglia activation in recent-onset schizophrenia: a quantitative (R)-[11C]PK11195 positron emission tomography study. *Biological Psychiatry*, 64(9), pp.820–822.

Bie, B., Wu, J., Foss, J.F., and Naguib, M., 2019. Activation of mGluR1 Mediates C1q-Dependent Microglial Phagocytosis of Glutamatergic Synapses in Alzheimer's Rodent Models. *Molecular Neurobiology*, 56(8), pp.5568–5585.

Blain, M., Miron, V.E., Lambert, C., Darlington, P.J., Cui, Q.-L., Saikali, P., Yong, V.W., and Antel, J.P., 2010. Isolation and culture of primary human CNS neural cells. In: L.C. Doering, ed., *Protocols for neural cell culture*, Springer Protocols Handbooks. Totowa, NJ: Humana Press, pp.87–104.

Boche, D., Gerhard, A., Rodriguez-Vieitez, E., and MINC Faculty, 2019. Prospects and challenges of imaging neuroinflammation beyond TSPO in Alzheimer's disease. *European Journal of Nuclear Medicine and Molecular Imaging*, 46(13), pp.2831–2847.

Bohlen, C.J., Bennett, F.C., Tucker, A.F., Collins, H.Y., Mulinyawe, S.B., and Barres, B.A., 2017. Diverse Requirements for Microglial Survival, Specification, and Function Revealed by Defined-Medium Cultures. *Neuron*, 94(4), p.759–773.e8.

Braak, H., and Braak, E., 1991. Neuropathological staging of Alzheimer-related changes. *Acta Neuropathologica*, 82(4), pp.239–259.

Bradt, B.M., Kolb, W.P., and Cooper, N.R., 1998. Complement-dependent proinflammatory properties of the Alzheimer's disease beta-peptide. *The Journal of Experimental Medicine*, 188(3), pp.431–438.

Brelstaff, J., Tolkovsky, A.M., Ghetti, B., Goedert, M., and Spillantini, M.G., 2018. Living Neurons with Tau Filaments Aberrantly Expose Phosphatidylserine and Are Phagocytosed by Microglia. *Cell reports*, 24(8), p.1939–1948.e4.

Browning, M.D., Dudek, E.M., Rapier, J.L., Leonard, S., and Freedman, R., 1993. Significant reductions in synapsin but not synaptophysin specific activity in the brains of some schizophrenics. *Biological Psychiatry*, 34(8), pp.529–535.

Buttgereit, A., Lelios, I., Yu, X., Vrohings, M., Krakoski, N.R., Gautier, E.L., Nishinakamura, R., Becher, B., and Greter, M., 2016. Sall1 is a transcriptional

regulator defining microglia identity and function. *Nature Immunology*, 17(12), pp.1397–1406.

Byun, Y.G., and Chung, W.-S., 2018. A Novel In Vitro Live-imaging Assay of Astrocyte-mediated Phagocytosis Using pH Indicator-conjugated Synaptosomes. *Journal of Visualized Experiments*, (132).

Caberlotto, L., Marchetti, L., Lauria, M., Scotti, M., and Parolo, S., 2016. Integration of transcriptomic and genomic data suggests candidate mechanisms for APOE4-mediated pathogenic action in Alzheimer's disease. *Scientific Reports*, 6, p.32583.

Cardno, A.G., Marshall, E.J., Coid, B., Macdonald, A.M., Ribchester, T.R., Davies, N.J., Venturi, P., Jones, L.A., Lewis, S.W., Sham, P.C., Gottesman, I.I., Farmer, A.E., McGuffin, P., Reveley, A.M., and Murray, R.M., 1999. Heritability estimates for psychotic disorders: the Maudsley twin psychosis series. *Archives of General Psychiatry*, 56(2), pp.162–168.

Carpanini, S.M., Torvell, M., and Morgan, B.P., 2019. Therapeutic inhibition of the complement system in diseases of the central nervous system. *Frontiers in immunology*, 10, p.362.

Chakrabarty, P., Ceballos-Diaz, C., Beccard, A., Janus, C., Dickson, D., Golde, T.E., and Das, P., 2010. IFN-gamma promotes complement expression and attenuates amyloid plaque deposition in amyloid beta precursor protein transgenic mice. *Journal of Immunology*, 184(9), pp.5333–5343.

Chartier-Harlin, M.C., Crawford, F., Houlden, H., Warren, A., Hughes, D., Fidani, L., Goate, A., Rossor, M., Roques, P., and Hardy, J., 1991. Early-onset Alzheimer's disease caused by mutations at codon 717 of the beta-amyloid precursor protein gene. *Nature*, 353(6347), pp.844–846.

Chiot, A., Zaïdi, S., Iltis, C., Ribon, M., Berriat, F., Schiaffino, L., Jolly, A., de la Grange, P., Mallat, M., Bohl, D., Millecamps, S., Seilhean, D., Lobsiger, C.S., and Boillée, S., 2020. Modifying macrophages at the periphery has the capacity to change microglial reactivity and to extend ALS survival. *Nature Neuroscience*, 23(11), pp.1339–1351.

Chung, W.-S., Clarke, L.E., Wang, G.X., Stafford, B.K., Sher, A., Chakraborty, C., Joung, J., Foo, L.C., Thompson, A., Chen, C., Smith, S.J., and Barres, B.A., 2013. Astrocytes mediate synapse elimination through MEGF10 and MERTK pathways. *Nature*, 504(7480), pp.394–400.

Chung, W.-S., Verghese, P.B., Chakraborty, C., Joung, J., Hyman, B.T., Ulrich, J.D., Holtzman, D.M., and Barres, B.A., 2016. Novel allele-dependent role for APOE in controlling the rate of synapse pruning by astrocytes. *Proceedings of the National Academy of Sciences of the United States of America*, 113(36), pp.10186–10191.

Colom-Cadena, M., Tulloch, J., Rose, J., Smith, C., and Spires-Jones, T., 2020. TMEM97 is a potential amyloid beta receptor in human Alzheimer's disease synapses. *Alzheimer's & Dementia*, 16(S2).

Colton, C.A., Brown, C.M., Cook, D., Needham, L.K., Xu, Q., Czapiga, M.,

- Saunders, A.M., Schmechel, D.E., Rasheed, K., and Vitek, M.P., 2002. APOE and the regulation of microglial nitric oxide production: a link between genetic risk and oxidative stress. *Neurobiology of Aging*, 23(5), pp.777–785.
- Combs, C.K., Karlo, J.C., Kao, S.C., and Landreth, G.E., 2001. beta-Amyloid stimulation of microglia and monocytes results in TNFalpha-dependent expression of inducible nitric oxide synthase and neuronal apoptosis. *The Journal of Neuroscience*, 21(4), pp.1179–1188.
- Comer, A.L., Jinadasa, T., Sriram, B., Phadke, R.A., Kretsge, L.N., Nguyen, T.P.H., Antognetti, G., Gilbert, J.P., Lee, J., Newmark, E.R., Hausmann, F.S., Rosenthal, S., Liu Kot, K., Liu, Y., Yen, W.W., Dejanovic, B., and Cruz-Martín, A., 2020. Increased expression of schizophrenia-associated gene C4 leads to hypoconnectivity of prefrontal cortex and reduced social interaction. *PLoS Biology*, 18(1), p.e3000604.
- Cong, Q., Soteros, B.M., Wollet, M., Kim, J.H., and Sia, G.-M., 2020. The endogenous neuronal complement inhibitor SRPX2 protects against complement-mediated synapse elimination during development. *Nature Neuroscience*, 23(9), pp.1067–1078.
- Correale, J., and Villa, A., 2007. The blood-brain-barrier in multiple sclerosis: functional roles and therapeutic targeting. *Autoimmunity*, 40(2), pp.148–160.
- Coughlin, J.M., Wang, Y., Ambinder, E.B., Ward, R.E., Minn, I., Vranesic, M., Kim, P.K., Ford, C.N., Higgs, C., Hayes, L.N., Schretlen, D.J., Dannals, R.F., Kassiou, M., Sawa, A., and Pomper, M.G., 2016. In vivo markers of inflammatory response in recent-onset schizophrenia: a combined study using [(11)C]DPA-713 PET and analysis of CSF and plasma. *Translational psychiatry*, 6, p.e777.
- Cserép, C., Pósfai, B., Lénárt, N., Fekete, R., László, Z.I., Lele, Z., Orsolits, B., Molnár, G., Heindl, S., Schwarcz, A.D., Ujvári, K., Környei, Z., Tóth, K., Szabadits, E., Sperlág, B., Baranyi, M., Csiba, L., Hortobágyi, T., Maglóczky, Z., Martinecz, B., Szabó, G., Erdélyi, F., Szipócs, R., Tamkun, M.M., Gesierich, B., Duering, M., Katona, I., Liesz, A., Tamás, G., and Dénes, Á., 2020. Microglia monitor and protect neuronal function through specialized somatic purinergic junctions. *Science*, 367(6477), pp.528–537.
- Davalos, D., Grutzendler, J., Yang, G., Kim, J.V., Zuo, Y., Jung, S., Littman, D.R., Dustin, M.L., and Gan, W.-B., 2005. ATP mediates rapid microglial response to local brain injury in vivo. *Nature Neuroscience*, 8(6), pp.752–758.
- Davies, D.S., Ma, J., Jegathees, T., and Goldsbury, C., 2017. Microglia show altered morphology and reduced arborization in human brain during aging and Alzheimer's disease. *Brain Pathology*, 27(6), pp.795–808.
- Dayan, E., and Cohen, L.G., 2011. Neuroplasticity subserving motor skill learning. *Neuron*, 72(3), pp.443–454.
- De Picker, L., Ottoy, J., Verhaeghe, J., Deleye, S., Wyffels, L., Fransen, E., Kosten, L., Sabbe, B., Coppens, V., Timmers, M., de Boer, P., Van Nueten, L., Op De Beeck, K., Oberacher, H., Vanhoenacker, F., Ceysens, S., Stroobants, S., Staelens, S., and Morrens, M., 2019. State-associated changes in longitudinal [18F]-PBR111 TSPO PET imaging of psychosis patients: Evidence for the accelerated

ageing hypothesis? *Brain, Behavior, and Immunity*, 77, pp.46–54.

De Picker, L.J., Morrens, M., Chance, S.A., and Boche, D., 2017. Microglia and Brain Plasticity in Acute Psychosis and Schizophrenia Illness Course: A Meta-Review. *Frontiers in psychiatry*, 8, p.238.

Dejanovic, B., Huntley, M.A., De Mazière, A., Meilandt, W.J., Wu, T., Srinivasan, K., Jiang, Z., Gandham, V., Friedman, B.A., Ngu, H., Foreman, O., Carano, R.A.D., Chih, B., Klumperman, J., Bakalarski, C., Hanson, J.E., and Sheng, M., 2018. Changes in the Synaptic Proteome in Tauopathy and Rescue of Tau-Induced Synapse Loss by C1q Antibodies. *Neuron*, 100(6), p.1322–1336.e7.

DeKosky, S.T., and Scheff, S.W., 1990. Synapse loss in frontal cortex biopsies in Alzheimer's disease: correlation with cognitive severity. *Annals of Neurology*, 27(5), pp.457–464.

Di Filippo, M., Chiasserini, D., Gardoni, F., Viviani, B., Tozzi, A., Giampà, C., Costa, C., Tantucci, M., Zianni, E., Boraso, M., Siliquini, S., de Iure, A., Ghiglieri, V., Colcelli, E., Baker, D., Sarchielli, P., Fusco, F.R., Di Luca, M., and Calabresi, P., 2013. Effects of central and peripheral inflammation on hippocampal synaptic plasticity. *Neurobiology of Disease*, 52, pp.229–236.

Doorduyn, J., de Vries, E.F.J., Willemsen, A.T.M., de Groot, J.C., Dierckx, R.A., and Klein, H.C., 2009. Neuroinflammation in schizophrenia-related psychosis: a PET study. *Journal of Nuclear Medicine*, 50(11), pp.1801–1807.

Dutta, R., Chang, A., Doud, M.K., Kidd, G.J., Ribaud, M.V., Young, E.A., Fox, R.J., Staugaitis, S.M., and Trapp, B.D., 2011. Demyelination causes synaptic alterations in hippocampi from multiple sclerosis patients. *Annals of Neurology*, 69(3), pp.445–454.

El Hajj, H., Savage, J.C., Bisht, K., Parent, M., Vallières, L., Rivest, S., and Tremblay, M.-È., 2019. Ultrastructural evidence of microglial heterogeneity in Alzheimer's disease amyloid pathology. *Journal of Neuroinflammation*, 16(1), p.87.

El Khoury, J., Hickman, S.E., Thomas, C.A., Loike, J.D., and Silverstein, S.C., 1998. Microglia, scavenger receptors, and the pathogenesis of Alzheimer's disease. *Neurobiology of Aging*, 19(1 Suppl), pp.S81-4.

Elward, K., and Gasque, P., 2003. "Eat me" and "don't eat me" signals govern the innate immune response and tissue repair in the CNS: emphasis on the critical role of the complement system. *Molecular Immunology*, 40(2–4), pp.85–94.

Engert, F., and Bonhoeffer, T., 1999. Dendritic spine changes associated with hippocampal long-term synaptic plasticity. *Nature*, 399(6731), pp.66–70.

Eroglu, C., and Barres, B.A., 2010. Regulation of synaptic connectivity by glia. *Nature*, 468(7321), pp.223–231.

Ertürk, A., Wang, Y., and Sheng, M., 2014. Local pruning of dendrites and spines by caspase-3-dependent and proteasome-limited mechanisms. *The Journal of Neuroscience*, 34(5), pp.1672–1688.

Faludi, G., and Mirnics, K., 2011. Synaptic changes in the brain of subjects with schizophrenia. *International Journal of Developmental Neuroscience*, 29(3), pp.305–309.

- Farfel, J.M., Yu, L., De Jager, P.L., Schneider, J.A., and Bennett, D.A., 2016. Association of APOE with tau-tangle pathology with and without β -amyloid. *Neurobiology of Aging*, 37, pp.19–25.
- Feinberg, I., 1982. Schizophrenia: caused by a fault in programmed synaptic elimination during adolescence? *Journal of Psychiatric Research*, 17(4), pp.319–334.
- Filipello, F., Morini, R., Corradini, I., Zerbi, V., Canzi, A., Michalski, B., Erreni, M., Markicevic, M., Starvaggi-Cucuzza, C., Otero, K., Piccio, L., Cignarella, F., Perrucci, F., Tamborini, M., Genua, M., Rajendran, L., Menna, E., Vetrano, S., Fahnestock, M., Paolicelli, R.C., and Matteoli, M., 2018. The microglial innate immune receptor TREM2 is required for synapse elimination and normal brain connectivity. *Immunity*, 48(5), p.979–991.e8.
- Fonseca, M.I., Zhou, J., Botto, M., and Tenner, A.J., 2004. Absence of C1q leads to less neuropathology in transgenic mouse models of Alzheimer's disease. *The Journal of Neuroscience*, 24(29), pp.6457–6465.
- Fu, M., Yu, X., Lu, J., and Zuo, Y., 2012. Repetitive motor learning induces coordinated formation of clustered dendritic spines in vivo. *Nature*, 483(7387), pp.92–95.
- Funk, A.J., Mielnik, C.A., Koene, R., Newburn, E., Ramsey, A.J., Lipska, B.K., and McCullumsmith, R.E., 2017. Postsynaptic Density-95 Isoform Abnormalities in Schizophrenia. *Schizophrenia Bulletin*, 43(4), pp.891–899.
- Galatro, T.F., Holtman, I.R., Lerario, A.M., Vainchtein, I.D., Brouwer, N., Sola, P.R., Veras, M.M., Pereira, T.F., Leite, R.E.P., Möller, T., Wes, P.D., Sogayar, M.C., Laman, J.D., den Dunnen, W., Pasqualucci, C.A., Oba-Shinjo, S.M., Boddeke, E.W.G.M., Marie, S.K.N., and Eggen, B.J.L., 2017. Transcriptomic analysis of purified human cortical microglia reveals age-associated changes. *Nature Neuroscience*, 20(8), pp.1162–1171.
- Garcia-Marin, V., Blazquez-Llorca, L., Rodriguez, J.-R., Boluda, S., Muntane, G., Ferrer, I., and Defelipe, J., 2009. Diminished perisomatic GABAergic terminals on cortical neurons adjacent to amyloid plaques. *Frontiers in Neuroanatomy*, 3, p.28.
- George, J., Cunha, R.A., Mülle, C., and Amédée, T., 2016. Microglia-derived purines modulate mossy fibre synaptic transmission and plasticity through P2X4 and A1 receptors. *The European Journal of Neuroscience*, 43(10), pp.1366–1378.
- George, J., Gonçalves, F.Q., Cristóvão, G., Rodrigues, L., Meyer Fernandes, J.R., Gonçalves, T., Cunha, R.A., and Gomes, C.A., 2015. Different danger signals differently impact on microglial proliferation through alterations of ATP release and extracellular metabolism. *Glia*, 63(9), pp.1636–1645.
- Gibson, E.M., and Monje, M., 2021. Microglia in Cancer Therapy-Related Cognitive Impairment. *Trends in Neurosciences*, 44(6), pp.441–451.
- Gibson, E.M., Nagaraja, S., Ocampo, A., Tam, L.T., Wood, L.S., Pallegar, P.N., Greene, J.J., Geraghty, A.C., Goldstein, A.K., Ni, L., Woo, P.J., Barres, B.A., Liddel, S., Vogel, H., and Monje, M., 2019. Methotrexate Chemotherapy Induces Persistent Tri-gial Dysregulation that Underlies Chemotherapy-Related Cognitive

Impairment. *Cell*, 176(1–2), p.43–55.e13.

Gilman, S., Koller, M., Black, R.S., Jenkins, L., Griffith, S.G., Fox, N.C., Eisner, L., Kirby, L., Rovira, M.B., Forette, F., Orgogozo, J.M., and AN1792(QS-21)-201 Study Team, 2005. Clinical effects of Abeta immunization (AN1792) in patients with AD in an interrupted trial. *Neurology*, 64(9), pp.1553–1562.

Ginhoux, F., Greter, M., Leboeuf, M., Nandi, S., See, P., Gokhan, S., Mehler, M.F., Conway, S.J., Ng, L.G., Stanley, E.R., Samokhvalov, I.M., and Merad, M., 2010. Fate mapping analysis reveals that adult microglia derive from primitive macrophages. *Science*, 330(6005), pp.841–845.

Ginhoux, F., Lim, S., Hoeffel, G., Low, D., and Huber, T., 2013. Origin and differentiation of microglia. *Frontiers in Cellular Neuroscience*, 7, p.45.

Goate, A., Chartier-Harlin, M.C., Mullan, M., Brown, J., Crawford, F., Fidani, L., Giuffra, L., Haynes, A., Irving, N., and James, L., 1991. Segregation of a missense mutation in the amyloid precursor protein gene with familial Alzheimer's disease. *Nature*, 349(6311), pp.704–706.

Goedert, M., and Spillantini, M.G., 2006. A century of Alzheimer's disease. *Science*, 314(5800), pp.777–781.

Gogtay, N., Vyas, N.S., Testa, R., Wood, S.J., and Pantelis, C., 2011. Age of onset of schizophrenia: perspectives from structural neuroimaging studies. *Schizophrenia Bulletin*, 37(3), pp.504–513.

Gomes, L.A., Hipp, S.A., Rijal Upadhaya, A., Balakrishnan, K., Ospitalieri, S., Koper, M.J., Largo-Barrientos, P., Uytterhoeven, V., Reichwald, J., Rabe, S., Vandenberghe, R., von Arnim, C.A.F., Tousseyn, T., Feederle, R., Giudici, C., Willem, M., Staufenbiel, M., and Thal, D.R., 2019. A β -induced acceleration of Alzheimer-related τ -pathology spreading and its association with prion protein. *Acta Neuropathologica*, 138(6), pp.913–941.

Gomez-Arboledas, A., Davila, J.C., Sanchez-Mejias, E., Navarro, V., Nuñez-Diaz, C., Sanchez-Varo, R., Sanchez-Mico, M.V., Trujillo-Estrada, L., Fernandez-Valenzuela, J.J., Vizuite, M., Comella, J.X., Galea, E., Vitorica, J., and Gutierrez, A., 2018. Phagocytic clearance of presynaptic dystrophies by reactive astrocytes in Alzheimer's disease. *Glia*, 66(3), pp.637–653.

Grabert, K., and McColl, B.W., 2018. Isolation and phenotyping of adult mouse microglial cells. *Methods in Molecular Biology*, 1784, pp.77–86.

Grabert, K., Michoel, T., Karavolos, M.H., Clohisey, S., Baillie, J.K., Stevens, M.P., Freeman, T.C., Summers, K.M., and McColl, B.W., 2016. Microglial brain region-dependent diversity and selective regional sensitivities to aging. *Nature Neuroscience*, 19(3), pp.504–516.

Greenhalgh, A.D., Zarruk, J.G., Healy, L.M., Baskar Jesudasan, S.J., Jhelum, P., Salmon, C.K., Formanek, A., Russo, M.V., Antel, J.P., McGavern, D.B., McColl, B.W., and David, S., 2018. Peripherally derived macrophages modulate microglial function to reduce inflammation after CNS injury. *PLoS Biology*, 16(10), p.e2005264.

Guerreiro, R., Wojtas, A., Bras, J., Carrasquillo, M., Rogaeva, E., Majounie, E.,

- Cruchaga, C., Sassi, C., Kauwe, J.S.K., Younkin, S., Hazrati, L., Collinge, J., Pocock, J., Lashley, T., Williams, J., Lambert, J.-C., Amouyel, P., Goate, A., Rademakers, R., Morgan, K., Powell, J., St George-Hyslop, P., Singleton, A., Hardy, J., and Alzheimer Genetic Analysis Group, 2013. TREM2 variants in Alzheimer's disease. *The New England Journal of Medicine*, 368(2), pp.117–127.
- Guttikonda, S.R., Sikkema, L., Tchieu, J., Saurat, N., Walsh, R.M., Harschnitz, O., Ciceri, G., Sneebouer, M., Mazutis, L., Setty, M., Zumbo, P., Betel, D., de Witte, L.D., Pe'er, D., and Studer, L., 2021. Fully defined human pluripotent stem cell-derived microglia and tri-culture system model C3 production in Alzheimer's disease. *Nature Neuroscience*, 24(3), pp.343–354.
- Harauzov, A., Spolidoro, M., DiCristo, G., De Pasquale, R., Cancedda, L., Pizzorusso, T., Viegi, A., Berardi, N., and Maffei, L., 2010. Reducing intracortical inhibition in the adult visual cortex promotes ocular dominance plasticity. *The Journal of Neuroscience*, 30(1), pp.361–371.
- Hardy, J., and Allsop, D., 1991. Amyloid deposition as the central event in the aetiology of Alzheimer's disease. *Trends in Pharmacological Sciences*, 12(10), pp.383–388.
- Hardy, J., and Selkoe, D.J., 2002. The amyloid hypothesis of Alzheimer's disease: progress and problems on the road to therapeutics. *Science*, 297(5580), pp.353–356.
- Harris, K.M., and Weinberg, R.J., 2012. Ultrastructure of synapses in the mammalian brain. *Cold Spring Harbor Perspectives in Biology*, 4(5).
- Hasel, P., Dando, O., Jiwaji, Z., Baxter, P., Todd, A.C., Heron, S., Márkus, N.M., McQueen, J., Hampton, D.W., Torvell, M., Tiwari, S.S., McKay, S., Eraso-Pichot, A., Zorzano, A., Masgrau, R., Galea, E., Chandran, S., Wyllie, D.J.A., Simpson, T.I., and Hardingham, G.E., 2017. Neurons and neuronal activity control gene expression in astrocytes to regulate their development and metabolism. *Nature Communications*, 8, p.15132.
- Hensch, T.K., and Fagiolini, M., 2005. Excitatory-inhibitory balance and critical period plasticity in developing visual cortex. *Progress in Brain Research*, 147, pp.115–124.
- Henstridge, C.M., Pickett, E., and Spires-Jones, T.L., 2016. Synaptic pathology: A shared mechanism in neurological disease. *Ageing Research Reviews*, 28, pp.72–84.
- Henstridge, C.M., Sideris, D.I., Carroll, E., Rotariu, S., Salomonsson, S., Tzioras, M., McKenzie, C.-A., Smith, C., von Arnim, C.A.F., Ludolph, A.C., Lulé, D., Leighton, D., Warner, J., Cleary, E., Newton, J., Swingler, R., Chandran, S., Gillingwater, T.H., Abrahams, S., and Spires-Jones, T.L., 2018. Synapse loss in the prefrontal cortex is associated with cognitive decline in amyotrophic lateral sclerosis. *Acta Neuropathologica*, 135(2), pp.213–226.
- Henstridge, C.M., Tzioras, M., and Paolicelli, R.C., 2019. Glial contribution to excitatory and inhibitory synapse loss in neurodegeneration. *Frontiers in Cellular Neuroscience*, 13, p.63.
- Hesse, R., Hurtado, M.L., Jackson, R.J., Eaton, S.L., Herrmann, A.G., Colom-Cadena, M., Tzioras, M., King, D., Rose, J., Tulloch, J., McKenzie, C.-A., Smith,

- C., Henstridge, C.M., Lamont, D., Wishart, T.M., and Spires-Jones, T.L., 2019. Comparative profiling of the synaptic proteome from Alzheimer's disease patients with focus on the APOE genotype. *Acta neuropathologica communications*, 7(1), p.214.
- Hierro-Bujalance, C., Infante-Garcia, C., Del Marco, A., Herrera, M., Carranza-Naval, M.J., Suarez, J., Alves-Martinez, P., Lubian-Lopez, S., and Garcia-Alloza, M., 2020. Empagliflozin reduces vascular damage and cognitive impairment in a mixed murine model of Alzheimer's disease and type 2 diabetes. *Alzheimer's research & therapy*, 12(1), p.40.
- Hippius, H., and Neundörfer, G., 2003. The discovery of Alzheimer's disease. *Dialogues in Clinical Neuroscience*, 5(1), pp.101–108.
- Holtmaat, A., and Svoboda, K., 2009. Experience-dependent structural synaptic plasticity in the mammalian brain. *Nature Reviews. Neuroscience*, 10(9), pp.647–658.
- Hong, S., Beja-Glasser, V.F., Nfonoyim, B.M., Frouin, A., Li, S., Ramakrishnan, S., Merry, K.M., Shi, Q., Rosenthal, A., Barres, B.A., Lemere, C.A., Selkoe, D.J., and Stevens, B., 2016. Complement and microglia mediate early synapse loss in Alzheimer mouse models. *Science*, 352(6286), pp.712–716.
- Hong, Y.K., and Chen, C., 2011. Wiring and rewiring of the retinogeniculate synapse. *Current Opinion in Neurobiology*, 21(2), pp.228–237.
- Hsia, A.Y., Malenka, R.C., and Nicoll, R.A., 1998. Development of excitatory circuitry in the hippocampus. *Journal of Neurophysiology*, 79(4), pp.2013–2024.
- Hubbard, J.A., Hsu, M.S., Seldin, M.M., and Binder, D.K., 2015. Expression of the Astrocyte Water Channel Aquaporin-4 in the Mouse Brain. *ASN Neuro*, 7(5).
- Hugo, J., and Ganguli, M., 2014. Dementia and cognitive impairment: epidemiology, diagnosis, and treatment. *Clinics in geriatric medicine*, 30(3), pp.421–442.
- Hui, C.W., Vecchiarelli, H.A., Gervais, É., Luo, X., Michaud, F., Scheefhals, L., Bisht, K., Sharma, K., Topolnik, L., and Tremblay, M.-È., 2020. Sex differences of microglia and synapses in the hippocampal dentate gyrus of adult mouse offspring exposed to maternal immune activation. *Frontiers in Cellular Neuroscience*, 14, p.558181.
- Hume, D.A., 2015. The many alternative faces of macrophage activation. *Frontiers in immunology*, 6, p.370.
- Husemann, J., Loike, J.D., Anankov, R., Febbraio, M., and Silverstein, S.C., 2002. Scavenger receptors in neurobiology and neuropathology: their role on microglia and other cells of the nervous system. *Glia*, 40(2), pp.195–205.
- Infante-Garcia, C., Ramos-Rodriguez, J.J., Galindo-Gonzalez, L., and Garcia-Alloza, M., 2016. Long-term central pathology and cognitive impairment are exacerbated in a mixed model of Alzheimer's disease and type 2 diabetes. *Psychoneuroendocrinology*, 65, pp.15–25.
- Ingelsson, M., Fukumoto, H., Newell, K.L., Growdon, J.H., Hedley-Whyte, E.T., Frosch, M.P., Albert, M.S., Hyman, B.T., and Irizarry, M.C., 2004. Early Aβ accumulation and progressive synaptic loss, gliosis, and tangle formation in AD

brain. *Neurology*, 62(6), pp.925–931.

Itagaki, S., McGeer, P.L., Akiyama, H., Zhu, S., and Selkoe, D., 1989. Relationship of microglia and astrocytes to amyloid deposits of Alzheimer disease. *Journal of Neuroimmunology*, 24(3), pp.173–182.

Jackson, R.J., Rose, J., Tulloch, J., Henstridge, C., Smith, C., and Spires-Jones, T.L., 2019. Clusterin accumulates in synapses in Alzheimer's disease and is increased in apolipoprotein E4 carriers. *Brain Communications*, 1(1), p.fc2003.

Janelins, M.C., Mastrangelo, M.A., Oddo, S., LaFerla, F.M., Federoff, H.J., and Bowers, W.J., 2005. Early correlation of microglial activation with enhanced tumor necrosis factor-alpha and monocyte chemoattractant protein-1 expression specifically within the entorhinal cortex of triple transgenic Alzheimer's disease mice. *Journal of Neuroinflammation*, 2, p.23.

Janelins, M.C., Mastrangelo, M.A., Park, K.M., Sudol, K.L., Narrow, W.C., Oddo, S., LaFerla, F.M., Callahan, L.M., Federoff, H.J., and Bowers, W.J., 2008. Chronic neuron-specific tumor necrosis factor-alpha expression enhances the local inflammatory environment ultimately leading to neuronal death in 3xTg-AD mice. *The American Journal of Pathology*, 173(6), pp.1768–1782.

Jonsson, T., Stefansson, H., Steinberg, S., Jonsdottir, I., Jonsson, P.V., Snaedal, J., Bjornsson, S., Huttenlocher, J., Levey, A.I., Lah, J.J., Rujescu, D., Hampel, H., Giegling, I., Andreassen, O.A., Engedal, K., Ulstein, I., Djurovic, S., Ibrahim-Verbaas, C., Hofman, A., Ikram, M.A., van Duijn, C.M., Thorsteinsdottir, U., Kong, A., and Stefansson, K., 2013. Variant of TREM2 associated with the risk of Alzheimer's disease. *The New England Journal of Medicine*, 368(2), pp.107–116.

Kahn, R.S., Sommer, I.E., Murray, R.M., Meyer-Lindenberg, A., Weinberger, D.R., Cannon, T.D., O'Donovan, M., Correll, C.U., Kane, J.M., van Os, J., and Insel, T.R., 2015. Schizophrenia. *Nature reviews. Disease primers*, 1, p.15067.

Karch, C.M., and Goate, A.M., 2015. Alzheimer's disease risk genes and mechanisms of disease pathogenesis. *Biological Psychiatry*, 77(1), pp.43–51.

Keller, J.N., 2006. Age-related neuropathology, cognitive decline, and Alzheimer's disease. *Ageing Research Reviews*, 5(1), pp.1–13.

Kenk, M., Selvanathan, T., Rao, N., Suridjan, I., Rusjan, P., Remington, G., Meyer, J.H., Wilson, A.A., Houle, S., and Mizrahi, R., 2015. Imaging neuroinflammation in gray and white matter in schizophrenia: an in-vivo PET study with [18F]-FEPPA. *Schizophrenia Bulletin*, 41(1), pp.85–93.

Kenkhuis, B., Somarakis, A., de Haan, L.M., Dzyubachyk, O., IJsselsteijn, M.E., de Miranda, N.F., Lelieveldt, B.P., Dijkstra, J., van Roon-Mom, W.M., Hollt, T., and van der Weerd, L., 2021. Iron-loading is a prominent feature of activated microglia in Alzheimer's disease patients. *BioRxiv*.

Kent, S.A., Spires-Jones, T.L., and Durrant, C.S., 2020. The physiological roles of tau and A β : implications for Alzheimer's disease pathology and therapeutics. *Acta Neuropathologica*, 140(4), pp.417–447.

Keren-Shaul, H., Spinrad, A., Weiner, A., Matcovitch-Natan, O., Dvir-Szternfeld, R., Ulland, T.K., David, E., Baruch, K., Lara-Astaiso, D., Toth, B., Itzkovitz, S.,

- Colonna, M., Schwartz, M., and Amit, I., 2017. A Unique Microglia Type Associated with Restricting Development of Alzheimer's Disease. *Cell*, 169(7), p.1276–1290.e17.
- Kielian, T., 2006. Toll-like receptors in central nervous system glial inflammation and homeostasis. *Journal of Neuroscience Research*, 83(5), pp.711–730.
- Kigerl, K.A., de Rivero Vaccari, J.P., Dietrich, W.D., Popovich, P.G., and Keane, R.W., 2014. Pattern recognition receptors and central nervous system repair. *Experimental Neurology*, 258, pp.5–16.
- Kikinis, Z., Fallon, J.H., Niznikiewicz, M., Nestor, P., Davidson, C., Bobrow, L., Pelavin, P.E., Fischl, B., Yendiki, A., McCarley, R.W., Kikinis, R., Kubicki, M., and Shenton, M.E., 2010. Gray matter volume reduction in rostral middle frontal gyrus in patients with chronic schizophrenia. *Schizophrenia Research*, 123(2–3), pp.153–159.
- Kim, S.-M., Mun, B.-R., Lee, S.-J., Joh, Y., Lee, H.-Y., Ji, K.-Y., Choi, H.-R., Lee, E.-H., Kim, E.-M., Jang, J.-H., Song, H.-W., Mook-Jung, I., Choi, W.-S., and Kang, H.-S., 2017. TREM2 promotes A β phagocytosis by upregulating C/EBP α -dependent CD36 expression in microglia. *Scientific Reports*, 7(1), p.11118.
- Kivipelto, M., Ngandu, T., Fratiglioni, L., Viitanen, M., Kåreholt, I., Winblad, B., Helkala, E.-L., Tuomilehto, J., Soininen, H., and Nissinen, A., 2005. Obesity and vascular risk factors at midlife and the risk of dementia and Alzheimer disease. *Archives of Neurology*, 62(10), pp.1556–1560.
- Klauser, P., Baker, S.T., Cropley, V.L., Bousman, C., Fornito, A., Cocchi, L., Fullerton, J.M., Rasser, P., Schall, U., Henskens, F., Michie, P.T., Loughland, C., Catts, S.V., Mowry, B., Weickert, T.W., Shannon Weickert, C., Carr, V., Lenroot, R., Pantelis, C., and Zalesky, A., 2017. White matter disruptions in schizophrenia are spatially widespread and topologically converge on brain network hubs. *Schizophrenia Bulletin*, 43(2), pp.425–435.
- Knopman, D.S., and Petersen, R.C., 2014. Mild cognitive impairment and mild dementia: a clinical perspective. *Mayo Clinic Proceedings*, 89(10), pp.1452–1459.
- Koffie, R.M., Hashimoto, T., Tai, H.-C., Kay, K.R., Serrano-Pozo, A., Joyner, D., Hou, S., Kopeikina, K.J., Frosch, M.P., Lee, V.M., Holtzman, D.M., Hyman, B.T., and Spires-Jones, T.L., 2012. Apolipoprotein E4 effects in Alzheimer's disease are mediated by synaptotoxic oligomeric amyloid- β . *Brain: A Journal of Neurology*, 135(Pt 7), pp.2155–2168.
- Koffie, R.M., Hyman, B.T., and Spires-Jones, T.L., 2011. Alzheimer's disease: synapses gone cold. *Molecular Neurodegeneration*, 6(1), p.63.
- Koffie, R.M., Meyer-Luehmann, M., Hashimoto, T., Adams, K.W., Mielke, M.L., Garcia-Alloza, M., Micheva, K.D., Smith, S.J., Kim, M.L., Lee, V.M., Hyman, B.T., and Spires-Jones, T.L., 2009. Oligomeric amyloid beta associates with postsynaptic densities and correlates with excitatory synapse loss near senile plaques. *Proceedings of the National Academy of Sciences of the United States of America*, 106(10), pp.4012–4017.
- Konno, T., Yoshida, K., Mizuno, T., Kawarai, T., Tada, M., Nozaki, H., Ikeda,

S.I., Nishizawa, M., Onodera, O., Wszolek, Z.K., and Ikeuchi, T., 2017. Clinical and genetic characterization of adult-onset leukoencephalopathy with axonal spheroids and pigmented glia associated with CSF1R mutation. *European Journal of Neurology*, 24(1), pp.37–45.

Kopeikina, K.J., Polydoro, M., Tai, H.-C., Yaeger, E., Carlson, G.A., Pitstick, R., Hyman, B.T., and Spires-Jones, T.L., 2013a. Synaptic alterations in the rTg4510 mouse model of tauopathy. *The Journal of Comparative Neurology*, 521(6), pp.1334–1353.

Kopeikina, K.J., Wegmann, S., Pitstick, R., Carlson, G.A., Bacskai, B.J., Betensky, R.A., Hyman, B.T., and Spires-Jones, T.L., 2013b. Tau causes synapse loss without disrupting calcium homeostasis in the rTg4510 model of tauopathy. *Plos One*, 8(11), p.e80834.

Kosik, K.S., Joachim, C.L., and Selkoe, D.J., 1986. Microtubule-associated protein tau (tau) is a major antigenic component of paired helical filaments in Alzheimer disease. *Proceedings of the National Academy of Sciences of the United States of America*, 83(11), pp.4044–4048.

Krasemann, S., Madore, C., Cialic, R., Baufeld, C., Calcagno, N., El Fatimy, R., Beckers, L., O’Loughlin, E., Xu, Y., Fanek, Z., Greco, D.J., Smith, S.T., Tweet, G., Humulock, Z., Zrzavy, T., Conde-Sanroman, P., Gacias, M., Weng, Z., Chen, H., Tjon, E., Mazaheri, F., Hartmann, K., Madi, A., Ulrich, J.D., Glatzel, M., Worthmann, A., Heeren, J., Budnik, B., Lemere, C., Ikezu, T., Heppner, F.L., Litvak, V., Holtzman, D.M., Lassmann, H., Weiner, H.L., Ochando, J., Haass, C., and Butovsky, O., 2017. The TREM2-APOE Pathway Drives the Transcriptional Phenotype of Dysfunctional Microglia in Neurodegenerative Diseases. *Immunity*, 47(3), p.566–581.e9.

Kunkle, B.W., Grenier-Boley, B., Sims, R., Bis, J.C., Damotte, V., Naj, A.C., Boland, A., Vronskaya, M., van der Lee, S.J., Amlie-Wolf, A., Bellenguez, C., Frizatti, A., Chouraki, V., Martin, E.R., Sleegers, K., Badarinarayan, N., Jakobsdottir, J., Hamilton-Nelson, K.L., Moreno-Grau, S., Olasso, R., Raybould, R., Chen, Y., Kuzma, A.B., Hiltunen, M., Morgan, T., Ahmad, S., Vardarajan, B.N., Epelbaum, J., Hoffmann, P., Boada, M., Beecham, G.W., Garnier, J.-G., Harold, D., Fitzpatrick, A.L., Valladares, O., Moutet, M.-L., Gerrish, A., Smith, A.V., Qu, L., Bacq, D., Denning, N., Jian, X., Zhao, Y., Del Zompo, M., Fox, N.C., Choi, S.-H., Mateo, I., Hughes, J.T., Adams, H.H., Malamon, J., Sanchez-Garcia, F., Patel, Y., Brody, J.A., Dombroski, B.A., Naranjo, M.C.D., Daniilidou, M., Eiriksdottir, G., Mukherjee, S., Wallon, D., Uphill, J., Aspelund, T., Cantwell, L.B., Garzia, F., Galimberti, D., Hofer, E., Butkiewicz, M., Fin, B., Scarpini, E., Sarnowski, C., Bush, W.S., Meslage, S., Kornhuber, J., White, C.C., Song, Y., Barber, R.C., Engelborghs, S., Sordon, S., Vojnovic, D., Adams, P.M., Vandenberghe, R., Mayhaus, M., Cupples, L.A., Albert, M.S., De Deyn, P.P., Gu, W., Himali, J.J., Beekly, D., Squassina, A., Hartmann, A.M., Orellana, A., Blacker, D., Rodriguez-Rodriguez, E., Lovestone, S., Garcia, M.E., Doody, R.S., Munoz-Fernandez, C., Sussams, R., Lin, H., Fairchild, T.J., Benito, Y.A., Holmes, C., Karamujic-Comic, H., Frosch, M.P., Thonberg, H., Maier, W., Roshchupkin, G., Ghetti, B., Giedraitis, V., Kawalia, A., Li, S., Huebinger, R.M., Kilander, L., Moebus, S., Hernandez, I., Kamboh, M.I., Brundin, R., Turton, J., Yang, Q.,

Katz, M.J., Concari, L., Lord, J., Beiser, A.S., Keene, C.D., Helisalmi, S., Kloszewska, I., Kukull, W.A., Koivisto, A.M., Lynch, A., Tarraga, L., Larson, E.B., Haapasalo, A., Lawlor, B., Mosley, T.H., Lipton, R.B., Solfrizzi, V., Gill, M., Longstreth, W.T., Montine, T.J., Frisardi, V., Diez-Fairen, M., Rivadeneira, F., Petersen, R.C., Deramecourt, V., Alvarez, I., Salani, F., Ciaramella, A., Boerwinkle, E., Reiman, E.M., Fievet, N., Rotter, J.I., Reisch, J.S., Hanon, O., Cupidi, C., Andre Uitterlinden, A.G., Royall, D.R., Dufouil, C., Maletta, R.G., de Rojas, I., Sano, M., Brice, A., Cecchetti, R., George-Hyslop, P.S., Ritchie, K., Tsolaki, M., Tsuang, D.W., Dubois, B., Craig, D., Wu, C.-K., Soininen, H., Avramidou, D., Albin, R.L., Fratiglioni, L., Germanou, A., Apostolova, L.G., Keller, L., Koutroumani, M., Arnold, S.E., Panza, F., Gkatzima, O., Asthana, S., Hannequin, D., Whitehead, P., Atwood, C.S., Caffarra, P., Hampel, H., Quintela, I., Carracedo, Á., Lannfelt, L., Rubinsztein, D.C., Barnes, L.L., Pasquier, F., Frölich, L., Barral, S., McGuinness, B., Beach, T.G., Johnston, J.A., Becker, J.T., Passmore, P., Bigio, E.H., Schott, J.M., and et al., 2019. Genetic meta-analysis of diagnosed Alzheimer's disease identifies new risk loci and implicates A β , tau, immunity and lipid processing. *Nature Genetics*, 51(3), pp.414–430.

Kwon, C.-H., Luikart, B.W., Powell, C.M., Zhou, J., Matheny, S.A., Zhang, W., Li, Y., Baker, S.J., and Parada, L.F., 2006. Pten regulates neuronal arborization and social interaction in mice. *Neuron*, 50(3), pp.377–388.

LaClair, K.D., Manaye, K.F., Lee, D.L., Allard, J.S., Savonenko, A.V., Troncoso, J.C., and Wong, P.C., 2013. Treatment with bexarotene, a compound that increases apolipoprotein-E, provides no cognitive benefit in mutant APP/PS1 mice. *Molecular Neurodegeneration*, 8, p.18.

Largo-Barrientos, P., Apóstolo, N., Creemers, E., Callaerts-Vegh, Z., Swerts, J., Davies, C., McInnes, J., Wierda, K., De Strooper, B., Spires-Jones, T., de Wit, J., Uytterhoeven, V., and Verstreken, P., 2021. Lowering Synaptogyrin-3 expression rescues Tau-induced memory defects and synaptic loss in the presence of microglial activation. *Neuron*, 109(5), p.767–777.e5.

Laudisi, F., Spreafico, R., Evrard, M., Hughes, T.R., Mandriani, B., Kandasamy, M., Morgan, B.P., Sivasankar, B., and Mortellaro, A., 2013. Cutting edge: the NLRP3 inflammasome links complement-mediated inflammation and IL-1 β release. *Journal of Immunology*, 191(3), pp.1006–1010.

Lee, J.H., Kim, J.Y., Noh, S., Lee, H., Lee, S.Y., Mun, J.Y., Park, H., and Chung, W.S., 2021. Astrocytes phagocytose adult hippocampal synapses for circuit homeostasis. *Nature*, 590(7847), pp.612–617.

Lehrman, E.K., Wilton, D.K., Litvina, E.Y., Welsh, C.A., Chang, S.T., Frouin, A., Walker, A.J., Heller, M.D., Umemori, H., Chen, C., and Stevens, B., 2018. CD47 Protects Synapses from Excess Microglia-Mediated Pruning during Development. *Neuron*, 100(1), p.120–134.e6.

Lenz, K.M., Nugent, B.M., Haliyur, R., and McCarthy, M.M., 2013. Microglia are essential to masculinization of brain and behavior. *The Journal of Neuroscience*, 33(7), pp.2761–2772.

Levkovitz, Y., Mendlovich, S., Riwkes, S., Braw, Y., Levkovitch-Verbin, H., Gal, G., Fennig, S., Treves, I., and Kron, S., 2010. A double-blind, randomized study of

- minocycline for the treatment of negative and cognitive symptoms in early-phase schizophrenia. *The Journal of Clinical Psychiatry*, 71(2), pp.138–149.
- Lewis, F., Schaffer, K., S., Sussex, J., O'Neill, P., Cockcroft, and L., 2014. The Trajectory of Dementia in the UK - Making a Difference. *Consulting Reports*.
- Li, Q., Cheng, Z., Zhou, L., Darmanis, S., Neff, N.F., Okamoto, J., Gulati, G., Bennett, M.L., Sun, L.O., Clarke, L.E., Marschallinger, J., Yu, G., Quake, S.R., Wyss-Coray, T., and Barres, B.A., 2019. Developmental Heterogeneity of Microglia and Brain Myeloid Cells Revealed by Deep Single-Cell RNA Sequencing. *Neuron*, 101(2), p.207–223.e10.
- Li, S., Hong, S., Shepardson, N.E., Walsh, D.M., Shankar, G.M., and Selkoe, D., 2009. Soluble oligomers of amyloid Beta protein facilitate hippocampal long-term depression by disrupting neuronal glutamate uptake. *Neuron*, 62(6), pp.788–801.
- Liddelow, S.A., Guttenplan, K.A., Clarke, L.E., Bennett, F.C., Bohlen, C.J., Schirmer, L., Bennett, M.L., Münch, A.E., Chung, W.-S., Peterson, T.C., Wilton, D.K., Frouin, A., Napier, B.A., Panicker, N., Kumar, M., Buckwalter, M.S., Rowitch, D.H., Dawson, V.L., Dawson, T.M., Stevens, B., and Barres, B.A., 2017. Neurotoxic reactive astrocytes are induced by activated microglia. *Nature*, 541(7638), pp.481–487.
- Lim, S.-H., Park, E., You, B., Jung, Y., Park, A.-R., Park, S.G., and Lee, J.-R., 2013. Neuronal synapse formation induced by microglia and interleukin 10. *Plos One*, 8(11), p.e81218.
- Liu, Y., Yang, X., Guo, C., Nie, P., Liu, Y., and Ma, J., 2013. Essential role of MFG-E8 for phagocytic properties of microglial cells. *Plos One*, 8(2), p.e55754.
- Long, J.M., and Holtzman, D.M., 2019. Alzheimer disease: an update on pathobiology and treatment strategies. *Cell*, 179(2), pp.312–339.
- Luengo-Fernandez, R., Leal, J., and Gray, A., 2015. UK research spend in 2008 and 2012: comparing stroke, cancer, coronary heart disease and dementia. *BMJ Open*, 5(4), p.e006648.
- Lui, H., Zhang, J., Makinson, S.R., Cahill, M.K., Kelley, K.W., Huang, H.-Y., Shang, Y., Oldham, M.C., Martens, L.H., Gao, F., Coppola, G., Sloan, S.A., Hsieh, C.L., Kim, C.C., Bigio, E.H., Weintraub, S., Mesulam, M.-M., Rademakers, R., Mackenzie, I.R., Seeley, W.W., Karydas, A., Miller, B.L., Borroni, B., Ghidoni, R., Farese, R.V., Paz, J.T., Barres, B.A., and Huang, E.J., 2016. Progranulin Deficiency Promotes Circuit-Specific Synaptic Pruning by Microglia via Complement Activation. *Cell*, 165(4), pp.921–935.
- Mathys, H., Davila-Velderrain, J., Peng, Z., Gao, F., Mohammadi, S., Young, J.Z., Menon, M., He, L., Abdurrob, F., Jiang, X., Martorell, A.J., Ransohoff, R.M., Hafler, B.P., Bennett, D.A., Kellis, M., and Tsai, L.-H., 2019. Single-cell transcriptomic analysis of Alzheimer's disease. *Nature*, 570(7761), pp.332–337.
- Matsuzaki, M., Ellis-Davies, G.C., Nemoto, T., Miyashita, Y., Iino, M., and Kasai, H., 2001. Dendritic spine geometry is critical for AMPA receptor expression in hippocampal CA1 pyramidal neurons. *Nature Neuroscience*, 4(11), pp.1086–1092.
- Matsuzaki, M., Honkura, N., Ellis-Davies, G.C.R., and Kasai, H., 2004. Structural

basis of long-term potentiation in single dendritic spines. *Nature*, 429(6993), pp.761–766.

McCull, B.W., Rothwell, N.J., and Allan, S.M., 2008. Systemic inflammation alters the kinetics of cerebrovascular tight junction disruption after experimental stroke in mice. *The Journal of Neuroscience*, 28(38), pp.9451–9462.

McGeer, P.L., Akiyama, H., Itagaki, S., and McGeer, E.G., 1989. Activation of the classical complement pathway in brain tissue of Alzheimer patients. *Neuroscience Letters*, 107(1–3), pp.341–346.

McGeer, P.L., Kawamata, T., Walker, D.G., Akiyama, H., Tooyama, I., and McGeer, E.G., 1993. Microglia in degenerative neurological disease. *Glia*, 7(1), pp.84–92.

McGeer, P.L., and McGeer, E.G., 1998. Glial cell reactions in neurodegenerative diseases: pathophysiology and therapeutic interventions. *Alzheimer Disease and Associated Disorders*, 12 Suppl 2, pp.S1-6.

McQuade, A., Kang, Y.J., Hasselmann, J., Jairaman, A., Sotelo, A., Coburn, M., Shabestari, S.K., Chadarevian, J.P., Fote, G., Tu, C.H., Danhash, E., Silva, J., Martinez, E., Cotman, C., Prieto, G.A., Thompson, L.M., Steffan, J.S., Smith, I., Davtyan, H., Cahalan, M., Cho, H., and Blurton-Jones, M., 2020. Gene expression and functional deficits underlie TREM2-knockout microglia responses in human models of Alzheimer's disease. *Nature Communications*, 11(1), p.5370.

Merlini, M., Rafalski, V.A., Rios Coronado, P.E., Gill, T.M., Ellisman, M., Muthukumar, G., Subramanian, K.S., Ryu, J.K., Syme, C.A., Davalos, D., Seeley, W.W., Mucke, L., Nelson, R.B., and Akassoglou, K., 2019. Fibrinogen Induces Microglia-Mediated Spine Elimination and Cognitive Impairment in an Alzheimer's Disease Model. *Neuron*, 101(6), p.1099–1108.e6.

Michailidou, I., Jongejan, A., Vreijling, J.P., Georgakopoulou, T., de Wissel, M.B., Wolterman, R.A., Ruizendaal, P., Klar-Mohamad, N., Grootemaat, A.E., Picavet, D.I., Kumar, V., van Kooten, C., Woodruff, T.M., Morgan, B.P., van der Wel, N.N., Ramaglia, V., Fluiter, K., and Baas, F., 2018. Systemic inhibition of the membrane attack complex impedes neuroinflammation in chronic relapsing experimental autoimmune encephalomyelitis. *Acta neuropathologica communications*, 6(1), p.36.

Michailidou, I., Naessens, D.M.P., Hametner, S., Guldenaar, W., Kooi, E.-J., Geurts, J.J.G., Baas, F., Lassmann, H., and Ramaglia, V., 2017. Complement C3 on microglial clusters in multiple sclerosis occur in chronic but not acute disease: Implication for disease pathogenesis. *Glia*, 65(2), pp.264–277.

Michailidou, I., Willems, J.G.P., Kooi, E.-J., van Eden, C., Gold, S.M., Geurts, J.J.G., Baas, F., Huitinga, I., and Ramaglia, V., 2015. Complement C1q-C3-associated synaptic changes in multiple sclerosis hippocampus. *Annals of Neurology*, 77(6), pp.1007–1026.

Mikuni, T., Uesaka, N., Okuno, H., Hirai, H., Deisseroth, K., Bito, H., and Kano, M., 2013. Arc/Arg3.1 is a postsynaptic mediator of activity-dependent synapse elimination in the developing cerebellum. *Neuron*, 78(6), pp.1024–1035.

- Mildner, A., Huang, H., Radke, J., Stenzel, W., and Priller, J., 2017. P2Y₁₂ receptor is expressed on human microglia under physiological conditions throughout development and is sensitive to neuroinflammatory diseases. *Glia*, 65(2), pp.375–387.
- Minett, T., Classey, J., Matthews, F.E., Fahrenhold, M., Taga, M., Brayne, C., Ince, P.G., Nicoll, J.A.R., Boche, D., and MRC CFAS, 2016. Microglial immunophenotype in dementia with Alzheimer's pathology. *Journal of Neuroinflammation*, 13(1), p.135.
- Miron, V.E., Boyd, A., Zhao, J.-W., Yuen, T.J., Ruckh, J.M., Shadrach, J.L., van Wijngaarden, P., Wagers, A.J., Williams, A., Franklin, R.J.M., and Ffrench-Constant, C., 2013. M2 microglia and macrophages drive oligodendrocyte differentiation during CNS remyelination. *Nature Neuroscience*, 16(9), pp.1211–1218.
- Miyaoka, T., Yasukawa, R., Yasuda, H., Hayashida, M., Inagaki, T., and Horiguchi, J., 2008. Minocycline as adjunctive therapy for schizophrenia: an open-label study. *Clinical neuropharmacology*, 31(5), pp.287–292.
- Mondal, M., Bali, J., Tzioras, M., Paolicelli, R.C., Jawaid, A., Malnar, M., Dominko, K., Udayar, V., Ben Halima, S., Vadodaria, K.C., Manesso, E., Thakur, G., Decressac, M., Petit, C., Sudharshan, R., Hecimovic, S., Simons, M., Klumperman, J., Bruestle, O., Ferguson, S., Nitsch, R., Schulz, P.E., Spires-Jones, T.L., Koch, P., Gunawan, R., and Rajendran, L., 2020. Nutrient signaling pathways regulate amyloid clearance and synaptic loss in Alzheimer's disease. *BioRxiv*.
- Montagne, A., Barnes, S.R., Sweeney, M.D., Halliday, M.R., Sagare, A.P., Zhao, Z., Toga, A.W., Jacobs, R.E., Liu, C.Y., Amezcua, L., Harrington, M.G., Chui, H.C., Law, M., and Zlokovic, B.V., 2015. Blood-brain barrier breakdown in the aging human hippocampus. *Neuron*, 85(2), pp.296–302.
- Morris, R.G., 1989. Synaptic plasticity and learning: selective impairment of learning rats and blockade of long-term potentiation in vivo by the N-methyl-D-aspartate receptor antagonist AP5. *The Journal of Neuroscience*, 9(9), pp.3040–3057.
- Morris, R.G., Anderson, E., Lynch, G.S., and Baudry, M., 1986. Selective impairment of learning and blockade of long-term potentiation by an N-methyl-D-aspartate receptor antagonist, AP5. *Nature*, 319(6056), pp.774–776.
- Morris, R.G., and Frey, U., 1997. Hippocampal synaptic plasticity: role in spatial learning or the automatic recording of attended experience? *Philosophical Transactions of the Royal Society of London. Series B, Biological Sciences*, 352(1360), pp.1489–1503.
- Moss, J., and Williams, A., 2020. Opening the floodgates to the brain. *Science*, 367(6483), pp.1195–1196.
- Mostany, R., Anstey, J.E., Crump, K.L., Maco, B., Knott, G., and Portera-Cailliau, C., 2013. Altered synaptic dynamics during normal brain aging. *The Journal of Neuroscience*, 33(9), pp.4094–4104.
- Nelson, L.H., Warden, S., and Lenz, K.M., 2017. Sex differences in microglial phagocytosis in the neonatal hippocampus. *Brain, Behavior, and Immunity*, 64,

pp.11–22.

Nimmerjahn, A., Kirchhoff, F., and Helmchen, F., 2005. Resting microglial cells are highly dynamic surveillants of brain parenchyma in vivo. *Science*, 308(5726), pp.1314–1318.

Njie, E.G., Boelen, E., Stassen, F.R., Steinbusch, H.W.M., Borchelt, D.R., and Streit, W.J., 2012. Ex vivo cultures of microglia from young and aged rodent brain reveal age-related changes in microglial function. *Neurobiology of Aging*, 33(1), p.195.e1-12.

Oberheim, N.A., Wang, X., Goldman, S., and Nedergaard, M., 2006. Astrocytic complexity distinguishes the human brain. *Trends in Neurosciences*, 29(10), pp.547–553.

Olah, M., Menon, V., Habib, N., Taga, M.F., Ma, Y., Yung, C.J., Cimpean, M., Khairallah, A., Coronas-Samano, G., Sankowski, R., Grün, D., Kroshilina, A.A., Dionne, D., Sarkis, R.A., Cosgrove, G.R., Helgager, J., Golden, J.A., Pennell, P.B., Prinz, M., Vonsattel, J.P.G., Teich, A.F., Schneider, J.A., Bennett, D.A., Regev, A., Elyaman, W., Bradshaw, E.M., and De Jager, P.L., 2020. Single cell RNA sequencing of human microglia uncovers a subset associated with Alzheimer's disease. *Nature Communications*, 11(1), p.6129.

Olmos-Alonso, A., Schettters, S.T.T., Sri, S., Askew, K., Mancuso, R., Vargas-Caballero, M., Holscher, C., Perry, V.H., and Gomez-Nicola, D., 2016. Pharmacological targeting of CSF1R inhibits microglial proliferation and prevents the progression of Alzheimer's-like pathology. *Brain: A Journal of Neurology*, 139(Pt 3), pp.891–907.

Onwordi, E.C., Halff, E.F., Whitehurst, T., Mansur, A., Cotel, M.-C., Wells, L., Creaney, H., Bonsall, D., Rogdaki, M., Shatalina, E., Reis Marques, T., Rabiner, E.A., Gunn, R.N., Natesan, S., Vernon, A.C., and Howes, O.D., 2020. Synaptic density marker SV2A is reduced in schizophrenia patients and unaffected by antipsychotics in rats. *Nature Communications*, 11(1), p.246.

Oosterhof, N., Chang, I.J., Karimiani, E.G., Kuil, L.E., Jensen, D.M., Daza, R., Young, E., Astle, L., van der Linde, H.C., Shivaram, G.M., Demmers, J., Latimer, C.S., Keene, C.D., Loter, E., Maroofian, R., van Ham, T.J., Hevner, R.F., and Bennett, J.T., 2019. Homozygous Mutations in CSF1R Cause a Pediatric-Onset Leukoencephalopathy and Can Result in Congenital Absence of Microglia. *American Journal of Human Genetics*, 104(5), pp.936–947.

Osimo, E.F., Beck, K., Reis Marques, T., and Howes, O.D., 2019. Synaptic loss in schizophrenia: a meta-analysis and systematic review of synaptic protein and mRNA measures. *Molecular Psychiatry*, 24(4), pp.549–561.

Païdassi, H., Tacnet-Delorme, P., Garlatti, V., Darnault, C., Ghebrehiwet, B., Gaboriaud, C., Arlaud, G.J., and Frchet, P., 2008. C1q binds phosphatidylserine and likely acts as a multiligand-bridging molecule in apoptotic cell recognition. *Journal of Immunology*, 180(4), pp.2329–2338.

Paolicelli, R.C., Bolasco, G., Pagani, F., Maggi, L., Scianni, M., Panzanelli, P., Giustetto, M., Ferreira, T.A., Guiducci, E., Dumas, L., Ragozzino, D., and Gross, C.T., 2011. Synaptic pruning by microglia is necessary for normal brain

development. *Science*, 333(6048), pp.1456–1458.

Paolicelli, R.C., Jawaid, A., Henstridge, C.M., Valeri, A., Merlini, M., Robinson, J.L., Lee, E.B., Rose, J., Appel, S., Lee, V.M.-Y., Trojanowski, J.Q., Spires-Jones, T., Schulz, P.E., and Rajendran, L., 2017. TDP-43 Depletion in Microglia Promotes Amyloid Clearance but Also Induces Synapse Loss. *Neuron*, 95(2), p.297–308.e6.

Parhizkar, S., Arzberger, T., Brendel, M., Kleinberger, G., Deussing, M., Focke, C., Nuscher, B., Xiong, M., Ghasemigharagoz, A., Katzmarski, N., Krasemann, S., Lichtenthaler, S.F., Müller, S.A., Colombo, A., Monasor, L.S., Tahirovic, S., Herms, J., Willem, M., Pettkus, N., Butovsky, O., Bartenstein, P., Edbauer, D., Rominger, A., Ertürk, A., Grathwohl, S.A., Neher, J.J., Holtzman, D.M., Meyer-Luehmann, M., and Haass, C., 2019. Loss of TREM2 function increases amyloid seeding but reduces plaque-associated ApoE. *Nature Neuroscience*, 22(2), pp.191–204.

Park, D., Tosello-Tramont, A.-C., Elliott, M.R., Lu, M., Haney, L.B., Ma, Z., Klibanov, A.L., Mandell, J.W., and Ravichandran, K.S., 2007. BAI1 is an engulfment receptor for apoptotic cells upstream of the ELMO/Dock180/Rac module. *Nature*, 450(7168), pp.430–434.

Parkhurst, C.N., Yang, G., Ninan, I., Savas, J.N., Yates, J.R., Lafaille, J.J., Hempstead, B.L., Littman, D.R., and Gan, W.-B., 2013. Microglia promote learning-dependent synapse formation through brain-derived neurotrophic factor. *Cell*, 155(7), pp.1596–1609.

Penzes, P., Cahill, M.E., Jones, K.A., VanLeeuwen, J.-E., and Woolfrey, K.M., 2011. Dendritic spine pathology in neuropsychiatric disorders. *Nature Neuroscience*, 14(3), pp.285–293.

Peretti, D., Bastide, A., Radford, H., Verity, N., Molloy, C., Martin, M.G., Moreno, J.A., Steinert, J.R., Smith, T., Dinsdale, D., Willis, A.E., and Mallucci, G.R., 2015. RBM3 mediates structural plasticity and protective effects of cooling in neurodegeneration. *Nature*, 518(7538), pp.236–239.

Petersen, R.C., 2004. Mild cognitive impairment as a diagnostic entity. *Journal of Internal Medicine*, 256(3), pp.183–194.

Petersen, R.C., Smith, G.E., Waring, S.C., Ivnik, R.J., Tangalos, E.G., and Kokmen, E., 1999. Mild cognitive impairment: clinical characterization and outcome. *Archives of Neurology*, 56(3), pp.303–308.

Pfeiffer, T., Poll, S., Bancelin, S., Angibaud, J., Inavalli, V.K., Keppler, K., Mittag, M., Fuhrmann, M., and Nägerl, U.V., 2018. Chronic 2P-STED imaging reveals high turnover of dendritic spines in the hippocampus in vivo. *eLife*, 7.

Pickett, E.K., Herrmann, A.G., McQueen, J., Abt, K., Dando, O., Tulloch, J., Jain, P., Dunnett, S., Sohrabi, S., Fjeldstad, M.P., Calkin, W., Murison, L., Jackson, R.J., Tzioras, M., Stevenson, A., d'Orange, M., Hooley, M., Davies, C., Colom-Cadena, M., Anton-Fernandez, A., King, D., Oren, I., Rose, J., McKenzie, C.-A., Allison, E., Smith, C., Hardt, O., Henstridge, C.M., Hardingham, G.E., and Spires-Jones, T.L., 2019. Amyloid beta and tau cooperate to cause reversible behavioral and transcriptional deficits in a model of alzheimer's disease. *Cell*

reports, 29(11), p.3592–3604.e5.

Pilz, G.-A., Carta, S., Stäuble, A., Ayaz, A., Jessberger, S., and Helmchen, F., 2016. Functional imaging of dentate granule cells in the adult mouse hippocampus. *The Journal of Neuroscience*, 36(28), pp.7407–7414.

Podcasy, J.L., and Epperson, C.N., 2016. Considering sex and gender in Alzheimer disease and other dementias. *Dialogues in Clinical Neuroscience*, 18(4), pp.437–446.

Podleśny-Drabiniok, A., Marcora, E., and Goate, A.M., 2020. Microglial Phagocytosis: A Disease-Associated Process Emerging from Alzheimer's Disease Genetics. *Trends in Neurosciences*.

Prince, M., Ali, G.-C., Guerchet, M., Prina, A.M., Albanese, E., and Wu, Y.-T., 2016. Recent global trends in the prevalence and incidence of dementia, and survival with dementia. *Alzheimer's research & therapy*, 8(1), p.23.

Prince, M., Bryce, R., Albanese, E., Wimo, A., Ribeiro, W., and Ferri, C.P., 2013. The global prevalence of dementia: a systematic review and metaanalysis. *Alzheimer's & Dementia*, 9(1), p.63–75.e2.

Prince, M., Knapp, M., Guerchet, M., McCrone, P., Prina, M., Comas-Herrera, A., Wittenberg, R., Adelaja, B., Hu, B., King, D., Rehill, A., and Salimkumar, D., 2014. Dementia UK: Second Edition - Overview.

Prince, M., Wimo, A., Guerchet, M., Ali, G., Wu, Y., and Prina, M., 2015. *World Alzheimer Report 2015*. London: Alzheimer's Disease International.

Prinz, M., and Priller, J., 2014. Microglia and brain macrophages in the molecular age: from origin to neuropsychiatric disease. *Nature Reviews. Neuroscience*, 15(5), pp.300–312.

Profenno, L.A., Porsteinsson, A.P., and Faraone, S.V., 2010. Meta-analysis of Alzheimer's disease risk with obesity, diabetes, and related disorders. *Biological Psychiatry*, 67(6), pp.505–512.

Qian, X., Shen, Q., Goderie, S.K., He, W., Capela, A., Davis, A.A., and Temple, S., 2000. Timing of CNS cell generation: a programmed sequence of neuron and glial cell production from isolated murine cortical stem cells. *Neuron*, 28(1), pp.69–80.

Reed-Geaghan, E.G., Croxford, A.L., Becher, B., and Landreth, G.E., 2020. Plaque-associated myeloid cells derive from resident microglia in an Alzheimer's disease model. *The Journal of Experimental Medicine*, 217(4).

Ritzel, R.M., Patel, A.R., Pan, S., Crapser, J., Hammond, M., Jellison, E., and McCullough, L.D., 2015. Age- and location-related changes in microglial function. *Neurobiology of Aging*, 36(6), pp.2153–2163.

Robinson, L., Tang, E., and Taylor, J.-P., 2015. Dementia: timely diagnosis and early intervention. *BMJ (Clinical Research Ed.)*, 350, p.h3029.

Rodriguez, G.A., Tai, L.M., LaDu, M.J., and Rebeck, G.W., 2014. Human APOE4 increases microglia reactivity at A β plaques in a mouse model of A β deposition. *Journal of Neuroinflammation*, 11, p.111.

Roses, A.D., 1996. Apolipoprotein E alleles as risk factors in Alzheimer's disease.

Annual Review of Medicine, 47, pp.387–400.

Satoh, J., Kino, Y., Asahina, N., Takitani, M., Miyoshi, J., Ishida, T., and Saito, Y., 2016. TMEM119 marks a subset of microglia in the human brain.

Neuropathology, 36(1), pp.39–49.

Scarmeas, N., and Stern, Y., 2003. Cognitive reserve and lifestyle. *Journal of Clinical and Experimental Neuropsychology*, 25(5), pp.625–633.

Schafer, D.P., Lehrman, E.K., Kautzman, A.G., Koyama, R., Mardinly, A.R., Yamasaki, R., Ransohoff, R.M., Greenberg, M.E., Barres, B.A., and Stevens, B., 2012. Microglia sculpt postnatal neural circuits in an activity and complement-dependent manner. *Neuron*, 74(4), pp.691–705.

Schizophrenia Psychiatric Genome-Wide Association Study (GWAS) Consortium, 2011. Genome-wide association study identifies five new schizophrenia loci. *Nature Genetics*, 43(10), pp.969–976.

Schizophrenia Working Group of the Psychiatric Genomics Consortium, 2014. Biological insights from 108 schizophrenia-associated genetic loci. *Nature*, 511(7510), pp.421–427.

Schultze, J.L., Freeman, T., Hume, D.A., and Latz, E., 2015. A transcriptional perspective on human macrophage biology. *Seminars in Immunology*, 27(1), pp.44–50.

Scott-Hewitt, N., Perrucci, F., Morini, R., Erreni, M., Mahoney, M., Witkowska, A., Carey, A., Faggiani, E., Schuetz, L.T., Mason, S., Tamborini, M., Bizzotto, M., Passoni, L., Filipello, F., Jahn, R., Stevens, B., and Matteoli, M., 2020. Local externalization of phosphatidylserine mediates developmental synaptic pruning by microglia. *The EMBO Journal*, 39(16), p.e105380.

Segawa, K., and Nagata, S., 2015. An apoptotic “eat me” signal: phosphatidylserine exposure. *Trends in Cell Biology*, 25(11), pp.639–650.

Segawa, K., Suzuki, J., and Nagata, S., 2011. Constitutive exposure of phosphatidylserine on viable cells. *Proceedings of the National Academy of Sciences of the United States of America*, 108(48), pp.19246–19251.

Sekar, A., Bialas, A.R., de Rivera, H., Davis, A., Hammond, T.R., Kamitaki, N., Tooley, K., Presumey, J., Baum, M., Van Doren, V., Genovese, G., Rose, S.A., Handsaker, R.E., Schizophrenia Working Group of the Psychiatric Genomics Consortium, Daly, M.J., Carroll, M.C., Stevens, B., and McCarroll, S.A., 2016. Schizophrenia risk from complex variation of complement component 4. *Nature*, 530(7589), pp.177–183.

Sellgren, C.M., Gracias, J., Watmuff, B., Biag, J.D., Thanos, J.M., Whittredge, P.B., Fu, T., Worringer, K., Brown, H.E., Wang, J., Kaykas, A., Karmacharya, R., Goold, C.P., Sheridan, S.D., and Perlis, R.H., 2019. Increased synapse elimination by microglia in schizophrenia patient-derived models of synaptic pruning. *Nature Neuroscience*, 22(3), pp.374–385.

Sheng, M., Sabatini, B.L., and Südhof, T.C., 2012. Synapses and Alzheimer’s disease. *Cold Spring Harbor Perspectives in Biology*, 4(5).

Sheppard, O., Coleman, M.P., and Durrant, C.S., 2019. Lipopolysaccharide-induced

neuroinflammation induces presynaptic disruption through a direct action on brain tissue involving microglia-derived interleukin 1 beta. *Journal of Neuroinflammation*, 16(1), p.106.

Shi, Q., Chowdhury, S., Ma, R., Le, K.X., Hong, S., Caldarone, B.J., Stevens, B., and Lemere, C.A., 2017a. Complement C3 deficiency protects against neurodegeneration in aged plaque-rich APP/PS1 mice. *Science Translational Medicine*, 9(392).

Shi, Q., Colodner, K.J., Matousek, S.B., Merry, K., Hong, S., Kenison, J.E., Frost, J.L., Le, K.X., Li, S., Dodart, J.-C., Caldarone, B.J., Stevens, B., and Lemere, C.A., 2015. Complement C3-Deficient Mice Fail to Display Age-Related Hippocampal Decline. *The Journal of Neuroscience*, 35(38), pp.13029–13042.

Shi, Y., Yamada, K., Liddelow, S.A., Smith, S.T., Zhao, L., Luo, W., Tsai, R.M., Spina, S., Grinberg, L.T., Rojas, J.C., Gallardo, G., Wang, K., Roh, J., Robinson, G., Finn, M.B., Jiang, H., Sullivan, P.M., Baufeld, C., Wood, M.W., Sutphen, C., McCue, L., Xiong, C., Del-Aguila, J.L., Morris, J.C., Cruchaga, C., Alzheimer's Disease Neuroimaging Initiative, Fagan, A.M., Miller, B.L., Boxer, A.L., Seeley, W.W., Butovsky, O., Barres, B.A., Paul, S.M., and Holtzman, D.M., 2017b. ApoE4 markedly exacerbates tau-mediated neurodegeneration in a mouse model of tauopathy. *Nature*, 549(7673), pp.523–527.

Sia, G.M., Clem, R.L., and Haganir, R.L., 2013. The human language-associated gene SRPX2 regulates synapse formation and vocalization in mice. *Science*, 342(6161), pp.987–991.

Sierra, A., Abiega, O., Shahraz, A., and Neumann, H., 2013. Janus-faced microglia: beneficial and detrimental consequences of microglial phagocytosis. *Frontiers in Cellular Neuroscience*, 7, p.6.

Sierra, A., de Castro, F., Del Río-Hortega, J., Rafael Iglesias-Rozas, J., Garrosa, M., and Kettenmann, H., 2016. The “Big-Bang” for modern glial biology: Translation and comments on Pío del Río-Hortega 1919 series of papers on microglia. *Glia*, 64(11), pp.1801–1840.

Silva, M.V.F., Loures, C. de M.G., Alves, L.C.V., de Souza, L.C., Borges, K.B.G., and Carvalho, M. das G., 2019. Alzheimer's disease: risk factors and potentially protective measures. *Journal of Biomedical Science*, 26(1), p.33.

Sipe, G.O., Lowery, R.L., Tremblay, M.È., Kelly, E.A., Lamantia, C.E., and Majewska, A.K., 2016. Microglial P2Y12 is necessary for synaptic plasticity in mouse visual cortex. *Nature Communications*, 7, p.10905.

Smith, C., McColl, B.W., Patir, A., Barrington, J., Armishaw, J., Clarke, A., Eaton, J., Hobbs, V., Mansour, S., Nolan, M., Rice, G.I., Rodero, M.P., Seabra, L., Ugenti, C., Livingston, J.H., Bridges, L.R., Jeffrey, I.J.M., and Crow, Y.J., 2020. Biallelic mutations in NRROS cause an early onset lethal microgliopathy. *Acta Neuropathologica*, 139(5), pp.947–951.

Smrz, D., Dráberová, L., and Dráber, P., 2007. Non-apoptotic phosphatidylserine externalization induced by engagement of glycosylphosphatidylinositol-anchored proteins. *The Journal of Biological Chemistry*, 282(14), pp.10487–10497.

Spires-Jones, T.L., and Hyman, B.T., 2014. The intersection of amyloid beta and tau at synapses in Alzheimer's disease. *Neuron*, 82(4), pp.756–771.

Srinivasan, K., Friedman, B.A., Etxeberria, A., Huntley, M.A., van der Brug, M.P., Foreman, O., Paw, J.S., Modrusan, Z., Beach, T.G., Serrano, G.E., and Hansen, D.V., 2020. Alzheimer's patient microglia exhibit enhanced aging and unique transcriptional activation. *Cell reports*, 31(13), p.107843.

Stephan, A.H., Madison, D.V., Mateos, J.M., Fraser, D.A., Lovelett, E.A., Coutellier, L., Kim, L., Tsai, H.-H., Huang, E.J., Rowitch, D.H., Berns, D.S., Tenner, A.J., Shamloo, M., and Barres, B.A., 2013. A dramatic increase of C1q protein in the CNS during normal aging. *The Journal of Neuroscience*, 33(33), pp.13460–13474.

Stevens, B., Allen, N.J., Vazquez, L.E., Howell, G.R., Christopherson, K.S., Nouri, N., Micheva, K.D., Mehalow, A.K., Huberman, A.D., Stafford, B., Sher, A., Litke, A.M., Lambris, J.D., Smith, S.J., John, S.W.M., and Barres, B.A., 2007. The classical complement cascade mediates CNS synapse elimination. *Cell*, 131(6), pp.1164–1178.

Streit, W.J., Braak, H., Xue, Q.-S., and Bechmann, I., 2009. Dystrophic (senescent) rather than activated microglial cells are associated with tau pathology and likely precede neurodegeneration in Alzheimer's disease. *Acta Neuropathologica*, 118(4), pp.475–485.

Tai, H.-C., Wang, B.Y., Serrano-Pozo, A., Frosch, M.P., Spires-Jones, T.L., and Hyman, B.T., 2014. Frequent and symmetric deposition of misfolded tau oligomers within presynaptic and postsynaptic terminals in Alzheimer's disease. *Acta neuropathologica communications*, 2, p.146.

Takeuchi, T., Duzskiewicz, A.J., and Morris, R.G.M., 2014. The synaptic plasticity and memory hypothesis: encoding, storage and persistence. *Philosophical Transactions of the Royal Society of London. Series B, Biological Sciences*, 369(1633), p.20130288.

Tanzi, R.E., and Hyman, B.T., 1991. Alzheimer's mutation. *Nature*, 350(6319), p.564.

Tay, T.L., Savage, J.C., Hui, C.W., Bisht, K., and Tremblay, M.-È., 2017. Microglia across the lifespan: from origin to function in brain development, plasticity and cognition. *The Journal of Physiology*, 595(6), pp.1929–1945.

Team, R.C., 2020. *R: A language and environment for statistical computing*. R Foundation for Statistical Computing, Vienna, Austria. RC Team.

Terry, R.D., Masliah, E., Salmon, D.P., Butters, N., DeTeresa, R., Hill, R., Hansen, L.A., and Katzman, R., 1991. Physical basis of cognitive alterations in Alzheimer's disease: synapse loss is the major correlate of cognitive impairment. *Annals of Neurology*, 30(4), pp.572–580.

Thal, D.R., Rüb, U., Orantes, M., and Braak, H., 2002. Phases of A beta-deposition in the human brain and its relevance for the development of AD. *Neurology*, 58(12), pp.1791–1800.

Tischer, J., Krueger, M., Mueller, W., Staszewski, O., Prinz, M., Streit, W.J., and

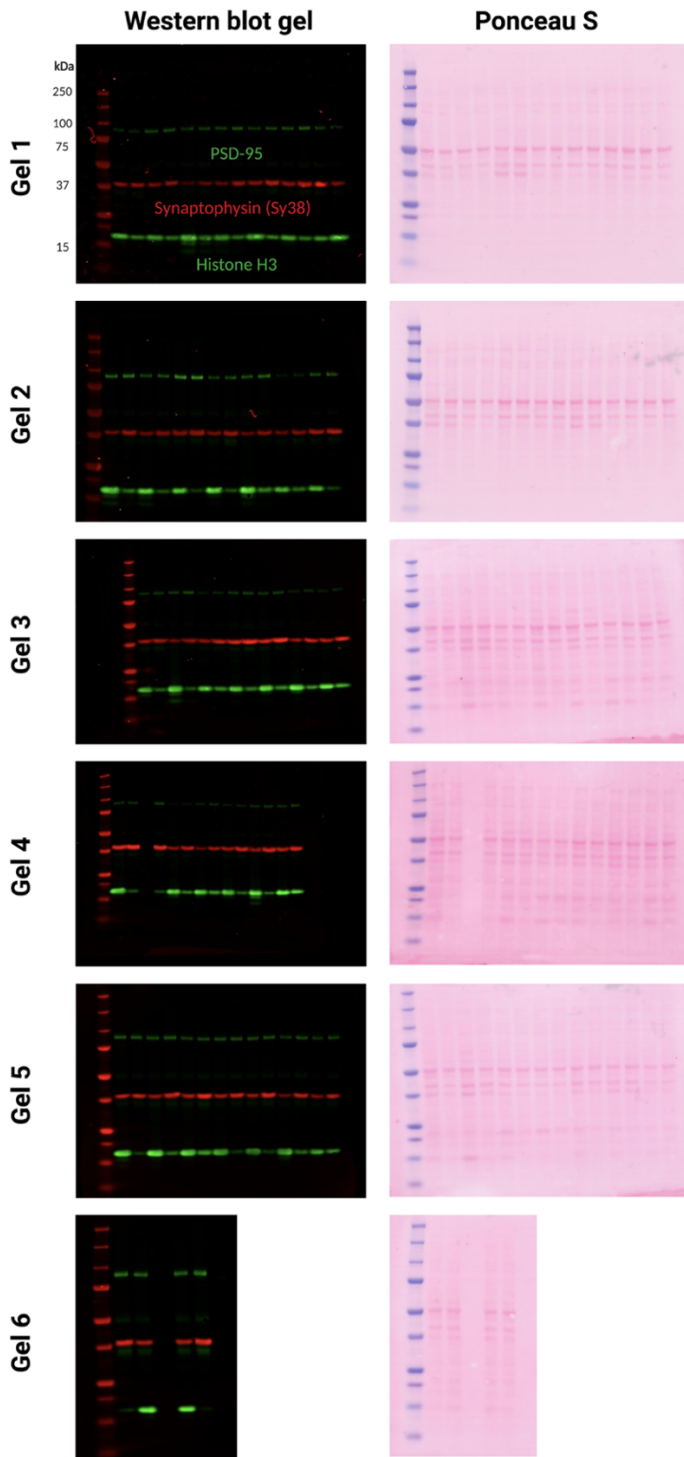
- Bechmann, I., 2016. Inhomogeneous distribution of Iba-1 characterizes microglial pathology in Alzheimer's disease. *Glia*, 64(9), pp.1562–1572.
- Toni, N., Buchs, P.A., Nikonenko, I., Bron, C.R., and Muller, D., 1999. LTP promotes formation of multiple spine synapses between a single axon terminal and a dendrite. *Nature*, 402(6760), pp.421–425.
- Torborg, C.L., and Feller, M.B., 2005. Spontaneous patterned retinal activity and the refinement of retinal projections. *Progress in Neurobiology*, 76(4), pp.213–235.
- Tremblay, M.-È., Lowery, R.L., and Majewska, A.K., 2010. Microglial interactions with synapses are modulated by visual experience. *PLoS Biology*, 8(11), p.e1000527.
- Turrigiano, G.G., and Nelson, S.B., 2004. Homeostatic plasticity in the developing nervous system. *Nature Reviews. Neuroscience*, 5(2), pp.97–107.
- Tzioras, M., Davies, C., Newman, A., Jackson, R., and Spires-Jones, T., 2019. Invited Review: APOE at the interface of inflammation, neurodegeneration and pathological protein spread in Alzheimer's disease. *Neuropathology and Applied Neurobiology*, 45(4), pp.327–346.
- Tzioras, M., and Spires-Jones, T.L., 2018. Research Plan - The effect of APOE genotype on microglial-mediated synapse loss in AD. *University of Edinburgh*.
- Tzioras, M., Stevenson, A.J., Boche, D., and Spires-Jones, T.L., 2021. Microglial contribution to synaptic uptake in the prefrontal cortex in schizophrenia. *Neuropathology and Applied Neurobiology*, 47(2), pp.346–351.
- Vainchtein, I.D., Chin, G., Cho, F.S., Kelley, K.W., Miller, J.G., Chien, E.C., Liddel, S.A., Nguyen, P.T., Nakao-Inoue, H., Dorman, L.C., Akil, O., Joshita, S., Barres, B.A., Paz, J.T., Molofsky, A.B., and Molofsky, A.V., 2018. Astrocyte-derived interleukin-33 promotes microglial synapse engulfment and neural circuit development. *Science*, 359(6381), pp.1269–1273.
- Vergheze, J., Wang, C., Lipton, R.B., Holtzer, R., and Xue, X., 2007. Quantitative gait dysfunction and risk of cognitive decline and dementia. *Journal of Neurology, Neurosurgery, and Psychiatry*, 78(9), pp.929–935.
- Viña, J., and Lloret, A., 2010. Why women have more Alzheimer's disease than men: gender and mitochondrial toxicity of amyloid-beta peptide. *Journal of Alzheimer's Disease*, 20 Suppl 2, pp.S527-33.
- Waller, R., Baxter, L., Fillingham, D.J., Coelho, S., Pozo, J.M., Mozumder, M., Frangi, A.F., Ince, P.G., Simpson, J.E., and Highley, J.R., 2019. Iba-1-/CD68+ microglia are a prominent feature of age-associated deep subcortical white matter lesions. *Plos One*, 14(1), p.e0210888.
- Wang, J.-Y., Chen, F., Fu, X.-Q., Ding, C.-S., Zhou, L., Zhang, X.-H., and Luo, Z.-G., 2014. Caspase-3 cleavage of dishevelled induces elimination of postsynaptic structures. *Developmental Cell*, 28(6), pp.670–684.
- Watkins, L.M., Neal, J.W., Loveless, S., Michailidou, I., Ramaglia, V., Rees, M.I., Reynolds, R., Robertson, N.P., Morgan, B.P., and Howell, O.W., 2016. Complement is activated in progressive multiple sclerosis cortical grey matter lesions. *Journal of Neuroinflammation*, 13(1), p.161.

- Weinhard, L., di Bartolomei, G., Bolasco, G., Machado, P., Schieber, N.L., Neniskyte, U., Exiga, M., Vadisiute, A., Raggioli, A., Schertel, A., Schwab, Y., and Gross, C.T., 2018. Microglia remodel synapses by presynaptic trogocytosis and spine head filopodia induction. *Nature Communications*, 9(1), p.1228.
- Werneburg, S., Jung, J., Kunjamma, R.B., Ha, S.-K., Luciano, N.J., Willis, C.M., Gao, G., Biscola, N.P., Havton, L.A., Crocker, S.J., Popko, B., Reich, D.S., and Schafer, D.P., 2020. Targeted complement inhibition at synapses prevents microglial synaptic engulfment and synapse loss in demyelinating disease. *Immunity*, 52(1), p.167–182.e7.
- Wible, C.G., Anderson, J., Shenton, M.E., Kricun, A., Hirayasu, Y., Tanaka, S., Levitt, J.J., O'Donnell, B.F., Kikinis, R., Jolesz, F.A., and McCarley, R.W., 2001. Prefrontal cortex, negative symptoms, and schizophrenia: an MRI study. *Psychiatry Research*, 108(2), pp.65–78.
- Wiesel, T.N., and Hubel, D.H., 1963. Effects of visual deprivation on morphology and physiology of cells in the cats lateral geniculate body. *Journal of Neurophysiology*, 26, pp.978–993.
- de Wilde, M.C., Overk, C.R., Sijben, J.W., and Masliah, E., 2016. Meta-analysis of synaptic pathology in Alzheimer's disease reveals selective molecular vesicular machinery vulnerability. *Alzheimer's & Dementia*, 12(6), pp.633–644.
- Wishart, T.M., Parson, S.H., and Gillingwater, T.H., 2006. Synaptic vulnerability in neurodegenerative disease. *Journal of Neuropathology and Experimental Neurology*, 65(8), pp.733–739.
- Wolters, F.J., Tinga, L.M., Dhana, K., Koudstaal, P.J., Hofman, A., Bos, D., Franco, O.H., and Ikram, M.A., 2019. Life Expectancy With and Without Dementia: A Population-Based Study of Dementia Burden and Preventive Potential. *American Journal of Epidemiology*, 188(2), pp.372–381.
- Wragg, M., Hutton, M., and Talbot, C., 1996. Genetic association between intronic polymorphism in presenilin-1 gene and late-onset Alzheimer's disease. Alzheimer's Disease Collaborative Group. *The Lancet*, 347(9000), pp.509–512.
- Wright, A.F., Goedert, M., and Hastie, N.D., 1991. Familial Alzheimer's disease. Beta amyloid resurrected. *Nature*, 349(6311), pp.653–654.
- Wu, H.-Y., Hudry, E., Hashimoto, T., Kuchibhotla, K., Rozkalne, A., Fan, Z., Spires-Jones, T., Xie, H., Arbel-Ornath, M., Grosskreutz, C.L., Bacskai, B.J., and Hyman, B.T., 2010. Amyloid beta induces the morphological neurodegenerative triad of spine loss, dendritic simplification, and neuritic dystrophies through calcineurin activation. *The Journal of Neuroscience*, 30(7), pp.2636–2649.
- Wu, T., Dejanovic, B., Gandham, V.D., Gogineni, A., Edmonds, R., Schauer, S., Srinivasan, K., Huntley, M.A., Wang, Y., Wang, T.-M., Hedehus, M., Barck, K.H., Stark, M., Ngu, H., Foreman, O., Meilandt, W.J., Elstrott, J., Chang, M.C., Hansen, D.V., Carano, R.A.D., Sheng, M., and Hanson, J.E., 2019. Complement C3 is activated in human AD brain and is required for neurodegeneration in mouse models of amyloidosis and tauopathy. *Cell reports*, 28(8), p.2111–2123.e6.
- Xu, T., Yu, X., Perlik, A.J., Tobin, W.F., Zweig, J.A., Tennant, K., Jones, T., and

- Zuo, Y., 2009. Rapid formation and selective stabilization of synapses for enduring motor memories. *Nature*, 462(7275), pp.915–919.
- Xu, W., Caracciolo, B., Wang, H.-X., Winblad, B., Bäckman, L., Qiu, C., and Fratiglioni, L., 2010. Accelerated progression from mild cognitive impairment to dementia in people with diabetes. *Diabetes*, 59(11), pp.2928–2935.
- Yoshiyama, Y., Higuchi, M., Zhang, B., Huang, S.-M., Iwata, N., Saido, T.C., Maeda, J., Suhara, T., Trojanowski, J.Q., and Lee, V.M.-Y., 2007. Synapse loss and microglial activation precede tangles in a P301S tauopathy mouse model. *Neuron*, 53(3), pp.337–351.
- Zhang, J., Wang, H., Ye, C., Ge, W., Chen, Y., Jiang, Z., Wu, C., Poo, M., and Duan, S., 2003. ATP released by astrocytes mediates glutamatergic activity-dependent heterosynaptic suppression. *Neuron*, 40(5), pp.971–982.
- Zhao, J., Bi, W., Xiao, S., Lan, X., Cheng, X., Zhang, J., Lu, D., Wei, W., Wang, Y., Li, H., Fu, Y., and Zhu, L., 2019. Neuroinflammation induced by lipopolysaccharide causes cognitive impairment in mice. *Scientific Reports*, 9(1), p.5790.
- Zhou, Y., Lai, B., and Gan, W.-B., 2017. Monocular deprivation induces dendritic spine elimination in the developing mouse visual cortex. *Scientific Reports*, 7(1), p.4977.
- Zhu, Y., Nwabuisi-Heath, E., Dumanis, S.B., Tai, L.M., Yu, C., Rebeck, G.W., and LaDu, M.J., 2012. APOE genotype alters glial activation and loss of synaptic markers in mice. *Glia*, 60(4), pp.559–569.
- Zrzavy, T., Hametner, S., Wimmer, I., Butovsky, O., Weiner, H.L., and Lassmann, H., 2017. Loss of “homeostatic” microglia and patterns of their activation in active multiple sclerosis. *Brain: A Journal of Neurology*, 140(7), pp.1900–1913.

Appendix

Appendix Figure 1. Complete list of Western blot gels and corresponding Ponceau S pages for Chapter 4, Figure 2.



Appendix R Script 1. R Studio Script used for the analysis in Chapter 3 (Modified version used for Re-analysis in Chapter 5).

```
---
title: "Microglia Human PM Statistical analysis"
output:
  word_document: default
  pdf_document: default
  html_document: default
---

### Packages
```{r}
library(readr)
library(table1)
library(ggplot2)
library(RColorBrewer)
library(tidyverse)
library(ggResidpanel)
library(dplyr)
library(car)
library(FSA)
library(rcompanion)
library(forecast)
library(gridExtra)
library(corrplot)
library(lmerTest)
library(emmeans)
library(knitr)
#library(kableExtra)
```

### Import dataframe
```{r}
#setwd("~/Desktop")

Load in dataframe (uses "readr")
Microglia <- read_csv("Human_3D_PM_analysis_R.csv", col_types = cols (
 CaseID = 'f',
 ImageNumber = "f",
 Disease = 'f',
 APOE = 'f',
 APOE4_allele = "f",
```

```

Sex = 'f',
Age = 'i',
BrainArea = 'f',
Plaque = 'f',
PMI = "i",
ObjectVolume = "d",
Total_volume_um = "d",
CD68Burden = "d",
CD68Syn1Burden = "d",
Syn1Burden = "d"))

```

```

Check structure of dataframe
str(Microglia)

```

```

Create a genotype ordered variable (as not sure how R will plot them)
levels(Microglia$Disease)
levels(Microglia$APOE)
levels(Microglia$APOE4_allele)
levels(Microglia$BrainArea)
levels(Microglia$Plaque)

```

```

Microglia$DiseaseOrder <- ordered(Microglia$Disease, levels=c("Control",
"AD"))
Microglia$APOE4_alleleOrder <- ordered(Microglia$APOE4_allele,
levels=c("N", "Y"))
...

```

```

Summary table of participant info

```

```

```{r}

```

```

# Create new dataframe with only one row per case (for info table)

```

```

MicroglialInfo <- Microglia %>%
  group_by(CaseID) %>%
  summarize(Disease = Disease[1],
            DiseaseOrder = DiseaseOrder[1],
            APOE = APOE[1],
            APOE4_allele = APOE4_allele[1],
            APOE4_alleleOrder = APOE4_alleleOrder[1],
            Age = Age[1],
            Sex = Sex[1],
            PMI = PMI[1],
            BrainArea = BrainArea[1])

```

```

# Then plot the table
info <- table1(~ Age + Sex + PMI | DiseaseOrder + APOE, data =
MicroglialInfo)
info
...

### Check whether groups are age-matched
```{r}
Plot ages in each group

Pick colours
display.brewer.pal(n=9, "Oranges")
brewer.pal(n=9,"Oranges")
"#FFF5EB" "#FEE6CE" "#FDD0A2" "#FDAE6B" "#FD8D3C" "#F16913"
"#D94801" "#A63603" "#7F2704"

display.brewer.pal(n=9, "Reds")
brewer.pal(n=9,"Reds")
"#FFF5F0" "#FEE0D2" "#FCBBA1" "#FC9272" "#FB6A4A" "#EF3B2C"
"#CB181D" "#A50F15" "#67000D"

display.brewer.pal(n=9, "BrBG")
brewer.pal(n=9,"BrBG")
"#8C510A" "#BF812D" "#DFC27D" "#F6E8C3" "#F5F5F5" "#C7EAE5"
"#80CDC1" "#35978F" "#01665E"

display.brewer.pal(n=12, "Set3")
brewer.pal(n=12,"Set3")
"#8DD3C7" "#FFFFFFB3" "#BEBADA" "#FB8072" "#80B1D3" "#FDB462"
"#B3DE69" "#FCCDE5" "#D9D9D9" "#BC80BD" "#CCEBC5" "#FFED6F"

Split dataframe - have made MicrogliaBA17 bc cases duplicated due to
brain area otherwise
MicrogliaBA17 <- subset(Microglia, BrainArea == "BA17")

MicrogliaBA17Info <- MicrogliaBA17 %>%
 group_by(CaseID) %>%
 summarize(Disease = Disease[1],
 DiseaseOrder = DiseaseOrder[1],
 APOE = APOE[1],
 APOE4_allele = APOE4_allele[1],
 APOE4_alleleOrder = APOE4_alleleOrder[1],
 Age = Age[1],
 Sex = Sex[1],
 PMI = PMI[1])

```



```

T-test
var.test(Age ~ Disease, data = MicrogliaBA17Info)
t.test(Age ~ Disease, data = MicrogliaBA17Info, var.equal = TRUE)
#p=0.1064 so age-matched

var.test(PMI ~ Disease, data = MicrogliaBA17Info)
t.test(PMI ~ Disease, data = MicrogliaBA17Info, var.equal = TRUE)
#p=0.2356 so PMI-matched

Check that meets the assumptions
Check for normality of residuals
hist(resid(AgeAOV))
shapiro.test(resid(AgeAOV)) # p-value = 0.001789

Levene's Test for Homogeneity of Variance (center = median)
leveneTest(Age ~ Disease * APOE, data = MicroglialInfo)
p-value = 0.6305

not normally distributed

Tukey transform the data to see if helps with assumptions (uses
rcompanion)
MicroglialInfo$Age_tukey =
 transformTukey(MicroglialInfo$Age,
 plotit=FALSE)

AgeAOV_tukey <- aov(Age_tukey ~ Disease * APOE, data = MicroglialInfo)
summary(AgeAOV_tukey)

shapiro.test(resid(AgeAOV_tukey)) # p-value = 0.0747
leveneTest(Age_tukey ~ Disease * APOE, data = MicroglialInfo)
p-value = 0.9482

Plot Age by Disease
ggplot(MicroglialInfo, aes(x = DiseaseOrder, y = Age, fill = DiseaseOrder)) +
 stat_boxplot(geom = 'errorbar', width = 0.2) + # adds the little horizontal
lines on top and bottom of whiskers
 geom_boxplot(outlier.size = -1, width=0.75) + # makes it not show outliers
twice (because of jitter)
 stat_summary(fun = max, fun.max = length, geom = "text", aes(label =
..ymax..), vjust = -2) + # adds group n's above bars
 geom_point(aes(shape=Sex, color = DiseaseOrder), position =
position_jitter(w = 0.1, h = 0.0), alpha = 0.9, size = 2) +
 ggtitle("Ages - by disease") + # title of the plot

```

```

 scale_y_continuous("Age (years)", limits = c(55,100), breaks =
c(55,60,65,70,75,80,85,90,95,100)) + # names the y axis, sets where ticks
are and sets limits of y-axis
 xlab("Group") + # sets the x-axis label
 theme_classic(base_size = 14) + #classic theme makes white background
without lines.
 theme(legend.position="right") + #removes legend since labels on x axis
sufficient
 guides(fill = FALSE) + # removes group legend
scale_color_manual(values = c("cornflowerblue", "deeppink")) +
manually set the colours you want - see word doc for link to list of colours
 # scale_fill_brewer(palette = "Blues") +
 scale_fill_brewer(palette = "Greys") +
 scale_color_manual(values = c("#e8b4a7", "#FB8072",
"#a3d9d1", "#35978F"))
```

```

```

### Check whether groups are PMI-matched
```{r}
Plot ages in each group

```

```

Plot
ggplot(MicrogliaBA17Info, aes(x = DiseaseOrder, y = PMI, fill =
DiseaseOrder)) +
 stat_boxplot(geom = 'errorbar', width = 0.2) + # adds the little horizontal
lines on top and bottom of whiskers
 geom_boxplot(outlier.size = -1, width=0.75) + # makes it not show outliers
twice (because of jitter)
 stat_summary(fun = max, fun.max = length, geom = "text", aes(label =
..ymax..), vjust = -2) + # adds group n's above bars
 geom_point(aes(shape=Sex), position = position_jitter(w = 0.1, h = 0.0),
alpha = 0.6, size = 1.5) +
 ggtitle("PMI") + # title of the plot
 scale_y_continuous("Post mortem interval (hours)", limits = c(0,110), breaks
= c(0,10,20,30,40,50,60,70,80,90,100,110)) + # names the y axis, sets where
ticks are and sets limits of y-axis
 xlab("Group") + # sets the x-axis label
 theme_classic(base_size = 14) + #classic theme makes white background
without lines.
 theme(legend.position="none") + #removes legend since labels on x axis
sufficient
 guides(fill = FALSE) + # removes group legend
scale_color_manual(values = c("cornflowerblue", "deeppink")) +
manually set the colours you want - see word doc for link to list of colours
 # scale_fill_brewer(palette = "Blues") +

```

```

 scale_fill_manual(values = c("#FEE0D2", "#FB8072",
"#C7EAE5", "#35978F"))
...

```{r}
# Run two-way ANOVA to assess whether there is a PMI difference - Go with
this as can get data to be normally distributed

PMIAOV <- aov(PMI ~ Disease * APOE, data = MicrogliaBA17Info)
summary(PMIAOV)

# Check that meets the assumptions
# Check for normality of residuals
hist(resid(PMIAOV))
shapiro.test(resid(PMIAOV)) # p-value = 0.6458

# normally distributed

# Plot Age by Disease
ggplot(MicrogliaBA17Info, aes(x = DiseaseOrder, y = Age, fill =
DiseaseOrder)) +
  stat_boxplot(geom = 'errorbar', width = 0.2) + # adds the little horizontal
lines on top and bottom of whiskers
  geom_boxplot(outlier.size = -1, width=0.75) + # makes it not show outliers
twice (because of jitter)
  stat_summary(fun = max, fun.max = length, geom = "text", aes(label =
..ymax..), vjust = -2) + # adds group n's above bars
  geom_point(aes(shape=Sex, color = DiseaseOrder), position =
position_jitter(w = 0.1, h = 0.0), alpha = 0.9, size = 1.5) +
  ggtitle("Ages") + # title of the plot
  scale_y_continuous("Age (years)", limits = c(55,100)) + # names the y axis,
sets where ticks are and sets limits of y-axis
  xlab("Group") + # sets the x-axis label
  theme_classic(base_size = 14) + #classic theme makes white background
without lines.
  theme(legend.position="right") + #removes legend since labels on x axis
sufficient
  guides(fill = FALSE) + # removes group legend
# scale_color_manual(values = c("cornflowerblue", "deeppink")) + #
manually set the colours you want - see word doc for link to list of colours
# scale_fill_brewer(palette = "Blues") +
scale_fill_brewer(palette = "Greys") +
scale_color_manual(values = c("#FEE0D2", "#FB8072",
"#C7EAE5", "#35978F"))

```

```
ggsave("CasesInfo.PNG", device = png, width = 2, height = 2, scale = 4)
```

```
```
```

```
Burdens
```

```
Create mean dataframe
```

```
```{r}
```

```
# Need to create a dataframe with the means/medians to plot with  
geom_point (will plot this over the spread of the data)
```

```
Microglia$NormCD68Syn1Burden <- (Microglia$CD68Syn1Burden /  
Microglia$CD68Burden) * 100
```

```
MicrogliaMean <- Microglia %>%
```

```
  group_by(CaseID) %>%
```

```
  summarize(Disease = Disease[1],
```

```
            DiseaseOrder = DiseaseOrder[1],
```

```
            BrainArea = BrainArea[1],
```

```
            APOE = APOE[1],
```

```
            APOE4_allele = APOE4_allele[1],
```

```
            APOE4_alleleOrder = APOE4_alleleOrder[1],
```

```
            Age = Age[1],
```

```
            Sex = Sex[1],
```

```
            PMI = PMI[1],
```

```
            Plaque = Plaque[1],
```

```
            CD68BurdenMed = median(CD68Burden, na.rm = TRUE),
```

```
            CD68Syn1BurdenMed = median(CD68Syn1Burden, na.rm =
```

```
TRUE),
```

```
            Syn1BurdenMed = median(Syn1Burden, na.rm = TRUE),
```

```
            NormCD68Syn1BurdenMed = median(NormCD68Syn1Burden,
```

```
na.rm = TRUE))
```

```
# Check whether to take means or medians
```

```
hist(Microglia$CD68Burden)
```

```
shapiro.test(Microglia$CD68Burden) # p-value < 2.2e-16 - MEDIAN
```

```
hist(Microglia$CD68Syn1Burden)
```

```
shapiro.test(Microglia$CD68Syn1Burden) # p-value < 2.2e-16 - MEDIAN
```

```
hist(Microglia$Syn1Burden)
```

```
shapiro.test(Microglia$Syn1Burden) # p-value = 2.2e-16 - MEDIAN
```

```
hist(Microglia$NormCD68Syn1Burden)
```

```
shapiro.test(Microglia$NormCD68Syn1Burden) # p-value < 2.2e-16 -  
MEDIAN
```


...

```
### Create mean dataframe for plaque AD only
```

```
```{r}
```

```
Need to create a dataframe with the means/medians to plot with
geom_point (will plot this over the spread of the data)
```

```
MicrogliaPlaqueMedian <- MicrogliaDisease %>%
 group_by(CaseID, Plaque) %>%
 summarize(Disease = Disease[1],
 DiseaseOrder = DiseaseOrder[1],
 BrainArea = BrainArea[1],
 APOE = APOE[1],
 APOE4_allele = APOE4_allele[1],
 APOE4_alleleOrder = APOE4_alleleOrder[1],
 Age = Age[1],
 Sex = Sex[1],
 PMI = PMI[1],
 CD68BurdenMed = median(CD68Burden, na.rm = TRUE),
 CD68Syn1BurdenMed = median(CD68Syn1Burden, na.rm =
TRUE),
 Syn1BurdenMed = median(Syn1Burden, na.rm = TRUE),
 NormCD68Syn1BurdenMed = median(NormCD68Syn1Burden,
na.rm = TRUE))
```

```
Check whether to take means or medians
```

```
hist(Microglia$CD68Burden)
shapiro.test(Microglia$CD68Burden) # p-value < 2.2e-16 - MEDIAN
```

```
hist(Microglia$CD68Syn1Burden)
shapiro.test(Microglia$CD68Syn1Burden) # p-value < 2.2e-16 - MEDIAN
```

```
hist(Microglia$Syn1Burden)
shapiro.test(Microglia$Syn1Burden) # p-value = 2.2e-16 - MEDIAN
```

```
hist(Microglia$NormCD68Syn1Burden)
shapiro.test(Microglia$NormCD68Syn1Burden) # p-value < 2.2e-16 -
MEDIAN
```

...

```

Plaque AD only CD68Syn1 burden graph
```{r}
# Plot
ggplot(MicrogliaPlaqueMedian, aes(x = Plaque, y = CD68Syn1BurdenMed,
fill = Plaque)) +
  stat_boxplot(geom = 'errorbar', width = 0.2) + # adds the little horizontal
lines on top and bottom of whiskers
  geom_boxplot(outlier.size = -1, width=0.75) + # makes it not show outliers
twice (because of jitter)
  stat_summary(fun = max, fun.max = length, geom = "text", aes(label =
..ymax..), vjust = -2) + # adds group n's above bars
  geom_point(aes (shape=Sex), position = position_jitter(w = 0.1, h = 0.0),
alpha = 0.6, size = 1.5) +
  ggtitle("CD68+Syn1 burden") + # title of the plot
  scale_y_continuous("CD68+Syn1 Burden (% volume)", limits = c(0,0.07),
breaks = c(0,0.01,0.02,0.03,0.04,0.05,0.06,0.07)) + # names the y axis, sets
where ticks are and sets limits of y-axis
  xlab("Plaque") + # sets the x-axis label
  theme_classic(base_size = 22) + #classic theme makes white background
without lines.
  theme(legend.position="none") + #removes legend since labels on x axis
sufficient
# guides(fill = FALSE) + # removes group legend
# scale_color_manual(values = c("cornflowerblue", "deeppink")) + #
manually set the colours you want - see word doc for link to list of colours
# scale_fill_brewer(palette = "Blues") +
scale_fill_manual(values = c("#FEE0D2", "#FB8072",
"#C7EAE5", "#35978F")) +
facet_wrap(~BrainArea)
ggsave("CD68Syn1Plaque.PNG", device = png, width = 2, height = 2, scale
= 4)
```

```

```

Plaque AD only CD68 burden graph
```{r}
# Plot
ggplot(MicrogliaPlaqueMedian, aes(x = Plaque, y = CD68BurdenMed, fill =
Plaque)) +
  stat_boxplot(geom = 'errorbar', width = 0.2) + # adds the little horizontal
lines on top and bottom of whiskers
  geom_boxplot(outlier.size = -1, width=0.75) + # makes it not show outliers
twice (because of jitter)
  stat_summary(fun = max, fun.max = length, geom = "text", aes(label =
..ymax..), vjust = -2) + # adds group n's above bars

```

```

  geom_point(aes (shape=Sex), position = position_jitter(w = 0.1, h = 0.0),
alpha = 0.6, size = 1.5) +
  ggtitle("CD68 burden") + # title of the plot
  scale_y_continuous("CD68 Burden (% volume)", limits = c(0,0.9), breaks =
c(0,0.1,0.2,0.3,0.4,0.5,0.6,0.7,0.8,0.9)) + # names the y axis, sets where ticks
are and sets limits of y-axis
  xlab("Plaque") + # sets the x-axis label
  theme_classic(base_size = 22) + #classic theme makes white background
without lines.
  theme(legend.position="none") + #removes legend since labels on x axis
sufficient
# guides(fill = FALSE) + # removes group legend
# scale_color_manual(values = c("cornflowerblue", "deeppink")) + #
manually set the colours you want - see word doc for link to list of colours
# scale_fill_brewer(palette = "Blues") +
scale_fill_manual(values = c("#FEE0D2", "#FB8072",
"#C7EAE5", "#35978F")) +
facet_wrap(~BrainArea)
ggsave("CD68Plaque.PNG", device = png, width = 2, height = 2, scale = 4)
```

```

```

Plaque AD only NormCD68Syn1 burden graph
```{r}

```

```

# Plot

```

```

ggplot(MicrogliaPlaqueMedian, aes(x = Plaque, y =
NormCD68Syn1BurdenMed, fill = Plaque)) +
  stat_boxplot(geom ='errorbar', width = 0.2) + # adds the little horizontal
lines on top and bottom of whiskers
  geom_boxplot(outlier.size = -1, width=0.75) + # makes it not show outliers
twice (because of jitter)
  stat_summary(fun = max, fun.max = length, geom = "text", aes(label =
..ymax..), vjust = -2) + # adds group n's above bars
  geom_point(aes (shape=Sex), position = position_jitter(w = 0.1, h = 0.0),
alpha = 0.6, size = 1.5) +
  ggtitle("Normalised CD68+Syn1 burden") + # title of the plot
  scale_y_continuous("Norm CD68+Syn1 Burden (% volume)", limits =
c(0,20), breaks = c(0,5,10,15,20)) + # names the y axis, sets where ticks are
and sets limits of y-axis
  xlab("Plaque") + # sets the x-axis label
  theme_classic(base_size = 22) + #classic theme makes white background
without lines.
  theme(legend.position="none") + #removes legend since labels on x axis
sufficient
# guides(fill = FALSE) + # removes group legend

```

```
# scale_color_manual(values = c("cornflowerblue", "deeppink")) + #
manually set the colours you want - see word doc for link to list of colours
# scale_fill_brewer(palette = "Blues") +
scale_fill_manual(values = c("#FEE0D2", "#FB8072",
"#C7EAE5", "#35978F")) +
facet_wrap(~BrainArea)
ggsave("NormCD68Syn1Plaque.PNG", device = png, width = 2, height = 2,
scale = 4)
```

```

```
#Stats for AD plaque CD68Syn1
```

```
Then run mixed effect model - because have multiple measurements from
each case (multiple images)
```

```
```{r}
```

```
# Set reference level
```

```
Microglia$APOE4_allele <- relevel(Microglia$APOE4_allele, ref = "N")
```

```
Microglia$Disease <- relevel(Microglia$Disease, ref = "Control")
```

```
Microglia$BrainArea <- relevel(Microglia$BrainArea, ref = "BA17")
```

```
Microglia$Plaque <- relevel(Microglia$Plaque, ref = "N")
```

```
# Mixed effect model - Plaques CD68Syn1
```

```
ME_CD68Syn1Burden_Plaque <- lmer(CD68Syn1Burden ~ Plaque *
```

```
BrainArea + APOE4_allele + Sex + (1|CaseID), data = MicrogliaDisease)
```

```
summary(ME_CD68Syn1Burden_Plaque)
```

```
resid_panel(ME_CD68Syn1Burden_Plaque)
```

```
shapiro.test(resid(ME_CD68Syn1Burden_Plaque)) # p-value = < 2.2e-16
```

```
# Mixed effect model - Plaques CD68
```

```
ME_CD68Burden_Plaque <- lmer(CD68Burden ~ Plaque * BrainArea +
```

```
APOE4_allele + Sex + (1|CaseID), data = MicrogliaDisease)
```

```
summary(ME_CD68Burden_Plaque)
```

```
resid_panel(ME_CD68Burden_Plaque)
```

```
shapiro.test(resid(ME_CD68Burden_Plaque)) # p-value = < 2.2e-16
```

```
# Mixed effect model - Plaques NormCD68Syn1
```

```
ME_NormCD68Syn1Burden_Plaque <- lmer(NormCD68Syn1Burden ~
```

```
Plaque * BrainArea + APOE4_allele + Sex + (1|CaseID), data =
```

```
MicrogliaDisease)
```

```
summary(ME_NormCD68Syn1Burden_Plaque)
```

```
resid_panel(ME_NormCD68Syn1Burden_Plaque)
```

```
shapiro.test(resid(ME_NormCD68Syn1Burden_Plaque)) # p-value = < 2.2e-16
```

```
# Tukey transformation Plaque CD68Syn1  
MicrogliaDisease$CD68Syn1Burden_Plaque_tukey =  
  transformTukey(MicrogliaDisease$CD68Syn1Burden,  
                 plotit=FALSE)
```

```
ME_CD68Syn1Burden_Plaque_tukey <-  
lmer(CD68Syn1Burden_Plaque_tukey ~ Plaque * BrainArea + APOE4_allele  
+ Sex + (1|CaseID), data = MicrogliaDisease)  
summary(ME_CD68Syn1Burden_Plaque_tukey)
```

```
resid_panel(ME_CD68Syn1Burden_Plaque_tukey)
```

```
shapiro.test(resid(ME_CD68Syn1Burden_Plaque_tukey)) # p-value = 0.7287
```

```
anova(ME_CD68Syn1Burden_Plaque_tukey)
```

```
emmeans(ME_CD68Syn1Burden_Plaque_tukey, pairwise ~ BrainArea *  
Plaque)
```

```
# Tukey transformation Plaque CD68  
MicrogliaDisease$CD68Burden_Plaque_tukey =  
  transformTukey(MicrogliaDisease$CD68Burden,  
                 plotit=FALSE)
```

```
ME_CD68Burden_Plaque_tukey <- lmer(CD68Burden_Plaque_tukey ~  
Plaque * BrainArea + APOE4_allele + Sex + (1|CaseID), data =  
MicrogliaDisease)  
summary(ME_CD68Burden_Plaque_tukey)
```

```
resid_panel(ME_CD68Syn1Burden_Plaque_tukey)
```

```
shapiro.test(resid(ME_CD68Burden_Plaque_tukey)) # p-value = 0.7287
```

```
anova(ME_CD68Burden_Plaque_tukey)
```

```
emmeans(ME_CD68Burden_Plaque_tukey, pairwise ~ BrainArea * Plaque)
```

```
# Tukey transformation Plaque CD68Syn1
```

```

MicrogliaDisease$NormCD68Syn1Burden_Plaque_tukey =
  transformTukey(MicrogliaDisease$NormCD68Syn1Burden,
    plotit=FALSE)

ME_NormCD68Syn1Burden_Plaque_tukey <-
  lmer(NormCD68Syn1Burden_Plaque_tukey ~ Plaque * BrainArea +
  APOE4_allele + Sex + (1|CaseID), data = MicrogliaDisease)
summary(ME_NormCD68Syn1Burden_Plaque_tukey)

resid_panel(ME_NormCD68Syn1Burden_Plaque_tukey)

shapiro.test(resid(ME_NormCD68Syn1Burden_Plaque_tukey)) # p-value =
0.7287

anova(ME_NormCD68Syn1Burden_Plaque_tukey)

emmeans(ME_NormCD68Syn1Burden_Plaque_tukey, pairwise ~ BrainArea
* Plaque)

...

### CD68SYN1 all APOE genotypes graph
```{r}
Plot
ggplot(MicrogliaMean, aes(x = APOE, y = CD68Syn1BurdenMed, fill =
APOE)) +
 stat_boxplot(geom = 'errorbar', width = 0.2) + # adds the little horizontal
lines on top and bottom of whiskers
 geom_boxplot(outlier.size = -1, width=0.75) + # makes it not show outliers
twice (because of jitter)
 stat_summary(fun = max, fun.max = length, geom = "text", aes(label =
..ymax..), vjust = -2) + # adds group n's above bars
 geom_point(position = position_jitter(w = 0.1, h = 0.0), alpha = 0.6, size =
1.5) +
 ggtitle("CD68+Syn1 burden") + # title of the plot
 scale_y_continuous("CD68+Syn1 Burden (% volume)", limits = c(0,0.04),
breaks = c(0,0.01,0.02,0.03,0.04)) + # names the y axis, sets where ticks are
and sets limits of y-axis
 xlab("APOE") + # sets the x-axis label
 theme_grey(base_size = 22) + #classic theme makes white background
without lines.
 theme(legend.position="right") + #removes legend since labels on x axis
sufficient
 guides(fill = FALSE) + # removes group legend

```

```

scale_color_manual(values = c("cornflowerblue", "deeppink")) +
manually set the colours you want - see word doc for link to list of colours
scale_fill_brewer(palette = "Blues") +
scale_fill_manual(values = c("#FEE0D2", "#FB8072",
"#C7EAE5", "#35978F")) +
facet_grid(BrainArea~DiseaseOrder)
ggsave("CD68Syn1APOE.PNG", device = png, width = 2, height = 2, scale =
4)
```

```

```

### CD68SYN1 APOE4 Y/N graph
```{r}

```

```

Plot

```

```

ggplot(MicrogliaMean, aes(x = APOE4_allele, y = CD68Syn1BurdenMed, fill
= APOE4_allele)) +
 stat_boxplot(geom = 'errorbar', width = 0.2) + # adds the little horizontal
lines on top and bottom of whiskers
 geom_boxplot(outlier.size = -1, width=0.75) + # makes it not show outliers
twice (because of jitter)
 stat_summary(fun = max, fun.max = length, geom = "text", aes(label =
..ymax..), vjust = -2) + # adds group n's above bars
 geom_point(position = position_jitter(w = 0.1, h = 0.0), alpha = 0.6, size =
1.5) +
 ggtitle("CD68+Syn1 burden") + # title of the plot
 scale_y_continuous("CD68+Syn1 Burden (% volume)", limits = c(0,0.04),
breaks = c(0,0.01,0.02,0.03,0.04)) + # names the y axis, sets where ticks are
and sets limits of y-axis
 xlab("APOE4") + # sets the x-axis label
 theme_grey(base_size = 22) + #classic theme makes white background
without lines.
 theme(legend.position="right") + #removes legend since labels on x axis
sufficient
 guides(fill = FALSE) + # removes group legend
scale_color_manual(values = c("cornflowerblue", "deeppink")) +
manually set the colours you want - see word doc for link to list of colours
scale_fill_brewer(palette = "Blues") +
scale_fill_manual(values = c("#FEE0D2", "#FB8072",
"#C7EAE5", "#35978F")) +
facet_grid(BrainArea~DiseaseOrder)
ggsave("CD68Syn1APOE4.PNG", device = png, width = 2, height = 2, scale
= 4)
```

```

```

### CD68 all APOE genotypes graph
```{r}

```

```

Plot

```

```

ggplot(MicrogliaMean, aes(x = APOE, y = CD68BurdenMed, fill = APOE)) +
 stat_boxplot(geom = 'errorbar', width = 0.2) + # adds the little horizontal
lines on top and bottom of whiskers
 geom_boxplot(outlier.size = -1, width=0.75) + # makes it not show outliers
twice (because of jitter)
 stat_summary(fun = max, fun.max = length, geom = "text", aes(label =
..ymax..), vjust = -2) + # adds group n's above bars
 geom_point(position = position_jitter(w = 0.1, h = 0.0), alpha = 0.6, size =
1.5) +
 ggtitle("CD68 burden") + # title of the plot
 scale_y_continuous("CD68 Burden (% volume)", limits = c(0,0.8), breaks =
c(0,0.1,0.2,0.3,0.4,0.5,0.6,0.7,0.8)) + # names the y axis, sets where ticks
are and sets limits of y-axis
 xlab("APOE") + # sets the x-axis label
 theme_grey(base_size = 22) + #classic theme makes white background
without lines.
 theme(legend.position="right") + #removes legend since labels on x axis
sufficient
 guides(fill = FALSE) + # removes group legend
scale_color_manual(values = c("cornflowerblue", "deeppink")) +
manually set the colours you want - see word doc for link to list of colours
 # scale_fill_brewer(palette = "Blues") +
 scale_fill_manual(values = c("#FEE0D2", "#FB8072",
"#C7EAE5", "#35978F")) +
 facet_grid(BrainArea~DiseaseOrder)
ggsave("CD68APOE.PNG", device = png, width = 2, height = 2, scale = 4)
```

```

```

### CD68 APOE4 Y/N graph
```{r}

```

```

Plot
ggplot(MicrogliaMean, aes(x = APOE4_allele, y = CD68BurdenMed, fill =
APOE4_allele)) +
 stat_boxplot(geom = 'errorbar', width = 0.2) + # adds the little horizontal
lines on top and bottom of whiskers
 geom_boxplot(outlier.size = -1, width=0.75) + # makes it not show outliers
twice (because of jitter)
 stat_summary(fun = max, fun.max = length, geom = "text", aes(label =
..ymax..), vjust = -2) + # adds group n's above bars
 geom_point(position = position_jitter(w = 0.1, h = 0.0), alpha = 0.6, size =
1.5) +
 ggtitle("CD68 burden") + # title of the plot
 scale_y_continuous("CD68 Burden (% volume)", limits = c(0,0.7), breaks =
c(0,0.1,0.2,0.3,0.4,0.5,0.6,0.7)) + # names the y axis, sets where ticks are
and sets limits of y-axis
 xlab("APOE4") + # sets the x-axis label

```



```

theme_grey(base_size = 22) + #classic theme makes white background
without lines.
theme(legend.position="right") + #removes legend since labels on x axis
sufficient
guides(fill = FALSE) + # removes group legend
scale_color_manual(values = c("cornflowerblue", "deeppink")) +
manually set the colours you want - see word doc for link to list of colours
scale_fill_brewer(palette = "Blues") +
scale_fill_manual(values = c("#FEE0D2", "#FB8072",
"#C7EAE5", "#35978F")) +
facet_grid(BrainArea~DiseaseOrder)
ggsave("CD68APOE4.PNG", device = png, width = 2, height = 2, scale = 4)
```

```

```

### NormCD68SYN1 all APOE genotypes graph
```{r}
Plot
ggplot(MicrogliaMean, aes(x = APOE, y = NormCD68Syn1BurdenMed, fill =
APOE)) +
stat_boxplot(geom = 'errorbar', width = 0.2) + # adds the little horizontal
lines on top and bottom of whiskers
geom_boxplot(outlier.size = -1, width=0.75) + # makes it not show outliers
twice (because of jitter)
stat_summary(fun = max, fun.max = length, geom = "text", aes(label =
..ymax..), vjust = -2) + # adds group n's above bars
geom_point(position = position_jitter(w = 0.1, h = 0.0), alpha = 0.6, size =
1.5) +
ggtitle("Normalised CD68+Syn1 burden") + # title of the plot
scale_y_continuous("Norm CD68+Syn1 Burden (% volume)", limits =
c(0,35), breaks = c(0,10,20,30)) + # names the y axis, sets where ticks are
and sets limits of y-axis
xlab("APOE") + # sets the x-axis label
theme_grey(base_size = 22) + #classic theme makes white background
without lines.
theme(legend.position="right") + #removes legend since labels on x axis
sufficient
guides(fill = FALSE) + # removes group legend
scale_color_manual(values = c("cornflowerblue", "deeppink")) +
manually set the colours you want - see word doc for link to list of colours
scale_fill_brewer(palette = "Blues") +
scale_fill_manual(values = c("#FEE0D2", "#FB8072",
"#C7EAE5", "#35978F")) +
facet_grid(BrainArea~DiseaseOrder)
ggsave("NormCD68Syn1APOE.PNG", device = png, width = 2, height = 2,
scale = 4)
```

```

```

### NormCD68SYN1 APOE4 Y/N graph
```{r}
Plot
ggplot(MicrogliaMean, aes(x = APOE4_allele, y =
NormCD68Syn1BurdenMed, fill = APOE4_allele)) +
 stat_boxplot(geom = 'errorbar', width = 0.2) + # adds the little horizontal
lines on top and bottom of whiskers
 geom_boxplot(outlier.size = -1, width=0.75) + # makes it not show outliers
twice (because of jitter)
 stat_summary(fun = max, fun.max = length, geom = "text", aes(label =
..ymax..), vjust = -2) + # adds group n's above bars
 geom_point(position = position_jitter(w = 0.1, h = 0.0), alpha = 0.6, size =
1.5) +
 ggtitle("Normalised CD68+Syn1 burden") + # title of the plot
 scale_y_continuous("Norm CD68+Syn1 Burden (% volume)", limits =
c(0,35), breaks = c(0,10,20,30)) + # names the y axis, sets where ticks are
and sets limits of y-axis
 xlab("APOE4") + # sets the x-axis label
 theme_grey(base_size = 22) + #classic theme makes white background
without lines.
 theme(legend.position="right") + #removes legend since labels on x axis
sufficient
 guides(fill = FALSE) + # removes group legend
scale_color_manual(values = c("cornflowerblue", "deeppink")) +
manually set the colours you want - see word doc for link to list of colours
 # scale_fill_brewer(palette = "Blues") +
 scale_fill_manual(values = c("#FEE0D2", "#FB8072",
"#C7EAE5", "#35978F")) +
 facet_grid(BrainArea~DiseaseOrder)
ggsave("NormCD68Syn1APOE4.PNG", device = png, width = 2, height = 2,
scale = 4)
```

```

```

### CD68SYN1 burden
```{r}
Plot
ggplot(MicrogliaMean, aes(x = BrainArea, y = CD68Syn1BurdenMed, fill =
BrainArea)) +
 stat_boxplot(geom = 'errorbar', width = 0.2) + # adds the little horizontal
lines on top and bottom of whiskers
 geom_boxplot(outlier.size = -1, width=0.75) + # makes it not show outliers
twice (because of jitter)

```

```

stat_summary(fun = max, fun.max = length, geom = "text", aes(label =
..ymax..), vjust = -2) + # adds group n's above bars
geom_point(position = position_jitter(w = 0.1, h = 0.0), alpha = 0.6, size =
1.5) +
ggtitle("CD68+Syn1 burden") + # title of the plot
scale_y_continuous("CD68+Syn1 Burden (% volume)", limits = c(0,0.04),
breaks = c(0,0.01,0.02,0.03,0.04)) + # names the y axis, sets where ticks are
and sets limits of y-axis
xlab("Brain Area") + # sets the x-axis label
theme_classic(base_size = 22) + #classic theme makes white background
without lines.
theme(legend.position="none") + #removes legend since labels on x axis
sufficient
guides(fill = FALSE) + # removes group legend
scale_color_manual(values = c("cornflowerblue", "deeppink")) +
manually set the colours you want - see word doc for link to list of colours
scale_fill_brewer(palette = "Blues") +
scale_fill_manual(values = c("#FEE0D2", "#FB8072",
"#C7EAE5", "#35978F")) +
facet_wrap(~DiseaseOrder)
ggsave("CD68Syn1.PNG", device = png, width = 2, height = 2, scale = 4)
```

```

Then run mixed effect model - because have multiple measurements from each case (multiple images)

```

```{r}
Set reference level
Microglia$APOE4_allele <- relevel(Microglia$APOE4_allele, ref = "N")
Microglia$Disease <- relevel(Microglia$Disease, ref = "Control")
Microglia$BrainArea <- relevel(Microglia$BrainArea, ref = "BA17")
Microglia$Plaque <- relevel(Microglia$Plaque, ref = "N")

Mixed effect model - Sex and Age as covariates
ME_CD68Syn1Burden <- lmer(CD68Syn1Burden ~ Disease * BrainArea +
APOE4_allele + Sex + (1|CaseID), data = Microglia)
summary(ME_CD68Syn1Burden)

ME_CD68Syn1BurdenAPOE4 <- lmer(CD68Syn1Burden ~ APOE4_allele *
BrainArea + Disease + Sex + (1|CaseID), data = Microglia)
summary(ME_CD68Syn1BurdenAPOE4)

resid_panel(ME_CD68Syn1Burden)
Residual plots look okay

shapiro.test(resid(ME_CD68Syn1Burden)) # p-value = < 2.2e-16

```

```

Tukey transformation
Microglia$CD68Syn1Burden_tukey =
 transformTukey(Microglia$CD68Syn1Burden,
 plotit=FALSE)

ME_CD68Syn1Burden_tukey <- lmer(CD68Syn1Burden_tukey ~ Disease *
BrainArea + APOE4_allele + Sex + (1|CaseID), data = Microglia)
summary(ME_CD68Syn1Burden_tukey)

ME_CD68Syn1BurdenAPOE_tukey <- lmer(CD68Syn1Burden_tukey ~
Disease * BrainArea + APOE + Sex + (1|CaseID), data = Microglia)
summary(ME_CD68Syn1BurdenAPOE_tukey)

ME_CD68Syn1BurdenAPOE4_tukey <- lmer(CD68Syn1Burden_tukey ~
APOE4_allele * Disease + BrainArea + Sex + (1|CaseID), data = Microglia)
summary(ME_CD68Syn1BurdenAPOE4_tukey)

resid_panel(ME_CD68Syn1Burden_tukey)

shapiro.test(resid(ME_CD68Syn1Burden_tukey)) # p-value = 0.56

anova(ME_CD68Syn1Burden_tukey) #>%>%
 #kable()

anova(ME_CD68Syn1BurdenAPOE_tukey)

anova(ME_CD68Syn1BurdenAPOE4_tukey)

...

CD68 burden
```{r}
# Plot
ggplot(MicrogliaMean, aes(x = BrainArea, y = CD68BurdenMed, fill =
BrainArea)) +
  stat_boxplot(geom = 'errorbar', width = 0.2) + # adds the little horizontal
lines on top and bottom of whiskers
  geom_boxplot(outlier.size = -1, width=0.75) + # makes it not show outliers
twice (because of jitter)
  stat_summary(fun = max, fun.max = length, geom = "text", aes(label =
..ymax..), vjust = -2) + # adds group n's above bars

```

```

geom_point(position = position_jitter(w = 0.1, h = 0.0), alpha = 0.6, size =
1.5) +
ggtitle("CD68 burden") + # title of the plot
scale_y_continuous("CD68 Burden (% volume)", limits = c(0,0.6), breaks =
c(0,0.1,0.2,0.3,0.4,0.5,0.6)) + # names the y axis, sets where ticks are and
sets limits of y-axis
xlab("Brain Area") + # sets the x-axis label
theme_classic(base_size = 22) + #classic theme makes white background
without lines.
theme(legend.position="none") + #removes legend since labels on x axis
sufficient
# guides(fill = FALSE) + # removes group legend
# scale_color_manual(values = c("cornflowerblue", "deeppink")) + #
manually set the colours you want - see word doc for link to list of colours
# scale_fill_brewer(palette = "Blues") +
scale_fill_manual(values = c("#FEE0D2", "#FB8072",
"#C7EAE5", "#35978F")) +
facet_wrap(~DiseaseOrder)
ggsave("CD68.PNG", device = png, width = 2, height = 2, scale = 4)
```

```

Then run mixed effect model - because have multiple measurements from each case (multiple images)

```

```{r}
# Set reference level
Microglia$APOE4_allele <- relevel(Microglia$APOE4_allele, ref = "N")
Microglia$Disease <- relevel(Microglia$Disease, ref = "Control")
Microglia$BrainArea <- relevel(Microglia$BrainArea, ref = "BA17")
Microglia$Plaque <- relevel(Microglia$Plaque, ref = "N")

# Mixed effect model - Sex and Age as covariates
ME_CD68Burden <- lmer(CD68Burden ~ Disease * BrainArea +
APOE4_allele + Sex + (1|CaseID), data = Microglia)
summary(ME_CD68Burden)

resid_panel(ME_CD68Burden)

shapiro.test(resid(ME_CD68Burden)) # p-value = < 2.2e-16

# Tukey transformation
Microglia$CD68Burden_tukey =
transformTukey(Microglia$CD68Burden,
plotit=FALSE)

```

```

ME_CD68Burden_tukey <- lmer(CD68Burden_tukey ~ Disease * BrainArea
+ APOE4_allele + Sex + (1|CaseID), data = Microglia)
summary(ME_CD68Burden_tukey)

ME_CD68BurdenAPOE_tukey <- lmer(CD68Burden_tukey ~ Disease *
BrainArea + APOE + Sex + (1|CaseID), data = Microglia)
summary(ME_CD68BurdenAPOE_tukey)

resid_panel(ME_CD68Burden_tukey)

shapiro.test(resid(ME_CD68Burden_tukey)) # p-value = 2.397e-07

anova(ME_CD68Burden_tukey)

anova(ME_CD68BurdenAPOE_tukey)

...

# Mixed effect model - NORMALISED BURDEN

```{r}
Plot
ggplot(MicrogliaMean, aes(x = BrainArea, y = NormCD68Syn1BurdenMed,
fill = BrainArea)) +
 stat_boxplot(geom = 'errorbar', width = 0.2) + # adds the little horizontal
lines on top and bottom of whiskers
 geom_boxplot(outlier.size = -1, width=0.75) + # makes it not show outliers
twice (because of jitter)
 stat_summary(fun = max, fun.max = length, geom = "text", aes(label =
..ymax..), vjust = -2) + # adds group n's above bars
 geom_point(position = position_jitter(w = 0.1, h = 0.0), alpha = 0.6, size =
1.5) +
 ggtitle("Normalised CD68+Syn1 burden") + # title of the plot
 scale_y_continuous("Norm CD68+Syn1 Burden (% volume)", limits =
c(0,35), breaks = c(0,5,10,15,20,25,30,35)) + # names the y axis, sets where
ticks are and sets limits of y-axis
 xlab("Brain Area") + # sets the x-axis label
 theme_classic(base_size = 22) + #classic theme makes white background
without lines.
 theme(legend.position="none") + #removes legend since labels on x axis
sufficient
guides(fill = FALSE) + # removes group legend
scale_color_manual(values = c("cornflowerblue", "deeppink")) +
manually set the colours you want - see word doc for link to list of colours

```

```

scale_fill_brewer(palette = "Blues") +
 scale_fill_manual(values = c("#FEE0D2", "#FB8072",
"#C7EAE5", "#35978F")) +
 facet_wrap(~DiseaseOrder)
ggsave("NormCD68Syn1.PNG", device = png, width = 2, height = 2, scale =
4)

```

```

ME_NormCD68Syn1Burden <- lmer(NormCD68Syn1Burden ~ Disease *
BrainArea + APOE4_allele + Sex + (1|CaseID), data = Microglia)
summary(ME_NormCD68Syn1Burden)

```

```

resid_panel(ME_NormCD68Syn1Burden)
Residual plots look okay

```

```

shapiro.test(resid(ME_NormCD68Syn1Burden)) # p-value = < 2.2e-16

```

```

Tukey transformation
Microglia$NormCD68Syn1Burden_tukey =
 transformTukey(Microglia$NormCD68Syn1Burden,
 plotit=FALSE)

```

```

ME_NormCD68Syn1Burden_tukey <- lmer(NormCD68Syn1Burden_tukey ~
Disease * BrainArea + APOE4_allele + Sex + Plaque + (1|CaseID), data =
Microglia)
summary(ME_NormCD68Syn1Burden_tukey)

```

```

ME_NormCD68Syn1BurdenAPOE_tukey <-
lmer(NormCD68Syn1Burden_tukey ~ Disease * BrainArea + APOE + Sex +
(1|CaseID), data = Microglia)
summary(ME_NormCD68Syn1BurdenAPOE_tukey)

```

```

resid_panel(ME_NormCD68Syn1Burden_tukey)

```

```

shapiro.test(resid(ME_NormCD68Syn1Burden_tukey)) # p-value = 0.02143

```

```

anova(ME_NormCD68Syn1Burden_tukey)

```

```

anova(ME_NormCD68Syn1BurdenAPOE_tukey)

```

```

...

```

```

Syn1 burden
```{r}
# Plot
ggplot(MicrogliaMean, aes(x = BrainArea, y = Syn1BurdenMed, fill =
BrainArea)) +
  stat_boxplot(geom = 'errorbar', width = 0.2) + # adds the little horizontal
lines on top and bottom of whiskers
  geom_boxplot(outlier.size = -1, width=0.75) + # makes it not show outliers
twice (because of jitter)
  stat_summary(fun = max, fun.max = length, geom = "text", aes(label =
..ymax..), vjust = -2) + # adds group n's above bars
  geom_point(aes (shape=Sex), position = position_jitter(w = 0.1, h = 0.0),
alpha = 0.6, size = 1.5) +
  ggtitle("Syn1 burden") + # title of the plot
  scale_y_continuous("Syn1 Burden (% volume)", limits = c(0,10), breaks =
c(0,1,2,3,4,5,6,7,8,9,10)) + # names the y axis, sets where ticks are and sets
limits of y-axis
  xlab("Brain Area") + # sets the x-axis label
  theme_classic(base_size = 14) + #classic theme makes white background
without lines.
  theme(legend.position="none") + #removes legend since labels on x axis
sufficient
# guides(fill = FALSE) + # removes group legend
# scale_color_manual(values = c("cornflowerblue", "deeppink")) + #
manually set the colours you want - see word doc for link to list of colours
# scale_fill_brewer(palette = "Blues") +
scale_fill_manual(values = c("#FEE0D2", "#FB8072",
"#C7EAE5", "#35978F")) +
facet_wrap(~DiseaseOrder)
```

```

Then run mixed effect model - because have multiple measurements from each case (multiple images)

```

```{r}
# Set reference level
Microglia$APOE4_allele <- relevel(Microglia$APOE4_allele, ref = "N")
Microglia$Disease <- relevel(Microglia$Disease, ref = "Control")
Microglia$BrainArea <- relevel(Microglia$BrainArea, ref = "BA17")
Microglia$Plaque <- relevel(Microglia$Plaque, ref = "N")

# Mixed effect model - Sex and Age as covariates
ME_Syn1Burden <- lmer(Syn1Burden ~ Disease * BrainArea +
APOE4_allele + Sex + Plaque + (1|CaseID), data = Microglia)
summary(ME_Syn1Burden)

resid_panel(ME_Syn1Burden)

```



```

shapiro.test(resid(ME_Syn1Burden)) # p-value = < 2.2e-16

# Tukey transformation
Microglia$Syn1Burden_tukey =
  transformTukey(Microglia$Syn1Burden,
                plotit=FALSE)

ME_Syn1Burden_tukey <- lmer(Syn1Burden_tukey ~ Disease * BrainArea +
  APOE4_allele + Sex + Plaque + (1|CaseID), data = Microglia)
summary(ME_Syn1Burden_tukey)

resid_panel(ME_Syn1Burden_tukey)

shapiro.test(resid(ME_Syn1Burden_tukey)) # p-value = 2.2e-16

anova(ME_Syn1Burden_tukey)

# Box-Cox transformation
lam.l = BoxCox.lambda(Microglia$Syn1Burden, method = "loglik")
Microglia$Syn1Burden_BCL = BoxCox(Microglia$Syn1Burden, lam.l)

ME_Syn1Burden_BCL <- lmer(Syn1Burden_BCL ~ Disease * BrainArea +
  APOE4_allele + Sex + Plaque + (1|CaseID), data = Microglia)
summary(ME_Syn1Burden_BCL)

resid_panel(ME_Syn1Burden_BCL)

shapiro.test(resid(ME_Syn1Burden_BCL)) # p-value = 0.09458

anova(ME_Syn1Burden_BCL)
```



```

### CD68SYN1 Sex stratified graph
```{r}
Plot
ggplot(MicrogliaMean, aes(x = Sex, y = CD68Syn1BurdenMed, fill = Sex)) +
 stat_boxplot(geom ='errorbar', width = 0.2) + # adds the little horizontal
lines on top and bottom of whiskers
 geom_boxplot(outlier.size = -1, width=0.75) + # makes it not show outliers
twice (because of jitter)

```


```

```

stat_summary(fun = max, fun.max = length, geom = "text", aes(label =
..ymax..), vjust = -2) + # adds group n's above bars
geom_point(position = position_jitter(w = 0.1, h = 0.0), alpha = 0.6, size =
1.5) +
ggtitle("CD68+Syn1 burden") + # title of the plot
scale_y_continuous("CD68+Syn1 Burden (% volume)", limits = c(0,0.04),
breaks = c(0,0.01,0.02,0.03,0.04)) + # names the y axis, sets where ticks are
and sets limits of y-axis
xlab("Sex") + # sets the x-axis label
theme_grey(base_size = 22) + #classic theme makes white background
without lines.
theme(legend.position="right") + #removes legend since labels on x axis
sufficient
guides(fill = FALSE) + # removes group legend
# scale_color_manual(values = c("cornflowerblue", "deeppink")) + #
manually set the colours you want - see word doc for link to list of colours
# scale_fill_brewer(palette = "Blues") +
scale_fill_manual(values = c("#FEE0D2", "#FB8072",
"#C7EAE5", "#35978F")) +
facet_grid(BrainArea~DiseaseOrder)
ggsave("CD68Syn1Sex.PNG", device = png, width = 2, height = 2, scale = 4)
```

```

```

CD68 Sex stratified graph
```{r}

```

```

# Plot

```

```

ggplot(MicrogliaMean, aes(x = Sex, y = CD68BurdenMed, fill = Sex)) +
stat_boxplot(geom = 'errorbar', width = 0.2) + # adds the little horizontal
lines on top and bottom of whiskers
geom_boxplot(outlier.size = -1, width=0.75) + # makes it not show outliers
twice (because of jitter)
stat_summary(fun = max, fun.max = length, geom = "text", aes(label =
..ymax..), vjust = -2) + # adds group n's above bars
geom_point(position = position_jitter(w = 0.1, h = 0.0), alpha = 0.6, size =
1.5) +
ggtitle("CD68 burden") + # title of the plot
scale_y_continuous("CD68 Burden (% volume)", limits = c(0,0.7), breaks =
c(0,0.1,0.2,0.3,0.4,0.5,0.6,0.7)) + # names the y axis, sets where ticks are
and sets limits of y-axis
xlab("Sex") + # sets the x-axis label
theme_grey(base_size = 22) + #classic theme makes white background
without lines.
theme(legend.position="right") + #removes legend since labels on x axis
sufficient
guides(fill = FALSE) + # removes group legend

```

```

# scale_color_manual(values = c("cornflowerblue", "deeppink")) + #
manually set the colours you want - see word doc for link to list of colours
# scale_fill_brewer(palette = "Blues") +
scale_fill_manual(values = c("#FEE0D2", "#FB8072",
"#C7EAE5", "#35978F")) +
facet_grid(BrainArea~DiseaseOrder)
ggsave("CD68Sex.PNG", device = png, width = 2, height = 2, scale = 4)
```

```




```

NormCD68SYN1 Sex stratified graph
```{r}
# Plot
ggplot(MicrogliaMean, aes(x = Sex, y = NormCD68Syn1BurdenMed, fill =
Sex)) +
stat_boxplot(geom = 'errorbar', width = 0.2) + # adds the little horizontal
lines on top and bottom of whiskers
geom_boxplot(outlier.size = -1, width=0.75) + # makes it not show outliers
twice (because of jitter)
stat_summary(fun = max, fun.max = length, geom = "text", aes(label =
..ymax..), vjust = -2) + # adds group n's above bars
geom_point(position = position_jitter(w = 0.1, h = 0.0), alpha = 0.6, size =
1.5) +
ggtitle("Normalised CD68+Syn1 burden") + # title of the plot
scale_y_continuous("Norm CD68+Syn1 Burden (% volume)", limits =
c(0,35), breaks = c(0,10,20,30)) + # names the y axis, sets where ticks are
and sets limits of y-axis
xlab("Sex") + # sets the x-axis label
theme_grey(base_size = 22) + #classic theme makes white background
without lines.
theme(legend.position="right") + #removes legend since labels on x axis
sufficient
guides(fill = FALSE) + # removes group legend
# scale_color_manual(values = c("cornflowerblue", "deeppink")) + #
manually set the colours you want - see word doc for link to list of colours
# scale_fill_brewer(palette = "Blues") +
scale_fill_manual(values = c("#FEE0D2", "#FB8072",
"#C7EAE5", "#35978F")) +
facet_grid(BrainArea~DiseaseOrder)
ggsave("NormCD68Syn1Sex.PNG", device = png, width = 2, height = 2,
scale = 4)
```

```

**Appendix Manuscript 1: Invited Review: APOE at the interface of inflammation, neurodegeneration and pathological protein spread in Alzheimer's disease**

# Invited Review: APOE at the interface of inflammation, neurodegeneration and pathological protein spread in Alzheimer's disease

M. Tzioras\*,<sup>a</sup> , C. Davies\*,<sup>a</sup> , A. Newman\*, R. Jackson\*,<sup>†</sup> and T. Spire-Jones\* 

\*UK Dementia Research Institute and Centre for Discovery Brain Sciences, The University of Edinburgh, Edinburgh, UK and <sup>†</sup>Massachusetts General Hospital and Harvard Medical School, Charlestown, MA, USA

M. Tzioras, C. Davies, A. Newman, R. Jackson and T. Spire-Jones (2019) *Neuropathology and Applied Neurobiology* 45, 327–346

## APOE at the interface of inflammation, neurodegeneration and pathological protein spread in Alzheimer's disease

Despite more than a century of research, the aetiology of sporadic Alzheimer's disease (AD) remains unclear and finding disease modifying treatments for AD presents one of the biggest medical challenges of our time. AD pathology is characterized by deposits of aggregated amyloid beta (A $\beta$ ) in amyloid plaques and aggregated tau in neurofibrillary tangles. These aggregates begin in distinct brain regions and spread throughout the brain in stereotypical patterns. Neurodegeneration, comprising loss of synapses and neurons, occurs in brain regions with high tangle pathology, and an inflammatory response of glial cells appears in brain regions with pathological aggregates. Inheriting an apolipoprotein E  $\epsilon$ 4 (*APOE4*) allele strongly increases the risk of developing AD for reasons that are not yet entirely clear. Substantial amounts of evidence support a role for APOE in

modulating the aggregation and clearance of A $\beta$ , and data have been accumulating recently implicating *APOE4* in exacerbating neurodegeneration, tau pathology and inflammation. We hypothesize that *APOE4* influences all the pathological hallmarks of AD and may sit at the interface between neurodegeneration, inflammation and the spread of pathologies through the brain. Here, we conducted a systematic search of the literature and review evidence supporting a role for *APOE4* in neurodegeneration and inflammation. While there is no direct evidence yet for *APOE4* influencing the spread of pathology, we postulate that this may be found in future based on the literature reviewed here. In conclusion, this review highlights the importance of understanding the role of APOE in multiple important pathological mechanisms in AD.

Keywords: Alzheimer's disease, APOE, Apolipoprotein E, glia, inflammation, neurodegeneration, tau

### Introduction

The greatest genetic risk factor for sporadic AD is a polymorphism in the apolipoprotein E (*APOE*) gene.

Correspondence: Tara Spire-Jones, UK Dementia Research Institute and Centre for Discovery Brain Sciences, The University of Edinburgh, 1 George Square, Edinburgh EH8 9JX, UK. Tel: +44 (0)1316511895; E-mail: Tara.spire-jones@ed.ac.uk

<sup>a</sup>Equal contributions.

The *APOE*  $\epsilon$ 4 (*APOE4*) allele is associated with increasing risk of AD in a dose-dependent manner when compared to the more common *APOE*  $\epsilon$ 3 (*APOE3*) allele; whereas the much rarer *APOE*  $\epsilon$ 2 (*APOE2*) allele has been shown to be protective [1]. The inheritance of two copies of *APOE4* increases the chance of developing AD by 12 times compared to the risk of a person with two copies of *APOE3*. Homozygous *APOE4* carriers who develop AD also have a lower average age of

© 2018 The Authors. *Neuropathology and Applied Neurobiology* published by John Wiley & Sons Ltd on behalf of British Neuropathological Society.

327

This is an open access article under the terms of the Creative Commons Attribution License, which permits use, distribution and reproduction in any medium, provided the original work is properly cited.

clinical onset of 68 years of age compared to an average age of onset of 84 for an individual with two copies of *APOE3*. One copy of *APOE4* increases the chance of AD by three times and lowers the average age of onset to 76 years of age [1]. Although mentioned in association with AD most frequently, APOE has also been linked to Parkinson's disease [2], frontotemporal dementia [3] and other neurological diseases (reviewed in [4]) as well as linked to lower cognition in nondemented aged individuals [5]. The pathways by which APOE impacts the development of AD have been widely studied both *in vitro* and *in vivo*, however, the exact mechanisms have yet to be uncovered.

Much of the work looking at APOE in AD investigates its relationship with A $\beta$ . Early *post mortem* work found a positive correlation between *APOE4* allele dose and A $\beta$  plaque density in individuals with AD [6]. A wide range of compelling studies indicate that *APOE4* affects the production, clearance and aggregation of A $\beta$  (reviewed in [4,7]). Recent genetic data that strongly suggest inflammation to play a role in AD risk have re-invigorated the investigations of the role of APOE in neuroinflammation and how this contributes to disease [8]; and there are emerging data suggesting that APOE may also influence tau-mediated neurodegeneration [9].

We hypothesize that *APOE4* acts beyond its well-known roles in influencing A $\beta$  pathology and lipid homeostasis and has a strong influence on neurodegeneration, inflammation and potentially the spread of pathological proteins through the brain. Here, we conducted a systematic literature search and review the current support in the literature for this hypothesis.

## Methods

A systematic literature search approach was taken for finding studies to review in this paper. In February 2018, Embase, Web of Science and MedLine were searched to identify primary research articles published from 1980 to the date searches were run. Search terms covering APOE, AD and inflammation/pathological protein spread/neurodegeneration were developed (Table S1) to suit each database. Initially, there were no language or selection restrictions on the type of study included or how outcomes were defined, measured or when they were taken. Searches identified 22 909 abstracts and titles that were exported to Endnote, where 12 638

duplicates were removed. 10 271 articles were uploaded into Covidence, where a further 767 duplicates were removed. A two-stage screening strategy was conducted on titles/abstracts and then on full texts using predetermined exclusion criteria (Table S2). Three researchers contributed to the abstract and title screening process such that 50% of abstracts/titles were screened by at least two people and 50% by one. All full-text articles were double screened. Of the 9502 titles/abstracts screened, 214 progressed to full-text review and 88 studies were included. Twenty hand-picked papers that were either published after the search date or were missed during the search but deemed pertinent to the review were also included as is standard practice for full systematic reviews (Figure 1; Table S3). In the results section, we synthesize the findings of the papers identified by the systematic search. Due to the heterogeneous nature of the studies, we did not perform standardized quality control checks of all of the papers, however, all papers included were published in peer-reviewed journals. Because systematic reviews are designed to test evidence of an intervention and due to the inability to conduct formal quality control due to the many types of experiments reviewed, this is not a fully registered systematic review but instead uses some of the principles of systematic reviews to perform a *systematic literature search* and screen for relevant papers which we review.

## Results of the systematic literature search

### APOE and neurodegeneration

To determine whether there is evidence that APOE influences neurodegeneration search terms were used to identify papers containing both APOE and indicators of neuron and synapse loss (papers relating to APOE and neurodegeneration identified in the systematic search are coloured blue and orange in Table S1).

### APOE-related atrophy and neuronal loss in AD

Imaging studies in AD populations repeatedly demonstrated possession of an *APOE4* allele to be associated with more extensive atrophy in disease-specific brain regions such as the medial temporal lobe [3,11–23],

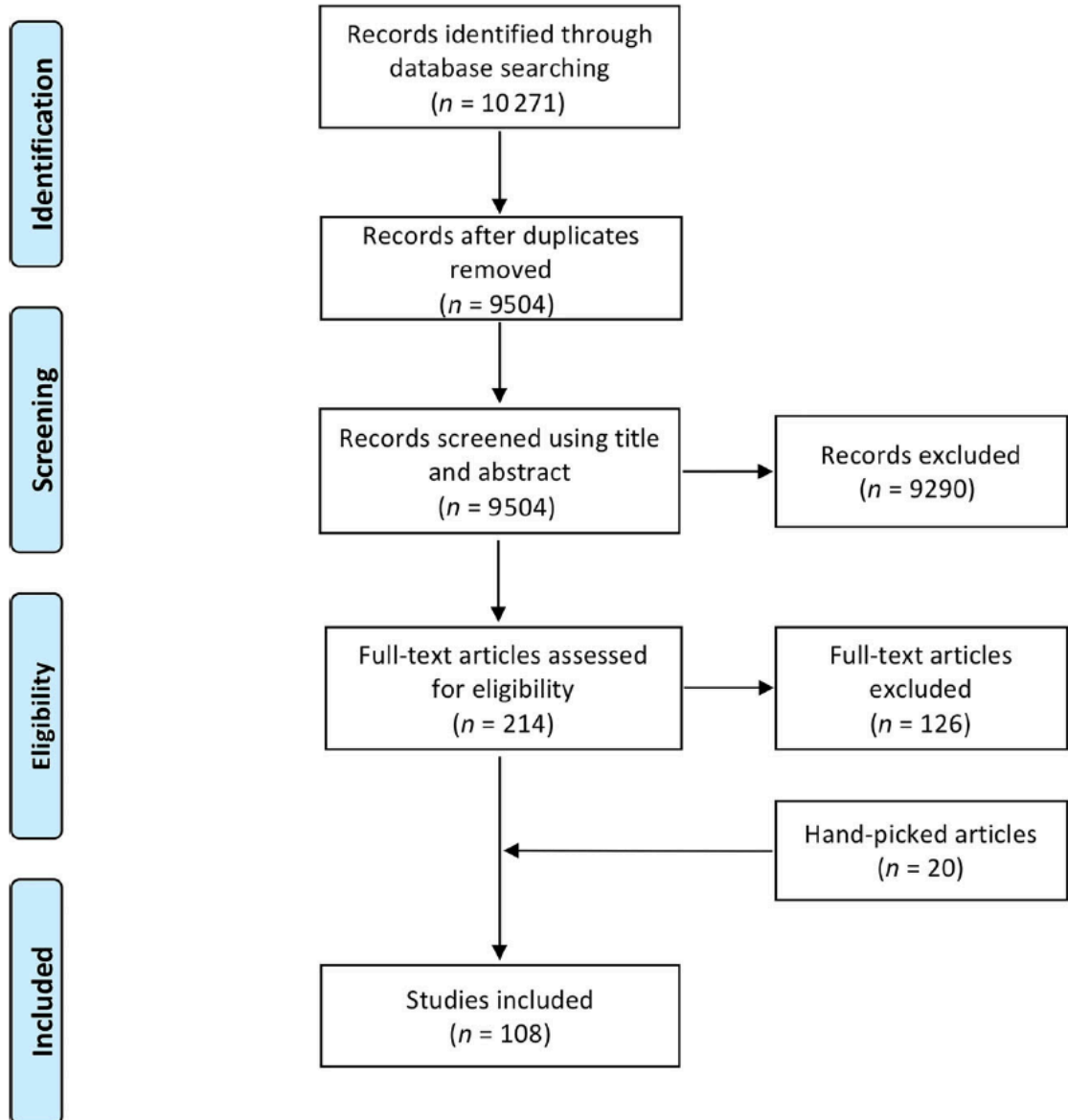


**Figure 1.** PRISMA flow diagram summarizing the review process. Template edited from [10]. Papers referenced in the main body of text were identified through our systematic search and can be found in Table S3.

although this was not universal [24,25]. This is unsurprising when considering that brain structures located here have clinical correlates to well-defined AD symptoms (e.g. memory impairments – hippocampus; altered emotional responses – amygdala), and that *APOE4* carriers are at increased risk of developing these symptoms

in the form of AD. *APOE4*-related atrophy of medial temporal lobe structures was suggested to occur in a gene-dose-dependent manner [15–17,19,21], with one study finding each *APOE4* allele to impart a 4.8% reduction in hippocampal volume and a 3.8% reduction in amygdala volume [16]. In longitudinal studies,

accelerated rates of hippocampal atrophy were associated with the *APOE4* allele [13,22,26–29], although this was not always observed [30,31]. *APOE4*-related atrophy was also observed in the parietal cortex [3,13] and some prefrontal areas [3,12], although again these were not consistently reported and may be related to the inclusion of younger AD patients in these studies.

Diffuse cerebral atrophy is a gross pathological feature of AD. Somewhat surprisingly, however, whole brain volume has been proposed to increase with increasing number of *APOE4* alleles in AD patients [19,32]. Greater *APOE4* allele dose was associated with larger volumes in the frontal lobes [11,17,20], although not always [12,14], which might potentially outweigh reductions in other brain regions and account for increased whole brain volume. Nonetheless, these studies indicate that the *APOE4* allele selectively influences the topography of regional brain atrophy, and thus neurodegeneration, in AD.

Studies of *post mortem* human AD brain have identified neuronal loss in vulnerable brain regions to be characteristic of AD. From our literature search, determining whether *APOE* influences this was less clear. In the nucleus basalis, *APOE4* was found to exacerbate neuronal loss [33], but have no impact in other studies [34,35]. These discrepancies may be due to the different methods employed in quantification of neuronal loss and groups studied. *APOE4* allele possession was also found to enhance neuronal loss in other subcortical structures [33,34], but have no effect on the CA1 region of the hippocampus or superior temporal sulcus [34,36].

*In vivo* and *in vitro* studies supported an association between *APOE4* and neuronal degeneration. In aged mice expressing human *APOE*, those expressing *APOE4* exhibited increased hippocampal and cortical atrophy compared to those expressing *APOE3* [37,38]. In *APOE4*, but not *APOE3* mice, activation of the amyloid cascade by inhibition of the  $A\beta$  degrading enzyme neprilysin was sufficient to induce degeneration of hippocampal and entorhinal cortex neurons, suggestive of a specific effect of *APOE4* in exacerbating  $A\beta$ -related neuronal loss [39]. Isoform-specific effects of *APOE* on  $A\beta$ -induced neurodegeneration were also suggested *in vitro*, with *APOE3* and *APOE2*, but not *APOE4*, protecting hippocampal and cortical neurons from  $A\beta$ -induced neurotoxicity [40–42]. *APOE4* has also been shown to exacerbate neurodegeneration in the absence

of  $A\beta$ , instead operating through a tau-dependent mechanism [9].

Animal studies support an isoform-specific role for *APOE* in the loss of GABAergic interneurons [43,44]. Mice expressing human *APOE4* exhibited greater age-dependent loss of GAD67- and somatostatin-positive interneurons in the dentate gyrus compared to those expressing *APOE3*. Interestingly, loss of somatostatin immunoreactivity was exacerbated by *APOE4* in the AD brain [45]. The detrimental effects of *APOE4* on GABAergic interneurons was sex-dependent, only being observed in female mice [44]. This is interesting when considering *APOE4* confers greater AD risk in females and some effects of *APOE4* on regional brain atrophy are more prominent in females [16,18,21].

In summary, there is strong evidence that *APOE4* influences neuron loss in AD, however, there are some conflicting reports and future well-powered, rigorous studies in both human brain and animal models are needed to fully understand the age, sex and region-specific effects of *APOE* on neuron death.

#### *APOE*-related synaptic and dendritic degeneration in AD

Prior to the onset of neuronal loss in AD, extensive synapse loss and dendritic changes occur. These can be considered early neurodegenerative processes that contribute to synaptic and neuronal dysfunction, which pave the way for more generalized neurodegeneration later in the disease. In contrast to neuronal loss, synaptic and dendritic degeneration are dynamic processes, with the potential to be reversed if targeted early enough. Thus, it is important to consider the role of *APOE* in these changes.

Whether synapse loss associates with *APOE* genotype was the subject of a few studies identified by our search. Electron microscopy coupled with stereological counting in *post mortem* tissue identified AD-related loss of synapses in the dentate gyrus, stratum radiatum of the CA1 region of the hippocampus and lamina III of the inferior temporal gyrus. However, this was not related to *APOE* status [46–48]. These findings contrast with results from aged *APOE* mice, which suggested *APOE4* to be associated with a reduced number of synapses in the dentate gyrus [49]. Although not accounting for these discrepancies, it is worth noting that electron microscopy is limited by its ability to only



accelerated rates of hippocampal atrophy were associated with the *APOE4* allele [13,22,26–29], although this was not always observed [30,31]. *APOE4*-related atrophy was also observed in the parietal cortex [3,13] and some prefrontal areas [3,12], although again these were not consistently reported and may be related to the inclusion of younger AD patients in these studies.

Diffuse cerebral atrophy is a gross pathological feature of AD. Somewhat surprisingly, however, whole brain volume has been proposed to increase with increasing number of *APOE4* alleles in AD patients [19,32]. Greater *APOE4* allele dose was associated with larger volumes in the frontal lobes [11,17,20], although not always [12,14], which might potentially outweigh reductions in other brain regions and account for increased whole brain volume. Nonetheless, these studies indicate that the *APOE4* allele selectively influences the topography of regional brain atrophy, and thus neurodegeneration, in AD.

Studies of *post mortem* human AD brain have identified neuronal loss in vulnerable brain regions to be characteristic of AD. From our literature search, determining whether APOE influences this was less clear. In the nucleus basalis, *APOE4* was found to exacerbate neuronal loss [33], but have no impact in other studies [34,35]. These discrepancies may be due to the different methods employed in quantification of neuronal loss and groups studied. *APOE4* allele possession was also found to enhance neuronal loss in other subcortical structures [33,34], but have no effect on the CA1 region of the hippocampus or superior temporal sulcus [34,36].

*In vivo* and *in vitro* studies supported an association between *APOE4* and neuronal degeneration. In aged mice expressing human APOE, those expressing *APOE4* exhibited increased hippocampal and cortical atrophy compared to those expressing *APOE3* [37,38]. In *APOE4*, but not *APOE3* mice, activation of the amyloid cascade by inhibition of the A $\beta$  degrading enzyme neprilysin was sufficient to induce degeneration of hippocampal and entorhinal cortex neurons, suggestive of a specific effect of *APOE4* in exacerbating A $\beta$ -related neuronal loss [39]. Isoform-specific effects of APOE on A $\beta$ -induced neurodegeneration were also suggested *in vitro*, with *APOE3* and *APOE2*, but not *APOE4*, protecting hippocampal and cortical neurons from A $\beta$ -induced neurotoxicity [40–42]. *APOE4* has also been shown to exacerbate neurodegeneration in the absence

of A $\beta$ , instead operating through a tau-dependent mechanism [9].

Animal studies support an isoform-specific role for APOE in the loss of GABAergic interneurons [43,44]. Mice expressing human *APOE4* exhibited greater age-dependent loss of GAD67- and somatostatin-positive interneurons in the dentate gyrus compared to those expressing *APOE3*. Interestingly, loss of somatostatin immunoreactivity was exacerbated by *APOE4* in the AD brain [45]. The detrimental effects of *APOE4* on GABAergic interneurons was sex-dependent, only being observed in female mice [44]. This is interesting when considering *APOE4* confers greater AD risk in females and some effects of *APOE4* on regional brain atrophy are more prominent in females [16,18,21].

In summary, there is strong evidence that *APOE4* influences neuron loss in AD, however, there are some conflicting reports and future well-powered, rigorous studies in both human brain and animal models are needed to fully understand the age, sex and region-specific effects of APOE on neuron death.

#### *APOE*-related synaptic and dendritic degeneration in AD

Prior to the onset of neuronal loss in AD, extensive synapse loss and dendritic changes occur. These can be considered early neurodegenerative processes that contribute to synaptic and neuronal dysfunction, which pave the way for more generalized neurodegeneration later in the disease. In contrast to neuronal loss, synaptic and dendritic degeneration are dynamic processes, with the potential to be reversed if targeted early enough. Thus, it is important to consider the role of APOE in these changes.

Whether synapse loss associates with *APOE* genotype was the subject of a few studies identified by our search. Electron microscopy coupled with stereological counting in *post mortem* tissue identified AD-related loss of synapses in the dentate gyrus, stratum radiatum of the CA1 region of the hippocampus and lamina III of the inferior temporal gyrus. However, this was not related to *APOE* status [46–48]. These findings contrast with results from aged APOE mice, which suggested *APOE4* to be associated with a reduced number of synapses in the dentate gyrus [49]. Although not accounting for these discrepancies, it is worth noting that electron microscopy is limited by its ability to only

quantify synaptic changes in small areas of tissue. Thus, its use for characterizing changes in a disease that stereotypically results in widespread pathology may not be entirely representative.

In AD, loss of the presynaptic vesicle protein, synaptophysin, is evident in various brain regions. In *post mortem* studies, APOE genotype did not modulate synaptophysin levels in frontal or temporal regions [50,51] although a trend towards lower synaptophysin immunoreactivity was observed in AD patients with an APOE4 allele [50]. A further study of another presynaptic vesicle protein, Rab3a, also found no association of synapse loss with APOE genotype [52]. This contrasts with animal studies demonstrating that mice expressing human APOE4 alone or in concurrence with human amyloid precursor protein display increased age-dependent degeneration of synaptophysin-positive presynaptic terminals in the neocortex and hippocampus [53,54]. Preservation of synaptophysin-positive presynaptic terminals in aged APOE4 mice has also been reported, however, [55]. Contradictory results have also been reported in APOE KO mice, with both age-dependent reductions in synaptophysin-positive terminals [56] and no changes [57] observed.

Although the findings discussed thus far tend to suggest that APOE4 does not contribute to synaptic degeneration, it is important to consider that techniques used may not be optimal for quantification of synapses or synaptic protein loss, and that many of these studies did not consider plaque proximity in the analyses which is known to drive substantial local synapse loss as will be discussed below. The axial resolution of even confocal microscopy is not sufficient to resolve individual synapses in standard tissue sections. In addition, immunoblotting is inferior to techniques that yield absolute synaptic protein concentrations. Indeed, using ELISA, presynaptic protein levels were found to be reduced in AD patients with an APOE4 allele, although only a trend towards reduction was seen for synaptophysin [58].

A relatively recently described histological technique, array tomography, has been used to overcome some of the limitations associated with synapse quantification using other methods, offering a means for high-resolution characterization of synapses in *post mortem* tissue. In addition, this approach avoids some issues associated with electron microscopy in that thousands of synapses can be analysed. Using this technique, synapse density

was found to be specifically reduced within the 'halo' surrounding amyloid plaques. In both AD human *post mortem* tissue and a mouse model, this was isoform-specific, with APOE4 exacerbating peri-plaque synapse loss [59,60].

APOE4-related peri-plaque synapse loss affects both pre- and post-synapses [59] and greater age-induced reductions in post-synaptic proteins have been observed in AD mouse models expressing APOE4 compared to other isoforms [61]. Dendritic abnormalities, such as dystrophic neurites, alterations in dendrite complexity and loss of spines are widespread in AD. Considering that dendritic abnormalities are closely linked to synaptic dysfunction, and thus potentially synaptic degeneration, the effect of APOE here is relevant.

The presence of dystrophic neurites are a neuropathological hallmark of AD and are exacerbated by APOE4 in AD mouse models when compared to other isoforms [59]. Such changes in dendritic morphology are predicted to alter synaptic function, and thus may influence degeneration. Indeed, neuritic degeneration requires the presence of APOE [62], with APOE4 mice showing increased age-dependent loss of neocortical and hippocampal dendrites compared to APOE3 mice [53].

The density of dendritic spines, the post-synaptic site of over 90% of excitatory neurons, has consistently been shown to be reduced in the presence of APOE4 in cortex, hippocampus, entorhinal cortex and amygdala *in vitro* [63], *in vivo* [64–68] and in humans [68]. A reduction in dendrite length was also observed in APOE4 mice [66,67], which contributes to reduced connectivity. Interestingly, expression of APOE2 can rescue reduced spine density in AD mouse models [69]. The morphology of dendritic spines has also been suggested to be influenced by APOE, with APOE4 being associated with shorter spines and APOE2 with longer spines [64]. In addition, APOE may influence spine morphology such that APOE4 specifically reduces the number of spines associated with learning and memory [65]. Finally, APOE4 is associated with reductions in dendritic arborization and less complicated branching patterns, impacting on neuronal function [64,65,67].

Collectively, these studies suggest that, in the context of dendritic and synaptic changes, APOE4 is less effective at maintaining synaptic and neuronal integrity in disease-specific brain areas than other isoforms, which likely contributes to synaptic and neuronal degeneration.

### Mechanisms of APOE-related neurodegeneration

Dendritic, synaptic and neuronal degeneration are all influenced by APOE in an isoform-specific manner. However, the mechanisms by which APOE4 impacts neurodegeneration are not completely understood. Elucidating these mechanisms may enable the development of appropriate therapies, particularly in relation to APOE effects on synapses and dendrites, which have potential to be reversible.

*In vivo* and *in vitro* studies suggested that APOE4 may drive neurodegeneration through an A $\beta$ -dependent mechanism [37,39–42]. Recent revisions of the amyloid hypothesis of AD, have suggested soluble oligomeric forms of A $\beta$  (oA $\beta$ ) to be the effectors of A $\beta$ -induced degeneration, with APOE4 exacerbating oA $\beta$ -associated degeneration relative to other isoforms [41,42,70] (Figure 2) (details of participants in Figures 2–5 found in Table S4). APOE and oA $\beta$  may act intracellularly to enact this degeneration, with APOE uptake into neurons correlating with neuronal death and intracellular accumulation of soluble A $\beta$  [71]. APOE4-specific increases in intraneuronal oA $\beta$  have been suggested to drive neurodegeneration through

impairments of mitochondria and lysosomes [39,72], although the role of intracellular A $\beta$  remains hotly debated in the field. Isoform-specific interactions between APOE and the C-terminal domain of soluble A $\beta$ , or lack of in the case of APOE4, have also been suggested to influence the propensity for APOE4 to promote A $\beta$ -mediated neuronal death [42]. Moreover, protection against oA $\beta$ -mediated synaptic loss by APOE3 has been suggested to be mediated by a novel intracellular protein kinase C pathway, which is not activated by APOE4 [70].

APOE and oA $\beta$  may also act extracellularly to impact neurodegeneration. Interestingly, oligomeric forms of A $\beta$  are increased in the 'halo' surrounding plaques, an area where synaptic degeneration is exacerbated by APOE4 [59,60]. Mechanistically, APOE4 might exacerbate peri-plaque synapse loss by facilitating the association of oA $\beta$  with synapses where it is toxic, thus resulting in synapse loss [60].

While APOE certainly influences A $\beta$ -dependent neurodegeneration, it is becoming increasingly clear that there are other mechanisms by which APOE influences degeneration (Figure 3). For example, in mice expressing a form of mutant human tau associated with

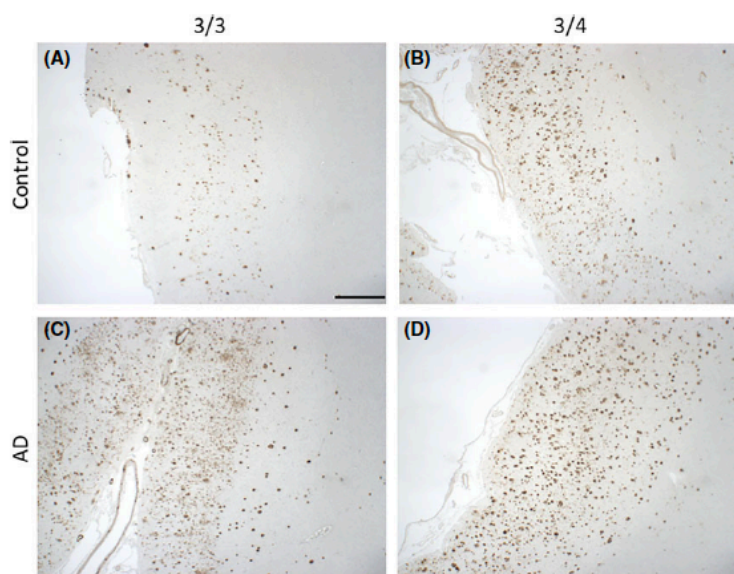


**Figure 2.** Amyloid- $\beta$  pathology in APOE3/3 and APOE3/4 carriers in normal ageing and AD. A $\beta$  plaque deposition is evident in aged controls (A) and is exacerbated in the presence of the APOE4 allele (B), resembling an AD-like phenotype. Both APOE3/3 and APOE3/4 AD cases (C and D, respectively) have substantial A $\beta$  deposition in all six layers of the cortex. Images taken from the grey matter of inferior temporal lobe (Brodmann area [BA] 20/21). Information about all participants donated tissue can be found in Table S4. A $\beta$  is stained with 6F/3D (mouse monoclonal, DAKO, M087201-2, 1:100, 98% formic acid, 5 minutes). Scale bar 1 mm.

frontotemporal dementia, co-expression of human APOE4 led to a drastic increase in neurodegeneration compared to that seen with other APOE isoforms. APOE was necessary for this tau-mediated neuronal death to occur [9], suggestive of APOE exerting a neurodegenerative effect through tau. APOE4 has also been shown to impair GABAergic interneurons through a tau-dependent mechanism *in vivo* [43]. Although known to be related to A $\beta$ , dysregulation of calcium homeostasis has also been implicated as a mechanism of APOE-related neurodegeneration, independent of A $\beta$ . Here, APOE4 increased levels of cytosolic calcium, an effect that was dose-dependently associated with cell death [73].

Another important consideration, and one that is often neglected, is the cellular source of APOE. Although primarily produced by glial cells, under conditions of stress or injury neurons also synthesize APOE [74]. Considering that the AD brain can be considered both a 'stressed' and 'injured' environment, the cellular source of APOE is likely to be relevant to its effect on neurodegeneration. Indeed, at the level of the dendrite,

loss of spines, reduced arborization and alterations in morphology were observed in mice expressing neuronal APOE4, but not astrocytic APOE4 [65,75]. This phenomenon has also been confirmed to occur at the level of the synapse, with only neuronal APOE4 promoting the degeneration of presynaptic terminals and cell death [75]. Consequently, the cellular source of APOE seems to impact upon its capacity to induce neurodegeneration. Further studies are needed to examine how neuronal and astrocytic APOE differ from one another, to characterize how these effects are mediated.

A potential mechanism by which neuronal APOE4 exerts increased neurotoxic effects may be due to the intraneuronal proteolytic processing of APOE, whereby APOE can be cleaved to generate C-terminally truncated fragments. In the human AD brain, these fragments are more numerous in individuals carrying an APOE4 allele. *In vitro*, APOE4 is more susceptible to proteolytic cleavage than APOE3 and, in mice, these APOE fragments are capable of eliciting AD-like neurodegeneration [76]. Further work has identified the lipid-binding region of APOE to be essential for

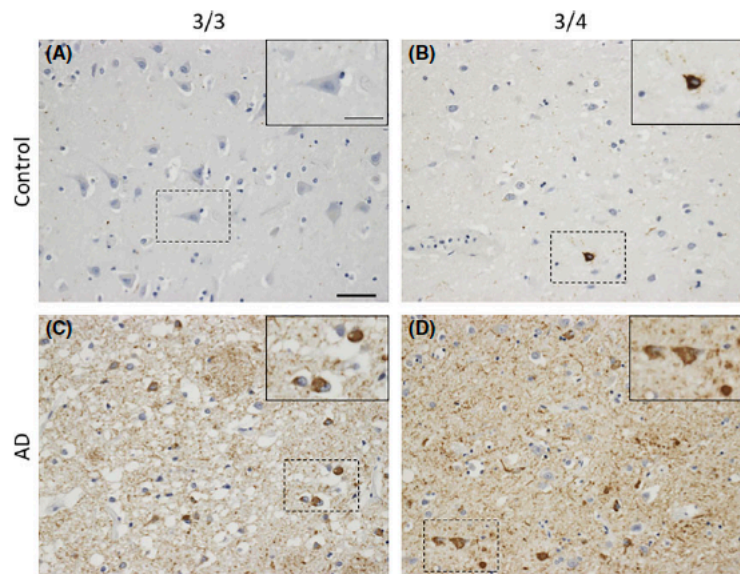


**Figure 3.** Tau pathology in APOE3/3 and APOE3/4 carriers in normal ageing and AD. In aged controls, phosphorylated tau species are absent in APOE 3/3 cases (A) and rarely found in APOE3/4 cases (B). In AD, both APOE3/3 (C) and APOE3/4 (D) have markedly increased numbers of tau-positive neurones. Images taken from the grey matter of inferior temporal lobe (BA20/21). Phosphorylated tau is stained with AT8 (mouse monoclonal, ThermoFisher, 1020, 1:2500). Scale bar 50  $\mu$ m, insert scale bar 25  $\mu$ m.

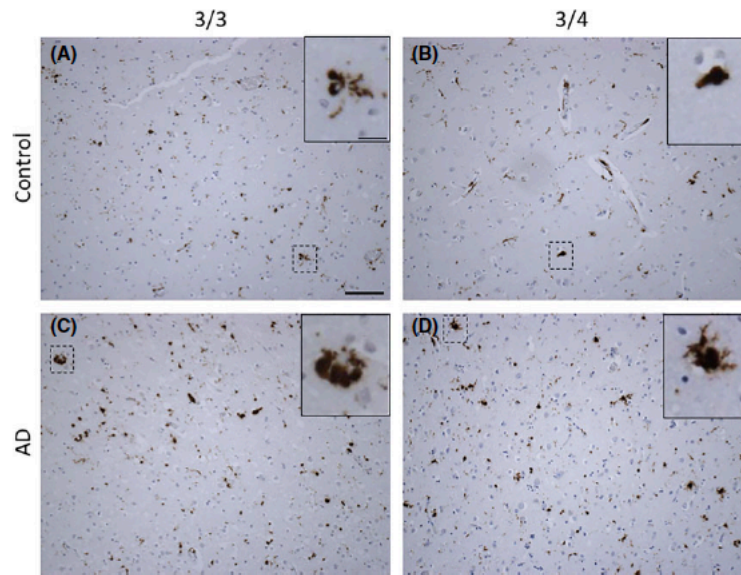


**Figure 4.** Activated microglia (CD68) in APOE3/3 and APOE3/4 carriers in normal ageing and AD. The lysosomal marker of microglia and macrophages, CD68, shown in AD (C-D) and age-matched control cases (A-B). Various microglial morphologies can be observed, for example, ramified (A and D) and amoeboid (B and C) in both ageing/AD and APOE3/x. Images taken from the grey matter of inferior temporal lobe (BA20/21). Microglia are stained with CD68 (mouse monoclonal, DAKO, M0876, 1:100, citric acid antigen retrieval). Scale bar 100  $\mu$ m, insert scale bar 25  $\mu$ m.

toxicity although not sufficient alone. Instead, the lipid- and receptor-binding regions appear to act in concert to mediate toxic effects [77]. APOE4 fragments have also been shown to interact synergistically with A $\beta$  and tau, exacerbating both pathologies and increasing the degree of neurodegeneration [43,78]. In relation to A $\beta$ , APOE4 fragments bind poorly to A $\beta$ , leading to reduced clearance and increased deposition [78], and these fragments also promote intraneuronal A $\beta$  accumulation [79]. In relation to tau, APOE fragments increase the degree of phosphorylation, likely exacerbating neurodegeneration [43]. Cleavage fragments of APOE may also exert neurodegenerative effects by increasing intracellular calcium [80], a mechanism that has previously been associated with full-length APOE4, as aforementioned, or by impairing mitochondrial function and integrity [77]. Finally, structural differences among APOE isoforms may also contribute to the more neurodegenerative phenotype associated with APOE4. Unlike APOE2 and APOE3, APOE4 exhibits a domain interaction, whereby a salt bridge mediates interaction between N- and C-terminal domains. Indeed, in mice, this domain interaction has been shown to be associated with pre-

and post-synaptic protein loss [81], thus suggesting another mechanism by which APOE4 might contribute to synaptic pathology and neurodegeneration.

APOE genotype may further contribute to synaptic degeneration, and subsequent neuronal degeneration, through its effects on dendrites. Dendritic changes are suggested to alter neuronal plasticity and regenerative capacity, leading to synaptic dysfunction and subsequent synapse and neuron loss. Indeed, more plastic changes are seen in the human AD brain in the absence of an APOE4 allele [33]. Various mechanisms have been proposed as to how APOE isoforms differentially regulate dendritic changes in AD. These range from altered binding of APOE to receptors and subsequent intracellular signalling cascades [82,83], impaired regulation of receptors within spines [63], elevations in calcineurin activity that is associated with reductions in spine density [84] and impairments of neuronal outgrowth [82], among others.

Overall, these results highlight the far-reaching and diverse biological effect APOE4 has on neurodegeneration in AD with particularly strong evidence supporting a role for APOE4 in synapse degeneration.

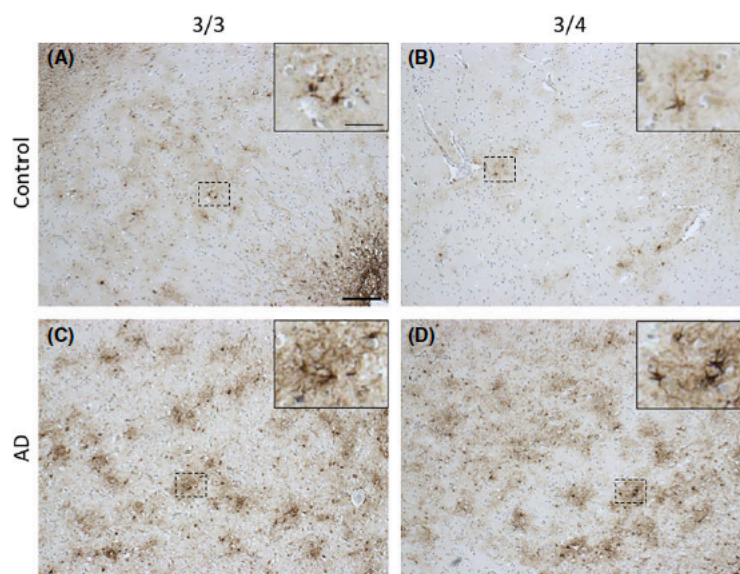


**Figure 5.** Activated astrocytes in APOE3/3 and APOE3/4 carriers in normal ageing and AD. Glial fibrillary acid protein (GFAP) is a cytoskeletal protein in activated astrocytes. Activated astrocytes are seen in both ageing (A–B) and AD (C–D), but more pronounced astroglial activation is observed in AD. In AD, astrocytes express more GFAP in the cell bodies, thus appearing darker, especially in APOE3/4 cases (D), and have more processes (C–D). Images taken from the grey matter of inferior temporal lobe (BA20/21). Astrocytes are stained with GFAP (rabbit polyclonal, DAKO, 0334, 1:800). Scale bar 200  $\mu\text{m}$ , insert scale bar 100  $\mu\text{m}$ .

#### APOE and inflammation

To determine whether there is evidence that APOE influences inflammation, search terms were used to identify papers containing both APOE and indicators of inflammation (papers from the systematic search that support a role for APOE in inflammation are coloured in green and orange in Table S1).

#### Increased glial activation and gliosis with APOE4

There is substantial reactive glial cell accumulation, termed gliosis, during AD which is enhanced in the presence of the APOE4 allele (Figures 4 and 5). Markers of glial activation are commonly used to reflect a variety of functional outcomes and to quantify the changes in glial numbers and their respective phenotype.

Human *post mortem* studies have quantified gliosis in different brain regions using multiple markers of activation. By immunophenotyping microglia in the frontal gyrus and correlating to APOE status in AD and control cases, markers of activation (CD68, Human

Leucocyte Antigen-DR isotype [HLA-DR], CD64) were found to be significantly associated with APOE4 carriers while APOE2 carriers were associated with higher levels of more homeostatic microglial markers (Iba1 and Macrophage Scavenger Receptor-A; MSR-A) and lower levels of the reactive ones [85]. Although the microglial phenotype was insufficient in predicting the APOE status in dementia, the elevated markers of phagocytosis, adaptive immune response and antigen recognition seen in APOE4 carriers point towards a more pathological environment. Other brain regions have been assessed for microglial levels, where in an APOE4 dose-dependent manner, there was extensive microgliosis in both the frontal and temporal cortices [86]. Similarly, there is elevated GFAP-positive astroglial activation in the grey matter of APOE4 AD patients compared to other APOE genotypes, and an overall greater astroglial activation between AD and age-matched control cases [87]. Interestingly, the APOE4 allele was associated with differences in GFAP burden in nondemented individuals, despite the increased plaque burden of nondemented aged APOE4 individuals, supporting the importance of glial cells in AD pathogenesis. As

always, the *post mortem* tissue only provides a snapshot of end-stage of disease, so we rely on mouse models for deciphering the mechanistic changes that APOE4 induces during AD.

Mouse studies looking at the effects of the human APOE allele with AD-like pathology have mostly replicated the gliosis data seen in human *post mortem* tissue. APOE4 mice crossed to the 5xFAD amyloidosis model showed increased microgliosis in deep cortical layers accompanied by a greater number of dystrophic microglial processes in the presence of the APOE4 allele, compared to APOE4 and APOE3 [88]. Of note, both APOE2 and APOE4 5xFAD mice had more A $\beta$ -associated microglia than APOE3 [88,89], suggesting that the APOE2 conformation may be protective not by preventing microglia/plaque interactions but by mediating more effective ways to respond to the plaques and making microglia more resistant to amyloid toxicity. These changes were not observed in the subiculum of these mice, reiterating regional differences in microglia. Furthermore, when APOE knock-in mice were crossed to a tauopathy model (P301S), CD68-positive microglial burdens in the hippocampus and entorhinal/piriform cortex were markedly increased in APOE4 mice compared APOE3 and APOE knock-out mice in a tau pathology mediated manner [9]. The same effect was also observed with GFAP immunoreactivity, further establishing an aberrant glial response to AD-like pathology in combination to the presence of the APOE4 allele. Similarly, there was neurodegeneration-associated microgliosis and astrogliosis in the hippocampus of APOE4 mice, compared to APOE3, but no differences were found in the septum [90]. However, in the hippocampus of APOE4 LPS-injected mice there was marked microgliosis although astrogliosis was found in the APOE3 mice [91]. In summary, in APOE4 amyloidosis (5xFAD) and tauopathy (P301S) mouse models there was exacerbated gliosis. Although, there was important regional variability, taken together these data strongly support a role for APOE4 in promoting inflammatory changes in microglia and astrocytes.

The precise mechanisms by which reactive gliosis is established in the APOE4 AD brain is unknown, but a key question that remains is whether this gliosis is a driver of the disease, accounting for the earlier onset and worse prognosis APOE4 carriers face, or a by-product of the exacerbated amyloid and tau pathology. To answer these questions, the inflammatory capacity of

glial cells and their transcriptomic signatures in the presence of the APOE4 are being currently assessed.

#### **ApoE-related glial transcriptional changes**

Transcriptional studies are becoming increasingly popular in the microglia and neuroinflammation field, with *ApoE* upregulation consistently being a top hit in AD-like mouse models. The advantages of RNA-sequencing are a nonbiased, high-yield output of all transcriptional changes as well as the ability to use these long data sets to investigate biological pathways. As such, this process speeds up the identification of genetic and molecular pathways involved in AD pathogenesis and ways they can be therapeutically targeted.

Recently, microglial *ApoE* mRNA transcript levels were quantified in two models of AD-like pathology (amyloidosis and tauopathy) and ageing [92]. Its high abundance in all conditions supports a role for APOE as a key part of the microglial signature, despite its expression not being restricted to microglial cells. In terms of its relative expression, *ApoE* was highly upregulated in ageing and disease models, with ageing female mice showing a marked increase. Pathway analysis puts APOE as the driver of a network whose downstream effectors are also highly upregulated in these models, like the chemoattractant CCL3, whose relevance to neuroinflammation will be discussed in the next section of this review.

*ApoE* transcription is also downstream of the activation of a microglial receptor TREM2 (Triggering Receptor Expressed on Myeloid cells 2), another AD risk gene [93]. This APOE activation pathway results in a more pro-inflammatory microglial response and a degenerative phenotype, as seen in the AD brain. Microglial and astrocytic pro-inflammatory genes were also profoundly upregulated in APOE4 knock-in mice crossed with a tauopathy model (P301S), compared to APOE3 [9]. Conversely, APOE knock-out/P301S mice showed attenuation of this impaired pro-inflammatory profile, highlighting APOE as a master regulator of glial inflammatory response with its APOE4 allele being associated to a pro-degeneration phenotype.

Single-cell RNA sequencing takes this a step further by identifying and characterizing clusters of subpopulations within a cell type, for instance disease-associated microglia (DAMs) [94]. Specifically, *ApoE* is upregulated early in DAMs of the 5xFAD AD-like model, even in

the absence of TREM2. A TREM2 independent pathway is thus proposed to initiate *Apoe* upregulation in the early phase of AD, with a later TREM2-dependent pathway activating *Apoe* transcription which induces neurodegenerative microglia. This potentially forms a therapeutic window where preventing the second *Apoe* induction via TREM2 may protect against the exacerbated inflammation and degeneration caused by microglia. Understanding the ways in which TREM2 is activated in the AD brain and the effectors mediating this TREM2-APOE pathway can provide new ways to halt AD progression and hinder neuroinflammation.

Human induced pluripotent stem cells (iPSCs) derived from AD patients were recently transcriptionally characterized after directing them towards a microglial-like lineage [95]. Importantly, the microglia-like cells were engineered with Crispr-Cas9 to correct APOE4 into APOE3. Not only did this result in attenuation of AD-associated morphological and transcriptional signatures, but immune-related genes were also upregulated.

Overall, *Apoe* is consistently one of the most upregulated genes in transcriptomic studies of microglia in AD-like models. Nevertheless, a limitation of transcriptomics involves the isolation process which pushes microglia into an activated phenotype [92]. There is a lack of detailed studies of human *post mortem* tissue profiling transcription in cases with different APOE genotypes, which will be needed to confirm the translational relevance of mouse studies. As this is still at the transcriptional level, studies looking a more functional level are imperative to understand how these RNA changes relate to disease.

#### Altered inflammatory response by glial cytokine release

Innate and adaptive immune cells respond to environmental stimuli by releasing signalling cytokines and chemokines. Our systematic literature search showed that the process of cytokine release by glia to maintain homeostasis and respond to damage is dysfunctional in the ageing and AD brain [96], with substantial evidence pointing towards the *APOE4* allele playing a crucial role in this [97–99], supporting the transcriptional profile changes seen in  $\epsilon 4$  microglia and astrocytes.

APOE4 alters the baseline pro-inflammatory response even in the absence of disease. Addition of

APOE4, but not APOE3 protein, to rat microglia cultures alone stimulated the secretion of prostaglandin E2 (PGE2), interleukin-1 $\beta$  (IL-1 $\beta$ ), and nitric oxide (NO) [100–103]. On the other hand, microglial and astrocyte stimulation with APOE4 and A $\beta$  attenuated the production of inflammatory mediators [103–105], indicating a more complex interaction of microglia, APOE, and A $\beta$  *in vivo*. A physiological concentration of A $\beta$  may therefore be beneficial to glial functioning by interacting with APOE.

LPS-activated microglia and astrocytes are a well-characterized model of glial activation by mimicking the inflammation seen in AD. Microglia induced with LPS in the APOE4 background released greater amounts of pro-inflammatory cytokines, like tumour necrosis factor- $\alpha$  (TNF- $\alpha$ ), IL-1 $\beta$ , and interleukin-6 (IL-6) [106], an effect replicated in AD-like models [88,107]. Simultaneously, APOE4 treated LPS-induced microglia suppressed the production of TNF- $\alpha$  less than the APOE3 and APOE2 isoforms [108] while APOE-/- mice secrete lower levels of anti-inflammatory cytokines [109], showing a physiological role of APOE in modulating inflammation. Indeed, knocking out murine *Apoe* increases glial production of nitric oxide (NO) [110] and other inflammatory mediators, like TNF- $\alpha$ , IL-1 $\beta$  and IL-6 transcripts in the CNS [111]. Murine *Apoe* is therefore required to suppress glial-mediated inflammation providing a physiological role in CNS homeostasis, which is disrupted in AD, potentially in an age-dependent manner. This evidence points to APOE4 expressing microglia being both more pro-inflammatory and less anti-inflammatory at the same time.

In contrast to the microglial data, astrocytes from APOE2 and APOE3 animals treated with LPS produced more of these pro-inflammatory cytokines than the APOE4 counterparts (IL-1 $\beta$ , TNF- $\alpha$ , and IL-6) [112]. APOE4 astrocytes also produce more CCL3 (chemokine C-C motif ligand 3) [113], similar to microglial *Ccl3* mRNA upregulation in AD-like models [92], which is downstream of the APOE-driven network while APOE-/- mice produce less CCL3 [109]. Despite the increase in CCL3, the chemoattraction ability of microglia is impaired in the presence of the *APOE4* allele, as they are less migratory and receptive to immune sensing [114–116]. Data so far suggest that APOE4 confers a more pro-inflammatory and less anti-inflammatory phenotype in microglia, with an opposing pattern in astrocytes.



### APOE at the interface of inflammation and neurodegeneration: glial-mediated synapse loss

The synaptic loss during the early phase of AD is now thought to be partly due to aberrant microglial and astrocyte complement-mediated phagocytosis [117,118]. Given APOE's role in synapse loss and inflammation, we postulate that the APOE4 genotype is implicated in synaptic loss through a glial-mediated mechanism (Figure 6).

LPS intracerebral injections in APOE4 mice led to decreased pre- and post-synaptic protein levels as well hippocampal gliosis and pro-inflammatory cytokine release [119]. Moreover, APOE4 is accompanied by greater complement activation [120], which is the proposed synaptic tag for synaptic clearance. Still, this evidence is correlative and there are other mediators than could affect synaptic loss. In development, astrocytes of the APOE4 background were less phagocytic towards pHrodo-labelled synaptosomes than those of APOE3 and APOE2 [121], leading to the hypothesis that some synapses are not pruned by APOE4 astrocytes, accumulating complement and making them more vulnerable in AD. Whether these synapses are

defective or not is a key question, as loss of healthy synapses with accumulated complement would explain the initial synapse loss in AD, and the earlier onset of APOE4 carriers.

Although a lot more evidence is required, particularly from the human perspective, to understand if and how glial cells drive the synapse loss during AD, understanding why APOE e4 carriers at greatest risk have this extensive synapse loss and greater onset will be crucial to tailor therapies for individuals of this genotype.

### Potential role for spread of pathological proteins through the brain

No studies were found in the systematic search that specifically investigated the role of APOE in pathological protein spread. Two of the current hypotheses about the spread of tau through the brain are that tau spreads trans-synaptically and that microglia eat tau-containing synapses facilitating its spread (Figure 7). Interestingly, in this review, APOE genotype is shown to affect both tau and microglia in multiple ways,

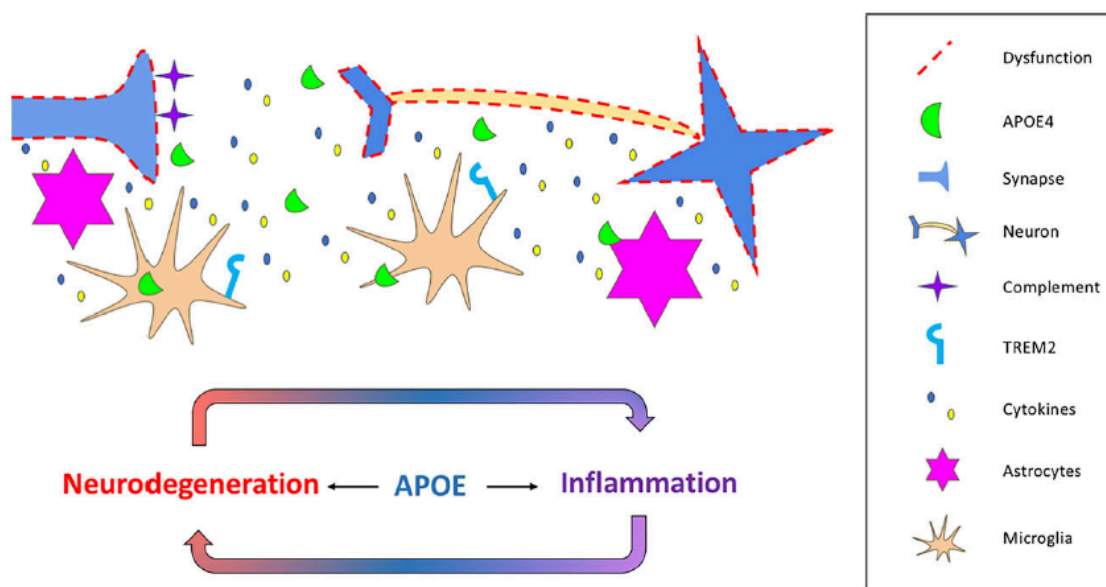


**Figure 6.** APOE at the interface of inflammation and neurodegeneration via glial-mediated mechanisms. Microglia and astrocytes expressing APOE4 promote parenchymal gliosis and release pro-inflammatory signals that are potentially associated with synaptic and neuronal loss. The paracrine signalling of microglial mediators along with the APOE-TREM2 pathway induces a pro-inflammatory phenotype, creating a vicious-cycle of inflammation and neurodegeneration. Ineffective clearance of excess synapses by astrocytes in APOE4 mice allows accumulating levels of C1q that can act as a tag for synaptic elimination later in life.

implicating APOE4 as a potential facilitator of misfolded proteins spreading between brain regions.

**Conclusion**

Our systematic literature search revealed strong links between APOE and synapse degeneration, which is further supported by relevant literature that did not fall into our search terms. The impaired phagocytic capacity of TREM2-/- microglia for synapses and synaptosomes in development [122] highlights yet again the TREM2/APOE pathway as a potential AD-related mechanism of synaptic elimination. The interplay between glia cell types in relation to APOE genotype is also a new avenue to be assessed considering that astrocytic IL-33 induces microglial synaptic engulfment of both excitatory and inhibitory synapses [123]. Conversely, microglia have been shown to induce a neurotoxic astrocyte phenotype via IL-1 $\alpha$ , C1q, and TNF [124], the two latter being increased with APOE4 expression. Moreover, APOE4-elevated soluble factors released by

microglia like NO and IL-6 can induce synapse loss in neurone culture systems [125], suggesting microglia may alter synaptic numbers both by phagocytosis and their secretome.

In studies identified by our systematic search, APOE4 was consistently associated with increased neurodegeneration within the medial temporal lobe; this region includes the entorhinal cortex, where tau pathology begins [126]. APOE4-associated degenerating synapses may release tau seeds via exosomes, stress-produced nanotubes [127], or passively as terminals degenerate. These may be taken up by recipient cells therefore propagating tau trans-synaptically. However, our recent data indicate that presynaptic terminal degeneration is not necessary for the spread of tau through neural circuits [128], making it important to investigate other mechanisms of pathological protein spread.

Microglia have also been suggested to mediate tau spread [129]. The exacerbated neurodegeneration in APOE4 likely induces microglia and astrocytes to phagocytose degenerating tau-containing synapses and

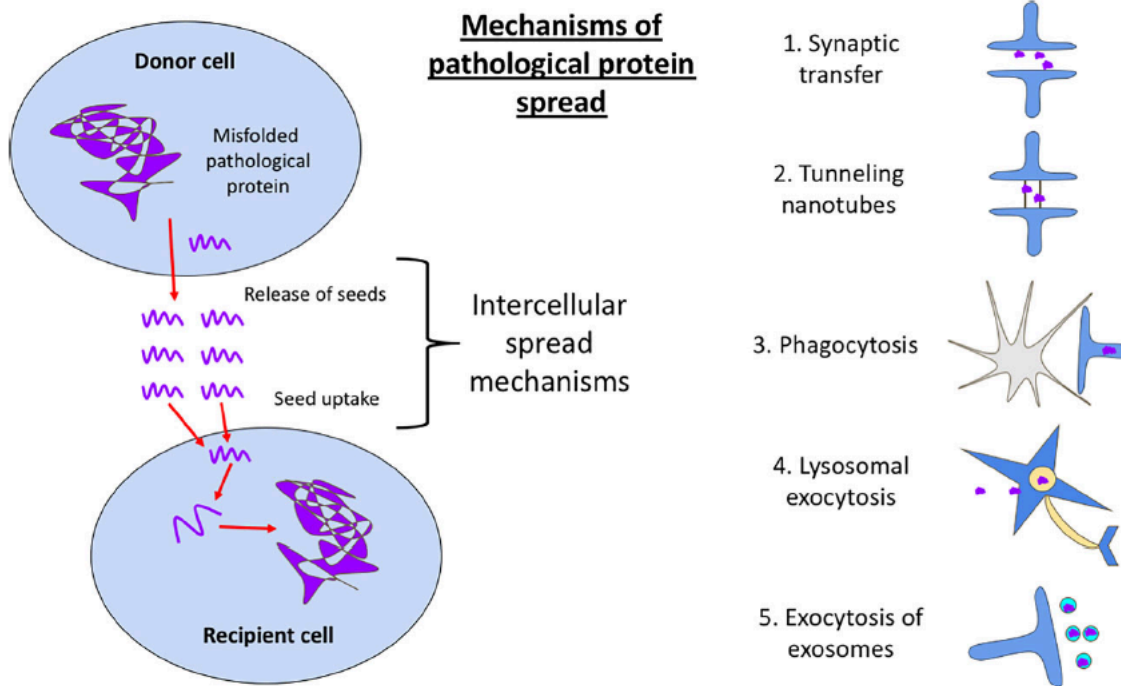


**Figure 7.** Schematic diagram of pathological protein spread. While direct evidence for APOE influencing the spread of tau through the brain is lacking, the papers in our systematic literature search implicate APOE in many processes that could influence spread. These include synaptic transfer through the synaptic cleft (1), via nanotubes (2), by glial phagocytosis (3) or vesicular secretion (4 & 5).

neurones. Exosomes synthesized from these microglia, containing synaptic-impairing micro-RNA [130] and tau seeds, may propagate tau pathology and neurodegeneration [131]. Astrocytes may also be involved in this, given their role in  $\alpha$ -synuclein transfer via tunnelling nanotubes in Parkinson's disease [132].

APOE, therefore, is potentially at the interface of inflammation, neurodegeneration, and the pathological protein spread (summarized in Figures 6 and 7). Tau pathology and synapse loss are the strongest correlates with cognitive impairments [133]; therefore, preventing these processes could have significant impact on disease progression. Further evidence is, however, needed to directly link APOE to these spreading mechanisms.

Our systematic literature search and review of the resulting papers highlights the need for multiple approaches to understand the complex role of APOE in disease, as has been observed recently for many fields in science [134]. Many findings remain contradictory and will need further support and investigation using different model systems to warrant moving forward to therapies targeting APOE. These caveats notwithstanding, our review of the literature supports the idea that understanding how APOE influences multiple pathological features of AD will be important for developing effective therapeutics to prevent or treat the disease. Currently, there is debate as to whether lowering or increasing levels of APOE will be beneficial in treating AD. Increasing astrocytic APOE levels can help displace synaptic A $\beta$  [135] and prevent subsequent synaptotoxicity. Such interventions, with the recent example of Bexarotene, have had mixed outcomes in mouse models of AD [136–139] and no direct benefits so far in human trials [140]. In contrast, lowering levels of APOE4 and increasing levels of APOE2 [59] and APOE3 [141], or decreasing total APOE [142] are promising alternative avenues for maintaining brain resilience and synaptic integrity.

### Acknowledgements

We wish to thank our human brain tissue donors and their families for their valuable contributions to this work. We also thank Marshall Dozier and Malcom McLeod from CAMARADES for their advice on the systematic search. This work was funded by the UK Dementia Research Institute, the European Research Council (ALZSYN), Alzheimer's Research UK and the

Scottish Government Chief Scientist Office, the Wellcome Trust, and Alzheimer's Society. TSJ gratefully acknowledges affiliations with the FENS-Kavli Network of Excellence, the Centre for Dementia Prevention, the Euan MacDonald Centre, and Edinburgh Neuroscience. The two control participants were from the Lothian Birth Cohort 1936, thus, we wish to thank the cohort and research team supported by Age UK (Disconnected Mind project) in The University of Edinburgh Centre for Cognitive Ageing and Cognitive Epidemiology, funded by the Biotechnology and Biological Sciences Research Council (BBSRC) and Medical Research Council (MRC) ((MR/K026992/1).

### Author contributions

MT – design of systematic search, paper screening, writing paper, staining and imaging tissue, revising paper. CD – design of systematic search, paper screening, writing paper, revising paper. AN – design of systematic search, paper screening, writing paper. RJJ – writing paper, revising paper. TS-J – design of systematic search, writing paper, revising paper.

### Ethics

Use of human tissue for *post mortem* studies has been reviewed and approved by the Edinburgh Brain Bank ethics committee and the ACCORD medical research ethics committee, AMREC (approval number 15-HV-016; ACCORD is the Academic and Clinical Central Office for Research and Development, a joint office of the University of Edinburgh and NHS Lothian). The Edinburgh Brain Bank is a Medical Research Council funded facility with research ethics committee (REC) approval (11/ES/0022). Tissue from four donors was used for this study and their details are found in supplementary information.

### Disclosures

Authors declare no conflicts of interest.

### References

- 1 Corder EH, Saunders AM, Strittmatter WJ, Schmechel DE, Gaskell PC, Small GW, *et al.* Gene dose of apolipoprotein E type 4 allele and the risk of

- Alzheimer's disease in late onset families. *Science* 1993; 261: 921–3
- 2 Li YJ, Hauser MA, Scott WK, Martin ER, Booze MW, Qin XJ, *et al.* Apolipoprotein E controls the risk and age at onset of Parkinson disease. *Neurology* 2004; 62: 2005–9
  - 3 Agosta F, Vessel KA, Miller BL, Migliaccio R, Bonasera SJ, Filippi M, *et al.* Apolipoprotein E epsilon4 is associated with disease-specific effects on brain atrophy in Alzheimer's disease and frontotemporal dementia. *Proc Natl Acad Sci USA* 2009; 106: 2018–22
  - 4 Huynh T-PV, Davis AA, Ulrich JD, Holtzman DM. Apolipoprotein E and Alzheimer's disease: the influence of apolipoprotein E on amyloid- $\beta$  and other amyloidogenic proteins. *J Lipid Res* 2017; 58: 824–36
  - 5 Deary IJ, Whiteman MC, Pattie A, Starr JM, Hayward C, Wright AF, *et al.* Apolipoprotein e gene variability and cognitive functions at age 79: a follow-up of the Scottish mental survey of 1932. *Psychol Aging* 2004; 19: 367–71
  - 6 Rebeck GW, Reiter JS, Strickland DK, Hyman BT. Apolipoprotein E in sporadic Alzheimer's disease: allelic variation and receptor interactions. *Neuron* 1993; 11: 575–80
  - 7 Liu C-C, Liu C-C, Kanekiyo T, Xu H, Bu G. Apolipoprotein E and Alzheimer disease: risk, mechanisms and therapy. *Nat Rev Neurol* 2013; 9: 106–18
  - 8 De Strooper B, Karran E. The cellular phase of Alzheimer's disease. *Cell* 2016; 164: 603–15
  - 9 Shi Y, Yamada K, Liddel SA, Smith ST, Zhao L, Luo W, *et al.* ApoE4 markedly exacerbates tau-mediated neurodegeneration in a mouse model of tauopathy. *Nature* 2017; 549: 523–7
  - 10 Moher D, Liberati A, Tetzlaff J, Altman DG, PRISMA Group. Preferred reporting items for systematic reviews and meta-analyses: the PRISMA statement. *PLoS Med* 2009; 6: e1000097
  - 11 Boccardi M, Sabatoli F, Testa C, Beltramello A, Soininen H, Frisoni GB. APOE and modulation of Alzheimer's and frontotemporal dementia. *Neurosci Lett* 2004; 356: 167–70
  - 12 Filippini N, Rao A, Wetten S, Gibson RA, Borrie M, Guzman D, *et al.* Anatomically-distinct genetic associations of APOE epsilon4 allele load with regional cortical atrophy in Alzheimer's disease. *NeuroImage* 2009; 44: 724–8
  - 13 Gispert JD, Rami L, Sánchez-Benavides G, Falcon C, Tucholka A, Rojas S, *et al.* Nonlinear cerebral atrophy patterns across the Alzheimer's disease continuum: impact of APOE4 genotype. *Neurobiol Aging* 2015; 36: 2687–701
  - 14 Lehtovirta M, Laakso MP, Soininen H, Helisalmi S, Mannermaa A, Helkala EL, *et al.* Volumes of hippocampus, amygdala and frontal lobe in Alzheimer patients with different apolipoprotein E genotypes. *Neuroscience* 1995; 67: 65–72
  - 15 Lehtovirta M, Soininen H, Laakso MP, Partanen K, Helisalmi S, Mannermaa A, *et al.* SPECT and MRI analysis in Alzheimer's disease: relation to apolipoprotein E epsilon 4 allele. *J Neurol Neurosurg Psychiatry* 1996; 60: 644–9
  - 16 Lupton MK, Strike L, Hansell NK, Wen W, Mather KA, Armstrong NJ, *et al.* The effect of increased genetic risk for Alzheimer's disease on hippocampal and amygdala volume. *Neurobiol Aging* 2016; 40: 68–77
  - 17 Geroldi C, Pihlajamäki M, Laakso MP, DeCarli C, Beltramello A, Bianchetti A, *et al.* APOE-epsilon4 is associated with less frontal and more medial temporal lobe atrophy in AD. *Neurology* 1999; 53: 1825–32
  - 18 Juottonen K, Lehtovirta M, Helisalmi S, Riekkinen PJ, Soininen H. Major decrease in the volume of the entorhinal cortex in patients with Alzheimer's disease carrying the apolipoprotein E epsilon4 allele. *J Neurol Neurosurg Psychiatry* 1998; 65: 322–7
  - 19 Hashimoto M, Yasuda M, Tanimukai S, Matsui M, Hirono N, Kazui H, *et al.* Apolipoprotein E epsilon 4 and the pattern of regional brain atrophy in Alzheimer's disease. *Neurology* 2001; 57: 1461–6
  - 20 Wolk DA, Dickerson BC, Alzheimer's Disease Neuroimaging Initiative. Apolipoprotein E (APOE) genotype has dissociable effects on memory and attentional-executive network function in Alzheimer's disease. *Proc Natl Acad Sci USA* 2010; 107: 10256–61
  - 21 Liu Y, Paajanen T, Westman E, Wahlund L-O, Simmons A, Tunnard C, *et al.* Effect of APOE  $\epsilon$ 4 allele on cortical thicknesses and volumes: the AddNeuroMed study. *J Alzheimers Dis* 2010; 21: 947–66
  - 22 Manning EN, Barnes J, Cash DM, Bartlett JW, Leung KK, Ourselin S, *et al.* APOE  $\epsilon$ 4 is associated with disproportionate progressive hippocampal atrophy in AD. *PLoS ONE* 2014; 9: e97608
  - 23 Susanto TAK, Pua EPK, Zhou J, Alzheimer's Disease Neuroimaging Initiative. Cognition, brain atrophy, and cerebrospinal fluid biomarkers changes from pre-clinical to dementia stage of Alzheimer's disease and the influence of apolipoprotein e. *J Alzheimers Dis* 2015; 45: 253–68
  - 24 Jack CR, Petersen RC, Xu YC, O'Brien PC, Waring SC, Tangalos EG, *et al.* Hippocampal atrophy and apolipoprotein E genotype are independently associated with Alzheimer's disease. *Ann Neurol* 1998; 43: 303–10
  - 25 Drzezga A, Grimmer T, Henriksen G, Mühlau M, Perneczky R, Miederer I, *et al.* Effect of APOE genotype on amyloid plaque load and gray matter volume in Alzheimer disease. *Neurology* 2009; 72: 1487–94
  - 26 Mori E, Lee K, Yasuda M, Hashimoto M, Kazui H, Hirono N, *et al.* Accelerated hippocampal atrophy in Alzheimer's disease with apolipoprotein E epsilon4 allele. *Ann Neurol* 2002; 51: 209–14
  - 27 Schuff N, Woerner N, Boreta L, Kornfield T, Shaw LM, Trojanowski JQ, *et al.* MRI of hippocampal

- volume loss in early Alzheimer's disease in relation to ApoE genotype and biomarkers. *Brain* 2009; 132: 1067–77
- 28 Lo RY, Hubbard AE, Shaw LM, Trojanowski JQ, Petersen RC, Aisen PS, et al. Longitudinal change of biomarkers in cognitive decline. *Arch Neurol* 2011; 68: 1257–66
  - 29 Risacher SL, Shen L, West JD, Kim S, McDonald BC, Beckett LA, et al. Longitudinal MRI atrophy biomarkers: relationship to conversion in the ADNI cohort. *Neurobiol Aging* 2010; 31: 1401–18
  - 30 Jack CR, Petersen RC, Xu Y, O'Brien PC, Smith GE, Ivnik RJ, et al. Rate of medial temporal lobe atrophy in typical aging and Alzheimer's disease. *Neurology* 1998; 51: 993–9
  - 31 Laakso MP, Frisoni GB, Könönen M, Mikkonen M, Beltramello A, Geroldi C, et al. Hippocampus and entorhinal cortex in frontotemporal dementia and Alzheimer's disease: a morphometric MRI study. *Biol Psychiatry* 2000; 47: 1056–63
  - 32 Yasuda M, Mori E, Kitagaki H, Yamashita H, Hirono N, Shimada K, et al. Apolipoprotein E epsilon 4 allele and whole brain atrophy in late-onset Alzheimer's disease. *Am J Psychiatry* 1998; 155: 779–84
  - 33 Arendt T, Schindler C, Brückner MK, Eschrich K, Bigl V, Zedlick D, et al. Plastic neuronal remodeling is impaired in patients with Alzheimer's disease carrying apolipoprotein epsilon 4 allele. *J Neurosci* 1997; 17: 516–29
  - 34 Camicioli R, Kaye J, Payami H, Ball MJ, Murdoch G. Apolipoprotein E epsilon4 is associated with neuronal loss in the substantia nigra in Alzheimer's disease. *Dement Geriatr Cogn Disord* 1999; 10: 437–41
  - 35 Gilmore ML, Erickson JD, Varoqui H, Hersh LB, Bennett DA, Cochran EJ, et al. Preservation of nucleus basalis neurons containing choline acetyltransferase and the vesicular acetylcholine transporter in the elderly with mild cognitive impairment and early Alzheimer's disease. *J Comp Neurol* 1999; 411: 693–704
  - 36 Gómez-Isla T, Hollister R, West H, Mui S, Growdon JH, Petersen RC, et al. Neuronal loss correlates with but exceeds neurofibrillary tangles in Alzheimer's disease. *Ann Neurol* 1997; 41: 17–24
  - 37 Yin J, Turner G, Coons S, Maalouf M, Reiman E, Shi J. Association of amyloid burden, brain atrophy and memory deficits in aged apolipoprotein ε4 mice. *Curr Alzheimer Res* 2014; 11: 283–90
  - 38 Buttini M, Akeefe H, Lin C, Mahley RW, Pitas RE, Wyss-Coray T, et al. Dominant negative effects of apolipoprotein E4 revealed in transgenic models of neurodegenerative disease. *Neuroscience* 2000; 97: 207–10
  - 39 Belinson H, Lev D, Masliah E, Michaelson DM. Activation of the amyloid cascade in apolipoprotein E4 transgenic mice induces lysosomal activation and neurodegeneration resulting in marked cognitive deficits. *J Neurosci* 2008; 28: 4690–701
  - 40 Jordán J, Galindo MF, Miller RJ, Reardon CA, Getz GS, LaDu MJ. Isoform-specific effect of apolipoprotein E on cell survival and beta-amyloid-induced toxicity in rat hippocampal pyramidal neuronal cultures. *J Neurosci* 1998; 18: 195–204
  - 41 Manelli AM, Bullfinch LC, Sullivan PM, LaDu MJ. Abeta42 neurotoxicity in primary co-cultures: effect of apoE isoform and Abeta conformation. *Neurobiol Aging* 2007; 28: 1139–47
  - 42 Drouet B, Fifre A, Pinçon-Raymond M, Vandekerckhove J, Rosseneu M, Guéant JL, et al. ApoE protects cortical neurones against neurotoxicity induced by the non-fibrillar C-terminal domain of the amyloid-beta peptide. *J Neurochem* 2001; 76: 117–27
  - 43 Andrews-Zwilling Y, Bien-Ly N, Xu Q, Li G, Bernardo A, Yoon SY, et al. Apolipoprotein E4 causes age- and Tau-dependent impairment of GABAergic interneurons, leading to learning and memory deficits in mice. *J Neurosci* 2010; 30: 13707–17
  - 44 Leung L, Andrews-Zwilling Y, Yoon SY, Jain S, Ring K, Dai J, et al. Apolipoprotein E4 causes age- and sex-dependent impairments of hilar GABAergic interneurons and learning and memory deficits in mice. *PLoS ONE* 2012; 7: e33569
  - 45 Grouselle D, Winsky-Sommerer R, David JP, Delacourte A, Dournaud P, Epelbaum J. Loss of somatostatin-like immunoreactivity in the frontal cortex of Alzheimer patients carrying the apolipoprotein epsilon 4 allele. *Neurosci Lett* 1998; 255: 21–4
  - 46 Scheff SW, Price DA, Schmitt FA, Mufson EJ. Hippocampal synaptic loss in early Alzheimer's disease and mild cognitive impairment. *Neurobiol Aging* 2006; 27: 1372–84
  - 47 Scheff SW, Price DA, Schmitt FA, DeKosky ST, Mufson EJ. Synaptic alterations in CA1 in mild Alzheimer disease and mild cognitive impairment. *Neurology* 2007; 68: 1501–8
  - 48 Scheff SW, Price DA, Schmitt FA, Scheff MA, Mufson EJ. Synaptic loss in the inferior temporal gyrus in mild cognitive impairment and Alzheimer's disease. *J Alzheimers Dis* 2011; 24: 547–57
  - 49 Cambon K, Davies HA, Stewart MG. Synaptic loss is accompanied by an increase in synaptic area in the dentate gyrus of aged human apolipoprotein E4 transgenic mice. *Neuroscience* 2000; 97: 685–92
  - 50 Heinonen O. Alzheimer pathology of patients carrying apolipoprotein E ε4 allele. *Neurobiol Aging* 1995; 16: 505–13
  - 51 Corey-Bloom J, Tiraboschi P, Hansen LA, Alford M, Schoos B, Sabbagh MN, et al. E4 allele dosage does not predict cholinergic activity or synapse loss in Alzheimer's disease. *Neurology* 2000; 54: 403–6
  - 52 Blennow K, Bogdanovic N, Alafuzoff I, Ekman R, Davidsson P. Synaptic pathology in Alzheimer's disease: relation to severity of dementia, but not to

- senile plaques, neurofibrillary tangles, or the ApoE4 allele. *J Neural Transm* 1996; 103: 603–18
- 53 Buttini M, Orth M, Bellosta S, Akeefe H, Pitas RE, Wyss-Coray T, *et al.* Expression of human apolipoprotein E3 or E4 in the brains of Apoe<sup>-/-</sup> mice: isoform-specific effects on neurodegeneration. *J Neurosci* 1999; 19: 4867–80
- 54 Buttini M, Yu G-Q, Shockley K, Huang Y, Jones B, Masliah E, *et al.* Modulation of Alzheimer-like synaptic and cholinergic deficits in transgenic mice by human apolipoprotein E depends on isoform, aging, and overexpression of amyloid beta peptides but not on plaque formation. *J Neurosci* 2002; 22: 10539–48
- 55 Veinbergs I, Mallory M, Mante M, Rockenstein E, Gilbert JR, Masliah E. Differential neurotrophic effects of apolipoprotein E in aged transgenic mice. *Neurosci Lett* 1999; 265: 218–22
- 56 Masliah E, Mallory M, Ge N, Alford M, Veinbergs I, Roses AD. Neurodegeneration in the central nervous system of apoE-deficient mice. *Exp Neurol* 1995; 136: 107–22
- 57 Anderson R, Barnes JC, Bliss TV, Cain DP, Cambon K, Davies HA, *et al.* Behavioural, physiological and morphological analysis of a line of apolipoprotein E knockout mouse. *Neuroscience* 1998; 85: 93–110
- 58 Tannenberg RK, Scott HL, Tannenberg AEG, Dodd PR. Selective loss of synaptic proteins in Alzheimer's disease: evidence for an increased severity with APOE varepsilon4. *Neurochem Int* 2006; 49: 631–9
- 59 Hudry E, Dashkoff J, Roe AD, Takeda S, Koffie RM, Hashimoto T, *et al.* Gene transfer of human Apoe isoforms results in differential modulation of amyloid deposition and neurotoxicity in mouse brain. *Sci Transl Med* 2013; 5: 212ra161
- 60 Koffie RM, Hashimoto T, Tai H-C, Kay KR, Serrano-Pozo A, Joyner D, *et al.* Apolipoprotein E4 effects in Alzheimer's disease are mediated by synaptotoxic oligomeric amyloid- $\beta$ . *Brain* 2012; 135: 2155–68
- 61 Liu D, Pan X, Zhang J, Shen H, Collins NC, Cole AM, *et al.* APOE4 enhances age-dependent decline in cognitive function by down-regulating an NMDA receptor pathway in EFAD-Tg mice. *Mol Neurodegener* 2015; 10: 7
- 62 Holtzman DM, Bales KR, Tenkova T, Fagan AM, Parsadanian M, Sartorius LJ, *et al.* Apolipoprotein E isoform-dependent amyloid deposition and neuritic degeneration in a mouse model of Alzheimer's disease. *Proc Natl Acad Sci USA* 2000; 97: 2892–7
- 63 Nwabuisi-Heath E, Rebeck GW, Ladu MJ, Yu C. ApoE4 delays dendritic spine formation during neuron development and accelerates loss of mature spines in vitro. *ASN Neuro* 2014; 6: e00134
- 64 Dumanis SB, Tesoriero JA, Babus LW, Nguyen MT, Trotter JH, Ladu MJ, *et al.* ApoE4 decreases spine density and dendritic complexity in cortical neurons in vivo. *J Neurosci* 2009; 29: 15317–22
- 65 Jain S, Yoon SY, Leung L, Knoferle J, Huang Y. Cellular source-specific effects of apolipoprotein (apo) E4 on dendrite arborization and dendritic spine development. *PLoS ONE* 2013; 8: e59478
- 66 Rodriguez GA, Burns MP, Weeber EJ, Rebeck GW. Young APOE4 targeted replacement mice exhibit poor spatial learning and memory, with reduced dendritic spine density in the medial entorhinal cortex. *Learn Mem* 2013; 20: 256–66
- 67 Wang C, Wilson WA, Moore SD, Mace BE, Maeda N, Schmechel DE, *et al.* Human apoE4-targeted replacement mice display synaptic deficits in the absence of neuropathology. *Neurobiol Dis* 2005; 18: 390–8
- 68 Ji Y, Gong Y, Gan W, Beach T, Holtzman DM, Wisniewski T. Apolipoprotein E isoform-specific regulation of dendritic spine morphology in apolipoprotein E transgenic mice and Alzheimer's disease patients. *Neuroscience* 2003; 122: 305–15
- 69 Lanz TA, Carter DB, Merchant KM. Dendritic spine loss in the hippocampus of young PDAPP and Tg2576 mice and its prevention by the ApoE2 genotype. *Neurobiol Dis* 2003; 13: 246–53
- 70 Sen A, Alkon DL, Nelson TJ. Apolipoprotein E3 (ApoE3) but not ApoE4 protects against synaptic loss through increased expression of protein kinase C epsilon. *J Biol Chem* 2012; 287: 15947–58
- 71 LaFerla FM, Troncoso JC, Strickland DK, Kawas CH, Jay G. Neuronal cell death in Alzheimer's disease correlates with apoE uptake and intracellular Abeta stabilization. *J Clin Invest* 1997; 100: 310–20
- 72 Belinson H, Kariv-Inbal Z, Kaye R, Masliah E, Michaelson DM. Following activation of the amyloid cascade, apolipoprotein E4 drives the in vivo oligomerization of amyloid- $\beta$  resulting in neurodegeneration. *J Alzheimers Dis* 2010; 22: 959–70
- 73 Veinbergs I, Everson A, Sagara Y, Masliah E. Neurotoxic effects of apolipoprotein E4 are mediated via dysregulation of calcium homeostasis. *J Neurosci Res* 2002; 67: 379–87
- 74 Xu Q, Bernardo A, Walker D, Kanegawa T, Mahley RW, Huang Y. Profile and regulation of apolipoprotein E (ApoE) expression in the CNS in mice with targeting of green fluorescent protein gene to the ApoE locus. *J Neurosci* 2006; 26: 4985–94
- 75 Buttini M, Masliah E, Yu G-Q, Palop JJ, Chang S, Bernardo A, *et al.* Cellular source of apolipoprotein E4 determines neuronal susceptibility to excitotoxic injury in transgenic mice. *Am J Pathol* 2010; 177: 563–9
- 76 Harris FM, Brecht WJ, Xu Q, Tesseur I, Kekonius L, Wyss-Coray T, *et al.* Carboxyl-terminal-truncated apolipoprotein E4 causes Alzheimer's disease-like neurodegeneration and behavioral deficits in transgenic mice. *Proc Natl Acad Sci USA* 2003; 100: 10966–71
- 77 Chang S, ran Ma T, Miranda RD, Balestra ME, Mahley RW, Huang Y. Lipid- and receptor-binding regions

- of apolipoprotein E4 fragments act in concert to cause mitochondrial dysfunction and neurotoxicity. *Proc Natl Acad Sci USA* 2005; 102: 18694–9
- 78 Bien-Ly N, Andrews-Zwilling Y, Xu Q, Bernardo A, Wang C, Huang Y. C-terminal-truncated apolipoprotein (apo) E4 inefficiently clears amyloid-beta (Abeta) and acts in concert with Abeta to elicit neuronal and behavioral deficits in mice. *Proc Natl Acad Sci USA* 2011; 108: 4236–41
- 79 Dafnis I, Argyri L, Sagnou M, Tzinia A, Tsilibary EC, Stratikos E, et al. The ability of apolipoprotein E fragments to promote intraneuronal accumulation of amyloid beta peptide 42 is both isoform and size-specific. *Sci Rep* 2016; 6: 30654
- 80 Tolar M, Keller JN, Chan S, Mattson MP, Marques MA, Crutcher KA. Truncated apolipoprotein E (ApoE) causes increased intracellular calcium and may mediate ApoE neurotoxicity. *J Neurosci* 1999; 19: 7100–10
- 81 Zhong N, Scearce-Levie K, Ramaswamy G, Weisgraber KH. Apolipoprotein E4 domain interaction: synaptic and cognitive deficits in mice. *Alzheimers Dement* 2008; 4: 179–92
- 82 Nathan BP, Jiang Y, Wong GK, Shen F, Brewer GJ, Struble RG. Apolipoprotein E4 inhibits, and apolipoprotein E3 promotes neurite outgrowth in cultured adult mouse cortical neurons through the low-density lipoprotein receptor-related protein. *Brain Res* 2002; 928: 96–105
- 83 Korwek KM, Trotter JH, Ladu MJ, Sullivan PM, Weeber EJ. ApoE isoform-dependent changes in hippocampal synaptic function. *Mol Neurodegener* 2009; 4: 21
- 84 Neustadt AL, Winston CN, Parsadanian M, Main BS, Villapol S, Burns MP. Reduced cortical excitatory synapse number in APOE4 mice is associated with increased calcineurin activity. *NeuroReport* 2017; 28: 618–24
- 85 Minett T, Classey J, Matthews FE, Fahrenhold M, Taga M, Brayne C, et al. Microglial immunophenotype in dementia with Alzheimer's pathology. *J Neuroinflammation* 2016; 13: 135
- 86 Egensperger R, Kösel S, von Eitzen U, Graeber MB. Microglial activation in Alzheimer disease: association with APOE genotype. *Brain Pathol* 1998; 8: 439–47
- 87 Overmyer M, Helisalmi S, Soininen H, Laakso M, Riekkinen P, Alafuzoff I. Astroglial and the ApoE genotype. an immunohistochemical study of post-mortem human brain tissue. *Dement Geriatr Cogn Disord* 1999; 10: 252–7
- 88 Rodriguez GA, Tai LM, LaDu MJ, Rebeck GW. Human APOE4 increases microglia reactivity at A $\beta$  plaques in a mouse model of A $\beta$  deposition. *J Neuroinflammation* 2014; 11: 111
- 89 Liu C-C, Zhao N, Fu Y, Wang N, Linares C, Tsai C-W, et al. ApoE4 accelerates early seeding of amyloid pathology. *Neuron* 2017; 96: 1024–1032.e3
- 90 Belinson H, Michaelson DM. ApoE4-dependent Abeta-mediated neurodegeneration is associated with inflammatory activation in the hippocampus but not the septum. *J Neural Transm* 2009; 116: 1427–34
- 91 Ophir G, Meilin S, Efrati M, Chapman J, Karussis D, Roses A, et al. Human apoE3 but not apoE4 rescues impaired astrocyte activation in apoE null mice. *Neurobiol Dis* 2003; 12: 56–64
- 92 Kang SS, Ebbert MTW, Baker KE, Cook C, Wang X, Sens JP, et al. Microglial translational profiling reveals a convergent APOE pathway from aging, amyloid, and tau. *J Exp Med* 2018; 215: 2235–45
- 93 Krasemann S, Madore C, Cialic R, Baufeld C, Calcagno N, El Fatimy R, et al. The TREM2-APOE Pathway Drives the Transcriptional Phenotype of Dysfunctional Microglia in Neurodegenerative Diseases. *Immunity* 2017; 47: 566–581.e9
- 94 Keren-Shaul H, Spinrad A, Weiner A, Matcovitch-Natan O, Dvir-Szternfeld R, Ulland TK, et al. A unique microglia type associated with restricting development of Alzheimer's disease. *Cell* 2017; 169: 1276–1290.e17
- 95 Lin Y-T, Seo J, Gao F, Feldman HM, Wen H-L, Penney J, et al. APOE4 causes widespread molecular and cellular alterations associated with Alzheimer's disease phenotypes in human iPSC-derived brain cell types. *Neuron* 2018; 98: 1141–1154.e7
- 96 Caberlotto L, Marchetti L, Lauria M, Scotti M, Parolo S. Integration of transcriptomic and genomic data suggests candidate mechanisms for APOE4-mediated pathogenic action in Alzheimer's disease. *Sci Rep* 2016; 6: 32583
- 97 Thangavel R, Bhagavan SM, Ramaswamy SB, Surpur S, Govindarajan R, Kempuraj D, et al. Co-expression of glia maturation factor and apolipoprotein E4 in Alzheimer's Disease brain. *J Alzheimers Dis* 2018; 61: 553–60
- 98 Vitek MP, Brown CM, Colton CA. APOE genotype-specific differences in the innate immune response. *Neurobiol Aging* 2009; 30: 1350–60
- 99 Tulloch J, Leong L, Thomson Z, Chen S, Lee E-G, Keene CD, et al. Glia-specific APOE epigenetic changes in the Alzheimer's disease brain. *Brain Res* 2018; 1698: 1798–186. Published Online First: 3 August 2018. <https://doi.org/10.1016/j.brainres.2018.08.006>
- 100 Colton CA, Brown CM, Cook D, Needham LK, Xu Q, Czapiga M, et al. APOE and the regulation of microglial nitric oxide production: a link between genetic risk and oxidative stress. *Neurobiol Aging* 2002; 23: 777–85
- 101 Brown CM, Wright E, Colton CA, Sullivan PM, Laskowitz DT, Vitek MP. Apolipoprotein E isoform mediated regulation of nitric oxide release. *Free Radic Biol Med* 2002; 32: 1071–5
- 102 Chen S, Averett NT, Manelli A, LaDu MJ, May W, Ard MD. Isoform-specific effects of apolipoprotein E

- on secretion of inflammatory mediators in adult rat microglia. *JAD* 2005; 7: 25–35
- 103 Guo L, LaDu MJ, Van Eldik LJ. A dual role for apolipoprotein e in neuroinflammation: anti- and pro-inflammatory activity. *J Mol Neurosci* 2004; 23: 205–12
- 104 Hu J, LaDu MJ, Van Eldik LJ. Apolipoprotein E attenuates beta-amyloid-induced astrocyte activation. *J Neurochem* 1998; 71: 1626–34
- 105 Dorey E, Bamji-Mirza M, Najem D, Li Y, Liu H, Callaghan D, *et al.* Apolipoprotein E isoforms differentially regulate Alzheimer's disease and amyloid- $\beta$ -induced inflammatory response in vivo and in vitro. *J Alzheimers Dis* 2017; 57: 1265–79
- 106 Maezawa I, Nivison M, Montine KS, Maeda N, Montine TJ. Neurotoxicity from innate immune response is greatest with targeted replacement of E4 allele of apolipoprotein E gene and is mediated by microglial p38MAPK. *FASEB J* 2006; 20: 797–9
- 107 Tai LM, Ghura S, Koster KP, Liakaitė V, Maischein-Cline M, Kanabar P, *et al.* APOE-modulated A $\beta$ -induced neuroinflammation in Alzheimer's disease: current landscape, novel data, and future perspective. *J Neurochem* 2015; 133: 465–88
- 108 Laskowitz DT, Thekdi AD, Thekdi SD, Han SK, Myers JK, Pizzo SV, *et al.* Downregulation of microglial activation by apolipoprotein E and apoE-mimetic peptides. *Exp Neurol* 2001; 167: 74–85
- 109 Ulrich JD, Ulland TK, Mahan TE, Nyström S, Nilsson KP, Song WM, *et al.* ApoE facilitates the microglial response to amyloid plaque pathology. *J Exp Med* 2018; 215: 1047–58
- 110 Laskowitz DT, Matthew WD, Bennett ER, Schmechel D, Herbstreith MH, Goel S, *et al.* Endogenous apolipoprotein E suppresses LPS-stimulated microglial nitric oxide production. *NeuroReport* 1998; 9: 615–8
- 111 Lynch JR, Morgan D, Mance J, Matthew WD, Laskowitz DT. Apolipoprotein E modulates glial activation and the endogenous central nervous system inflammatory response. *J Neuroimmunol* 2001; 114: 107–13
- 112 Maezawa I, Maeda N, Montine TJ, Montine KS. Apolipoprotein E-specific innate immune response in astrocytes from targeted replacement mice. *J Neuroinflammation* 2006; 3: 10
- 113 Ophir G, Amariglio N, Jacob-Hirsch J, Elkon R, Rechavi G, Michaelson DM. Apolipoprotein E4 enhances brain inflammation by modulation of the NF-kappaB signaling cascade. *Neurobiol Dis* 2005; 20: 709–18
- 114 Blain J-F, Sullivan PM, Poirier J. A deficit in astroglial organization causes the impaired reactive sprouting in human apolipoprotein E4 targeted replacement mice. *Neurobiol Dis* 2006; 21: 505–14
- 115 Cudaback E, Li X, Montine KS, Montine TJ, Keene CD. Apolipoprotein E isoform-dependent microglia migration. *FASEB J* 2011; 25: 2082–91
- 116 Cudaback E, Yang Y, Montine TJ, Keene CD. APOE genotype-dependent modulation of astrocyte chemokine CCL3 production. *Glia* 2015; 63: 51–65
- 117 Gomez-Arboledas A, Davila JC, Sanchez-Mejias E, Navarro V, Nuñez-Diaz C, Sanchez-Varo R, *et al.* Phagocytic clearance of presynaptic dystrophies by reactive astrocytes in Alzheimer's disease. *Glia* 2018; 66: 637–53
- 118 Hong S, Beja-Glasser VF, Nfonoyim BM, Frouin A, Li S, Ramakrishnan S, *et al.* Complement and microglia mediate early synapse loss in Alzheimer mouse models. *Science* 2016; 352: 712–6
- 119 Zhu Y, Nwabuisi-Heath E, Dumanis SB, Tai LM, Yu C, Rebeck GW, *et al.* APOE genotype alters glial activation and loss of synaptic markers in mice. *Glia* 2012; 60: 559–69
- 120 McGeer PL, Walker DG, Pitas RE, Mahley RW, McGeer EG. Apolipoprotein E4 (ApoE4) but not ApoE3 or ApoE2 potentiates  $\beta$ -amyloid protein activation of complement in vitro. *Brain Res* 1997; 749: 135–8
- 121 Chung W-S, Verghese PB, Chakraborty C, Joung J, Hyman BT, Ulrich JD, *et al.* Novel allele-dependent role for APOE in controlling the rate of synapse pruning by astrocytes. *Proc Natl Acad Sci USA* 2016; 113: 10186–91
- 122 Filipello F, Morini R, Corradini I, Zerbi V, Canzi A, Michalski B, *et al.* The microglial innate immune receptor TREM2 is required for synapse elimination and normal brain connectivity. *Immunity* 2018; 48: 979–991.e8
- 123 Vainchtein ID, Chin G, Cho FS, Kelley KW, Miller JG, Chien EC, *et al.* Astrocyte-derived interleukin-33 promotes microglial synapse engulfment and neural circuit development. *Science* 2018; 359: 1269–73
- 124 Liddel SA, Guttenplan KA, Clarke LE, Bennett FC, Bohlen CJ, Schirmer L, *et al.* Neurotoxic reactive astrocytes are induced by activated microglia. *Nature* 2017; 541: 481–7
- 125 Azevedo EP, Ledo JH, Barbosa G, Sobrinho M, Diniz L, Fonseca ACC, *et al.* Activated microglia mediate synapse loss and short-term memory deficits in a mouse model of transthyretin-related oculoleptomeningeal amyloidosis. *Cell Death Dis* 2013; 4: e789
- 126 Braak H, Braak E. Neuropathological staging of Alzheimer-related changes. *Acta Neuropathol* 1991; 82: 239–59
- 127 Victoria GS, Zurzolo C. The spread of prion-like proteins by lysosomes and tunneling nanotubes: Implications for neurodegenerative diseases. *J Cell Biol* 2017; 216: 2633–44
- 128 Pickett EK, Henstridge CM, Allison E, Pitstick R, Pooler A, Wegmann S, *et al.* Spread of tau down neural circuits precedes synapse and neuronal loss in the rTgTauEC mouse model of early Alzheimer's disease.



- Synapse* 2017; 71: e21965. <https://doi.org/10.1002/syn.21965>
- 129 Maphis N, Xu G, Kokiko-Cochran ON, Jiang S, Cardona A, Ransohoff RM, *et al.* Reactive microglia drive tau pathology and contribute to the spreading of pathological tau in the brain. *Brain* 2015; 138: 1738–55
- 130 Prada I, Gabrielli M, Turola E, Iorio A, D'Arrigo G, Parolisi R, *et al.* Glia-to-neuron transfer of miRNAs via extracellular vesicles: a new mechanism underlying inflammation-induced synaptic alterations. *Acta Neuropathol* 2018; 135: 529–50
- 131 Asai H, Ikezu S, Tsunoda S, Medalla M, Luebke J, Haydar T, *et al.* Depletion of microglia and inhibition of exosome synthesis halt tau propagation. *Nat Neurosci* 2015; 18: 1584–93
- 132 Rostami J, Holmqvist S, Lindström V, Sigvardson J, Westermark GT, Ingelsson M, *et al.* Human astrocytes transfer aggregated alpha-synuclein via tunneling nanotubes. *J Neurosci* 2017; 37: 11835–53
- 133 DeKosky ST, Scheff SW. Synapse loss in frontal cortex biopsies in Alzheimer's disease: correlation with cognitive severity. *Ann Neurol* 1990; 27: 457–64
- 134 Munafò MR, Davey Smith G. Robust research needs many lines of evidence. *Nature* 2018; 553: 399–401
- 135 Lane-Donovan C, Herz J. Apoe, apoe receptors, and the synapse in alzheimer's disease. *Trends Endocrinol Metab* 2017; 28: 273–84
- 136 O'Hare E, Jeggo R, Kim E-M, Barbour B, Walczak J-S, Palmer P, *et al.* Lack of support for bexarotene as a treatment for Alzheimer's disease. *Neuropharmacology* 2016; 100: 124–30
- 137 LaClair KD, Manaye KF, Lee DL, Allard JS, Savonenko AV, Troncoso JC, *et al.* Treatment with bexarotene, a compound that increases apolipoprotein-E, provides no cognitive benefit in mutant APP/PS1 mice. *Mol Neurodegener* 2013; 8: 18
- 138 Cramer PE, Cirrito JR, Wesson DW, Lee CYD, Karlo JC, Zinn AE, *et al.* ApoE-directed therapeutics rapidly clear  $\beta$ -amyloid and reverse deficits in AD mouse models. *Science* 2012; 335: 1503–6
- 139 Teseur I, Lo AC, Roberfroid A, Dietvorst S, Van Broeck B, Borgers M, *et al.* Comment on "ApoE-directed therapeutics rapidly clear  $\beta$ -amyloid and reverse deficits in AD mouse models". *Science* 2013; 340: 924–e
- 140 Cummings JL, Zhong K, Kinney JW, Heaney C, Moll-Tudla J, Joshi A, *et al.* Double-blind, placebo-controlled, proof-of-concept trial of bexarotene in moderate Alzheimer's disease. *Alzheimers Res Ther* 2016; 8: 4
- 141 McColl BW, McGregor AL, Wong A, Harris JD, Amalitano A, Magnoni S, *et al.* APOE epsilon3 gene transfer attenuates brain damage after experimental stroke. *J Cereb Blood Flow Metab* 2007; 27: 477–87
- 142 Huynh T-PV, Liao F, Francis CM, Robinson GO, Serrano JR, Jiang H, *et al.* Age-dependent effects of apoe reduction using antisense oligonucleotides in a model of  $\beta$ -amyloidosis. *Neuron* 2017; 96: 1013–1023.e4

### Supporting information

Additional Supporting Information may be found in the online version of this article at the publisher's web-site:

**Table S1.** Search terms used for Embase, Web of Science, and Med Science

**Table S2.** Exclusion Criteria

**Table S3.** Papers included in the systematic review (Discussed in the Results sections) (\* denotes hand-picked papers included in the systematic literature search)

**Table S4.** Details of human *post mortem* cases used for Figures 2-5. MRC BBN: Medical Research Council Brain Bank Number, AD: Alzheimer's disease, PM: *post mortem*.

Received 11 October 2018

Accepted after revision 27 October 2018

Published online Article Accepted on 5 November 2018

**Supplemental Information 1:** Search terms used for Embase, Web of Science, and Med Science

**Database: Med Science**

**Inflammation**

1. exp Apolipoproteins E/
2. Alzheimer Disease/
3. 1 and 2
4. Astrocytes/
5. Microglia/
6. microglia\*.mp.
7. compound granular corpuscle.mp.
8. glitter cell.mp.
9. hortega cell.mp.
10. glia cell.mp.
11. 5 or 6 or 7 or 8 or 9 or 10
12. reactiv\*.mp.
13. 4 and 12
14. 11 and 12
15. activ\*.mp.
16. 4 and 15
17. 11 and 15
18. exp Complement C4/
19. Complement C1q/
20. Complement C3/
21. Interleukin-1beta/
22. Tumor Necrosis Factor-alpha/
23. cytokine\*.mp.
24. GLIOSIS/
25. pro inflammatory.mp.
26. anti inflammatory.mp.
27. Inflammat\* mediat\*.mp.
28. neuroinflammatory.mp.
29. neuroinflammation.mp.

30. phagocyt\*.mp.
31. immun\*.mp.
32. 4 or 11 or 13 or 14 or 16 or 17 or 18 or 19 or 20 or 21 or 22 or 23 or 24 or 25 or 26 or 27 or 28 or 29 or 30 or 31
33. 3 and 32

### **Neurodegeneration**

1. exp Apolipoproteins E/
2. Alzheimer Disease/
3. 1 and 2
4. neuron\*.mp.
5. synap\*.mp.
6. 4 or 5
7. dysfunction\*.mp.
8. degenerate\*.mp.
9. degeneration.mp.
10. Death.mp.
11. Impair\*.mp.
12. Loss.mp.
13. dysregulate\*.mp.
14. dysregulation\*.mp.
15. prun\*.mp.
16. phagocyt\*.mp.
17. 7 or 8 or 9 or 10 or 11 or 12 or 13 or 14 or 15 or 16
18. 6 and 17
19. neurodegenerat\*.mp.
20. Neurotoxic\*.mp.
21. synaptotoxic\*.mp.
22. Myelin\*.mp.
23. Demyelin\*.mp.
24. 19 or 20 or 21 or 22 or 23
25. 18 or 24
26. 3 and 25

## **Prion-like spread**

1. exp Apolipoproteins E/
2. Alzheimer Disease/
3. 1 and 2
4. Amyloid/
5. Amyloid beta-Peptides/
6. AMYLOID BETA-PROTEIN PRECURSOR/
7. Plaque, Amyloid/
8. tau Proteins/
9. tau.mp.
10. phf.mp.
11. tangles.mp.
12. Neurofibrillary Tangles/
13. paired helical filament.mp.
14. straight filament.mp.
15. tauopathy.mp.
16. neurofibrill\*.mp.
17. 4 or 5 or 6 or 7 or 8 or 9 or 10 or 11 or 12 or 13 or 14 or 15 or 16
18. prion\*.mp.
19. move\*.mp.
20. moving.mp.
21. dynamic\*.mp.
22. Propagat\*.mp.
23. attenuat\*.mp.
24. spread\*.mp.
25. secret\*.mp.
26. transfer\*.mp.
27. transmiss\*.mp.
28. progress\*.mp.
29. Trans-synaptic\*.mp.
30. seed\*.mp.
31. infect\*.mp.
32. tunnel\*.mp.
33. conver\*.mp.
34. aggregat\*.mp.

35. 18 or 19 or 20 or 21 or 22 or 23 or 24 or 25 or 26 or 27 or 28 or 29 or 30 or 31 or 32 or 33 or

36. 3 and 17 and 35

**Database: Embase**

**Inflammation**

1. apolipoprotein E/
2. APOE.mp.
3. APO-E.mp.
4. apolipoprotein e isoproteins.mp.
5. apoe isoproteins.mp.
6. apo e isoproteins.mp.
7. Apoproteins E.mp.
8. APOE-epsilon2.mp.
9. APOE epsilon2.mp.
10. ApoE2.mp.
11. APOE-epsilon 2.mp.
12. APOE epsilon 2.mp.
13. Apo E-2.mp.
14. Apo E 2.mp.
15. APO E2.mp.
16. Apolipoprotein-epsilon2.mp.
17. Apolipoprotein epsilon2.mp.
18. Apolipoprotein E-2.mp.
19. Apolipoprotein E 2.mp.
20. apolipoprotein E2.mp.
21. APOE-epsilon3.mp.
22. APOE epsilon3.mp.
23. ApoE3.mp.
24. APOE-epsilon 3.mp.
25. APOE epsilon 3.mp.
26. APO E-3.mp.
27. Apo E 3.mp.
28. APO E3.mp.

29. Apolipoprotein-epsilon3.mp.
30. Apolipoprotein epsilon3.mp.
31. Apolipoprotein E-3.mp.
32. Apolipoprotein E 3.mp.
33. Apolipoprotein E3.mp.
34. apoprotein E3.mp.
35. APOE-epsilon4.mp.
36. APOE epsilon4.mp.
37. APOE4.mp.
38. APOE-epsilon 4.mp.
39. APOE epsilon 4.mp.
40. Apo E-4.mp.
41. Apo E 4.mp.
42. apo e4.mp.
43. Apolipoprotein-epsilon4.mp.
44. Apolipoprotein epsilon4.mp.
45. Apolipoprotein E-4.mp.
46. Apolipoprotein E 4.mp.
47. Apolipoprotein E4.mp.
48. 1 or 2 or 3 or 4 or 5 or 6 or 7 or 8 or 9 or 10 or 11 or 12 or 13 or 14 or 15 or 16 or 17 or 18 or 19 or 20 or 21 or 22 or 23 or 24 or 25 or 26 or 27 or 28 or 29 or 30 or 31 or 32 or 33 or 34 or 35 or 36 or 37 or 38 or 39 or 40 or 41 or 42 or 43 or 44 or 45 or 46 or 47
49. Alzheimer disease.mp.
50. Alzheimer.mp.
51. Alzheimer's.mp.
52. Alzheimer Dementia.mp.
53. Dementia Alzheimer.mp.
54. Alzheimer-Type Dementia.mp.
55. Dementia Alzheimer-Type.mp.
56. Primary Senile Degenerative Dementia.mp.
57. Dementia Senile.mp.
58. senile dementia.mp.
59. Dementia Alzheimer Type.mp.
60. Alzheimer Type Dementia.mp.

61. Senile Dementia Alzheimer Type.mp.
62. Alzheimer Type Senile Dementia.mp.
63. Dementia Primary Senile Degenerative.mp.
64. Disease Alzheimer.mp.
65. Alzheimer Disease Late Onset.mp.
66. Focal Onset Alzheimer's Disease.mp.
67. Familial Alzheimer Disease.mp.
68. Sporadic Alzheimer disease.mp.
69. Alzheimer Disease Early Onset.mp.
70. Early Onset Alzheimer Disease.mp.
71. alzheimer disease.mp.
72. 49 or 50 or 51 or 52 or 53 or 54 or 55 or 56 or 57 or 58 or 59 or 60 or 61 or 62 or 63 or 64 or 65 or 66 or 67 or 68 or 69 or 70 or 71
73. astrocyte/
74. microglia/
75. 73 or 74
76. reactiv\*.mp.
77. activ\*.mp.
78. 75 and 76
79. 75 and 77
80. complement component C4/
81. complement component C1q/
82. complement component C3/
83. interleukin 1beta/
84. tumor necrosis factor/
85. cytokine\*.mp.
86. gliosis.mp.
87. pro-inflammat\*.mp.
88. anti-inflammat\*.mp.
89. Inflammat\* mediat\*.mp.
90. neuroinflammat\*.mp.
91. phagocyt\*.mp.
92. immun\*.mp.
93. 80 or 81 or 82 or 83 or 84 or 85 or 86 or 87 or 88 or 89 or 90 or 91 or 92

94. 73 or 74 or 78 or 79 or 93

95. 48 and 72 and 94

### **Neurodegeneration**

1. apolipoprotein E/
2. APOE.mp.
3. APO-E.mp.
4. apolipoprotein e isoproteins.mp.
5. apoe isoproteins.mp.
6. apo e isoproteins.mp.
7. Apoproteins E.mp.
8. APOE-epsilon2.mp.
9. APOE epsilon2.mp.
10. ApoE2.mp.
11. APOE-epsilon 2.mp.
12. APOE epsilon 2.mp.
13. Apo E-2.mp.
14. Apo E 2.mp.
15. APO E2.mp.
16. Apolipoprotein-epsilon2.mp.
17. Apolipoprotein epsilon2.mp.
18. Apolipoprotein E-2.mp.
19. Apolipoprotein E 2.mp.
20. apolipoprotein E2.mp.
21. APOE-epsilon3.mp.
22. APOE epsilon3.mp.
23. ApoE3.mp.
24. APOE-epsilon 3.mp.
25. APOE epsilon 3.mp.
26. APO E-3.mp.
27. Apo E 3.mp.
28. APO E3.mp.
29. Apolipoprotein-epsilon3.mp.
30. Apolipoprotein epsilon3.mp.
31. Apolipoprotein E-3.mp.



32. Apolipoprotein E 3.mp.
33. Apolipoprotein E3.mp.
34. apoprotein E3.mp.
35. APOE-epsilon4.mp.
36. APOE epsilon4.mp.
37. APOE4.mp.
38. APOE-epsilon 4.mp.
39. APOE epsilon 4.mp.
40. Apo E-4.mp.
41. Apo E 4.mp.
42. apo e4.mp.
43. Apolipoprotein-epsilon4.mp.
44. Apolipoprotein epsilon4.mp.
45. Apolipoprotein E-4.mp.
46. Apolipoprotein E 4.mp.
47. Apolipoprotein E4.mp.
48. 1 or 2 or 3 or 4 or 5 or 6 or 7 or 8 or 9 or 10 or 11 or 12 or 13 or 14 or 15 or 16 or 17 or 18 or 19 or 20 or 21 or 22 or 23 or 24 or 25 or 26 or 27 or 28 or 29 or 30 or 31 or 32 or 33 or 34 or 35 or 36 or 37 or 38 or 39 or 40 or 41 or 42 or 43 or 44 or 45 or 46 or 47
49. Alzheimer disease.mp.
50. Alzheimer.mp.
51. Alzheimer's.mp.
52. Alzheimer Dementia.mp.
53. Dementia Alzheimer.mp.
54. Alzheimer-Type Dementia.mp.
55. Dementia Alzheimer-Type.mp.
56. Primary Senile Degenerative Dementia.mp.
57. Dementia Senile.mp.
58. senile dementia.mp.
59. Dementia Alzheimer Type.mp.
60. Alzheimer Type Dementia.mp.
61. Senile Dementia Alzheimer Type.mp.
62. Alzheimer Type Senile Dementia.mp.
63. Dementia Primary Senile Degenerative.mp.

64. Disease Alzheimer.mp.
65. Alzheimer Disease Late Onset.mp.
66. Focal Onset Alzheimer's Disease.mp.
67. Familial Alzheimer Disease.mp.
68. Sporadic Alzheimer disease.mp.
69. Alzheimer Disease Early Onset.mp.
70. Early Onset Alzheimer Disease.mp.
71. alzheimer disease.mp.
72. 49 or 50 or 51 or 52 or 53 or 54 or 55 or 56 or 57 or 58 or 59 or 60 or 61 or 62 or 63 or 64 or 65 or 66 or 67 or 68 or 69 or 70 or 71
73. neuron\*.mp.
74. synap\*.mp.
75. 73 or 74
76. degenerat\*.mp.
77. dysfunction\*.mp.
78. death.mp.
79. impair\*.mp.
80. loss.mp.
81. dysregulat\*.mp.
82. prun\*.mp.
83. phagocyt\*.mp.
84. 76 or 77 or 78 or 79 or 80 or 81 or 82 or 83
85. 75 and 84
86. neurodegenerat\*.mp.
87. neurotoxic\*.mp.
88. synaptotoxic\*.mp.
89. myelin\*.mp.
90. demyelin\*.mp.
91. 86 or 87 or 88 or 89 or 90
92. 85 or 91
93. 48 and 72 and 92

### **Prion-like spread**

1. apolipoprotein E/
2. APOE.mp.

3. APO-E.mp.
4. apolipoprotein e isoproteins.mp.
5. apoe isoproteins.mp.
6. apo e isoproteins.mp.
7. Apoproteins E.mp.
8. APOE-epsilon2.mp.
9. APOE epsilon2.mp.
10. ApoE2.mp.
11. APOE-epsilon 2.mp.
12. APOE epsilon 2.mp.
13. Apo E-2.mp.
14. Apo E 2.mp.
15. APO E2.mp.
16. Apolipoprotein-epsilon2.mp.
17. Apolipoprotein epsilon2.mp.
18. Apolipoprotein E-2.mp.
19. Apolipoprotein E 2.mp.
20. apolipoprotein E2.mp.
21. APOE-epsilon3.mp.
22. APOE epsilon3.mp.
23. ApoE3.mp.
24. APOE-epsilon 3.mp.
25. APOE epsilon 3.mp.
26. APO E-3.mp.
27. Apo E 3.mp.
28. APO E3.mp.
29. Apolipoprotein-epsilon3.mp.
30. Apolipoprotein epsilon3.mp.
31. Apolipoprotein E-3.mp.
32. Apolipoprotein E 3.mp.
33. Apolipoprotein E3.mp.
34. apoprotein E3.mp.
35. APOE-epsilon4.mp.
36. APOE epsilon4.mp.
37. APOE4.mp.

38. APOE-epsilon 4.mp.
39. APOE epsilon 4.mp.
40. Apo E-4.mp.
41. Apo E 4.mp.
42. apo e4.mp.
43. Apolipoprotein-epsilon4.mp.
44. Apolipoprotein epsilon4.mp.
45. Apolipoprotein E-4.mp.
46. Apolipoprotein E 4.mp.
47. Apolipoprotein E4.mp.
48. 1 or 2 or 3 or 4 or 5 or 6 or 7 or 8 or 9 or 10 or 11 or 12 or 13 or 14 or 15 or 16 or 17 or 18 or 19 or 20 or 21 or 22 or 23 or 24 or 25 or 26 or 27 or 28 or 29 or 30 or 31 or 32 or 33 or 34 or 35 or 36 or 37 or 38 or 39 or 40 or 41 or 42 or 43 or 44 or 45 or 46 or 47
49. Alzheimer disease.mp.
50. Alzheimer.mp.
51. Alzheimer's.mp.
52. Alzheimer Dementia.mp.
53. Dementia Alzheimer.mp.
54. Alzheimer-Type Dementia.mp.
55. Dementia Alzheimer-Type.mp.
56. Primary Senile Degenerative Dementia.mp.
57. Dementia Senile.mp.
58. senile dementia.mp.
59. Dementia Alzheimer Type.mp.
60. Alzheimer Type Dementia.mp.
61. Senile Dementia Alzheimer Type.mp.
62. Alzheimer Type Senile Dementia.mp.
63. Dementia Primary Senile Degenerative.mp.
64. Disease Alzheimer.mp.
65. Alzheimer Disease Late Onset.mp.
66. Focal Onset Alzheimer's Disease.mp.
67. Familial Alzheimer Disease.mp.
68. Sporadic Alzheimer disease.mp.
69. Alzheimer Disease Early Onset.mp.

70. Early Onset Alzheimer Disease.mp.
71. alzheimer disease.mp.
72. 49 or 50 or 51 or 52 or 53 or 54 or 55 or 56 or 57 or 58 or 59 or 60 or 61 or 62 or 63 or 64 or 65 or 66 or 67 or 68 or 69 or 70 or 71
73. amyloid beta protein/
74. amyloid protein/
75. amyloid plaque/
76. "amyloid beta protein[1-40]"/
77. "amyloid beta protein[1-42]"/
78. amyloid precursor protein/
79. amyloid/
80. tau protein/
81. tau.mp.
82. phf.mp.
83. tangles.mp.
84. neurofibrillary tangle/
85. paired helical filament/
86. straight filament.mp.
87. tauopathy/
88. neurofibrill\*.mp.
89. 73 or 74 or 75 or 76 or 77 or 78 or 79 or 80 or 81 or 82 or 83 or 84 or 85 or 86 or 87 or 88
90. prion\*.mp.
91. move\*.mp.
92. moving.mp.
93. dynamic\*.mp.
94. propagat\*.mp.
95. attenuat\*.mp.
96. spread\*.mp.
97. secret\*.mp.
98. transfer\*.mp.
99. transmiss\*.mp.
100. progress\*.mp.
101. Trans-synaptic\*.mp.
102. seed\*.mp.

- 103. infect\*.mp.
- 104. tunnel\*.mp.
- 105. conver\*.mp.
- 106. aggregat\*.mp.
- 107. 90 or 91 or 92 or 93 or 94 or 95 or 96 or 97 or 98 or 99 or 100 or 101 or 102 or 103 or 104 or 105 or 106
- 108. 48 and 72 and 89 and 107

**Database: Web of science**

**Inflammation**

- #14 #13 AND #3
- #13 #12 OR #11 OR #10 OR #8 OR #7 OR #5 OR #4
- #12 TS= ("complement\*" OR "complement component 4" OR "complement component, c4" OR "component 4, complement" OR "component, c4 complement" OR "c4, complement" OR "c4 complement component" OR "complement 4" OR "complement c4" OR "C1q" OR "c1q, complement" OR "complement 1q" OR "complement c1q" OR "complement component 1q" OR "component 1q, complement" OR "C3" OR "c3, complement" OR "complement 3" OR "complement c3" OR "complement component 3" OR "component 3, complement" OR "interleukin\*" OR "IL1 $\beta$ " OR IL1- $\beta$  OR "Interleukin 1 beta" OR "Interleukin- 1 beta" OR "il-1 beta" OR "interleukin 1beta" OR "interleukin-1 beta" OR "interleukin-1beta" OR "tumor necrosis factor alpha" OR "tumor necrosis factor-alpha" OR "tnf-alpha" OR "tnfalpha" OR "cachectin" OR "cachectin tumor necrosis factor" OR "cachectin-tumor necrosis factor" OR "tumor necrosis factor ligand superfamily member 2" OR "tnf superfamily, member 2" OR TNF $\alpha$ " OR "cytokine\*" OR "gliosis" OR "pro-inflammat\*" OR "anti-inflammat\*" OR "inflammat\* NEAR/2 mediat\*" OR "neuroinflammat\*" OR "phagocyt\*" OR "immun\*")
- #11 #9 AND #4
- #10 #9 AND #5
- #9 ts=("Reactiv\*")
- #8 #6 AND #4
- #7 #6 AND #5
- #6 TS= ("Activat\*")
- #5 TS= ("microglia" OR "cell microglia" OR "compound granular corpuscle" OR

"glitter cell" OR "hortega cell" OR "microglia cell" OR "microglial cell" OR  
 "neuromicroglia cell" OR "glia cell")

#4 TS= ("astro\*" OR "astroglia cell" OR "astroglial cell" OR "glia cell" OR "type 1  
 astrocytes" OR "type 2 astrocytes")

#3 #2 AND #1

#2 TS= ("Alzheimer" OR "Alzheimer's" OR "Alzheimer Dementia" OR  
 "Dementia Alzheimer" OR "Alzheimer-Type Dementia" OR "Dementia Alzheimer-  
 Type" OR "Primary Senile Degenerative Dementia" OR "Dementia Senile" OR  
 "Senile Dementia" OR "Dementia Alzheimer Type" OR "Alzheimer Type Dementia"  
 OR "Senile Dementia Alzheimer Type" OR "Alzheimer Type Senile Dementia" OR  
 "Dementia Primary Senile Degenerative" OR "Alzheimer's Disease" OR "Disease  
 Alzheimer" OR "Acute Confusional Senile Dementia" OR "Senile Dementia Acute  
 Confusional" OR "Alzheimer Disease Late Onset" OR "Late onset Alzheimer's  
 Disease" OR "Alzheimer's Disease Focal Onset" OR "Focal Onset Alzheimer's  
 Disease" OR "Familial Alzheimer Disease" OR "Sporadic Alzheimer disease" OR  
 "Alzheimer Disease Early Onset" OR "Early Onset Alzheimer Disease" OR  
 "Alzheimer disease" OR "Alzeimer disease" OR "Alzeimer's disease" OR "Alzheimer  
 dementia" OR "alzheimer sclerosis" OR "alzheimer syndrome" OR "alzheimer's  
 disease" OR "dementia, alzheimer")

#1 TS=("apolipoprotein E" OR "APOE" OR "apo-e" OR "apolipoprotein e  
 isoproteins" OR "apoe isoproteins" OR "APO E" OR "apo e isoproteins" OR  
 "Apoproteins E" OR "Apoprotein E" OR "APOE-epsilon2" OR "APOE epsilon2" OR  
 "ApoE2" OR "APOE-epsilon 2" OR "APOE epsilon 2" OR "Apo E-2" OR "Apo E 2"  
 OR "apo e2" OR "Apolipoprotein-epsilon2" OR "Apolipoprotein epsilon2" OR  
 "Apolipoprotein E-2" OR "Apolipoprotein E 2" OR "APOE-epsilon3" OR "apoe  
 epsilon3" OR "ApoE3" OR "APOE-epsilon 3" OR "APOE epsilon 3" OR "APO E-3"  
 OR "Apo E 3" OR "APO E3" OR "Apolipoprotein-epsilon3" OR "Apolipoprotein  
 epsilon3" OR "Apolipoprotein E-3" OR "Apolipoprotein E 3" OR "APOE-epsilon4"  
 OR "APOE epsilon4" OR "APOE4" OR "APOE-epsilon 4" OR "APOE epsilon 4" OR  
 "Apo E-4" OR "Apo E 4" OR "apo e4" OR "Apolipoprotein-epsilon4" OR  
 "Apolipoprotein epsilon4" OR "Apolipoprotein E-4" OR "Apolipoprotein E 4" OR  
 "apolipoprotein ε" OR "APOε" OR "apo-ε" OR "apolipoprotein ε isoproteins" OR  
 "apoε isoproteins" OR "APO ε" OR "apo ε isoproteins" OR "Apoproteins ε" OR  
 "Apoprotein ε" OR "APOE-ε2" OR "APOE ε2" OR "Apoε2" OR "APOE-ε2" OR  
 "APOE ε 2" OR "Apo ε-2" OR "Apo ε 2" OR "apo ε2" OR "Apolipoprotein-ε2" OR

"Apolipoprotein ε2" OR "Apolipoprotein ε-2" OR "Apolipoprotein ε 2" OR "APOE-ε3"  
 OR "apoe ε3" OR "Apoε3" OR "APOE-ε3" OR "APOE ε 3" OR "APO ε-3" OR "Apo ε  
 3" OR "APO ε3" OR "Apolipoprotein-ε3" OR "Apolipoprotein ε3" OR "Apolipoprotein  
 ε-3" OR "Apolipoprotein ε 3" OR "APOE-ε4" OR "APOE ε4" OR "APOε4" OR  
 "APOE-ε 4" OR "APOE ε 4" OR "Apo ε-4" OR "Apo ε 4" OR "apo ε4" OR  
 "Apolipoprotein-ε4" OR "Apolipoprotein ε4" OR "Apolipoprotein ε-4" OR  
 "Apolipoprotein ε 4")

## **Neurodegeneration**

#9 #8 AND #3

#8 #7 OR #6

#7 TS=("Neurodegeneration" OR "Neurotoxic\*" OR "Synaptotoxic\*" OR  
 "Myelin\*", "demyelin\*")

#6 #5 AND #4

#5 ts=("degenerat\*" OR "Dysfunction\*" OR "Death" OR "Impair\*" OR "loss" OR  
 "Dysregulat\*" OR "prun\*" OR "phagocyt\*")

#4 ts=("Neuron\*" OR "synap\*")

#3 #2 AND #1

#2 TS= ("Alzheimer" OR "Alzheimer's" OR "Alzheimer Dementia" OR  
 "Dementia Alzheimer" OR "Alzheimer-Type Dementia" OR "Dementia Alzheimer-  
 Type" OR "Primary Senile Degenerative Dementia" OR "Dementia Senile" OR  
 "Senile Dementia" OR "Dementia Alzheimer Type" OR "Alzheimer Type Dementia"  
 OR "Senile Dementia Alzheimer Type" OR "Alzheimer Type Senile Dementia" OR  
 "Dementia Primary Senile Degenerative" OR "Alzheimer's Disease" OR "Disease  
 Alzheimer" OR "Acute Confusional Senile Dementia" OR "Senile Dementia Acute  
 Confusional" OR "Alzheimer Disease Late Onset" OR "Late onset Alzheimer's  
 Disease" OR "Alzheimer's Disease Focal Onset" OR "Focal Onset Alzheimer's  
 Disease" OR "Familial Alzheimer Disease" OR "Sporadic Alzheimer disease" OR  
 "Alzheimer Disease Early Onset" OR "Early Onset Alzheimer Disease" OR  
 "Alzheimer disease" OR "Alzeimer disease" OR "Alzeimer's disease" OR "Alzheimer  
 dementia" OR "alzheimer sclerosis" OR "alzheimer syndrome" OR "alzheimer's  
 disease" OR "dementia, alzheimer")

#1 TS=("apolipoprotein E" OR "APOE" OR "apo-e" OR "apolipoprotein e  
 isoproteins" OR "apoe isoproteins" OR "APO E" OR "apo e isoproteins" OR



"Apoproteins E" OR "Apoprotein E" OR "APOE-epsilon2" OR "APOE epsilon2" OR "ApoE2" OR "APOE-epsilon 2" OR "APOE epsilon 2" OR "Apo E-2" OR "Apo E 2" OR "apo e2" OR "Apolipoprotein-epsilon2" OR "Apolipoprotein epsilon2" OR "Apolipoprotein E-2" OR "Apolipoprotein E 2" OR "APOE-epsilon3" OR "apoe epsilon3" OR "ApoE3" OR "APOE-epsilon 3" OR "APOE epsilon 3" OR "APO E-3" OR "Apo E 3" OR "APO E3" OR "Apolipoprotein-epsilon3" OR "Apolipoprotein epsilon3" OR "Apolipoprotein E-3" OR "Apolipoprotein E 3" OR "APOE-epsilon4" OR "APOE epsilon4" OR "APOE4" OR "APOE-epsilon 4" OR "APOE epsilon 4" OR "Apo E-4" OR "Apo E 4" OR "apo e4" OR "Apolipoprotein-epsilon4" OR "Apolipoprotein epsilon4" OR "Apolipoprotein E-4" OR "Apolipoprotein E 4" OR "apolipoprotein ε" OR "APOε" OR "apo-ε" OR "apolipoprotein ε isoproteins" OR "apoε isoproteins" OR "APO ε" OR "apo ε isoproteins" OR "Apoproteins ε" OR "Apoprotein ε" OR "APOE-ε2" OR "APOE ε2" OR "Apoε2" OR "APOE-ε2" OR "APOE ε 2" OR "Apo ε-2" OR "Apo ε 2" OR "apo ε2" OR "Apolipoprotein-ε2" OR "Apolipoprotein ε2" OR "Apolipoprotein ε-2" OR "Apolipoprotein ε 2" OR "APOE-ε3" OR "apoe ε3" OR "Apoε3" OR "APOE-ε3" OR "APOE ε 3" OR "APO ε-3" OR "Apo ε 3" OR "APO ε3" OR "Apolipoprotein-ε3" OR "Apolipoprotein ε3" OR "Apolipoprotein ε-3" OR "Apolipoprotein ε 3" OR "APOE-ε4" OR "APOE ε4" OR "APOε4" OR "APOE-ε 4" OR "APOE ε 4" OR "Apo ε-4" OR "Apo ε 4" OR "apo ε4" OR "Apolipoprotein-ε4" OR "Apolipoprotein ε4" OR "Apolipoprotein ε-4" OR "Apolipoprotein ε 4")

### **Prion-like spread**

#8 #7 AND #6 AND #3

#7 TS= ("Prion\*" OR "move\*" OR "Moving" OR "dynamic\*" OR "Propagat\*" OR "Attenuat\*" OR "Spread\*" OR "Secret\*" OR "Transfer\*" OR "transmiss\*" OR "progress\*" OR "trans-synaptic\*" or "seed\*" or "conver\*" or "infect\*" or "tunnel\*" or "aggregat\*")

#6 #5 OR #4

#5 TS= ("tau" OR "τ" OR "PHF" OR "tau-protein" OR "microtubule associated protein tau" OR "microtubule protein tau" OR "tau proteins" OR "Neurofibrillary tangles" OR "tangles" OR "paired helical filament" OR "paired-helical filament" OR "Straight filament" OR "tauopathy" OR "neurofibrill\*")

#4 TS= ("Amyloid" OR "Amyloido\*" OR "Alzheimer's Amyloid Fibril Protein" OR "ABP Alzheimer's" OR "Alzheimer ABP" OR "Alzheimer's ABP" OR "Amyloid AD-

AP" OR "AD-AP Amyloid" OR "Amyloid AD AP" OR "beta-Amyloid Protein" OR "Protein beta-Amyloid" OR "beta Amyloid Protein" OR "Amyloid beta-Protein" OR "Amyloid beta Protein" OR "beta-Protein Amyloid" OR "Amyloid Fibril Protein Alzheimer's" OR Amyloid Protein A4 OR "Protein A4 Amyloid" OR "Alzheimer beta-Protein" OR "Alzheimer beta Protein" OR "beta-Protein Alzheimer" OR "Amyloid beta-Peptide" OR "beta-Peptide Amyloid" OR "β-amyloid" OR "amyloid β" OR "Aβ" OR "Amyloid-β" OR "β-Amyloid Protein" OR "Protein β-Amyloid" OR "β Amyloid Protein" OR "Amyloid β-Protein" OR "Amyloid β Protein" OR "β-Protein Amyloid" OR "Alzheimer β-Protein" OR "Alzheimer βProtein" OR "β-Protein Alzheimer" OR "Amyloid -βPeptide" OR "β-Peptide Amyloid")

#3 #2 AND #1

#2 TS= ("Alzheimer" OR "Alzheimer's" OR "Alzheimer Dementia" OR "Dementia Alzheimer" OR "Alzheimer-Type Dementia" OR "Dementia Alzheimer-Type" OR "Primary Senile Degenerative Dementia" OR "Dementia Senile" OR "Senile Dementia" OR "Dementia Alzheimer Type" OR "Alzheimer Type Dementia" OR "Senile Dementia Alzheimer Type" OR "Alzheimer Type Senile Dementia" OR "Dementia Primary Senile Degenerative" OR "Alzheimer's Disease" OR "Disease Alzheimer" OR "Acute Confusional Senile Dementia" OR "Senile Dementia Acute Confusional" OR "Alzheimer Disease Late Onset" OR "Late onset Alzheimer's Disease" OR "Alzheimer's Disease Focal Onset" OR "Focal Onset Alzheimer's Disease" OR "Familial Alzheimer Disease" OR "Sporadic Alzheimer disease" OR "Alzheimer Disease Early Onset" OR "Early Onset Alzheimer Disease" OR "Alzheimer disease" OR "Alzeimer disease" OR "Alzeimer's disease" OR "Alzheimer dementia" OR "alzheimer sclerosis" OR "alzheimer syndrome" OR "alzheimer's disease" OR "dementia, alzheimer")

#1 TS=("apolipoprotein E" OR "APOE" OR "apo-e" OR "apolipoprotein e isoproteins" OR "apoe isoproteins" OR "APO E" OR "apo e isoproteins" OR "Apoproteins E" OR "Apoprotein E" OR "APOE-epsilon2" OR "APOE epsilon2" OR "ApoE2" OR "APOE-epsilon 2" OR "APOE epsilon 2" OR "Apo E-2" OR "Apo E 2" OR "apo e2" OR "Apolipoprotein-epsilon2" OR "Apolipoprotein epsilon2" OR "Apolipoprotein E-2" OR "Apolipoprotein E 2" OR "APOE-epsilon3" OR "apoe epsilon3" OR "ApoE3" OR "APOE-epsilon 3" OR "APOE epsilon 3" OR "APO E-3" OR "Apo E 3" OR "APO E3" OR "Apolipoprotein-epsilon3" OR "Apolipoprotein epsilon3" OR "Apolipoprotein E-3" OR "Apolipoprotein E 3" OR "APOE-epsilon4" OR "APOE epsilon4" OR "APOE4" OR "APOE-epsilon 4" OR "APOE epsilon 4" OR

"Apo E-4" OR "Apo E 4" OR "apo e4" OR "Apolipoprotein-epsilon4" OR  
"Apolipoprotein epsilon4" OR "Apolipoprotein E-4" OR "Apolipoprotein E 4" OR  
"apolipoprotein ε" OR "APOε" OR "apo-ε" OR "apolipoprotein ε isoproteins" OR  
"apoε isoproteins" OR "APO ε" OR "apo ε isoproteins" OR "Apoproteins ε" OR  
"Apoprotein ε" OR "APOE-ε2" OR "APOE ε2" OR "Apoε2" OR "APOE-ε2" OR  
"APOE ε 2" OR "Apo ε-2" OR "Apo ε 2" OR "apo ε2" OR "Apolipoprotein-ε2" OR  
"Apolipoprotein ε2" OR "Apolipoprotein ε-2" OR "Apolipoprotein ε 2" OR "APOE-ε3"  
OR "apoε ε3" OR "Apoε3" OR "APOE-ε3" OR "APOE ε 3" OR "APO ε-3" OR "Apo ε  
3" OR "APO ε3" OR "Apolipoprotein-ε3" OR "Apolipoprotein ε3" OR "Apolipoprotein  
ε-3" OR "Apolipoprotein ε 3" OR "APOE-ε4" OR "APOE ε4" OR "APOε4" OR  
"APOE-ε 4" OR "APOE ε 4" OR "Apo ε-4" OR "Apo ε 4" OR "apo ε4" OR  
"Apolipoprotein-ε4" OR "Apolipoprotein ε4" OR "Apolipoprotein ε-4" OR  
"Apolipoprotein ε 4")

## Supplemental Information 2: Exclusion Criteria

1. Not studying APOE in AD-related neurodegeneration, inflammation or pathological protein spread
2. Not studying AD (exclude other neurological diseases)
3. Not focused on the brain
4. Studies of APOE and A $\beta$  or APOE and tau without studying protein spread
5. Human studies involving patients with mild cognitive impairment or animal studies using young APOE mice without additional AD pathology (e.g. no cross with tau or A $\beta$  models or no lipopolysaccharide stimulation)
6. Human studies with evidence of mental health history (e.g. depression)
7. Evidence of neurological trauma (e.g. traumatic brain injury)
8. Evidence of infection (e.g. Herpes Simplex virus)
9. Studies of blood brain barrier dysfunction
10. Studies on olfactory system or retina
11. Studies of biomarkers
12. Reviews, editorials, case reports, case series studies, conference proceedings or posters
13. Duplicates
14. Studies not in English language
15. Studies where full text unavailable

**Supplemental Table 3:** Papers included in the systematic review (Discussed in the Results sections) (\* denotes hand-picked papers included in the systematic literature search)

| First author (Date)     | Inflammation/ Neurodegeneration/ Neurodegeneration and Inflammation | Study design   | Main Findings                                                                                                                                                                                                                                                                         | Reference |
|-------------------------|---------------------------------------------------------------------|----------------|---------------------------------------------------------------------------------------------------------------------------------------------------------------------------------------------------------------------------------------------------------------------------------------|-----------|
| Agosta (2009)           | Neurodegeneration                                                   | Human - MRI    | AD <i>APOE4</i> carriers had greater atrophy in bilateral parietal cortex, right precuneus, hippocampus and middle frontal gyrus vs. non-carriers and controls.                                                                                                                       | [3]       |
| Anderson (1998)         | Neurodegeneration                                                   | <i>In vivo</i> | <i>APOE</i> KO and WT mice had similar synaptic and dendritic densities.                                                                                                                                                                                                              | [57]      |
| Andrews-Zwilling (2010) | Neurodegeneration                                                   | <i>In vivo</i> | Female <i>APOE4</i> -KI mice had age-dependent decrease in hilar GABAergic interneurons vs. <i>APOE3</i> -KI. In neurotoxic <i>APOE4</i> fragment transgenic mice, interneuron loss was even more pronounced.                                                                         | [43]      |
| Arendt (1997)           | Neurodegeneration                                                   | Human - PM     | AD <i>APOE4</i> carriers had more severe neurodegeneration in all areas investigated vs. non-carriers. Carriers had less plastic dendritic changes. Number of <i>APOE4</i> alleles influenced the pattern of dendritic arborisation.                                                  | [33]      |
| Belinson (2008)         | Neurodegeneration                                                   | <i>In vivo</i> | In <i>APOE4</i> -TR mice, activation of the amyloid cascade via inhibition of neprilysin resulted in degeneration of hippocampal CA1, entorhinal and septal neurons. This was accompanied by accumulation of intracellular A $\beta$ and <i>APOE</i> along with lysosomal activation. | [39]      |
| Belinson (2010)         | Neurodegeneration                                                   | <i>In vivo</i> | In <i>APOE4</i> -TR mice, activation of the amyloid cascade via inhibition of neprilysin resulted in A $\beta$ , oA $\beta$ and apoE4 co-localising with enlarged lysosomes and mitochondrial pathology. Kinetics of the lysosomal                                                    | [72]      |

|                              |                                  |                |                                                                                                                                                                                                                                                                                                                                                                                                                |       |
|------------------------------|----------------------------------|----------------|----------------------------------------------------------------------------------------------------------------------------------------------------------------------------------------------------------------------------------------------------------------------------------------------------------------------------------------------------------------------------------------------------------------|-------|
|                              |                                  |                | effects paralleled CA1 neuronal loss.                                                                                                                                                                                                                                                                                                                                                                          |       |
| Belinson & Michaelson (2009) | Neurodegeneration & Inflammation | <i>In vivo</i> | APOE4-related CA1 neurodegeneration was associated with activation of astrogliosis and microgliosis. Microgliosis occurred earlier and was more prolonged compared to astrogliosis. Neurodegeneration within the septum was not associated with microgliosis or astrogliosis in either APOE3 or APOE4 mice.                                                                                                    | [90]  |
| Bien-Ly (2011)               | Neurodegeneration                | <i>In vivo</i> | C-terminal truncated APOE4/AD mice had greater A $\beta$ levels and A $\beta$ deposition, and displayed neuronal deficits such as reduced MAP2, calbindin and Fos immunoreactivity vs. AD mice expressing full length APOE3 or APOE4.                                                                                                                                                                          | [78]  |
| Blain (2006)                 | Inflammation                     | <i>In vivo</i> | Impairment in reactive sprouting in hE4 mice compared to hE3 mice. hE4 mice had more reactive astrocytes as well as a defective outward migration pattern of the astrocytes in the dentate gyrus. The expression of the anti-inflammatory cytokine IL-1ra was delayed in hE4 mice compared to hE3 mice. presence of apoE4 delays the astroglial repair process and indirectly compromises synaptic remodeling. | [114] |
| Blennow (1996)               | Neurodegeneration                | Human - PM     | Rab3a levels were reduced in AD in hippocampus and frontal cortex, but not in cerebellum. No significant differences in rab3a levels in any brain region between AD patients possessing different numbers of the APOE4 allele.                                                                                                                                                                                 | [52]  |
| Boccardi (2004)              | Neurodegeneration                | Human - MRI    | Greater atrophy in medial temporal lobe of AD APOE4 carriers vs. non-carriers.                                                                                                                                                                                                                                                                                                                                 | [11]  |

|                |                   |                 |                                                                                                                                                                                                                                                                                                                                                                                                    |       |
|----------------|-------------------|-----------------|----------------------------------------------------------------------------------------------------------------------------------------------------------------------------------------------------------------------------------------------------------------------------------------------------------------------------------------------------------------------------------------------------|-------|
| Brown (2002)   | Inflammation      | <i>In vitro</i> | Macrophages from male APOE4/4-TR mice produced significantly higher levels of nitric oxide than from male APOE3/3-TR mice, while macrophages from female APOE3/3-TR and female APOE4/4-TR mice produced the similar levels of nitric oxide. Primary cultures of microglial cells of APOE4 transgenic mice also produced significantly more nitric oxide than microglia from APOE3 transgenic mice. | [101] |
| Buttini (1999) | Neurodegeneration | <i>In vivo</i>  | APOE3 protected against excitotoxin-induced neurodegeneration but APOE4 did not - seen as reduction in synaptophysin, MAP-2 positive neuronal dendrites and neurofilament positive axons.                                                                                                                                                                                                          | [53]  |
| Buttini (2000) | Neurodegeneration | <i>In vivo</i>  | Hemizygous and homozygous APOE3 mice were protected against age-related and excitotoxin-induced neurodegeneration, but APOE4 mice were not. APOE3/E4 bigenic mice were as susceptible to neurodegeneration as APOE4 singly-transgenic mice. Neurodegeneration was more severe in homozygous than in hemizygous APOE4 mice consistent with a dose effect.                                           | [38]  |
| Buttini (2002) | Neurodegeneration | <i>In vivo</i>  | In hAPP/APOE3 and hAPP/APOE mice, APOE3 but not APOE4, delayed age-dependent synaptic loss through a plaque-independent mechanism.                                                                                                                                                                                                                                                                 | [54]  |
| Buttini (2010) | Neurodegeneration | <i>In vivo</i>  | Regardless of cellular source, APOE3 protected synapses and dendrites against excitotoxic injury, as did astrocytic APOE4. Neuronal APOE4 was associated with loss of neocortical and hippocampal pyramidal neurons, and increased fragmented APOE4.                                                                                                                                               | [75]  |

|                    |                                  |                               |                                                                                                                                                                                              |       |
|--------------------|----------------------------------|-------------------------------|----------------------------------------------------------------------------------------------------------------------------------------------------------------------------------------------|-------|
| Caberlotto (2016)  | Inflammation                     | Computational                 | Identification of an alteration in aging-associated processes such as inflammation, oxidative stress and metabolic pathways.                                                                 | [96]  |
| Cambon (2000)      | Neurodegeneration                | <i>In vivo</i>                | In aging, only human APOE4 mice displayed a decrease in synapse per neuron ratio, accompanied by an increase in synaptic size when compared with human APOE2, APOE KO and WT mice.           | [49]  |
| Camicioli (1999)   | Neurodegeneration                | Human - PM                    | In AD, neuron loss in the substantia nigra was associated with possession of APOE4 allele, but not in nucleus basalis of Meynert or CA1 region of the hippocampus.                           | [34]  |
| Chang (2005)       | Neurodegeneration                | <i>In vitro</i>               | Fragments of APOE4 were neurotoxic, but full-length APOE4 was not. The lipid- and receptor-binding regions in APOE4 fragments act together to cause dysfunction and neurotoxicity.           | [77]  |
| Chen (2005)        | Inflammation                     | <i>In vitro</i>               | APOE4 but not APOE3 with presence of lipoprotein HDL or serum stimulated an inflammatory response in microglia by release of PGE2 & IL-1 $\beta$ .                                           | [102] |
| Chung (2016)       | Neurodegeneration & Inflammation | <i>In vitro &amp; in vivo</i> | Synaptosome phagocytosis assays on APOE TR astrocytes.                                                                                                                                       | [121] |
| Colton (2002)      | Inflammation                     | <i>In vitro</i>               | Significantly more NO was produced in APOE4 mice compared to APOE3 transgenic mice.                                                                                                          | [100] |
| Corey-Bloom (2000) | Neurodegeneration                | Human - PM                    | No correlation between APOE4 allele dosage and synapse loss in AD.                                                                                                                           | [51]  |
| Cudaback (2011)    | Inflammation                     | <i>In vitro</i>               | Activation of ATP or C5a complement receptor on microglia, causes microglial migration following APOE3>APOE2=APOE4.                                                                          | [115] |
| Cudaback (2015)    | Inflammation                     | <i>In vitro &amp; human</i>   | TLR4/LPS- and TLR3/Poly I:C-induced production of chemokine CCL3 followed APOE3< APOE2 = APOE4. The APOE expression levels followed apoE2>apoE3> apoE4. Post-mortem AD brains homozygous for | [116] |



|                    |                   |                               |                                                                                                                                                                                                                                                                                                                                |       |
|--------------------|-------------------|-------------------------------|--------------------------------------------------------------------------------------------------------------------------------------------------------------------------------------------------------------------------------------------------------------------------------------------------------------------------------|-------|
|                    |                   |                               | APOE4 allele had increased CCL3 than those homozygous for APOE3.                                                                                                                                                                                                                                                               |       |
| Dorey (2017)       | Inflammation      | <i>In vitro &amp; in vivo</i> | APOE4 promoted A $\beta$ -induced neuroinflammation while APOE2 was protective. APOE4/AD mice had higher inflammatory cytokines than APOE2/AD mice. Lipidated APOE4 increased inflammation in astrocytes while recombinant APOE4 did not. Both forms of APOE2 offered protection against A $\beta$ -induced neuroinflammation. | [105] |
| Drouet (2001)      | Neurodegeneration | <i>In vitro</i>               | APOE2 and APOE3 protected cortical neurons against apoptotic cell death induced by non-fibrillar A $\beta$ . APOE4 had no protective effect. Effect involves interaction of APOE with C-terminal domain of A $\beta$ 1-40.                                                                                                     | [42]  |
| Drzezga (2009) *   | Neurodegeneration | Human - MRI                   | No correlation between APOE4 allele dose and grey matter loss in AD patients.                                                                                                                                                                                                                                                  | [25]  |
| Dumanis (2009)     | Neurodegeneration | <i>In vitro &amp; in vivo</i> | APOE4-TR mice had reduced dendritic spine density and spine length compared to APOE2-TR and APOE3-TR mice in the cortex but not in hippocampus.                                                                                                                                                                                | [64]  |
| Egensperger (1998) | Inflammation      | Human study                   | APOE4 allele dependent increase in the number of activated microglia and the tissue taken up by activated microglia.                                                                                                                                                                                                           | [86]  |
| Filippini (2009)   | Neurodegeneration | Human - MRI                   | In AD, grey matter volume decreased with increasing APOE4 allele load in the bilateral medial and anterior temporal lobes.                                                                                                                                                                                                     | [12]  |
| Geroldi (1999) *   | Neurodegeneration | Human - MRI                   | Smaller volumes with increasing dose of the APOE4 allele in the hippocampus, entorhinal cortex and anterior temporal lobes in AD patients. Larger volumes in the frontal lobes with increasing APOE4 alleles.                                                                                                                  | [17]  |

|                   |                   |                        |                                                                                                                                                                                                                                                                                                                                        |       |
|-------------------|-------------------|------------------------|----------------------------------------------------------------------------------------------------------------------------------------------------------------------------------------------------------------------------------------------------------------------------------------------------------------------------------------|-------|
| Gilmor (1999)     | Neurodegeneration | Human - PM             | Non-significant reduction in the number of cholinergic neurons in the nucleus basalis of Meynert in AD cases. No relationship to APOE allele status.                                                                                                                                                                                   | [35]  |
| Gispert (2015)    | Neurodegeneration | Human - MRI            | APOE4 carriers showed steeper hippocampal volume reductions with AD progression. APOE4 carriers showed lower gray matter volume in the bilateral hippocampus, amygdala, parahippocampal cortex and temporal pole, the left angular and inferior parietal cortex, the right insula, the posterior cingulate and precuneus.              | [13]  |
| Gómez-Isla (1997) | Neurodegeneration | Human - PM             | In AD, more than 50% of neurons were lost in the superior temporal sulcus. Neither the amount nor the rate of neuronal loss correlated with APOE genotype.                                                                                                                                                                             | [36]  |
| Grouselle (1998)  | Neurodegeneration | Human - PM             | Somatostatin concentrations were significantly lower in patients carrying an APOE4 allele.                                                                                                                                                                                                                                             | [45]  |
| Guo (2004)        | Inflammation      | <i>In vitro</i>        | APOE3 and APOE4 blocked A $\beta$ -induced proinflammatory response in activated glia. Without A $\beta$ , APOE3 and APOE4 stimulate IL-1 $\beta$ levels in a concentration and isoform dependent manner, with APOE4 more effective than APOE3.                                                                                        | [103] |
| Harris (2003)     | Neurodegeneration | <i>In vivo</i> & human | Ratios of APOE fragments to full-length APOE higher in AD cases vs. nondemented controls. AD and control cases with APOE4 had more APOE fragments than those without APOE4. APOE4 is more susceptible than APOE3 to proteolysis <i>in vitro</i> . Mice with high-level expression of C-terminal truncated APOE4 had neurodegeneration. | [76]  |

|                    |                   |                 |                                                                                                                                                                                                                                                                                                                                                                                                    |       |
|--------------------|-------------------|-----------------|----------------------------------------------------------------------------------------------------------------------------------------------------------------------------------------------------------------------------------------------------------------------------------------------------------------------------------------------------------------------------------------------------|-------|
| Hashimoto (2001) * | Neurodegeneration | Human - MRI     | In AD patients, hippocampal volume decreased with increasing number of <i>APOE4</i> alleles. Amygdala volume also decreased with increasing <i>APOE4</i> gene dose. Whole brain volume increased with increasing <i>APOE4</i> gene dose.                                                                                                                                                           | [19]  |
| Heinonen (1995)    | Neurodegeneration | Human - PM      | Synaptophysin-like immunoreactivity did not differ significantly in AD patients with or without and <i>APOE4</i> allele.                                                                                                                                                                                                                                                                           | [50]  |
| Holtzman (2000)    | Neurodegeneration | <i>In vivo</i>  | Plaque-associated neuritic dystrophy developed in App(V717F) TG mice expressing mouse or human APOE. Formation of dystrophic neurites required APOE. More fibrillar deposits and neuritic plaques were observed in <i>APOE4</i> -expressing App(V717F) mice vs. those with <i>APOE3</i> .                                                                                                          | [62]  |
| Hu (1998)          | Inflammation      | <i>In vitro</i> | In 3 experimental paradigms APOE inhibited A $\beta$ -induced astrocytic activation. No APOE isoform-specific effects were found.                                                                                                                                                                                                                                                                  | [104] |
| Hudry (2013)       | Neurodegeneration | <i>In vivo</i>  | In APP/PS1 mice, <i>APOE4</i> increased oA $\beta$ , plaques, peri-plaque synapse loss, and dystrophic neurons compared to <i>APOE3</i> . Greater reduction in presynaptic synaptophysin near plaques with <i>APOE3</i> and <i>APOE4</i> , but not <i>APOE2</i> . Post-synaptic proteins were unchanged with <i>APOE2</i> and <i>APOE3</i> , but <i>APOE4</i> had greater PSD95 loss near plaques. | [59]  |
| Jack (1998) *      | Neurodegeneration | Human - MRI     | Hippocampal volumes were smaller in AD patients. Hippocampal volumes did not differ based on <i>APOE</i> genotype.                                                                                                                                                                                                                                                                                 | [24]  |
| Jack (1998) *      | Neurodegeneration | Human - MRI     | Mean annual rate of hippocampal and temporal horn volume loss was greater in AD patients. <i>APOE</i> genotype was not associated with                                                                                                                                                                                                                                                             | [30]  |

|                      |                   |                                  |                                                                                                                                                                                                                                                                                                                                                                                                                                    |      |
|----------------------|-------------------|----------------------------------|------------------------------------------------------------------------------------------------------------------------------------------------------------------------------------------------------------------------------------------------------------------------------------------------------------------------------------------------------------------------------------------------------------------------------------|------|
|                      |                   |                                  | the annual rate of volume change.                                                                                                                                                                                                                                                                                                                                                                                                  |      |
| Jain (2013)          | Neurodegeneration | <i>In vivo</i>                   | Impairments in dendritic arborisation and a loss of spines in the hippocampus and entorhinal cortex of female NSE-APOE4 and APOE4-KI mice compared to their respective APOE3-expressing counterparts. NSE-APOE4 mice had more severe deficits in dendritic arborisation, spine density and morphology than apoE4-KI mice. GFAP-apoE4 mice did not have impairments in their dendrite arborisation or spine density and morphology. | [65] |
| Ji (2003) *          | Neurodegeneration | <i>In vivo</i> & human           | APOE4 mice had a lower density of dendritic spines than WT or APOE3 mice. In humans, APOE4 dose inversely correlated with dendritic spine density in AD.                                                                                                                                                                                                                                                                           | [68] |
| Jórdan (1998)        | Neurodegeneration | <i>In vitro</i>                  | APOE4 alone was toxic to cultures, whereas APOE3 had no effect. APOE3 treatment prevented the A $\beta$ -induced toxicity.                                                                                                                                                                                                                                                                                                         | [40] |
| Juottonen (1998) *   | Neurodegeneration | Human - MRI                      | Greater volume loss in the entorhinal cortex of AD patients with an APOE4 allele vs. those without an APOE4 allele. This effect was especially prominent in females vs. males.                                                                                                                                                                                                                                                     | [18] |
| Kang (2018) *        | Inflammation      | <i>In vitro</i> & <i>in vivo</i> | Transcriptomic study comparing sex, age, and isolation-method of microglia in multiple models of AD-like pathology (amyloid, tau, ageing, and inflammation).                                                                                                                                                                                                                                                                       | [92] |
| Keren-Shaul (2017) * | Inflammation      | <i>In vitro</i> & <i>in vivo</i> | Transcriptomic study (single-cell RNA seq) of microglia subsets in AD-like a mouse model.                                                                                                                                                                                                                                                                                                                                          | [94] |
| Koffie (2012)        | Neurodegeneration | <i>In vitro</i> & <i>in vivo</i> | Higher oA $\beta$ and synapse loss near plaques in AD APOE4 carriers compared to APOE3 carriers. Lipidated APOE4 co-localised with oA $\beta$ and increased                                                                                                                                                                                                                                                                        | [60] |

|                  |                                  |                        |                                                                                                                                                                                                                                                                                                                                                                                                                             |       |
|------------------|----------------------------------|------------------------|-----------------------------------------------------------------------------------------------------------------------------------------------------------------------------------------------------------------------------------------------------------------------------------------------------------------------------------------------------------------------------------------------------------------------------|-------|
|                  |                                  |                        | synaptic localization of the $\alpha$ A $\beta$ . This required APOE receptors.                                                                                                                                                                                                                                                                                                                                             |       |
| Krasemann (2017) | Neurodegeneration & Inflammation | <i>In vivo</i> & human | Identified a neurodegenerative phenotype of microglia after phagocytosis of apoptotic neurons which is driven by APOE-TREM2 pathway, this switches the microglia from homeostatic to disease-associated.                                                                                                                                                                                                                    | [93]  |
| Laakso (2000)    | Neurodegeneration                | Human - MRI            | Trend towards accelerated volume loss in the AD group vs. controls. No significant interactions between volume change and APOE status.                                                                                                                                                                                                                                                                                      | [31]  |
| LaFerla (1997)   | Neurodegeneration                | Human - PM             | Neuronal death, as shown by TUNEL, correlated with APOE uptake and intracellular A $\beta$ stabilization. Cells with the most nuclear DNA fragmentation had the highest level of cell surface gp330 which binds APOE.                                                                                                                                                                                                       | [71]  |
| Lanz (2003)      | Neurodegeneration                | <i>In vivo</i>         | Presence of human APOE2 in the APPSw+/- mice restored spine density to levels seen in Tg- controls.                                                                                                                                                                                                                                                                                                                         | [69]  |
| Laskowitz (1998) | Inflammation                     | <i>In-vitro</i>        | Brain cultures from APOE-deficient mouse pups showed enhanced NO production relative to cultures from wildtype mice and from transgenic mice expressing the human APOE3 isoform, demonstrating that endogenous APOE produced by glial cultures is capable of inhibiting microglial function. APOE produced within the brain may suppress microglial reactivity and thus alter the CNS response to acute and chronic injury. | [110] |
| Laskowitz (2001) | Inflammation                     | <i>In vitro</i>        | APOE4 was less effective at reducing microglia activation and the release of TNF $\alpha$ and NO. Peptides from the APOE receptor binding region mimicked these effects, and deletions of the amino acids 146-149 abolished this effect.                                                                                                                                                                                    | [108] |

|                   |                                  |                                        |                                                                                                                                                                                                                         |      |
|-------------------|----------------------------------|----------------------------------------|-------------------------------------------------------------------------------------------------------------------------------------------------------------------------------------------------------------------------|------|
| Lehtovirta (1995) | Neurodegeneration                | Human - MRI                            | AD patients with APOE4/4 genotype had smaller volumes of the hippocampus and the amygdala than those with APOE3/4 and those with APOE3/3 or APOE2/3. Volumes of frontal lobes were similar across the AD subgroups.     | [14] |
| Lehtovirta (1996) | Neurodegeneration                | Human - MRI                            | AD APOE4 carriers had the most extensive volume loss in the medial temporal lobe, hippocampus and amygdala compared to those without APOE4. This was greatest within APOE4 homozygotes.                                 | [15] |
| Leung (2012)      | Neurodegeneration                | <i>In vivo</i>                         | Age-dependent loss of hilar GABAergic interneurons, whereby GAD67- or somatostatin-positive—but not NPY- or parvalbumin-positive—interneuron loss was exacerbated by APOE4. This effect was sex-dependent.              | [44] |
| Lin (2018) *      | Neurodegeneration & Inflammation | <i>In vitro</i> - iPSCs & gene editing | Generated iPSCs of neurons, astrocytes and microglia from APOE3 and APOE4 individuals that were genetically engineered with Crispr-Cas9 to correct the APOE genotype and did transcriptomics on the altered cell types. | [95] |
| Liu (2010) *      | Neurodegeneration                | Human - MRI                            | AD APOE4 carriers had smaller volume in hippocampus and amygdala.                                                                                                                                                       | [21] |
| Liu (2015)        | Neurodegeneration                | <i>In vivo</i>                         | Greater age-induced reduction in PSD95, drebrin and NMDAR subunits in the APOE4/FAD and 5xFAD/APOE-KO mice compared with APOE2/FAD and APOE3/FAD mice.                                                                  | [61] |
| Liu (2017)        | Inflammation                     | <i>In vivo</i>                         | APOE isoforms differentially affect amyloid plaque-associated neuroinflammation. APOE4 expression increased whereas APOE3 reduced amyloid-related gliosis in the mouse brains.                                          | [89] |

|                  |                                  |                               |                                                                                                                                                                                                                              |       |
|------------------|----------------------------------|-------------------------------|------------------------------------------------------------------------------------------------------------------------------------------------------------------------------------------------------------------------------|-------|
| Lo (2011) *      | Neurodegeneration                | Human - MRI                   | APOE4 in AD patients accelerated the hippocampal atrophy.                                                                                                                                                                    | [28]  |
| Lupton (2016)    | Neurodegeneration                | Human - MRI                   | APOE4 was associated with reduced hippocampal and amygdala volume in AD patients.                                                                                                                                            | [16]  |
| Lynch (2001)     | Inflammation                     | <i>In vivo &amp; in vitro</i> | APOE downregulates CNS production of TNF $\alpha$ , IL-1b, and IL-6 mRNA following stimulation with lipopolysaccharide (LPS).                                                                                                | [111] |
| Maezawa (2006a)  | Inflammation                     | <i>In vitro</i>               | Astrocyte stimulation and production of inflammatory cytokines.                                                                                                                                                              | [112] |
| Maezawa (2006b)  | Neurodegeneration & inflammation | <i>In vitro</i>               | Most paracrine-mediated neurodegeneration was due to microglia not astrocytes. Microglial damage to neurons followed TR-APOE4>TR-APOE3>TR-APOE2. Microglial p38MAPK-dependent cytokine secretion followed a similar pattern. | [106] |
| Manelli (2007)   | Neurodegeneration                | <i>In vitro</i>               | Dose-dependent neurotoxicity was induced by $\alpha$ A $\beta$ with a ranking order of apoE4-TR > KO = apoE2-TR = apoE3-TR > WT.                                                                                             | [41]  |
| Manning (2014) * | Neurodegeneration                | Human - MRI                   | Hippocampal atrophy rates in APOE4 carriers were significantly higher in AD compared with non-carriers.                                                                                                                      | [22]  |
| Masliah (1995)   | Neurodegeneration                | <i>In vivo</i>                | In APOE KO mice, there was an age-dependent loss of synaptophysin-immunoreactive nerve terminals and MAP2-immunoreactive dendrites in the neocortex and hippocampus, compared to controls.                                   | [56]  |
| McGeer (1997)    | Inflammation                     | <i>In vitro</i>               | APOE4 only significantly enhanced complement activation with A $\beta$ .                                                                                                                                                     | [120] |
| Minett (2016)    | Inflammation                     | Human - PM                    | APOE2 allele was associated with expression of Iba1 and MSR-A, and APOE4 with CD68, HLA-DR and CD64.                                                                                                                         | [85]  |
| Mori (2002) *    | Neurodegeneration                | Human - MRI                   | APOE4 dose was significantly correlated with the rate of hippocampal atrophy in AD.                                                                                                                                          | [26]  |

|                       |                   |                 |                                                                                                                                                                                                                                                                                                        |       |
|-----------------------|-------------------|-----------------|--------------------------------------------------------------------------------------------------------------------------------------------------------------------------------------------------------------------------------------------------------------------------------------------------------|-------|
| Nathan (2002)         | Neurodegeneration | <i>In vitro</i> | Cortical neurons from APOE KO mice have significantly shorter neurites than neurons from WT mice. Human APOE3 increased neurite outgrowth, whereas APOE4 decreased outgrowth dose-dependently.                                                                                                         | [82]  |
| Neustadtl (2017)      | Neurodegeneration | <i>In vivo</i>  | APOE4 mice have higher cortical calcineurin activity compared with APOE3 mice. Elevation in calcineurin associated with fewer dendritic spine number in layer II/III of the cortex.                                                                                                                    | [84]  |
| Nwabuisi-Heath (2014) | Neurodegeneration | <i>In vivo</i>  | During spine maintenance phase, density of GluN1 + GluA2 spines did not change with APOE2, while density of these spines decreased with APOE4 vs. APOE3, primarily due to the loss of GluA2 in spines. During spine loss phase, total spine density was lower in neurons with APOE4 compared to APOE3. | [63]  |
| Ophir (2003)          | Inflammation      | <i>In vivo</i>  | APOE3 (but not APOE4) transgenic mice have marked increased astrocyte activation 72 hrs after LPS. There was no effect on astrocytic proliferation only morphology. APOE4 had a similar phenotype to APOE-deficiency.                                                                                  | [91]  |
| Ophir (2005)          | Inflammation      | <i>In vivo</i>  | Expression of inflammation related genes were higher and more prolonged in apoE4 compared to apoE3 transgenic mice treated with LPS after 24hrs. Microglia activation and NF- $\beta$ K regulated genes were higher in apoE4 than apoE3 transgenic mice.                                               | [113] |
| Overmyer (1999)       | Inflammation      | Human - PM      | APOE4 carriers have more GFAP expression than those without APOE4 allele.                                                                                                                                                                                                                              | [87]  |
| Risacher (2010)       | Neurodegeneration | Human - MRI     | The presence of one or more APOE4 alleles increased annual rate of atrophy in hippocampus and entorhinal cortex.                                                                                                                                                                                       | [29]  |



|                    |                                  |                               |                                                                                                                                                                                                                                                                                                    |      |
|--------------------|----------------------------------|-------------------------------|----------------------------------------------------------------------------------------------------------------------------------------------------------------------------------------------------------------------------------------------------------------------------------------------------|------|
| Rodriguez (2013)   | Neurodegeneration                | <i>In vivo</i>                | Shorter dendrites and lower spine densities in basal shaft dendrites of APOE4 mice compared to APOE3 mice. Spine densities did not differ between APOE2 and APOE3.                                                                                                                                 | [66] |
| Rodriguez (2014)   | Neurodegeneration & Inflammation | <i>In vivo</i>                | Cortical levels of IL-1 $\beta$ were higher in E4FAD mice compared to E3FAD mice. Increased microglial reactivity in E4FAD mice and higher density of reactive cells surrounding cortical plaques, than in E3FAD mice. No APOE dependent differences in microglia reactivity within the subiculum. | [88] |
| Scheff (2006)<br>* | Neurodegeneration                | Human - PM                    | AD patients had fewer synapses in the outer molecular layer of the dentate gyrus. This was not related to APOE genotype.                                                                                                                                                                           | [46] |
| Scheff (2007)      | Neurodegeneration                | Human - PM                    | AD patients had fewer synapses in the stratum radiatum of the hippocampal CA1 subfield. This was not related to APOE genotype.                                                                                                                                                                     | [47] |
| Scheff (2011)      | Neurodegeneration                | Human - PM                    | AD patients had fewer synapses in lamina 3 of the inferior temporal gyrus. This was not related to APOE genotype.                                                                                                                                                                                  | [48] |
| Schuff (2009)<br>* | Neurodegeneration                | Human - MRI                   | AD patients showed hippocampal volume loss over 6 months and accelerated loss over 1 year. Increased rates of hippocampal loss were associated with presence of the APOE4 gene in AD.                                                                                                              | [27] |
| Sen (2012)         | Neurodegeneration                | <i>In vitro &amp; in vivo</i> | APOE3 but not APOE4, acts via LRP1 to protect synapses against $\alpha\beta$ by inducing PKC $\epsilon$ synthesis. This was lipidation and APOE receptor dependent.                                                                                                                                | [70] |
| Shi (2017)         | Neurodegeneration & inflammation | <i>In vitro &amp; in vivo</i> | APOE4 causes more extensive atrophy and neurodegeneration but absence of APOE is protective. APOE4 also causes higher neuroinflammation while                                                                                                                                                      | [9]  |

|                             |                   |                                  |                                                                                                                                                                                                                                                                                                                                         |       |
|-----------------------------|-------------------|----------------------------------|-----------------------------------------------------------------------------------------------------------------------------------------------------------------------------------------------------------------------------------------------------------------------------------------------------------------------------------------|-------|
|                             |                   |                                  | APOE-KO was protective.                                                                                                                                                                                                                                                                                                                 |       |
| Susanto (2015)              | Neurodegeneration | Human - MRI                      | In AD A $\beta$ + subjects, APOE4 carriers had more severe atrophy of the medial temporal lobe and thalamus compared to non-carriers.                                                                                                                                                                                                   | [23]  |
| Tai (2015)                  | Inflammation      | <i>In vitro</i> and animal model | APOE4 affected A $\beta$ -induced inflammatory receptor signaling, with increased detrimental (toll-like receptor 4-p38 $\alpha$ ) and reduced beneficial (IL-4R-nuclear receptor) pathways. $\alpha$ A $\beta$ induced TNF- $\alpha$ secretion which followed APOE-KO > APOE4 > APOE3 > APOE2. This was inhibited by TLR4 antagonists. | [107] |
| Tannenberg (2006)           | Neurodegeneration | Human - PM                       | Presence of APOE4 resulted in significantly lower levels of pre-synaptic proteins in AD cases.                                                                                                                                                                                                                                          | [58]  |
| Thangavel (2017)            | Inflammation      | Human - PM                       | APOE4 and glia maturation factor were colocalised within amyloid plaques of AD brains as well as in the activated astrocytes surrounding the plaques                                                                                                                                                                                    | [97]  |
| Tolar (1999)                | Neurodegeneration | <i>In vitro</i>                  | Truncated APOE and APOE peptide elicit an increase in intracellular calcium levels, followed by death of hippocampal neurons in culture                                                                                                                                                                                                 | [80]  |
| Tulloch (2018) <sup>*</sup> | Inflammation      | Human - Methylation              | Lower APOE DNA methylation in non-neuronal cells, mainly glia, in AD cases.                                                                                                                                                                                                                                                             | [99]  |
| Ulrich (2018) <sup>*</sup>  | Inflammation      | <i>In vitro</i> & <i>in vivo</i> | APOE and plaque interaction in the APP/PS1 mouse AD-like model.                                                                                                                                                                                                                                                                         | [109] |
| Veinbergs (1999)            | Neurodegeneration | <i>In vivo</i>                   | Mice expressing human APOE4 exhibited dendritic alterations compared to APOE3 mice. However, both APOE3 and APOE4 mice had preserved density of synaptophysin-immunoreactive pre-synaptic terminals.                                                                                                                                    | [55]  |
| Veinbergs (2002)            | Neurodegeneration | <i>In vitro</i>                  | APOE4-mediated neurotoxicity was associated with calcium dysregulation via                                                                                                                                                                                                                                                              | [73]  |

|                             |                                  |                               |                                                                                                                                                                                                                                                                                                                                                                                                           |       |
|-----------------------------|----------------------------------|-------------------------------|-----------------------------------------------------------------------------------------------------------------------------------------------------------------------------------------------------------------------------------------------------------------------------------------------------------------------------------------------------------------------------------------------------------|-------|
|                             |                                  |                               | increased influx through calcium channels and reduced clearance. Mediated by APOE receptors.                                                                                                                                                                                                                                                                                                              |       |
| Vitek (2009) *              | Inflammation                     | <i>In vitro &amp; in vivo</i> | Characterising inflammatory responses of innate immune response in APOE TR mice                                                                                                                                                                                                                                                                                                                           | [98]  |
| Wang (2005)                 | Neurodegeneration                | <i>In vivo</i>                | APOE4 mice displayed significantly reduced excitatory synaptic transmission and dendritic arborisation. Despite these changes there were no signs of gliosis, amyloid deposition or neurofibrillary tangles in these mice.                                                                                                                                                                                | [67]  |
| Wolk and Dickerson (2010) * | Neurodegeneration                | Human - MRI                   | AD APOE4 carriers exhibited greater medial temporal lobe atrophy, whereas non-carriers had greater frontoparietal atrophy.                                                                                                                                                                                                                                                                                | [20]  |
| Yasuda (1998)               | Neurodegeneration                | Human - MRI                   | Positive correlation between whole brain volume and number of APOE4 alleles in AD.                                                                                                                                                                                                                                                                                                                        | [32]  |
| Yin (2014)                  | Neurodegeneration                | <i>In vivo</i> - MRI          | Increased hippocampal and cortical atrophy in aged APOE4 mice compared to APOE3 mice. Increased soluble and insoluble A $\beta$ in aged APOE4 mice.                                                                                                                                                                                                                                                       | [37]  |
| Zhong (2008)                | Neurodegeneration                | <i>In vivo</i>                | Arg-61 APOE mice (domain interaction) had no gross structural abnormalities or significant loss of neurons. Age-dependent loss of synaptophysin in neocortex and hippocampus and lower levels of the postsynaptic neuroligin-1. Fewer bassoon-immunoreactive presynaptic boutons in hippocampus vs. WT mice. No significant difference observed in the neocortex. No differences in total dendritic area. | [81]  |
| Zhu (2012)                  | Neurodegeneration & Inflammation | <i>In vivo</i>                | After LPS APOE4 mice had increased glial activation with higher levels of microglia and astrocytes, and higher prolonged cytokine release (IL-1 $\beta$ , IL-6, TNF-                                                                                                                                                                                                                                      | [119] |

|  |  |  |                                                                                                                                                                                               |  |
|--|--|--|-----------------------------------------------------------------------------------------------------------------------------------------------------------------------------------------------|--|
|  |  |  | <p>α) compared to APOE2 and APOE3 mice. APOE-KO mice were similar to APOE4. APOE4 caused greater synaptic protein loss measured by three synaptic markers; PSD-95, drebin, synaptophysin.</p> |  |
|--|--|--|-----------------------------------------------------------------------------------------------------------------------------------------------------------------------------------------------|--|

**Supplementary Table 4.** Details of human post-mortem cases used for Figures 2-5. MRC BBN: Medical Research Council Brain Bank Number, AD: Alzheimer's disease, PM: Post-mortem.

| MRC BBN   | Control vs AD | Age | Sex | APOE genotype           | PM delay (hours) | Brain weight (g) | Brain pH | Braak Stage |
|-----------|---------------|-----|-----|-------------------------|------------------|------------------|----------|-------------|
| BBN 28402 | Control       | 78  | M   | $\epsilon 3/\epsilon 3$ | 49               | 1503             | 6.33     | I           |
| BBN 29082 | Control       | 79  | F   | $\epsilon 3/\epsilon 4$ | 80               | 1339             | 5.96     | III         |
| BBN 28771 | AD            | 85  | M   | $\epsilon 3/\epsilon 3$ | 91               | 1183             | 5.95     | VI          |
| BBN 19690 | AD            | 57  | M   | $\epsilon 3/\epsilon 4$ | 58               | 1200             | 5.90     | VI          |

---

## Epilogue

---

I had the best and worst times during these years. I lost myself, only to find myself again stronger.

I felt the laughter in my ribs and the tears on my face.

I don't know if I will ever understand (or accept) why we have to go through the tough things in life to grow, but we did quite some growing.

I am glad I was open to every learning opportunity. I always remember my mom telling me about how her grandmother survived the concentration camp because she knew how to sew and could fix their uniforms, getting lemon rinds in exchange to live. Nothing is beneath you and you are not superior to anyone. Find the opportunity in everything.

I thought being a successful scientist was all there is to it, and I couldn't be more wrong. People are too complicated to only be defined by one thing.

I do hope I will be remembered for the good stuff.

Long story short, it was...



